ABSTRACT

Reactive transport of arsenic through basaltic porous media

Bergur Sigfússon

This thesis studied the volcanic and geothermal source of arsenic (As) and its fate in shallow ground waters and upon entering the ocean by means of experimental and field measurements combined with geochemical modeling.

Arsenic enters the atmosphere and hydrosphere from degassing magmas and during volcanic eruptions. The November 2004 eruption within the Vatnajökull Glacier, Iceland, provided an opportunity to study elemental fluxes from volcanic eruptions into the environment. According to geochemical modeling, lowering of pH due to magma gases during the eruption led to rapid tephra dissolution with corresponding change in flood water chemistry. Geochemical modeling of floodwater/seawater mixing indicated localised decrease in dissolved arsenic and sulphur due to adsorption on the suspended floodwater materials. As the floodwater was diluted the As desorbed and limited effect of the floodwater was predicted after thousand fold dilution.

Laboratory experiments were carried out to generate and validate sorption coefficients for arsenite and arsenate in contact with basaltic glass at pH 3 to 10. The mobility of arsenite decreased with increasing pH. The opposite was true for arsenate, being nearly immobile at pH 3 to being highly mobile at pH 10.

A 1D reactive transport model constrained by a long time series of field measurements of chemical composition of geothermal effluent fluids from a power plant was constructed. Thioarsenic species were the dominant form of dissolved As in the waters exiting the power plant but converted to some extent to arsenite and arsenate before feeding into a basaltic lava field. Chloride, moved through the basaltic lava field (4100 m) in less than 10 yrs but arsenate was retarded considerably due to surface reactions and has entered a groundwater well 850 m down the flow path in accordance to prediction by the 1D model, which further predicted a complete breakthrough of arsenate in the year 2100 while arsenite will be retained for about 1000 yrs.

KEYWORDS: Arsenic; basaltic glass, Nesjavellir, Grímsvötn; Skeiðará.

Reactive transport of arsenic through basaltic porous media

by

Bergur Sigfússon
University of Aberdeen

B.Sc. Geology (University of Iceland)
M.Sc. Geology (University of Iceland)

A thesis submitted for the degree of Doctor of Philosophy
at the University of Aberdeen,
Aberdeen, UK.

October 2009

DECLARATION

I hereby declare that the work presented in this thesis has been performed by myself in the Department of Plant and Soil Science and has not been presented in any previous application for a degree. All verbatim extracts have been distinguished by quotation marks and all sources of information specifically acknowledged by reference to the authors.

BERGUR SIGFÚSSON

ACKNOWLEDGEMENTS

First and foremost I am forever grateful to my wonderful lovely wife Rannveig Anna Guicharnaud, which has put up with me for the last years while in the meantime did one of these theses herself. She has encouraged me greatly throughout the study and has been a source of enormous inspiration and joy since I first met her in Þórsmörk all these years ago.

My supervisor Professor Andy A. Meharg deserves gratitude for his endless help and suggestions throughout this study.

Further I would like to thank my co supervisor Dr. Sigurður R. Gíslason, which initially employed me to sieve his massive river suspended material samples in the year 2000. These endless attempts to wreck my back while sampling large river samples from bridges ended up in this thesis in the form of the suspended materials chemical analyses from River Skeiðará.

At the University of Aberdeen I would like to thank Dr. Graeme I Paton, Dr. Paul Williams and Dr. Andrea Raab for valuable discussions and priceless help in the lab. Dot MacKinnon and Norman Little deserve special thanks for help with analytical equipment and bits and bobs needed to carry out "low" budget experiments.

At the University of Iceland I would like to thank Eydís Eiríksdóttir, Andri Stefánsson, Niels Giroud, Stefán Arnórsson and Jón Örn Bjarnason for endless discussions and help on the subject, being experimental, field related or mathematical derivation of kinetic models.

At Reykjavik Energy I would like to thank Einar Gunnlaugsson, Gretar Ívarsson, Bjarni Reyr Kristjansson and Selma Olsen for their help. I would specially like to thank Einar Örn Þrastarson; it takes a quite skilled driver to transport an ion chromatograph coupled to atomic fluorescence detector over 4 km long lava field in the middle of the winter without smashing the equipment to pieces.

I would like to thank my family, Sigfús Jóhannesson, Sigríður Elefsen, Ari Sigfússon, Hildur Sigfússon and Ingunn Sigfúsdóttir for their patience; I suppose I will see more of you from now on.

Finally, I would like to thank my sons Alexander and Benedikt for their endless patience during the final stages of this work. Now it's just back to the kitchen.

This project was funded by the Icelandic Centre of Research, The Icelandic Governmental fund for Graduate Education, Reykjavik Energy and Landsvirkjun.

SUMMARY

The importance of geothermal energy as a source for electricity generation and district heating has increased over recent decades. Arsenic (As) can be a significant constituent of the geothermal fluids pumped to the surface during power generation. This thesis studied the volcanic and geothermal source of As and its fate in shallow ground waters, and upon entering the ocean, by means of experimental and field measurements combined with geochemical modeling.

Dissolved As exists in different oxidation states, mainly as the reduced arsenite (As(III)) and oxidised arsenate (As(V)), and the charge of individual species varies with pH. In sulphidic waters As is primarily bound to sulphur on thioarsenic forms. Basaltic glass is one of the most important rock types in many high-temperature geothermal fields. Static batch and dynamic column experiments were combined to generate and validate sorption coefficients for As(III) and As(V) in contact with basaltic glass at pH 3 to 10. Five surface reactions were chosen to represent As/basaltic glass interactions. These reactions produced one monodentate and one bidentate As(III) surface complexes and one monodentate and two bidentate As(V) surface complexes:

Reaction	log K (25°C)
As(III)	
$2Glass\text{-}OH + H_3AsO_3 = (Glass\text{-}O)_2AsOH + 2H_2O$	4.7
$Glass\text{-}OH + H_3AsO_3 = Glass\text{-}H_4AsO_4$	2.8
As(V)	
$Glass\text{-}OH + H_3AsO_4 = Glass\text{-}OAsO_3^{-2} + 2H_+ + H_2O$	-2.4
$2Glass\text{-}OH + H_3AsO_4 = (Glass\text{-}O)_2AsO_2^- + H^+ + 2H_2O$	2.3
$2Glass\text{-}OH + H_3AsO_4 = (Glass\text{-}O)_2AsOOH + 2H_2O$	4.3

Validation of experiments was carried out by two empirical kinetic models and a surface complexation model (SCM). The SCM provided a better fit to the experimental column data than kinetic models at high pH values. However, in certain circumstances an adequate estimation of As transport in the column could not be attained without incorporation of kinetic reactions. The varying mobility with pH was due to the combined effects of the variable charge of the basaltic glass and the individual As species as pH shifted, respectively. The mobility of arsenite decreased with increasing pH. The opposite was true for arsenate, being nearly immobile at pH 3 to being highly mobile at pH 10.

The laboratory measured adsorption coefficients for aquatic As(III) and As(V) species on basaltic glass surfaces were applied to a shallow basaltic rock aquifer near the Nesjavellir geothermal power plant in Iceland. A one dimensional (1 D) reactive transport model constrained by a long time series of field measurements of chemical

composition of geothermal effluent fluids, pH, Eh and sometimes Fe- and As-dissolved species measurements was constructed for this purpose. Di-, tri- and tetrathioarsenic species ($As(OH)S_2^{2-}$,AsS_3H^{2-} ,AsS_3^{3-} and $As(SH)_4$) were the dominant form of dissolved As in geothermal waters exiting the power plant but converted to some extent to arsenite (H_3AsO_3) and arsenate ($HAsO_4^{2-}$) oxyanions coinciding with rapid oxidation of sulphide (S_2^-) to thiosulphide ($S_2O_3^{2-}$) and finally to sulphate (SO_4^{2-}) during surface runoff before feeding into a basaltic lava field. A continuous 25 year data set monitoring groundwater chemistry along a traverse of warm springs on the Lake Thingvallavatn shoreline allowed calibration of the 1D model. The conservative ion, chloride (Cl^-), moved through the basaltic lava field (4100 m) in less than 10 years but As was retarded considerably due to surface reactions and has entered a groundwater well 850 m down the flow path as arsenate in accordance to prediction by the 1D model. The 1D model predicted a complete breakthrough of arsenate in the year 2100 while arsenite will be retained for about 1000 years. Due to increased deep well injection of geothermal effluents, adsorption to the basalt surfaces and dilution from ground waters, As concentrations in springs discharging into Lake Thingvallavatn will not reach those of the inlet concentrations during the years 1990-2006.

Arsenic enters the atmosphere and hydrosphere from degassing magmas and during volcanic eruptions. The November 2004 eruption within the Vatnajökull Glacier, Iceland, provides an opportunity to study elemental fluxes from volcanic eruptions. On 28th October, Lake Grímsvötn started draining sub glacially with the floodwater entering River Skeiðará 50 km south of the lake. Following four d draining of Lake Grímsvötn an eruption started at 21:50 GMT on 1st November 2004 forming an eruption column up to 12-14 km. Maximum discharge of the glacial flood rose from 50 to3,300 m^3 sec^{-1} on 2 November at 16:40. A distinct change in the floodwater chemistry was observed between 8:20 and 12:15 on 2 November where dissolved $S_2O_3^{2-}$ and Hg were first detected with corresponding peak flux of Na, Cl, B and V. Further change occurred between 12:15 and 19:15 where other elemental fluxes peaked with concurrent decrease in δ34S values from 7.5‰ to 3.5‰. According to geochemical modeling, lowering of pH due to magma gases during the eruption led to rapid tephra dissolution with corresponding change in flood water chemistry. The modeling of floodwater/seawater mixing indicated localised decrease in dissolved arsenic and sulphur due to adsorption on suspended materials. As the floodwater was diluted the As desorbed and limited effect of the floodwater was predicted after thousand fold dilution.

TABLE OF CONTENTS

LIST OF FIGURES

LIST OF TABLES

LIST OF EQUATIONS

CHAPTER 5

GLOSSARY

AAS	Atomic Absorption Spectrometry
AEC	Anion Exchange Chromatography
AES	Atomic Emission Spectrometry
AFS	Atomic Fluorescence Spectrometry
ARD	Advection-Reaction-Dispersion equation
ars system	Arsenate Reductase system
As(III)	Arsenite
As(V)	Arsenate
AsB	Arsenobetaine
AsC	Arsenochline
BET	Brunauer, Emmett and Teller surface area
BSM	Basic Stern Model
CA	Cellulose Acetate
CAMP	Central Atlantic Magma Province
CCM	Constant Capacitance Model
CFB	Continental Flood Basalt
CZE	Capillary Zone Electrophoresis
DDLM	Diffuse Double Layer Model
DMA^{III}	Dimethylarsinic Acid
DMA^{V}	Dimethylarsonic Acid
DOC	Dissolved Organic Carbon
EDS	Energy Dispersive Spectrometry
EIA	Environmental Impact Assessment
ES	Electro spray Ionisation
EXAFS	Extended X-ray Absorption Fine Structure
FESEM	Field Emission Scanning Electron Microscopy
GC	General Composite approach
GF	Graphite furnace
HDPE	High Density Polyethylene
HFO	Hydrous Ferric Oxide
HG	Hydride Generation
HPLC	High Pressure Liquid Chromatography
IC	Ion Chromatography
ICP	Inductively Coupled Plasma
LDPE	Low Density Polyethylene
MMA^{V}	Monomethylarsonic Acid
MRM	Multi-Reaction Model
MS	Mass Spectrometry
NAIP	North Atlantic Igneous Province
ORS	Octopole Reaction System
PTFE	Polytetrafluoroethylene (Teflon)
PV	Pore Volumes
SMS	Sector Mass Spectrometry

TCC	Total Carbonate Carbon
TLM	Triple Layer Model
TMAO	Trimethylarsine Oxide
UV	Ultra Violet
XANES	X-ray Absorption Near Edge Spectroscopy
XAS	X-ray Absorption Spectroscopy

1 Literature review

The review gives a brief discussion on the Geology of Iceland followed by a more detailed description of the speciation and detection of arsenic. Prediction of arsenic speciation in terms of thermodynamics is discussed as well as comprehensive review is provided on analytical techniques on arsenic speciation. Empirical and mechanistic adsorption models are discussed in detail and finally, methods for geochemical modeling of arsenic transport are described.

1.1 Introduction

The current production of geothermal energy places it fourth in the world with respect to renewable energy sources, behind hydroelectricity, wind power and biomass (REN21, 2008). The current usage pales in comparison to its potential. Although geothermal energy utilisation leads to some emission of gases and effluent water that require disposal, it is a relatively benign energy source compared to nuclear and fossil fuels. The first environmental impact assessment (EIA) of geothermal utilization was compiled in the USA in 1970, and considerable research on the side effects and environmental impacts of geothermal utilisation have been carried out since then (Kristmannsdottir and Armannsson, 2003), partly due to increased public awareness of the impact of anthropogenic activities.

The main environmental issues involved in geothermal development are (Kristmannsdottir and Armannsson, 2003):

- Chemical pollution
- Physical effects of fluid withdrawal
- Noise
- Thermal effects
- Biological effects
- Protection of natural features

One important constituent of chemical pollution is the element arsenic (As). Arsenic is a third row, group V, metalloid element and thus has an excess of electrons and unfilled orbital's that stabilise formal oxidation states from +5 to -3. The assignment of formal oxidation states to As is not very meaningful from a chemical

standpoint because As bonding overall is essentially covalent (Cotton and Wilkinson, 1988). However from toxicological point of view, redox chemistry plays an important role in As toxicology, and the most toxic form of As being the gas arsine (AsH_3) followed by the aqueous forms arsenite ($As^{(III)}O_3^{3-}$) and arsenate ($As^{(V)}O_4^{3-}$). The organic (methylated) forms of As are generally considered to be less toxic while there is still considerable uncertainty regarding the toxicity of some organic species (Vaughan, 2006; Hopenhayn, 2006). While As can combine with many other elements to form covalent compounds, it most commonly bonds to oxygen and sulphur in nature (O'Day, 2006).

Volcanic ash forms due to rapid cooling of magma in atmosphere or in contact with water. The rapid cooling results in insufficient time for crystallisation and if the magma is mafic in origin, basaltic glass can form (Jakobsson and Gudmundsson, 2008). The ratio of crystalline to non-crystalline rock depends on such factors as magma composition, temperature, the difference in vapour pressure between the magma and the ambient environment (Jakobsson and Gudmundsson, 2008).

The concentration of As in a limited dataset of Icelandic rocks, which are primarily volcanic in origin, ranges from less than 5 μg kg^{-1} to 1.28 mg kg^{-1} (Arnorsson, 2003), while that of basaltic volcanic materials ranges from 0.02 mg kg^{-1} to 0.18 mg kg^{-1} with a mean of 0.08 mg kg^{-1} (Arnorsson, 2003). Arnorsson (2003) reported a positive relationship between As and rubidium (Rb) ($p=0.008$) and K_2O ($p=0.06$), respectively, in rocks ranging from basic to silicic volcanics from the active volcanic belt of NE-Iceland and Krafla central volcanic complex. Rubidium and K are incompatible during production and evolution of magmas in the mantle (Cox et al., 1979). The strongly positive correlation between Rb, K_2O and As indicates the same magma processes affect As, Rb and K_2O concentrations of basaltic to silicic volcanic rocks. Therefore, in spite of limited database, As concentrations in Icelandic volcanic rocks may be estimated with some degree of certainty from published Rb and K_2O values (Arnorsson, 2003).

1.1.1 Geology of Iceland

Iceland is mainly composed of basaltic rocks where active seafloor spreading coincides with the occurrence of upwelling mantle plume resulting in intense volcanism (Schilling, 1973). The island lies in the centre of North Atlantic Igneous Province (NAIP) which is a result of Continental Flood Basalt (CFB) volcanism which is

commonly associated with spatially constrained melting anomalies located within the upper mantle (Ernst and Buchan, 2003). Iceland may be considered as an analogue to other CFB provinces such as Central Atlantic Magma Province (CAMP) in America and Africa, The Columbia River Flood Basalts in N-America, Parana-Etendeka in S-America and Africa, Deccan traps in India, Siberian traps in Russia and Emeishan in China. The crest of the Mid-Atlantic Ridge marks the boundary between the North American and Eurasian tectonic plates. The two plates move towards the west-northwest and east-southeast respectively, with an average calculated spreading rate of ~2 cm year^{-1} (Einarsson, 2008). The main volcanic activity in Iceland occurs in active central volcanoes situated within fissure swarms usually nearly parallel to the plate boundaries (rift zones) (Figure 1).

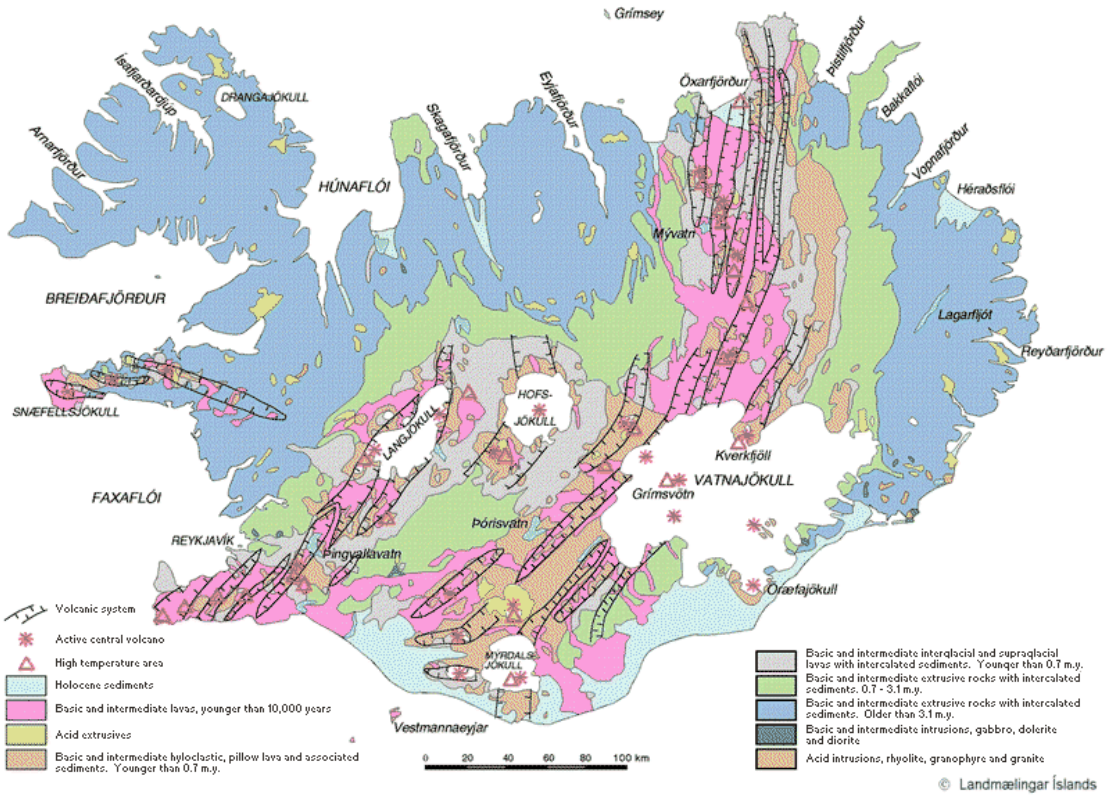

Figure 1 Geology map of Iceland. The main volcanic activity occurs within the volcanic systems located in the main volcanic rift zones. From Johannesson and Saemundsson (1998).

The volcanics formed in the rift zone were continuously buried by younger lavas, then transported out of the rift zones by tectonic movement, and finally the largest lavas resurfaced due to erosion during the Pleistocene (Palmason, 1973; Eiriksson, 2008). Therefore, the youngest lavas of Iceland are located in the centre of the rift zones with increasingly older lavas to the east and west. Iceland‘s rocks can be divided into four geological formations (Johannesson and Saemundsson, 1998): the Later Tertiary Basalt

formation (>3.2 Ma) primarily composed of basaltic lavas with intercalated sediments, The Late Pliocene and Early Pleistocene Basalt formation (0.7 – 3.2 Ma), The Late Pleistocene *Móberg* formation (<0.7 Ma), and the Holocene formation (<10 ka) (Figure 1). *Móberg* is consolidated, mafic to intermediate, hyaloclastite (Table 1) (Kjartansson, 1959). After the eruptions the materials are partially cemented together by alteration and the primary weathering product is palagonite formed as a result of basaltic glass interaction with water (Jakobsson and Gudmundsson, 2008). Table 1 defines the most common geological formations associated with glacio-volcanism relevant to this study. Rocks formed during the Ice Age (<3.2 Ma) are either predominantly hyaloclastite ridges formed between the hyaloclastite ridges at interglacial periods (Figure 2). The hyaloclastite ridges are, therefore, the subglacial equivalents of basaltic lavas erupted from fissures sub aerially.

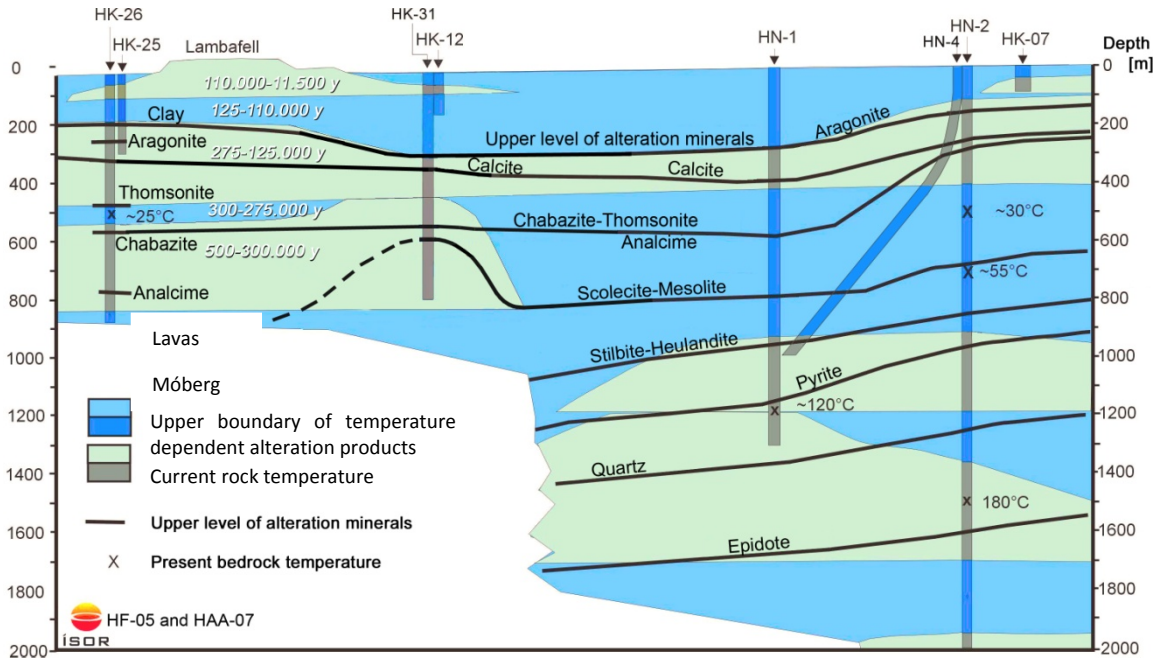

Figure 2 Bedrock sequence near the Hengill Central volcano complex in SW-Iceland. Basaltic lavas, erupted at interglacial periods fill up the gaps between hyaloclastite ridges formed at glacial periods. Superimposed are the zones for low- and high-temperature hydrothermal alteration. From Alfredsson et al. (2007).

Table 1 Definitions of common rock constituents associated with volcanism in Iceland.

Constituent	Defintion	
Flow-foot Breccia	Sediments that are deposited on the advancing frontal slope of lava which flows into water.	Jones, 1969
Hyaloclastite	A hydrated tuff-like breccia rich in black volcanic glass.	Fischer and Schmincke, 1984
Móberg	Consolidated, mafic to intermediate, hyaloclastite.	Kjartansson, 1959
Palagonite	An alteration product from the interaction of water with basaltic volcanic glass.	Stroncik and Schmincke, 2002
Pillow lava	A rock type formed when lava emerges from an underwater or subglacial volcanic vent into water.	Batiza and White, 2000
Sideromelane	Basaltic volcanic glass that is translucent	White and Houghton, 2000
Tachylite	Basaltic volcanic glass (opaque) due to microlite christalisation and is inferred to result from slightly slower chilling than that of sideromelane.	White and Houghton, 2000
Tephra	Air-fall material produced by volcanic eruption regardless of composition or fragment size.	Thorarinsson, 1944
Tuya	A flat-topped steep-sided volcano formed when lava erupts through a thick glacier or ice sheet.	Mathews, 1947
Tuff	A rock consisting of consolidated volcanic ash.	Encyclopædia Brittanica, 2009
Volcanic ash	Volcanic tephra smaller than 2 mm.	Heiken and Wohletz, 1985
Volcanic glass	Any glassy rock formed from lava or magma that may have reached very low temperature without crystallisating, but its viscosity may have become very high.	Encyclopædia Brittanica, 2009

1.1.2 **Geothermal activity in Iceland**

Geothermal areas in Iceland have been divided into two categories, high temperature and low temperature areas (Figure 3). High temperature geothermal activity of varying degree is always associated with the central volcano complexes in Iceland with the temperature of the system and permeability of the aquifers being the main determining factors on the system's capacity for energy utilisation. Nearly all the high temperature geothermal systems (where temperature is >200°C at 1 km depth) are located in the rift zone where lavas and hyaloclastite ridges build up the bedrock sequence (Figures 2 and 4). The main aquifers in these systems are composed of some form of volcanic materials, being un-weathered or partially altered to palagonite (Figure 2). Furthermore, the permeability is increased by large number of fractures cutting through the systems allowing preferential flow in the fracture orientation.

Low temperature geothermal areas (where temperature is <150°C) occur where regional groundwater flow meets localized heat source and is as a consequence elevated to the surface. The low temperature areas are primarily located outside the active volcanic zones (Figure 3).

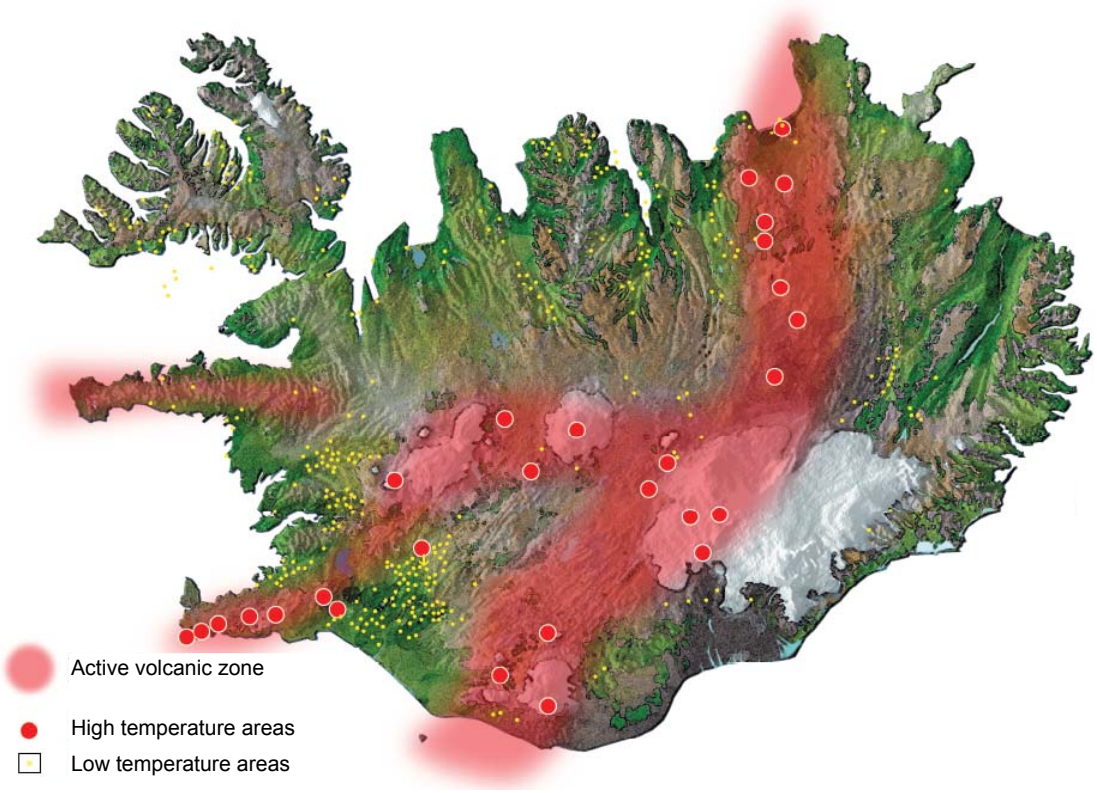

Figure 3 Geothermal areas in Iceland. All high temperature areas are located within the active volcanic zones but low temperature areas can be located elsewhere provided that the permeability of the bedrock is sufficient to allow for groundwater movement. Figure from Reykjavik Energy.

1.1.3 Hydrology of main Icelandic aquifers

Permeability of Icelandic rocks is highest in the rift zones but decreases to the east and west and is overall highest at the surface. The low permeability is primarily due to regional low temperature alteration of primary minerals into secondary minerals such as silica, smectites and zeolites (Walker, 1960; Neuhoff et al., 1999; Sigurdsson and Ingimarsson, 1990). The molar volume of secondary minerals is greater than the molar volume of the primary minerals. Therefore, alteration of primary to secondary minerals fills pore space by addition of water and sometimes CO_2 to the mineral matrix. High temperature alteration with associated loss in permeability mainly occurs during the active volcanism phase in and around extinct central volcanoes in the Tertiary formation. Dike and fissure swarms are associated with these extinct central volcanoes leading preferential groundwater flow usually parallel to the nearest volcanic rift axis. The highest permeability is associated with rocks younger than 0.7 Ma in the rift zones. The relatively young rocks have not been subject of regional low temperature alteration

and therefore have high permeability. New fractures associated with plate movements and central volcanoes form regularly allowing easy flow of ground-waters.

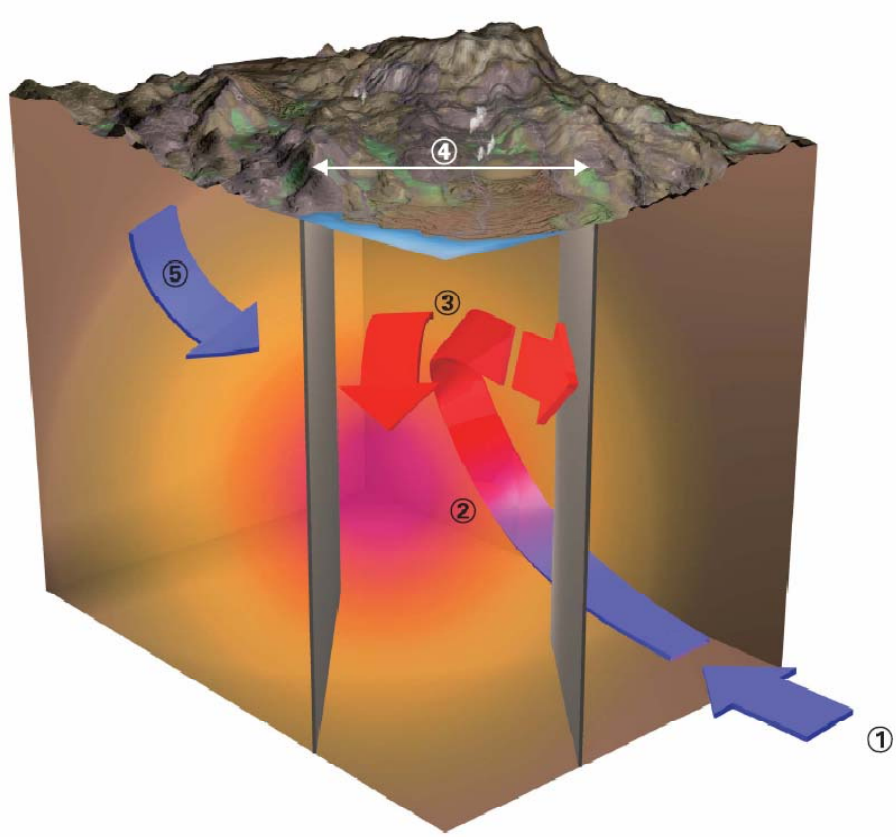

Figure 4 Conceptual model of the Hengill high temperature geothermal system. (1) Cold water originating from the highlands flows underground towards Mount Hengill. (2) The water comes into contact with hot bedrock, heats up and is forced out through cracks and faults. (3) Boiling water and steam flows from Mount Hengill between tectonic and volcanic boundaries towards the surface. (4) Between these boundaries, geothermal heat is much nearer the surface than outside therefore facilitating utilisation. (5) Groundwater from local precipitation can also seep into the geothermal system. Figure from Reykjavik Energy.

1.2 Arsenic

High concentrations of As in ground waters have been reported from different regions of the world (Smedley and Kinniburgh, 2002). The most widespread As enrichment occurs in regions of large continental basins such as West Bengal, Bangladesh, Vietnam, Cambodia, Chile, Argentina, USA and China (Mandal and Suzuki, 2002; Kuan et al., 2000; Charlet and Polya, 2006) where suspended materials are carried with major rivers from mountainous areas to the river floodplains and are there subject to sedimentation and subsequent biogeochemical cycling at or below the Earth's surface.

Naturally elevated As levels can be a result of diverse chemical reactions occurring under a variety of environmental conditions. Occurrence of elevated As in ground waters has primarily been attributed to dissolution of Fe(III) oxyhydroxide mineral coatings caused by bacterial oxidation of organic carbon under reduced conditions (Smedley and Kinniburgh, 2002; Harvey et al., 2002; Nickson et al., 1998). These oxyhydroxides had previously precipitated under oxidising conditions, co precipitating or adsorbing As from the aqueous solution onto their surfaces during precipitation and transport in the oxidised river environment (Smedley and Kinniburgh, 2002; Harvey et al., 2002; Nickson et al., 1998).

Another source of As to ground waters is the oxidative dissolution of sulphides. High temperature (>100 °C) geothermal ground-waters often contain elevated As levels (Webster and Nordstrom, 2003), which can be lowered by precipitation of sulphides at high H_2S levels (Cleverley et al., 2003). Arsenic in reduced geothermal waters forms the minerals realgar (As_2S_2) and/or, orpiment (As_2S_3) that co-exist with pyrite (FeS_2) (Cleverley et al., 2003). These pyrites dissolve under oxidizing conditions, creating sulphuric acid and, therefore, mobilise any As present in the mineral structure or adsorbed on the surface (Cleverley et al., 2003). The subsequent transport of As then depends on the chemical composition of the water, and as a result speciation of As and the nature of the mineral surfaces of the aquifer (Stauder et al., 2005).

High temperature geothermal waters also serve as a carrier of As to surface waters. This process may be described studying Figure 4 using the same numbering system as in the figure text

(1) Cold water originating from the highlands in SW Iceland flows underground towards Mount Hengill.
(2) The water comes into contact with hot bedrock, which is primarily basaltic in origin and contains some As. The water heats up, is forced through cracks and faults, reacts with the rocks and releases As into the water by dissolving the basaltic glass, primary silicates and oxides containing As as well as releasing As resting on crystal surfaces. At deep levels the As is primarily on the As(III) form and is mainly associated with sulphur originating from the rocks and volcanic gases originating from cooling magmas and intrusions.
(3) Boiling water and steam flows upwards carrying the As from Mount Hengill between tectonic and volcanic boundaries towards Nesjavellir.

(4) Between these boundaries, geothermal heat is much nearer the surface than outside, some water and steam enters the surface and the H_2S gas in the water starts to oxidize to thiosulphate ($S_2O_3^{2-}$) and eventually to sulphate (SO_4^{2-}) as well as degassing into the atmosphere. Once the H_2S has been eliminated from the water the As-S species start to disintegrate into As-oxyanions and finally As(III) is oxidised to As(V) (Chapter 4).

1.2.1 **Speciation of As**

Speciation of As is the most important factor controlling its bioavailability and mobility, depending on environmental parameters such as pH and redox potential, temperature and salinity of the solution. Arsenic is mostly present in most aqueous environments as the +III and +V oxidation states as arsenite and arsenate oxyanions and their hydrolysis species, respectively (Ferguson and Gavis, 1972) with minor amount of methyl and dimethyl organoarsenic compounds being detected (Hung et al., 2004). The pH of natural waters range from 2-12 whereas acid mine drainage can reach as low as -0.5, the Eh of surface waters in contact with atmosphere ranges from <800 mV at acidic to <400 mV under alkaline conditions (Figure 5). High temperature geothermal waters in Iceland range in pH from ~6 to ~9.5 (Stefansson and Arnorsson, 2002, Reykjavik Energy, unpublished data) and are reduced, although redox equilibrium is seldom attained (Stefansson and Arnorsson, 2002). At these conditions the primary As oxyanion is $H_3AsO_3^0{}_{(aq)}$. Recently, the importance of thioarsenates in sulfidic geothermal waters has been reported accounting for up to 83% of dissolved As under alkaline conditions (Planer-Friedrich et al., 2007).

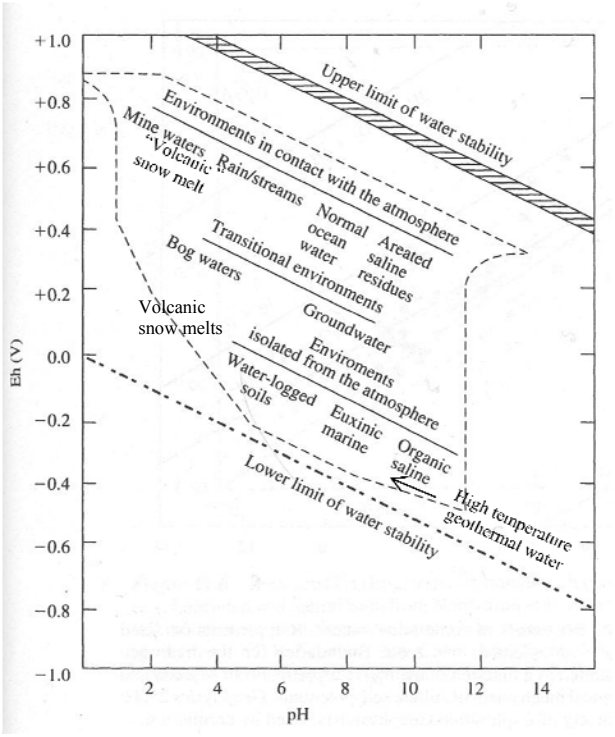

Figure 5. Approximate positions of some natural environments in terms of Eh and pH. The crossed line represents the limits of measurements in natural environments (Baas-Becking et al., 1960). Waters in high temperature geothermal systems are frequently positioned near the lower limit of water stability at pH between 6-9.5 (Stefansson and Arnorsson, 2002), Reykjavik Energy, unpublished data). In addition snow melts in the vicinity of erupting volcanoes yield pH 2.8 (Flaathen et al., 2009).

The following discussion of As speciation thermodynamic systems only takes into account the formation and solubility of As bearing minerals in equilibrium with aqueous species in water, but not with surface species. The effect of surface speciation will be discussed in preceding chapters.

1.2.1.1 The As-O-H system

Speciation of As can be conveniently described in a series of complex thermodynamic systems (Brookins, 1986; Vink, 1996) shown on Eh vs. pH diagrams. The formation of $H_3AsO_3^0{}_{(aq)}$ from the solid As_2O_3 polymorphs arsenolite and claudetite may be described by the reaction:

$$As_3 0_{3(s)} + 3H_2O \rightarrow 2H_3AsO^0_{3(aq)} \qquad \text{Eq. 1}$$

The reaction described by eq. 1 is independent of Eh and pH and, therefore, depends only on $H_3AsO_3^0{}_{(aq)}$ activity and H_2O activity as the activity of $H_3AsO_3^0{}_{(aq)}$ reaches 0.15 m. This equilibrium is reached at 0.15 m $H_3AsO_3^0{}_{(aq)}$ at 25°C (Vink, 1996) and, therefore, arsenolite and claudetite will dissolve at lower $H_3AsO_3^0{}_{(aq)}$ activities. In the

As-O-H system (Figure 6), the As is predominantly found as aqueous species unless the total dissolved As reaches the high arsenolite solubility and is therefore highly mobile. Native As(s) can only occur under very reducing conditions at both acidic and alkaline conditions (Figure 6). Both arsenite and arsenate form protolytes, which may release protons stepwise similar to carbonic acid (Figure 6). Arsenate forms negatively charged oxyanions ($H_2AsO_4^-$ and $HAsO_4^{-2}$) at natural pH values (Brookins, 1986; Vink, 1996) while As (III) forms the uncharged oxyanion (H_3AsO_3) (Loehr and Plane, 1968) at pH up to around 9 (pKa= 9.2) (Pokrovski et al., 1996). Above pH 9.2 the predominant arsenite species is $H_2AsO_3^-$.

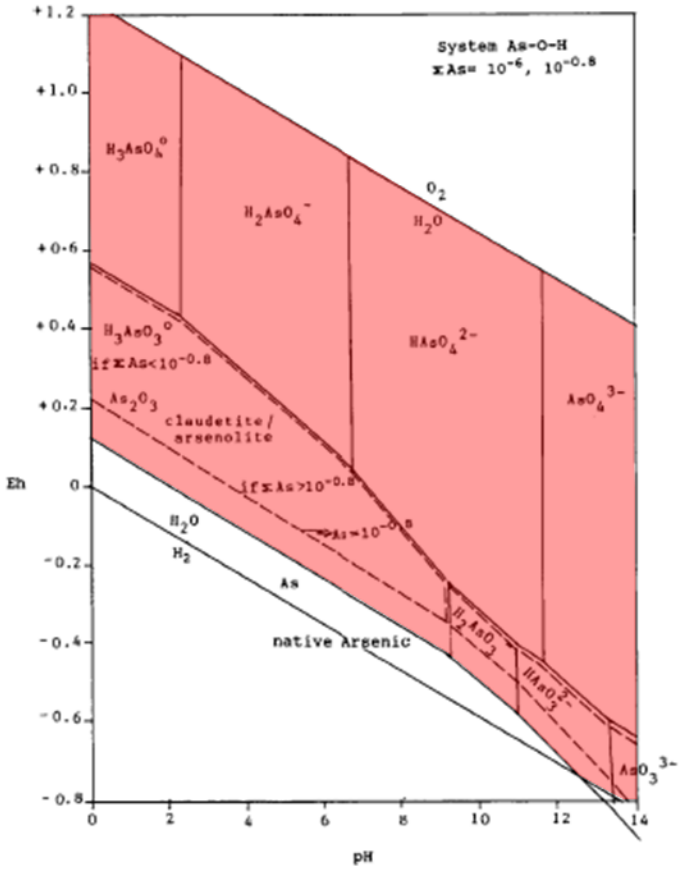

Figure 6 Eh – pH diagram for the system As-O-H at 25°C. Activities of ∑As = 10^{-6} m, contoured for $10^{-0.8}$ m. Modified from Vink (1996)

1.2.1.2 The As-S-O-H system

When sulphur is added as a component the system becomes As-S-O-H (Figure 7). The polymorphs of As_2O_3 are still insignificant due to their very high solubility (Vink, 1996) whereas realgar (As_2S_2) is stable at both acidic and alkaline strongly reducing

conditions. Orpiment (As_2S_3) occurs at less reduced conditions, mainly acidic but also at slightly alkaline conditions (Vink, 1996). Pokrovski et al. (1996) reported the hydrolysis of orpiment according to the reaction:

$$As_3S_{3(s)} + 3H_2O \rightarrow 2H_3AsO^0_{3(aq)} + H_2S^0_{(aq)} \quad \text{Eq. 2}$$

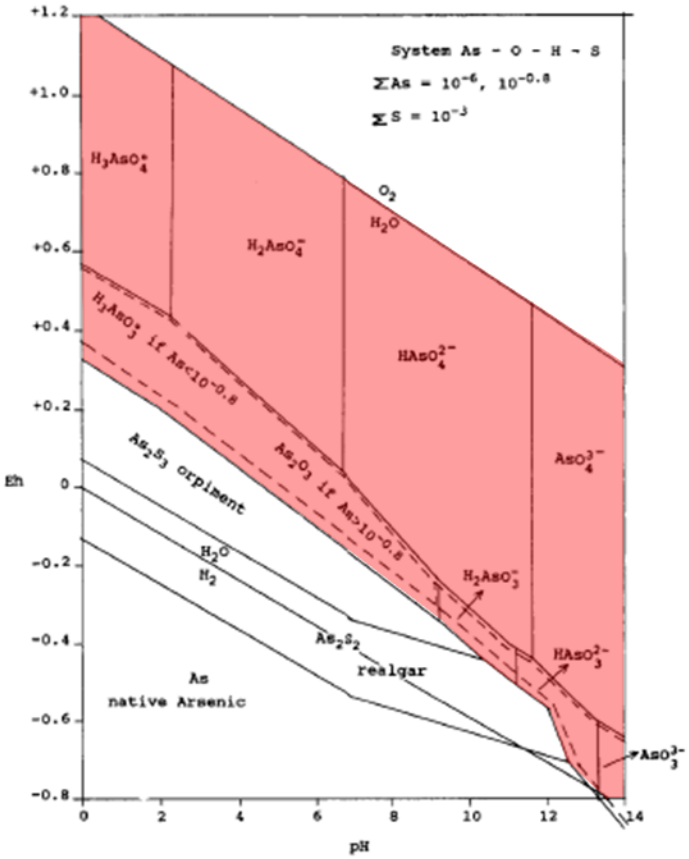

Figure 7 Eh-pH diagram for the system As-O-H-S at 25°C. Activities of ∑As = 10^{-6} m, contoured for $10^{-0.8}$ m, and activities of ∑S = 10^{-3} m. Red area represents conditions where As is mobile (the primary As phase is on aqueous form). Modified from Vink (1996).

However, recent research has stated that the solubility of amorphous and crystalline orpiment under neutral to alkaline conditions is controlled by at least four thioarsenite species each with multiple protonation states (Stauder et al., 2005; Wilkin et al., 2003; Rochette et al., 2000; Beak et al., 2008) forming according to the reactions:

$$As_3S_{3(s)} + 4H_2O \rightarrow 2As(OH)_2S^-_{(aq)} + HS^-_{(aq)} + 3H^+_{(aq)} \quad \text{Eq. 3}$$

$$As_3S_{3(s)} + HS^-_{(aq)} + 2H_2O \rightarrow 2As(OH)S_2^{2-}{}_{(aq)} + 3H^+ \quad \text{Eq. 4}$$

$$As_3S_{3(s)} + 3HS^-_{(aq)} \rightarrow 2AsS_3H^{2-}{}_{(aq)} + H^+ \quad \text{Eq. 5}$$

$$As_3S_{3(s)} + 5HS^-_{(aq)} + 3H^+ \rightarrow 2As(SH)^-_{4(aq)} \quad \text{Eq. 6}$$

These thioarsenite species dominate under experimental conditions where sulphide concentrations exceeded 0.1-1 mM (Figure 8). The thioarsenite species can be considered to form when -SH groups progressively substitute –OH groups in the As species (Wilkin et al., 2003) according to:

$$As(OH)^0_{3(aq)} + HS^- + H^+ \rightarrow As(OH)_2(SH)^0_{(aq)} + H_2O \quad \text{Eq. 7}$$

$$As(OH)^0_{3(aq)} + HS^- \rightarrow As(OH)_2S^- + H_2O \quad \text{Eq. 8}$$

$$As(OH)_2S^- + HS^- \rightarrow As(OH)S_2^{-2} + H_2O \quad \text{Eq. 9}$$

$$As(OH)S_2^{-2} + HS^- + H^+ \rightarrow AsS_3H^{-2} + H_2O \quad \text{Eq. 10}$$

$$As(OH)S_2^{-2} + HS^- \rightarrow AsS_3{}^{-3} + H_2O \quad \text{Eq. 11}$$

$$AsS_3H^{-2} + HS^- + 2H^+ \rightarrow As(SH)_{4(aq)} \quad \text{Eq. 12}$$

Sulphide concentrations in low temperature aquatic systems are generally controlled by the rate of bacterial sulphate reduction (Canfield et al., 2006) the form and abundance of iron in the solid matrix. Dissolved sulphide is generally low when iron hydroxides are present since it is consumed during reduction of the hydroxides and formation of sulphides (Jensen et al., 2003) and does not accumulate in the water therefore precluding the formation of thioarsenite species. High temperature geothermal water can contain high amounts of dissolved sulphides, due to its reduced state, influx of sulphur gases from the heat source and host rock, which can readily complex any dissolved As in the water (Planer-Friedrich et al., 2007).

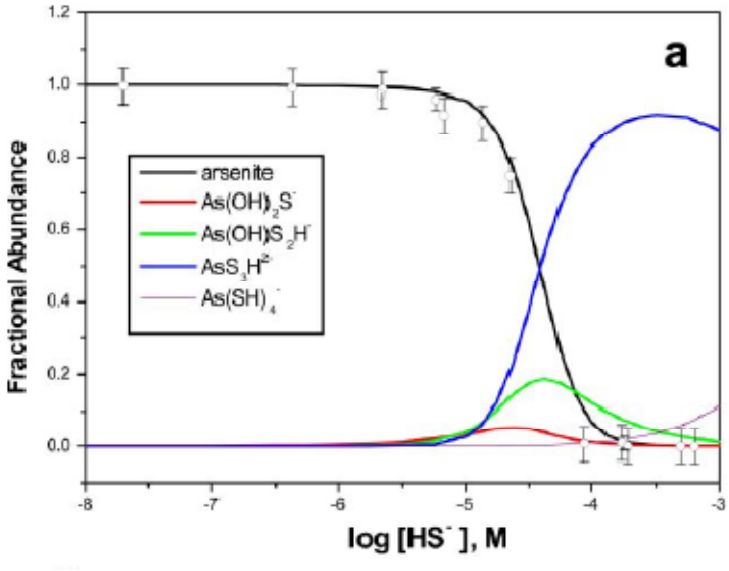

Figure 8 Distribution of arsenite and thioarsenite as a function of bisulphide concentration at pH 7, 25°C. Data points correspond to the measured fractional abundance fo arsenite at pH 7. From Wilkin et al., (2003).

1.2.1.3 The As-S-Fe-O-H system

The abovementioned system can be further expanded by adding Fe as a component. The most common occurrence of As in nature is in the mineral arsenopyrite (FeAsS) (Vink, 1996). Furthermore, as mentioned above; reactive Fe has detrimental effect on the possible formation of thioarsenite species.

Once Fe has been introduced to the system (Figure 9), realgar is the stable As form at reduced acidic conditions whereas at reducing alkaline conditions it coexists with magnetite (Fe_3O_4), where arsenopyrite is only stable at extremely reducing alkaline conditions (Vink 1996). The mineral scorodite ($FeAsO_4$ or $FeAsO_4 \cdot 2H_2O$), which can be expressed to form according to:

$$Fe_2O_{3(S)} + 2H_3AsO_{4(aq)} \rightarrow 2FeAsO_{4(s)} + 3H_2O \qquad \text{Eq. 13}$$

is stable under oxidising acidic conditions and, therefore, As should only exist in the soluble from under oxidising neutral to alkaline conditions and at weakly reducing conditions (Figure 9).

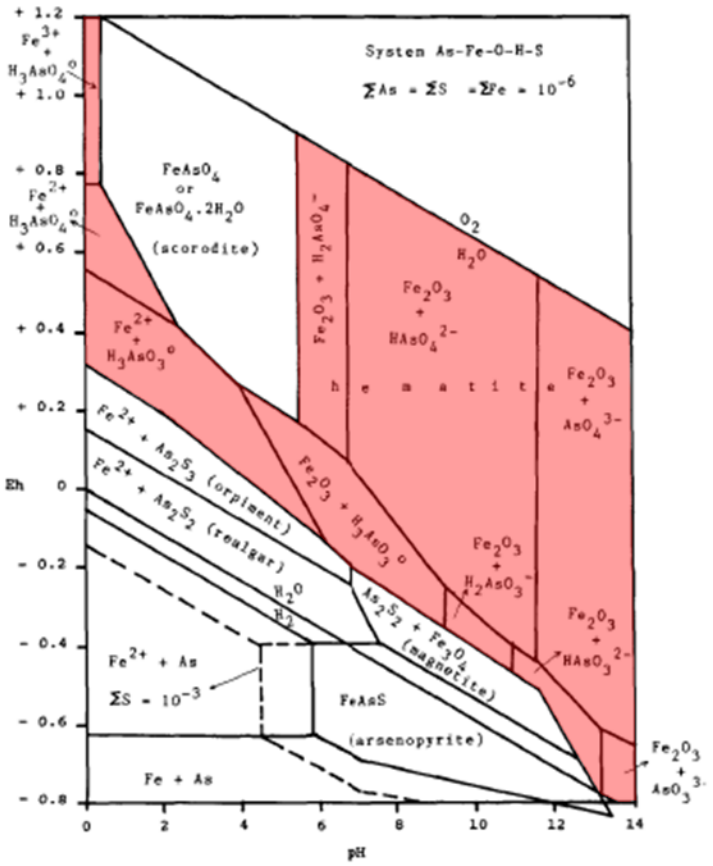

Figure 9 Eh-pH diagram for the system As-Fe-O-H-S at 25°C. Activities of ∑As and ∑Fe and ∑S = 10^{-6} m. Only partial contouring is shown for ∑S = 10^{-3} m. Red area represents conditions where As is mobile (the primary As phase is on aqueous form). Modified from Vink (1996).

1.2.2 Measurement of As

1.2.2.1 Sample preservation

Determination of speciation, including oxidation state, of As is important for interpreting its toxicity, mobility, geochemical and biogeochemical cycling in the environment. Suitable filtration and preservation of water samples is essential for stabilizing the arsenite/arsenate ratio prior to analysis if the analysis cannot be carried out immediately on site.

Although oxidation/reduction reactions for As are generally slow (Gmelins, 1908; Cherry et al., 1979) a series of inorganic processes can occur in water such as:

- Reduction of arsenate by H_2S (Cherry et al., 1979).
- Reduction of arsenate by S_2O_3 and consequent precipitation of As_2S_3 (Chapin, 1914)

- Photocatalysed oxidation of arsenite by Fe(III) (Emett and Khoe, 2001).
- Oxidation of arsenite by dissolved Fe(III) (Cherry et al., 1979).
- Oxidation of arsenite by oxygen in air (Batley, 1989).
- Oxidation of thioarsenites to arsenate (Planer-Friedrich et al., 2007).

Microbes play a large role in determining As speciation in natural waters because they can oxidize and reduce dissolved As over a large range of temperature, pH and solution composition. Dissolved As(V) is reduced rapidly only by strong reducing agents, catalysis or by microbial activity (Cherry et al., 1979). A large number of bacteria and archaea have been identified that use arsenate as a terminal electron acceptor for anaerobic respiration (Mukhopadhyay et al., 2002; Newman et al., 1998) and arsenite oxidizing microbes are also common (Salmassi et al., 2002). As a response to elevated As concentrations in certain environments, microbes have evolved mechanisms to oxidise arsenite to arsenate and reduce arsenate to arsenite. The process of detoxifying As involves an arsenate reductase enzyme coupled with an arsenite efflux pump (the *ars* system) which appears to be common in both anoxic and oxic waters (Mukhopadhyay et al., 2002). A range of microbes are capable of methylating inorganic As, and some can produce further organoarsenic metabolites. Many forms of dissolved organic carbon (DOC) are microbial substrates, and if these substrates are present at high enough concentrations their microbial utilization consumes dissolved O_2, causing anoxia and subsequent arsenate reduction during storage if not properly preserved. Mixed microbial cultures were found to oxidise arsenite and reduce arsenate in geothermally influenced water (Freeman et al., 1986) and arsenite oxidised rapidly by microbes in hot springs (Wilkie and Hering, 1998). Membrane filters with 0.2-0.4 micron pores remove microbes from samples, stabilizing As speciation (McCleskey et al., 2004).

The following solutions may be applied to prevent some of the problems listed above.

Reduction of arsenate can be avoided by purging the sample with N_2 gas to expel all H_2S from the sample (Arnorsson et al., 2006). Nitrogen purging also removes oxygen from the sample and can prevent oxidation of arsenite (Batley, 1989).

Photocatalysed oxidation of arsenite can be inhibited by the formation of Fe(III) sulphate complex that absorbs photons and prevents the production of reactive free radicals (Emett and Khoe, 2001).

Oxidation of arsenite can be slowed down by the addition of acid, by storing the sample at 0-6°C or a combination of acidification and cooling e.g. (Batley, 1989). Acidification breaks down all thioarsenates present in samples and is, therefore, not suitable treatment for preserving speciation in sulphidic waters (Planer-Friedrich et al., 2007). Furthermore, acidification of sulphidic samples has been reported to lead to precipitation of As sulphides (Smieja and Wilkin, 2003). To eliminate the precipitation of As-sulphides prior to detection, Beak et al. (2008), raised the pH to >10 with NaOH, oxidised the H_2S to SO_4^{2-} with 0.5 ml of 30% H_2O_2 for 30 minutes before acidifying it again with HCl to pH <2.

Oxidation of arsenite can be stopped by freezing (Andreae, 1979) and is the preferred way of storage for preservation of thioarsenate species (Planer-Friedrich et al., 2007) which are to be analysed by HPLC methods.

Microbial activity can be stopped by filtering (McCleskey et al., 2004) and/or freezing/chilling.

Separation of arsenite (uncharged) and arsenate (negatively charged) species in the field in acidic solution with ion exchange resins therefore eliminating the need to preserve speciation (Wilkie and Hering, 1998; Ficklin, 1983). Thioarsenites are negatively charged at neutral pH and can be mistakenly interpreted as As(V) in those waters (Jay et al., 2004).

Addition of ethylenediaminetetraacetic acid **(**EDTA) to complex redox active cations, such as iron and manganese, inhibits oxidation of arsenite (e.g. Gallagher et al., 2001) although Oliviera et al. (2005) reported on the inefficiency of EDTA addition for long term storage.

1.2.2.2 Arsenic speciation analysis – Separation techniques

The determination of the total As concentration in a sample is insufficient for environmental considerations since its toxicity depends on the speciation (Gong et al., 2002). Numerous methods have been suggested to separate and quantify As species.

The most commonly used speciation techniques for As often involve a combination by chromatographic separation with spectrometric detection. Of the separation techniques, High Pressure Liquid Chromatography (HPLC) is the most commonly used technique (B'Hymer and Caruso, 2004). The majority of the work on As speciation in the literature utilizes ion-exchange (Wei and Liu, 2007) or ion pair (Sathrugnan and Hirata, 2004) chromatography and to lesser extent ion exclusion

chromatography (Taniguchi et al., 1999), micellar chromatography, capillary electrophoresis (CE) (Wu and Ho, 2004), stripping potentiometry (Munoz and Palmero, 2005), stripping voltammetry (Rasul et al., 2002), selective formation of As species into As-hydrides (Masscheleyn et al., 1991) and photometry (Dasgupta et al., 2002).

1.2.2.2.1 Ion exchange chromatography

Ion exchange chromatography is used for the separation of ions and easily ionized substances. It utilizes the mechanism of exchange equilibrium between a stationary phase, which contains surface ions, and opposite charged ions in the mobile phase. Ion exchange HPLC may be used in either anion (more commonly used for As species) or cation exchange modes. The ionic strength of the solute, the pH of the mobile phase, the ionic strength and concentration of the buffer, temperature of column, flow rate and organic modifiers can all influence the separation and retention times of analytes in ion-exchange HPLC (B'Hymer and Caruso, 2004). Common buffer systems for As ion-exchange chromatography include phosphate (Wei and Liu, 2007), carbonate (Brisbin et al., 2002), phthalic acid (Sheppard et al., 1990), tetra methyl ammonium hydroxide (Lintschinger et al., 1998) and formate buffers (Shiobara et al., 2001). Both isocratic and gradient ion-exchange chromatographic systems have been used to separate As compounds. Gradient systems offer better resolution of rapidly eluting compounds and in addition have the ability to reduce retention times of slowly eluting compounds. Anion exchange chromatography is most widely carried out with the aid of Hamilton PRP-X100 column with any of the above mentioned buffers (Gong et al., 2002) while Dionex Ionpac columns are either used with the abovementioned buffers or more recently with automatically generated potassium- or sodium hydroxide eluent with or without eluent suppression (Planer-Friedrich et al., 2007). The choice of eluent and column depends on the analytes under investigation and the detector for the As species. Arsenite, arsenate, monomethylarsonic acid (MMA^{V}), dimethylarsinic acid (DMA^{III}) are commonly measured by anion exchange methods while arsenobetaine (AsB), arsenochline (AsC), trimethylarsine oxide (TMAO) and tetramethylarsonium ion (Me_4As^{+}) are measured by cation exchange chromatography (Gong et al., 2002). Arsenite is uncharged under neutral conditions (pKa =9.2) and co-elutes with AsB from PRP-X100 column. Separation of arsenite and AsB can be achieved by forming anionic complex when tartaric acid was used as the complex phase. Separation can also be achieved by increasing the pH of the eluent using ammonium carbonate as the eluent on

a PRP-X100 column. Gradient runs with Ionpac columns have achieved separation of Asb, arsenite, arsenate, MMA^V and DMA^V (Lintschinger et al., 1998). Finally thioarsenic species have been separated on Ionpac columns (Stauder et al., 2005; Planer-Friedrich et al., 2007; Wilkin et al., 2003) but the oxidation state of these thioarsenic species cannot be determined from chromatography and have to be confirmed by X-ray absorption spectroscopy (XAS) (Beak et al., 2008).

1.2.2.2.2 Ion-pair chromatography

Ion-pair chromatography (reversed phase HPLC) can both separate ionic species and uncharged molecular species. The separation of analytes is performed using stationary phases that have a surface less polar than the mobile phase. In reversed phase ion-pair chromatography, a counter ion is added to the mobile phase, and a secondary chemical equilibrium of the ion-pair formation is used to control retention and selectivity. Elution and separation are achieved using aqueous solutions with an organic modifier, usually methanol for As speciation analysis. The separation of analytes in ion-pair chromatography is influenced by hydrophobicity of the counter ion, the concentration of the ion-pair reagent, buffer concentration, the pH and ionic strength of the mobile phase and properties of the stationary phase (B'Hymer and Caruso, 2004).

1.2.2.2.3 Ion-exclusion chromatography

Ion-exclusion chromatography involves the use of strong anion- or cation-exchange resins for the separation of weakly ionized or neutral compounds. The charge of the resin is the same as that of the ionic species and the method has three types of interactions, ion-exclusion, ion exchange, and hydrophobic interaction which are suitable to separate various As species (Taniguchi et al., 1999). This method separated arsenite, arsenate and MMA successfully but DMA was not eluted in highly saline biological materials (Nakazato et al., 2000) and seawater (Nakazato et al., 2002).

1.2.2.2.4 Micellar chromatography

Micellar chromatography is a variation of reversed-phase HPLC and has been used to separate arsenite, arsenate, MMA^V and DMA^V in urine samples (Ding et al., 1995). In micellar chromatography, a relatively high concentration of surfactant is used as counter ions and the formation of "micelles" occurs.

1.2.2.2.5 Capillary zone electrophoresis

Capillary zone electrophoresis (CZE) has been used to separate arsenite, arsenate, MMA and DMA^V (Wu and Ho, 2004). The method separates the species by electric current on a surface immersed in a background electrolyte of choice. The method was used in conjunction with indirect ultra-violet (UV) light detection to determine As speciation in realgar and orpiment alkali extracts (Wu and Ho, 2004) and with mass spectrometry (MS) for organoarsenic complexes (Debusschere et al., 2000).

1.2.2.2.6 Hydride generation techniques

Analysis of As is frequently carried out by formation of arsine (AsH_3) hydride followed by detection with either atomic absorption spectrometry (AAS), atomic fluorescence spectrometry (AFS), atomic emission spectrometry (AES) or ICP-MS. Hydride generation (HG) is a chemical derivatization process that produces volatile hydrides upon chemical treatment of a sample with a reducing agent, typically sodium borohydride ($NaBH_4$). The target As species can be separated from almost all other accompanying materials in the sample through the HG process. Only gaseous hydrides are introduced to the detector, and the sample matrix is left in the liquid waste. The As hydride generation reaction can by described in two major steps, the formation of arsine from arsenite upon contact with tetrahydroborate ion (BH_4^-) :

$$As^{III}(OH)_{3(aq)} + 3\,BH_{4(aq)}^{-} \rightarrow AsH_{3(g)} + 3\,BH_{3(aq)} + 3\,H_2O \qquad \text{Eq. 14}$$

and production of H_2 gas that carries the arsine towards and maintains the flame in the AFS detector:

$$BH_{3(aq)} + 3\,H_2O \rightarrow H_3BO_{3(aq)} + 3H_{2(g)} \qquad \text{Eq. 15}$$

A steady flow of $H_2(g)$ is frequently used to carry arsine to the detector. The hydride generation procedure can be used for differential determination of arsenite and arsenate based on the fact that arsenite reacts with tetraborohydride at a higher pH than arsenate (Hung et al., 2004; Masscheleyn et al., 1991). A successful determination of the inorganic species arsenate and arsenate can be achieved by maintaining a high pH in the HG system with a strong buffer. Total As can then be determined followed by a pre-reduction of arsenate to arsenite with any of the reductants mentioned in the electrochemical section below. The difference between total As and arsenite then gives an estimate of arsenate in the sample. Pre-reduction with an acid mixture of KI/ascorbic acid where the ascorbic acid prevents the oxidation of iodide to triiodide by air is the

most applied methodology for the total determination of As in aqueous samples (Chen et al., 1992).

1.2.2.3 Arsenic speciation analysis - Detection techniques

Speciation and detection of trace levels of As in environmental samples requires high-sensitivity detection. Atomic spectrometry provides the best sensitivity for As detection (Gong et al., 2002).

1.2.2.3.1 Inductively coupled plasma (ICP) mass spectrometry (MS)

Due to its extremely high sensitivity, multi element capability, large dynamic range, and isotope ratio measurement capability the ICP-MS coupled with HPLC is now the most effective tool in many As research laboratories (Gong et al., 2002). In ICP-MS, the high efficiency of atomization and ion formation of the ICP is coupled with the specific and sensitive detection capability offered by MS (B'Hymer and Caruso, 2004). Essentially, an aerosol of the sample is introduced into the plasma source where vaporization, atomization and ionization of the analytes occur nearly simultaneously. Elemental ions are passed on into a mass spectrometer. Arsenic does have a spectral interference under certain conditions. Chloride from the sample matrix may combine with argon from the plasma gas to form $^{40}Ar^{35}Cl$ which has the same nominal mass-to-charge ratio (m/z) as As of 75. This problem can be overcome by few ways. A mathematical correction can be used to eliminate this interference. Chlorine has two isotopes, ^{35}Cl and ^{37}Cl so $^{40}Ar^{37}Cl$ should also form in the plasma at the isotopic ratio of chlorine 35 and 37. By monitoring m/z 77, the proportion of the signal m/z 75 generated from argon chloride may be subtracted allowing for the accurate determination of the As signal (B'Hymer and Caruso, 2004). This mathematical correction though requires High-Resolution ICP-MS. Other methods to eliminate $^{40}Ar^{35}Cl$ interference include introducing octopole reaction system (ORS) where helium gas is introduced into the plasma where it collides with ArCl molecules and consequently dissociates the molecules or reduces their kinetic energy and as a consequence, the ArCl molecules can hardly enter the MS while the As ion predominantly passes through the reaction cell into the MS detector (Nakazato et al., 2002; Tao et al., 1993). A HG system has also been coupled to the ICP-MS where arsines are only introduced to the system and chlorine flows to waste with the rest of the sample matrix (Gong et al., 2002; Naykki et al., 2001).

Determination of total As in samples is determined routinely by ICP-MS. For speciation, coupling of HPLC in any form with ICP-MS is very widespread procedure (B'Hymer and Caruso, 2004). Addition of HG into the HPLC-ICP-MS system was reported by Nakazato et al. (2002) which also reported the use of ORS instead of HG system.

1.2.2.3.2 Inductively coupled plasma atomic emission spectrometry (ICP-AES)

The ICP-AES has poorer detection limit than the ICP-MS but has the advantage over many techniques being a multi-element technique, as is ICP-MS, and can, therefore, be useful for As detection when concentrations are high enough. The ICP section of the technique works similarly as in ICP-MS whereas the respective analytes are detected by an optical spectrometer (AES). The sample is pumped into a nebulizer where it is atomized and introduced directly inside the plasma flame. The sample immediately collides with the electrons and other charged ions in the plasma and is broken down into charged ions. The various molecules break up into their respective atoms which then lose electrons and recombine repeatedly in the plasma, giving off the characteristic wavelengths of the elements involved. Sensitivity for As has been increased by coupling HG to the HPLC-ICP-AES system (Rubio et al., 1993).

1.2.2.3.3 Atomic fluorescence spectrometry

The most attractive feature of fluorescence methods is their inherent high sensitivity. Briefly, a sample is introduced into a light beam of a fixed wavelength. A photon is absorbed by the molecule and electrons are excited from their ground electronic state to a higher energy state. Within each of these electronic states are various vibrational states. Collisions with other molecules cause the excited molecule to lose vibrational energy until it reaches the lowest vibrational state of the excited electronic state. Then excited electrons jump to the ground electronic state and as a consequence emit photons in the form of fluorescent light**.** The quality of conventional atomic fluorescence methods based on liquid sample injection suffers due to light scattering and background due to the sample matrix. The, separation of arsines with HG-systems as described above has dramatically improved the detection limits of As (Gong et al., 2002).

Transition metals might interfere with As determination when hydride generation is used although KI/ascorbic acid was found to be the most effective prereductant/masking agent for As interference when iron content was very high (Naykki et al., 2001). The

predominant mechanism is probably due to the reaction of the interfering transition metal ions with $NaBH_4$ reductant, with the formed precipitate being able to capture and catalytically decompose evolved hydrides (Howard and Salou, 1996). Although not as common detector as the ICP-MS for HPLC, HG-AFS has been coupled with success to IC-HG (Wei, Liu 2007) and is regularly used to measure total As.

1.2.2.3.4 Atomic absorption spectrometry

Arsenic can be detected by atomic absorption spectrometry, AAS and is traditionally either introduced to the AAS as arsine produced by HG or as free As atoms produced from the sample deposited in a small graphite tube. Most reported methods for As detection by graphite furnace atomic absorption spectrometry (GF-AAS) require pre-concentration in addition to the treatment in the furnace in order to increase sensitivity. AAS is regularly combined to HG because it suffers from low sensitivity and high background noise for As determination (Howard and Hunt, 1993). The usage of AAS as a detector for HPLC has declined since the 1980s and ICP-MS is now the preferred choice.

1.2.2.3.5 Mass spectrometry

Unlike ICP-MS, ICP-AES, AAS and AFS, where elemental As is detected, electrospray ionisation (ES) mass spectrometry (MS) can provide molecular information of As compounds for positive identification (Gong et al., 2002). This method requires a set of highly sophisticated apparatus and will not be dealt with further in this thesis.

1.2.2.3.6 Electrochemical methods

Electrochemical methods can be used to separate and analyse inorganic As species. Briefly anodic stripping voltammetry involves the deposition of As on an electrode surface:

$$As^{3+} + 3e^- \rightarrow As^0 \quad \text{Eq. 16}$$

Followed by anodic stripping:

$$As^0 \rightarrow As^{3+} + 3e^- \quad \text{Eq. 17}$$

The process is usually carried out on a solid gold or gold coated electrodes (Feeney and Kounaves, 2002).

Electrochemical methods provide high sensitivity and excellent selectivity of the As species but are only possible in simple solutions. In a complex matrix, As

determination is only possible after separation from the interfering matrix (Munoz and Palmero, 2005). Arsenic has been detected by both potentiometry (Munoz and Palmero, 2005) and voltammetry (Rasul et al., 2002). Potentiometry has been shown to possess advantages in sensitivity and selectivity over voltammetric methods. In stripping potentiometry, no external current passes through the working electrode making the technique insensitive to interferences from electro-active substances in the sample. In voltammetric stripping, such substances give rise to background currents that overlap the current stripping peaks. The main advantage of these techniques is the low weight of apparatus, low cost per sample without using or producing any significant toxic substances such as arsine (Rasul et al., 2002; Feeney and Kounaves, 2002). Arsenite and arsenite show different electrochemical behaviour. Conventionally arsenite is electro active ion while arsenate is electrochemically inert under normal conditions (Feeney and Kounaves, 2002). Some chemicals recommended to reduce arsenate to arsenite include, sodium sulphite (Na_2SO_3), hydrazine (N_2H_4)+HCl+HBr, NaBr + N_2H_4+H_2SO_4, gaseous SO_4, potassium iodide (KI), KI + ascorbic acid ($C_6H_8O_6$), cysteine ($C_3H_7NO_2S$), and mannitol ($C_6H_{14}O_6$) (Munoz and Palmero, 2005). Furthermore, solid samples and samples containing organic As compounds have to be mineralised with appropriate methods but digestion of As compounds is beyond the scope of this thesis. Chemical reduction of arsenate to arsenite has been successfully carried out under field conditions with Na_2SO_3 (Rasul et al., 2002; Feeney and Kounaves, 2002) and the difference between arsenite measured prior to chemical reduction and arsenite measured after reduction assumed to represent arsenate in solution.

1.2.2.3.7 Bacterial biosensors

Bioluminescence-based biosensors offer a powerful tool for assessing pollutant bioavailability and toxicity (Paton et al., 1997). Bacterial biosensors have been suggested as a potential complementary, and in some cases alternative, technique to chemical methods for giving environmentally relevant interpretation of samples (Flynn et al., 2002) A combination of metabolic biosensors (*E. coli* and *P. fluorescens*) and As specific biosensor (*E. coli* CM1166 pC200 (Corbisier et al., 1993)) was applied to As and Cu contaminated Chilean soils (Flynn et al., 2002). The metabolic biosensors demonstrated overall toxicity of the soils by showing decreased activity as pollution increased while the As specific biosensor was constructed with *luxAB* genes from *V.*

fischeri which are induced by the *ars* operon that confers resistance to As, so that luminescence is induced by the availability of As in the form of arsenite (Flynn et al., 2002).

1.2.2.3.8 Photometric measurement

Finally, As has been analysed by forming arsnenomolybdate, followed by reduction to heteropoly blue before detecting the complex by photometry (Dasgupta et al., 2002). This method suffers from interference with phosphorus (P) and silicon (Si) in solution as they produce molybdate complexes but P and Si are often encountered in at least one order of magnitude higher concentrations than As in water. Interference by Si has been solved by addition of sodium fluoride (NaF) to the sample to complex the Si in solution (Dasgupta et al., 2002).

1.2.2.3.9 X-ray adsorption spectroscopy

Although chromatographic methods have been used to confirm the existence of thioarsenic species in environmental samples the oxidation state of As in these samples is not probed directly (Beak et al., 2008) and as a consequence these species have been referred to as thioarsenites (Wilkin et al., 2003) or thioarsenates (Stauder et al., 2005). Spectroscopic methods offer the possibility to determine the oxidation state and bonding of As with their nearest neighbour. X-ray absorption near edge spectroscopy (XANES) can demonstrate distinguishable absorption edge positions of As-O bonds compared to As-S bonds as well as valence state of the As (Beak et al., 2008). Extended X-ray absorption fine structure (EXAFS) spectroscopy can further be used to determine the distance of As-O and As-S bonds and coordination number of the central As atom which varies with different As-S ratio of the thioarsenic species (Beak et al., 2008). These methods rely on complex apparatus not widely available and environmental samples need to be preserved before determination can take place.

1.2.3 **Arsenic in Icelandic and geothermal waters**

The Provisional WHO guideline limit for As in drinking waters is 133.5 nmol l^{-1} (10 µg l^{-1}) (World Health Organization, 2004). Furthermore, criteria of five levels (Table 2) have been set up for As concentrations in the environment the protection of aquatic life (e.g. CCME, 1995; Government News, 1999). These levels may be described in terms

of the impact of As on freshwater biota as: I) very low or no probability of effects, II) low probability of effects, III) Effects can be expected in case of sensitive ecosystems, IV) Effect expected on biota and V) Permanently unacceptable levels for biota. Although, from toxicological point of view, the determination of As speciation is more meaningful then the quantification of total As concentration (Gong et al., 2002), no data have been reported on measured concentrations of individual species of As in Icelandic natural waters to the authors knowledge.

In precipitation As concentration is generally below 13.3 nmol l^{-1} (Bauer and Onishi, 1978). In central Iceland, As concentration in precipitation is low; 0.16 to 0.67 nmol l^{-1} (Gislason et al., 2000; Gislason et al., 2002). Arsenic concentrations in Icelandic river waters are most often under the detection limits of the ICP-MS method (0.67 nmol/l) (Gislason et al., 2004). Arsenic was detected in elevated concentrations, up to 31 nmol l^{-1} in Jökulhlaup waters, and river waters in vicinity of active volcanoes, 3 nmol l^{-1}, and rivers draining acid intrusive and extrusive rocks (0.9 nmol/l) (Gislason et al., 2000; Gislason et al., 2002; Gislason et al., 2004).

Arnorsson (2003) reported increase in As concentrations of ground waters with increasing temperature; 1 to 133 nmol l^{-1} at the highest temperature (90°C). Although $Fe^{(III)}$hydroxides in surface and particularly peat waters were abundant, As/B ratio of the waters did not lower relative to ground waters indicating lack of co-precipitation of As with $Fe^{(III)}$-hydroxides (Arnorsson, 2003). Sigfusson (unpublished data) found that As concentrations in soil water increased from below detection limits at surface to 3 nmol l^{-1} near bedrock at 2 m depth. The increase in As concentrations were generally observed at deeper levels compared to other redox dependent elements (Fe, Mn, N) and As was most frequently detected in horizons with lowest concentrations of the oxyhydroxide ferrihydrite.

Table 2. The range of measured dissolved As-concentration in Icelandic waters.

Water type	low nmol/l	high nmol/l	Reference
Precipitation	0.16		Gislason et al. (2000)
Rivers	<0.67	3	Gislason et al. (2000, 2002 and 2004)
Jökulhlaup rivers	1	31	Gislason et al. (2004)
Reduced soil water	1	3	Sigfusson (unpubl)
Groundwater and low temperature waters	1	133	Arnorsson (2003)
High-temperature geothermal waters	26	2840	Olafsson and Riley (1978); Olafsson (1992); Arnorsson et al. (1999)
High-temperature geothermal vapours	<0.67	23.5	Giroud (2008)
Volcanic pollution		640	Flaathen and Gislason (2007)
Runoff from streets in Reykjavik		15000	Gislason et al. (1999)
Wastewater at Nesjavellir		700	Wetang'ula and Snorrason (2005)
Level I water*	<5.3		
Level II water	5.3	67	
Level III water	67	200	
Level IV water	200	1000	
Level V water	>1000		

*Level I) very low or no probability of effects, II) low probability of effects, III) Effects can be expected in case of sensitive ecosystems, IV) Effect expected on biota and V) Permanently unacceptable levels for biota. (CCME 1995, Government News 1999).

Gislason et al. (1999) studied river waters and soil solution compositions at 50 cm depth around industrial area in Hvalfjörður, Iceland. They reported that As concentrations were always below critical limits for drinking water. Heavy metals in the soil water generally decreased with increased pH of the soil water.

Arsenic concentrations in geothermal waters are frequently high, with measured concentrations up to $6.7*10^5$ nmol/l while more typical concentrations range from $1.3*10^4$ nmol/l to $1.3*10^5$ nmol/l (cited by Arnorsson, 2004). Icelandic high temperature geothermal waters showed a variety of concentrations between 10.6 and 2840 nmol l^{-1} while their co-discharging vapour phase constituted up to 25.3 nmol l^{-1}

(Giroud, 2008). A 250°C geothermal sea water at Reykjanes contained 1280-1960 nmol l^{-1} (Olafsson and Riley, 1978). Well waters from Námafjall and Krafla geothermal fields contained 26.7 –640 nmol l^{-1} (Arnorsson et al., 1999). Nesjavellir well waters and water in the power station ranged from 1600 to 2140 nmol l^{-1} (Olafsson, 1992).

Wetang'ula and Snorrason (2005) reported As concentrations of 671 nmol l^{-1} in separator water from Nesjavellir geothermal co-generation power-plant wastewater at pH of 9.39. The concentration at Lækjarhvarf where the wastewaters disappear in the lava near the power-plant was 699 nmol l^{-1} at pH 9.12. The highest concentration of As seeping from this same lava was reported at 81.9 nmol/l at Grámelur classifying the water as Level III water as mentioned above.

Volcanic degassing represents an important natural source of As to shallow aqueous systems. Arsenic is a minor but recurrent constituent of volcanic gases (Symonds et al., 1987). Aiuppa et al. (2005) studied As concentrations in ground waters around active volcanoes in Italy and reported that As concentrations were highest where active hydrothermal circulation takes place at shallow levels. They concluded that dissolution of As-bearing sulphites was the main source of As. Highest concentrations were 92600 nmol/l but lower concentrations were observed where shallow ground waters were heated by steam.

Melted snow in contact with volcanic ash from the volcanic eruption of Hekla 2000 had total dissolved concentration as high as 640 nmol/l (Flaathen and Gislason, 2007).

Runoff from the streets in Reykjavík has been measured to be as high as 15 000 nmol/l (Gislason et al., 1998). This high pulse was associated with the first thawing event after a period of days where temperatures were below freezing point with snow on the streets. Gislason et al. (1998) suggested this was due to the fact that the As was primarily situated on ice grain boundaries which melt before the bulk ice during thawing events.

Arnorsson (2003) reported that As in basaltic rocks was primarily bound in titanomagnetite which is a stable mineral in most surface and ground waters. The available source for As to natural waters was therefore As in soluble salts on mineral grain boundaries and to lesser extent silicate minerals. Arnorsson did not consider As-sulphite precipitation to be significant in reducing As levels nor coprecipitation with Fe(III)-hydroxides.

1.2.4 **Sorption of As**

The rate and extent of chemical sorption onto surfaces is described by a combination of kinetic and equilibrium expressions such as the Freundlich and Langmuir isotherms (Langmuir, 1918; Ho and McKay, 1999; Limousin et al., 2007). Empirical data can be modelled to acceptable degree without interpreting the exact mechanism of surface reactions, although not specifically providing any information regarding the reactions involved in the sorption phenomenon. Surface complexation models use mechanistic approach to interpret and develop sorption isotherms (Sahai and Sverjensky, 1997a). These models are validated by spectroscopic methods on the molecular scale and, therefore, give insight into the actual mechanism taking place.

When studying adsorption and subsequent modeling, a comparison of reaction and the mean residence times of the mobile phase should be conducted (Limousin et al., 2007). If reaction times are much shorter than the residence time thermodynamic equilibrium may be reached and the reactions can be considered instantaneously reversible. Otherwise they are irreversible phenomenon and kinetic experiments must be carried out to further interpret and model the natural systems.

Experiments on the kinetics and extension of As sorption onto various surfaces has been carried out for decades and a brief outline is tabulated in table 3.

Table 3 Compilation of selected experiments involving sorption processes for As species.

Mineral/surface	Relevant findings of experiments	Reference
Arsenate ($H_3As^VO_4$)		
Alpha-Al_2O_3	Arsenate was strongly adsorbed at low pH and was progressively released to the fluid with increasing pH above 7. At any pH, increasing temperature favoured aqueous species of As over surface species. Increasing temperature favoured less negatively charged species below a pH of 9 and more negatively charged species above a pH of 10. Comparison with the stability of As surface complexes with Fe suggested that surface complexes with Al are more stable.	(Halter and Pfeifer, 2001)
Zero valent iron (Fe^0)	Borate and organic matter decreased the sorption of arsenate	(Biterna et al., 2007)
Cu(II), Ni(II)- and Co(II)-doped goethite	Arsenate adsorption decreased in the order of Cu(II)-doped goethite >= Ni(II)-doped goethite > Co(II) doped goethite > pure goethite at all pH values.	(Davis et al., 2006)
Sandy, clayey and loamy soils	Adsorption of arsenate was initially fast followed by slower uptake. Desorption was hysteretic in nature indicating lack of equilibrium retention and/or irreversible processes.	(Zhang and Selim, 2005)
Hematite (Fe_2O_3)	Carbonate competed with arsenate for sorption sites and quantification of adsorbed carbonate may be important when predicting arsenate transport in groundwater where iron oxide-coated aquifer materials are exposed to seasonally fluctuating partial pressures of CO_2(g).	(Arai et al., 2004)
Aluminium oxide (Al_2O_3)	Desorption of arsenate decreased with longer residence times. Surface transformations such as (i) a rearrangement of surface complexes and/or (ii) a conversion of surface complexes into aluminium arsenate-like precipitates might be important chemical factors responsible for the decrease in arsenate reversibility with aging.	(Arai and Sparks, 2002)
Goethite (α-FeO(OH))	Arsenate adsorption was fast initially followed by slower adsorption. Desorption was quite rapid initially and after 24 hours only small amount desorbed. Phosphate had much more influence than sulphate on arsenate desorption. High phosphate concentrations could not desorb all arsenate.	(Arai and Sparks, 2002)
Hematite, feldspar	Arsenate was removed by first order reaction and	(Singh et al.,

	maximum amount was adsorbed at pH 4 on hematite and pH 6.2 on feldspar. Below these pH adsorption decreased perhaps due to dissolution of the minerals.	1996)
Iron oxide (Fe_2O_3) and Aluminium oxide (Al_2O_3)	The maximum arsenate uptake values were observed at pH 6. Iron oxide removed more arsenate per mass than aluminium oxide. The adsorption was mainly controlled by the specific surface area of adsorbents.	(Jeong et al., 2007)
Ferrihydrite ($Fe_5HO_8 \cdot 4H_2O$)	Arsenate formed a surface precipitate on ferrihydrite at low pH (3-5) but no surface precipitation was observed at pH 8. Surface precipitation probably involved initial uptake of arsenate by surface complexation followed by transition to ferric arsenate formation.	(Jia et al., 2006)
Arsenite ($H_3As^{III}O_4$)		
Kaolinite, illite, montmorillonite and amorphous aluminium hydroxide (am-$Al(OH)_3$)	Arsenite oxidised homogenously to arsenate alkaline conditions (pH > 9) in solutions without mineral solids In addition, recovery of adsorbed As from arsenite-treated clay mineral solids showed that oxidation of arsenite to arsenate was enhanced by heterogeneous oxidation on kaolinite and illite surfaces. This leads to As being more strongly adsorbed as arsenate on these surfaces therefore decreasing As mobility in the environment.	(Manning and Goldberg, 1997)
Zero valent iron	Arsenite was removed by a two step process, fast initial disappearance followed by slow subsequent removal process. Arsenite uptake by green rust may be a major mechanism in arsenite removal by zero valent iron.	(Lien and Wilkin, 2005)
Goethite (α-FeO(OH))	The lack of competition observed between arsenite and Fe (II) for sorption sites indicated that the concurrent release of Fe(II) and arsenite during reductive dissolution of iron oxides, inferred as the mechanism of As mobilization in many reducing ground waters, may have relatively minor effects on the subsequent resorption of arsenite to residual iron oxides remaining in the sediment.	(Dixit and Hering, 2006)
Goethite (α-FeO(OH))	Arsenite formed inner sphere bidentate surface complex. Arsenite-alpha-FeOOH surface complex was stable toward heterogeneous oxidation to arsenate	(Manning et al., 1998)

Arsenate/Arsenite

Gamma-Al_2O_3	Arsenite adsorption increased with increasing pH and was insensitive to ionic strength (I) changes (0.01 and 0.8 M $NaNO_3$) at pH 3-4.5, while adsorption decreased with increasing I between pH 4.5 and 9.0, and Arsenate adsorption decreased with increasing pH and was insensitive to I changes at pH 3.5-10. For arsenite both inner- and outer-sphere adsorption coexisted whereas for arsenate inner-sphere complexes were predominant at studied experimental conditions.	(Arai et al., 2001)
Activated alumina	pH was a strong factor in the uptake of both arsenite and arsenate by activated alumina. Uptake of arsenite was much less than for arsenate at most pH conditions.	(Lin and Wu, 2001)
Zero valent iron	At oxic conditions arsenate and arsenite removal where much higher than at anoxic conditions and arsenate removal was faster than arsenite. This was caused by adsorption on ferric hydroxides formed readily through oxidation of Fe(0) by dissolved oxygen.	(Bang et al., 2005)
Various clays	Halloysite and chlorite had much greater arsenate sorption than two kaolinites, illite and illite/montmorillonite. The clay had lower arsenite adsorption than arsenate adsorption and the adsorption was affected by pH. The quantities of extractable arsenite and arsenate decreased with increasing aging time.	(Lin and Puls, 2000)
Ferrihydrite ($Fe_5HO_8 \cdot 4H_2O$)	A distinct adsorption maximum was observed for arsenite adsorption at approximately pH 9.0, which corresponds closely to the first pKa(a) (9.2) of $H_3AsO_3^0$, whereas there was a continuous drop in arsenate adsorption with increasing pH from 3 to 11.	(Raven et al., 1998)
Muscovite/Biotite mica	The amount of As adsorbed increased with increasing pH, exhibiting a maximum value, before decreasing at higher pH values. Biotite provided greater reactivity than muscovite toward As adsorption.	(Chakraborty et al., 2007)
Siderite ($FeCO_3$)	High As retention capacity of a siderite filter arose from coprecipitation of Fe oxides with As and subsequently adsorption of As on the fresh Fe oxides/hydroxides. Arsenic adsorption in the filter from As-spiked tap water was relatively lower than that from artificial As solution because high HCO_3^- concentration restrained siderite	(Guo et al., 2007)

	dissolution and thus suppressed production of the fresh Fe oxides on the siderite grains.	
Coprecipated Aluminium:iron hydroxides	In soils where iron hydroxides often have appreciable Al substitution, arsenite might not be retained to the same extent as that observed with pure iron hydroxides. On the contrary, Al substitution in iron hydroxides might not be a limiting factor for arsenate adsorption although arsenate might be retained less strongly on Al sites than Fe sites.	(Masue et al., 2007)
Humic acids	At all pH values, arsenate was more strongly bound than arsenite. Maximum binding was observed around pH 7, which is consistent with H^+ competition for binding sites at low pH values and OH- competition for the As at high pH. Arsenic had higher affinity to terrestrial humic acid than aquatic humic acid.	(Buschmann et al., 2006)
Zero valent iron	Arsenic removal was dramatically affected by the dissolved oxygen (DO) content and the pH of the solution. Under oxic conditions, arsenate removal by Fe(0) filings was faster than arsenite. The removal of As by Fe(0) was attributed to adsorption by iron hydroxides generated from the oxic corrosion of Fe(0).	(Bang et al., 2005)
Muscovite / Montmorillonite	Arsenate was completely reduced to arsenite on the muscovite surface. For montmorillonite, arsenate was reduced to arsenite on the surface in the presence of ferrous iron in solution.	(Charlet et al., 2005)
Goethite, lepidocrocite, machinawite and pyrite	Arsenic species retained original oxidation states and occupied similar environments on the oxyhydroxide substrates. Inner sphere complexes formed, apparently involving bidentate (bridging) arsenate or arsenite.	(Farquhar et al., 2002)

1.2.4.1 Kinetics of sorption

Kinetic models may describe reaction pathways toward equilibrium and reaction position and times along those pathways (Langmuir, 1997). Observation has shown that the sorption rate of arsenite and arsenate on minerals was initially rapid and was followed by a slow phase (Arai et al., 2004; Arai and Sparks, 2002; Arai et al., 2005; O'Reilly et al., 2001). The rate limiting adsorption steps are generally described as being controlled by slow diffusion to the adsorption sites on the surface. Studies with the aid of EXAFS measurements have provided microscopic evidence of rearrangement

of As surface complexes and surface precipitation during extended exposure time of surfaces to dissolved As. Decreased desorption was observed as initial adsorption time was increased (Arai and Sparks, 2002). Lin and Puls (2000) reported that desorption rate of arsenite and arsenate clay minerals decreased with increasing aging time. They explained this phenomenon with the diffusion of As into internal adsorption sites (absorption) not accessible to the bulk solution. Zhang and Selim (2005) used kinetic batch adsorption/desorption experiments and subsequent sequential extraction to study arsenate in contact with soils and reported desorption was hysteretic in nature indicating lack of equilibrium retention and or irreversible or slowly reversible processes.

Widely used kinetic models for the description of contaminants such as As species include:

1) The dynamic Langmuir kinetic model (Langmuir, 1918) which can be represented as:

$$\frac{dq}{dt} = k_a(C_0 - q_m\Phi)(1-\Phi) - k_d\Phi \qquad \text{Eq. 18}$$

Where q is adsorbate concentration (mol kg^{-1}), t is time (sec) k_a is the first order constant for adsorption, C_0 is the initial solute concentration (mol l^{-1}), q_m is the maximum amount of adsorbate (mol kg^{-1}) (derived from experimental data described in next section), Φ is the fraction of covered surface and k_d is the first order rate constant for desorption.

2). The pseudo-second order model for sorption of metals in soils (Ho and McKay, 1999) which is represented as:

$$\frac{dq_t}{dt} = k\frac{\Theta}{\rho}(q_e - q_t)^2 \qquad \text{Eq. 19}$$

Where q_t is the amount of adsorbate (mol kg^{-1}) at time t (sec), k is the rate constant of sorption (kg sec mol^{-1}), θ is the water content (l l^{-1}), ρ is the soil bulk density (kg l^{-1}), q_e is the amount of soluted As adsorbed at equilibrium (mol kg^{-1}).

3) The multi-reaction model (MRM) (Zhang and Selim, 2005) considers soil heterogeneity and kinetics of adsorption. The model assumes that a fraction of the surface sites are kinetic in nature whereas the remaining fractions react rapidly or instantaneously with solutes in the soil solution. The model accounts for reversible and irreversible sorption (Figure 10) and can be presented in the following formulations:

$$q_e = K_e \frac{\Theta}{\rho} c^n \qquad \text{Eq. 20}$$

$$\frac{dq_k}{dt} = k_1 \frac{\Theta}{\rho} c^n - k_2 q_k \qquad \text{Eq. 21}$$

$$\frac{dq_i}{dt} = k_3 s_k \qquad \text{Eq. 22}$$

Where q_e, q_k and q_i are the amount adsorbed at equilibrium, kinetic and irreversible sites respectively (mol kg^{-1}), K_e is a dimensionless equilibrium constant, k_1 and k_2 (s^{-1}) are forward and backward reaction rates associated with kinetic sites respectively, k3 (s^{-1}) is the irreversible rate coefficient. The continuum between chemisorption and precipitation is controlled by several factors including (i) the ratio of number of sites to the number of ions in solution, (ii) the strength of the metal-oxide bond, and (iii) the degree to which the bulk solution is under-saturated with respect to the metal hydroxide precipitate (Selim and Zhang, 2007). Chemisorption and precipitation are consistent with one or more irreversible reactions in the MRM models.

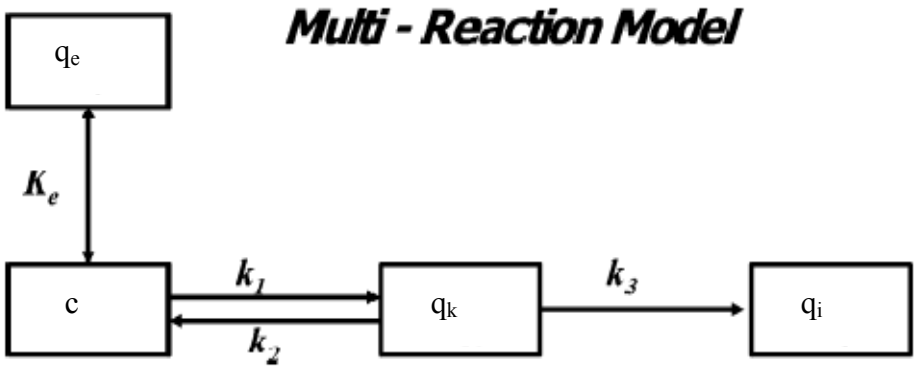

Figure 10 Schematic diagram of the multi reaction model (MRM). Here, C is concentration in solution, q_e, q_k, and q_i are the amounts sorbed on equilibrium, kinetic, and irreversible sites, respectively, where Ke is equilibrium constant and k_1, k_2, and k_3 are the respective rate constants. Modified from Zhang and Selim (2005).

Figure 10 indicates that the irreversible sorption sites are filled consecutively to the kinetic sites, however more recent version of the MRM model (Selim and Zhang, 2007) accounts for more types of reactions where two types of kinetic sites are active and the irreversible retention can either occur consecutively as in the model above where formation of q_s phase is controlled by the concentration of one kinetic site or concurrently where solute is removed directly from solution by e.g. chemisorption, precipitation or immobilisation rather than sorption and is referred to as sink term, q_{irr}

(Figure 11). The extended MRM model (Selim and Zhang, 2007) can be presented by the following formulations:

$$q_e = K_e c^n \qquad \text{Eq. 23} \qquad \text{reversible equilibrium}$$

$$\frac{dq_1}{dt} = k_1 \frac{\Theta}{\rho} c^n - k_2 q_1 \qquad \text{Eq. 24} \qquad \text{reversible kinetic 1}$$

$$\frac{dq_2}{dt} = \left(k_3 \frac{\Theta}{\rho} c^n - k_4 q_2 \right) - k_s q_2 \qquad \text{Eq. 25} \qquad \text{reversible kinetic 2}$$

$$Q = \rho \frac{dq_{irr}}{dt} = k_{irr} \Theta c \qquad \text{Eq. 26} \qquad \text{irreversible concurrent}$$

$$\frac{dq_s}{dt} = k_s q_2 \qquad \text{Eq. 27} \qquad \text{irreversible consecutive}$$

Where c is the solution concentration, q_e, q_1, q_2, are the amounts sorbed at equilibrium, kinetic 1 and 2 sites respectively and q_{irr} and q_s are the amounts sorbed (or precipitated, immobilised) at the concurrent and consecutive irreversible sites respectively, k_1 and k_2 (s^{-1}) are adsorption and desorption coefficients for kinetic site 1, k_3 and k_4 (s^{-1}) are adsorption and desorption coefficients for kinetic site 2, and k_{irr} and k_s (s^{-1}) are rate coefficients for irreversible concurrent and consecutive reactions respectively.

Multi Reaction Model II

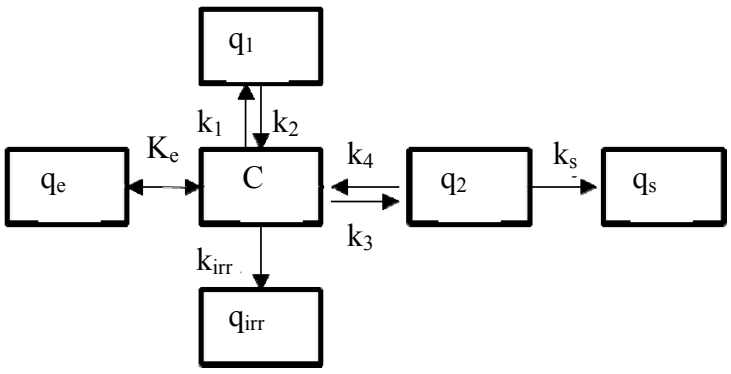

Figure 11 The extended multi reaction model (Selim and Zhang, 2007). Here c is concentration in solution, q_e, q_1, q_2, are the amounts sorbed at equilibrium, kinetic 1 and 2 sites respectively and q_{irr} and q_s are the amounts sorbed (or precipitated, immobilised) at the concurrent and consecutive irreversible sites respectively, k_3 and k_4 (s^{-1}) are adsorption and desorption coefficients for kinetic site 2, and k_{irr} and k_s (s^{-1}) are rate coefficients for irreversible concurrent and consecutive reactions respectively.

4) A Second-order model (SOM) (Selim and Zhang, 2007) considers two types of sorption sites, an equilibrium type and a kinetically controlled type. In addition,

maximum adsorption (q_{max}) derived from a Langmuir isotherm is included in the model. q_{max} is assumed to be intrinsic soil property that is time invariant represented as:

$$q_{\max} = q_{e_{\max}} + q_{k_{\max}} \qquad \text{Eq. 28}$$

Where q_{emax} and q_{kmax} are the adsorption maxima for equilibrium and kinetic type sites respectively. If f represents fraction of equilibrium type sites to the total sites we have:

$$q_{e_{\max}} = fq_{\max} \; and \; q_{k_{\max}} = (1-f)q_{\max} \qquad \text{Eq. 29}$$

Assuming Φ_e and Φ_k as the vacant available sites for adsorption at equilibrium and kinetic sites (q_e and q_k) we have:

$$\begin{aligned} \Phi e &= q_{e_{\max}} - q_e = fq_{\max} - q_e \; and \\ \Phi e &= q_{k_{\max}} - q_k = (1-f)q_{\max} - q_k \end{aligned} \qquad \text{Eq. 30}$$

As the vacant sites become filled or occupied by the retained solute, the amount of vacant sites approaches zero, and the amount of retained by the soil matrix approaches the sorption maxima. Selim and Amacher (1988) assumed q_{max} was not partitioned between q_e and q_k, instead they assumed vacant sites were available both for q_e and q_k. Therefore, the amount of solute adsorbed on each type of sites is only determined by the associated rate coefficients and the total vacant sites. In the second order model following the same overall a structure as the extended MRM model (Figure 11) the governing retention reactions can be expressed as (Selim and Ma, 2001):

$$q_e = K_e \Theta c \Phi \qquad \text{Eq. 31 reversible equilibrium}$$

$$\frac{dq_1}{dt} = k_1 \Theta c \Phi - k_2 q_1 \qquad \text{Eq. 32 reversible kinetic 1}$$

$$\frac{dq_2}{dt} = \left(k_3 \Theta c \Phi - k_4 q_2\right) - k_s q_2 \qquad \text{Eq. 33 reversible kinetic 2}$$

$$\frac{dq_{irr}}{dt} = k_{irr} \Theta c \qquad \text{Eq. 34 irreversible concurrent}$$

$$\frac{dq_s}{dt} = k_s c_2 \qquad \text{Eq. 35 irreversible consecutive}$$

All the models described above can be applied to empirical data but do not necessarily provide mechanistic information on the reactions involved without being verified by spectroscopic methods.

1.2.4.2 Empirical equilibrium sorption isotherms

On the contrary to kinetic models, sorption isotherms describe equilibrium state between solute and sorption concentrations of a compound but do not explain the reaction steps involved to acquire this equilibrium.

Giles et al. (1974) proposed a general modeling of sorption isotherms of which 4 particular cases are now used as the 4 main shapes of isotherms commonly observed (Figure 12). These isotherms were reviewed by Limousin et al. (2007).

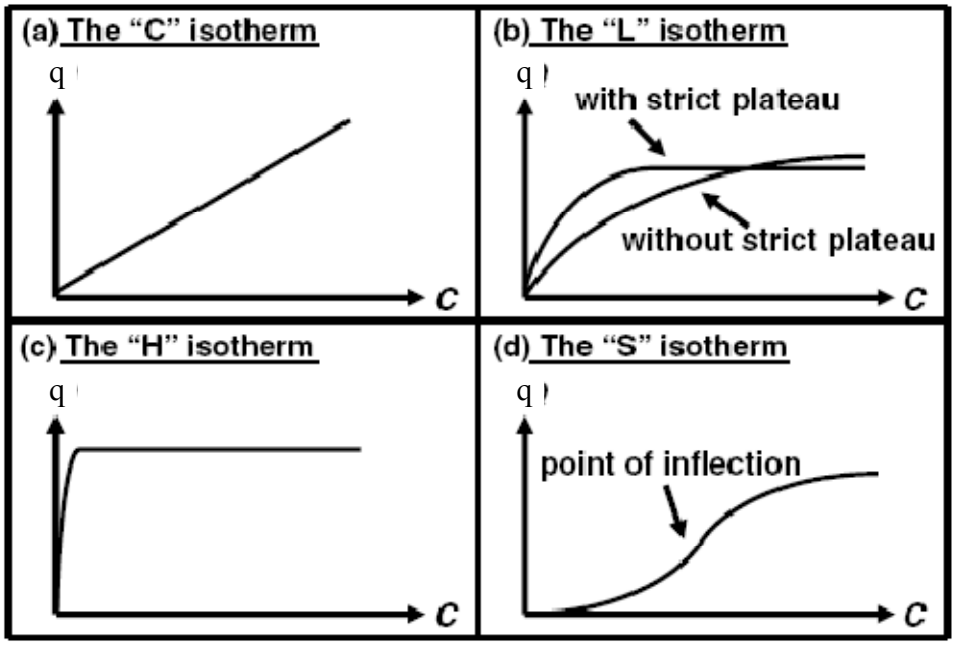

Figure 12 The four main types of adsorption isotherms (Giles et al., 1974). q is the sorbed concentration and C is the solute concentration.

The "C" isotherm is a line of zero-origin (Figure 12). This means the relation between solute, C and sorbed concentration, q independent of concentration. This ratio is usually called partition coefficient of K_d (l kg^{-1}). The "C" isotherm serves as an approximation rather than accurate description of solute/sorbate relationships and is usually only observed at very narrow range or at very low concentrations.

The "L" isotherm (Figure 12) suggests a progressive saturation of the solid. The ratio between the concentration of solute remaining in solution and adsorbed on the surface decreases providing a concave curve. The curve can either reach a strict plateau when the solid has limited sorption capacity or the curve does not reach any plateau. It is often difficult to distinguish between the two types.

The "H" isotherm is a particular case of "L" isotherm where the initial slope is very steep. This case was distinguished from the others because a compound sometimes

exhibits such a high affinity for the solid that the initial slope cannot be distinguished from infinity, even if it does not make sense from thermodynamic point of view (Tóth, 1994).

The "S" isotherm is sigmoidal and thus is always a result of two opposite mechanisms. The presence of soluble ligand can provide sigmoidal isotherm for metallic species. At low metal concentrations adsorption is limited by the presence of the ligand. As the ligand is saturated the adsorption proceeds naturally (Sposito, 1984).

Isotherm models by definition, assume chemical equilibrium between solute and sorbed concentrations.

Two sorption isotherms are the most widely used to describe the relationship between concentration of soluted and sorbed chemicals at equilibrium, the Freundlich and Langmuir isotherm (Langmuir, 1918). Both describe the "L" type isotherms. A sorption isotherm is a common approach, describes common sorption phenomena and predicts mobility of sorbing substances in the environment. However, it does not provide any mechanistic information on the reactions involved in the overall sorption process. Verification of thermodynamic equilibrium is important for accurate prediction with sorption isotherms, otherwise kinetic aspects have to be taken into account.

The Freundlich isotherm has the form of :

$$q = K_F c^n \qquad \text{Eq. 36}$$

where q and c are the sorbed and solute concentrations of chemical at equilibrium respectively, K_F and n are adjustable coefficients. If n is 1 the Freundlich is simply a "C" isotherm and the K_F can be considered a K_d. With the Freundlich equation, sorption extends indefinitely as concentration increases which is unrealistic since the surface is bound to become saturated at some point as solute concentration is increased.

The Langmuir Isotherm can be derived from the law of mass action for a sorption reaction:

$$q + I \leftrightarrow q_I \qquad \text{Eq. 37}$$

$$\text{with } K_{s_I} = \frac{[q_I]}{[q][I]} \qquad \text{Eq. 38}$$

With the mass balance for sorption sites:

$$q + q_I \leftrightarrow q_{total} \qquad \text{Eq. 39}$$

the law of mass action gives:

$$q_I = \frac{q_{\max} K_L c_I}{1 + K_L c_I} \qquad \text{Eq. 40}$$

Where q_{max} is maximum sorbed concentration corresponding to a monolayer at the surface, K_L is the Langmuir constant related to energy of sorption. It can be derived from the Langmuir eq. that q_I increases linearly with c_I if $c_I << K_L$. However, as c_I becomes very high and $c_I >> K_L$ the surface becomes saturated and $q_I = q_{total}$.

The Langmuir can be modified for multisite or competitive sorption. The q_{max} remains available for all species which are on the one hand either competing for the sorption sites and on the other hand show different affinities for the sorption sites and have therefore varying affinity coefficients (K_L). The competitive Langmuir model can be presented as (Murali and Aylmore, 1983):

$$q_I = \frac{q_{\max} K_{L_i} c_i}{1 + \sum_{j=1}^{q} K_{L_j} c_j} \qquad \text{Eq. 41}$$

When the competitive phenomenon between species is ion exchange, Limousin et al. (2007) recommended construction of isotherms on the basis of ion exchange approach rather than on Langmuir isotherm. A Langmuir isotherm where multiple sorption sites are active can be considered as the sum of intrinsic Langmuir isotherms each representing the isotherm for the respective sorption site (Limousin et al., 2007).

1.2.4.3 Ion exchange isotherms

When concentration of a studied ion is studied at low concentration compared to other competing ions the bulk can be considered as a constant and a single species Langmuir isotherm applied. However once the ion in question reaches the same order of magnitude as the bulk solution, the bulk solution cannot longer be considered a constant and a multispecies isotherm is needed. An ion exchange isotherm does not describe the relationship between q and c but rather the molar fraction of charges of ion adsorbed on the solid versus molar fraction of charges of the ion remaining in solution. It is assumed that the number of adsorption sites is constant and is called the "intrinsic charge" of the solid. The exchange isotherm essentially describes cation (anion) exchange capacity of a soil. The exchange capacity is strongly dependent on the measuring conditions such as pH and ionic strength.

1.2.4.4 Mechanistic isotherms by surface complexation models

A variety of models have been proposed to describe surface complex formation such as; The diffuse double layer model (DDLM) (Dzombak and Morel, 1990), the constant capacitance model (CCM), basic Stern model (BSM) and the triple layer model (TLM) (Langmuir, 1997). A review of the physical bases of surface complexation models is provided by Goldberg (1992).

Hydrous oxide surfaces with variable charge can be considered as >SOH (where >S signifies any –OH binding atom at the surface) (Sahai and Sverjensky, 1997b) which can either accept proton represented by the reaction:

$$> SOH + H^{+}_{(aq)} \leftrightarrow > SOH^{+}_{2} \qquad \text{Eq. 42}$$

associated with the intrinsic equilibrium constant $K_{S,1}$ or donate proton to the solution represented by the reaction:

$$> SOH \leftrightarrow > SO^{-} + H^{+}_{(aq)} \qquad \text{Eq. 43}$$

associated with the intrinsic equilibrium constant $K_{S,2}$. The equilibrium constants $K_{S,1}$ and $K_{S,2}$ differ between the respective surfaces and consequently their zero point of charge lie at varying pH. The main mechanism of ligand adsorption (like the arsenite and arsenate primarily form in solution) is ligand exchange when the surface hydroxyl is exchanged by another ligand (Stumm and Morgan 1996). The overall adsorption constant on hydrous oxide can be represented as:

$$K_{ads} = K_{\text{int}} \times e^{(-\Delta Z \Psi F / RT)} \qquad \text{Eq. 44}$$

Where K_{int} is the intrinsic adsorption constant representing a chemical component of adsorption and the expression in brackets called the electrostatic (Boltzman) term, accounts for the electrostatic component of adsorption with ΔZ is the change in surface charge due to adsorption, Ψ is the surface potential, F is the Faraday constant, R is the universal gas constant and T is temperature in Kelvin. The extent of surface complex formation is strongly pH dependent (due to pH dependence of the surface potential, Ψ) and since the adsorption is coupled with a release of OH^- ions, adsorption is favoured at low pH.

A sorption isotherm based on mechanistic approach involves reaction of the chemical with a surface and measuring the surface complex formed by spectroscopic methods. This has the advantage over methods when the adsorbed amount is either estimated by measuring the difference of initial and final concentration of chemical in solution. Surface complexation modeling further allows quantitative description and

modeling of competing ions. However, spectroscopic approaches rely on sophisticated and expensive experimental apparatus which are not as widely accessible as instruments for solution chemistry.

The surface complexation modeling is complicated by complex mineral assemblages on surface of adsorbents. Two principal modeling approaches can be used in that case (Davis et al., 1998). In the general composite (GC) approach, it is assumed the surface mineral assemblage is too complex to be characterised properly. The surface is treated as "generic" surface groups in equilibrium with water and formation constants derived from experimental data at different pH values. In the component additivity approach (CA), it is assumed that a surface is composed by a mixture of mineral assemblages of which properties are known from studies of the individual components. The adsorption is then predicted by the sum of contribution from each component on adsorption.

1.2.4.5 Experimental methods to derive kinetic and isotherm coefficients

The information contained in a sorption isotherm depends on the experimental conditions of which it was obtained. Therefore, a brief description of the experimental conditions should always be provided with the data (Schweich and Sardin, 1981).

The shape of an isotherm usually does not change if the solid/solution ratio is within the same order of magnitude. However adsorption has been shown to be nonlinearly dependent on solid/solution ratio (e.g. Bajracharya et al., 1996). Adsorption is often observed to decrease with the solid concentration and has been attributed to: (i) the occupied volume of the solid particles (Celorie et al., 1989); and (ii) their aggregation (Voice et al., 1983) that would prevent the optimal adsorption of the solutes. The optimal experimental solid/solution ratio should represent natural conditions. The choice of an adequate solid/solution ratio consists of finding a good intermediate between experimental constraints and representative conditions. Batch experiments should be carried out when solid/solution ratio is sufficiently low (lower than 1:2) for solids to be suspended in the water. Soils frequently have the solid/solution ratio of 1:1 and aquifers solid/solution ratio 3:1 and column experiments may be the most suitable procedure to for deriving sorption isotherms

Closed batch experiments are the easiest to conduct. A solid is shaken in solution until sorption equilibrium is reached, then the remaining solute concentration is measured. In batch experiments, the solid/solution ratio is frequently either too high to represent rivers, lakes and oceans, or to low compared to natural porous media such as soils and aquifers. The closed batch method is therefore considered as a very useful preliminary experiment but extrapolation to porous media requires further investigations (Limousin et al., 2007).

Open batch experiments involve injecting a blank solution into the inlet of a reactor, then the reactive solute is injected into the reactor. The outlet of the experiment can then be either discarded (provided new injection solution is continuously injected) or re-injected into the column. The flow rate can be adjusted so the mean residence time of water in the reactor is either lower, similar or higher than the mean reaction time. This method therefore allows easier kinetic investigations than for closed batch where a series of experiments occurring over varying timescales have to be carried out to provide similar kinetic data.

Repacked column experiments involve packing the solid material into a column and pumping a solution containing the reactive chemical through the column. The method is an open flow method and allows study of the chemical kinetics of adsorption and desorption can be studied with more ease than with the batch method (Sparks and Rechcigl, 1982).

The solid/solution ratio of repacked columns is representative of natural porous media. The main disadvantage of the column method is that the system is not perfectly mixed and the reactive compound is dispersed by the medium. Therefore, a comparison with an inert tracer is unavoidable to distinguish chemical reactions from hydrological factors.

1.3 Geochemical modeling of As transport

The transport of a As (or any other contaminant) can be described with the Advection-Reaction-Dispersion (ARD) eq. and, if necessary, with the addition of a diffusion term. This eq. can be incorporated into geochemical models provided enough information is available for describing the transport sufficiently and is represented as:

$$\frac{\partial c}{\partial t} = -v\frac{\partial c}{\partial x} - \frac{\partial q}{\partial t} + D_L \frac{\partial^2 c}{\partial x^2} \qquad \text{Eq. 45}$$

Where the left hand term describes the difference in chemical concentration with time and is dependent on three terms, the first describing Advective flow, the second representing all chemical Reactions and the third indicating Dispersion. These terms will now be discussed further.

1.3.1 **Advection**

Advection of a solute takes place as a result of groundwater flow, being either unsaturated or saturated. Water in the unsaturated zone percolates vertically downwards along the maximal gradient of the soil moisture potential (Appelo and Postma, 2005). The process is driven by infiltrating water that pushes the old water ahead. The rate of percolation can be derived from mass balance dividing the precipitation surplus by the water filled porosity of the soil (Allison et al., 1994). Once the water enters the groundwater table the pore space is saturated and the flow is dependent of the hydraulic gradient and hydraulic conductivity of the aquifer or soil according to Darcy's law:

$$v_D = -kdh/dx \qquad \text{Eq. 46}$$

Where v_D is the Darcy velocity, k is the hydraulic conductivity, dh/dx is the hydraulic gradient (can also be expressed as difference in water potential between two connected sites in the aquifer).

1.3.2 **Reaction**

Geochemical modeling can be divided into two principal categories: (i) forward modeling and (ii) inverse modeling. Forward modeling is used to predict water chemistry after completion of predetermined reactions. Inverse modeling is used to suggest which processes might take place along a flow path. Inverse modeling is not the subject of this thesis and will not be dealt with further here. Coupled transport and geochemical models are needed to carry out modeling of transport of reactive species in the groundwater environments. Chemical reactions of soluble As with the solid phase can be modelled as series of adsorption/desorption reactions which obey predetermined kinetic expressions and isotherms based on empirical data where As is either measured in remaining solution (non mechanistic) or surface complexes are measured by spectroscopy (mechanistic models). The surface reactions can, furthermore, be a

combination of dissolution and precipitation reactions. In any case, a firm knowledge of the possible reactions should be preferably established for reliable prediction of As transport in the environment. Forward modeling of As should be able to incorporate the effect of different solid/solution ratios, adsorption site densities, pH changes and competition with other species for sorption sites. Surface complexation models can often accommodate such variation in conditions whereas adsorption isotherms are applicable under narrow range of pH water chemistry conditions (Sracek et al., 2004). A partial solution to this constraint of adsorption isotherms might be to carry out adsorption experiments for a wide variety of conditions and interpolate any coefficients applicable between each two sets of conditions. Geochemical modeling can either assume equilibrium, that is, geochemical reactions are very fast compared to groundwater residence time or that reactions proceed according to kinetic laws (Sracek et al., 2004).

Equilibrium models have to take the speciation of solutions into account. The stability of the phases in solution depends on the speciation of solution. The model however does not take into account how or if they will occur. Furthermore uncertainties in thermodynamic data for the speciation and formation of phases from solution is well documented (e.g. Cleverley et al., 2003). The model may be described in its simplest form by the reaction:

$$inital\ water + reacting\ phases \leftrightarrow predicted\ water + product\ phases \qquad \text{Eq. 47}$$

During each small step the program transfers a small amount of mass from reactants to products. Then the program calculates mass distribution between the products and calculates their saturation indices. Pre-determined phases, to which the water is supersaturated, are allowed to precipitate. The reaction steps are then repeated until equilibrium is attained.

Kinetic models are carried out by programming the kinetic expression into the model reactions allowed to proceed for a predetermined amount of time before a transport step is carried out. An example of such procedure may be found in the methods chapter 2.2.5.2.

1.3.3 **Diffusion**

Molecular diffusion occurs as a result in concentration difference between two points where molecules will flow from high to low concentration zones by random Brownian

movement of molecules according to Fick's laws. Fick's first law relates the flux of a chemical to the concentration gradient:

$$F = -D\frac{\partial c}{\partial x} \qquad \text{Eq. 48}$$

Where F is the flux (mol s^{-1} m^{-2}), D is the diffusion coefficient (m^2 s^{-1}), c is the concentration (mol m^{-3}) and x is the distance (m) between two zones. Fick's second law of diffusion may be represented as:

$$\frac{\partial c}{\partial t} = D\frac{\partial^2 c}{\partial x^2} \qquad \text{Eq. 49}$$

and describes difference in concentration at a given point with time and can therefore be incorporated directly into the ARD equation (eq. 45) (Appelo and Postma, 2005).

Differences in mobility of ions are a function of the friction they experience travelling through water and are related to the ion-size and viscosity. Overall differences in diffusion coefficients for ions in simple electrolytes are small and can be estimated as $D \approx 10^{-9}$ m^2 s^{-1} at 25°C (Appelo and Postma, 2005). Therefore, when advective flow is significant, the diffusion can be omitted from modeling calculations leading to lower processor demand. In clay dominated soils and peat when advective flow is sufficiently slow, diffusion can be the primary mechanism of groundwater flow.

1.3.4 **Dispersion**

Groundwater flowing through an aquifer is forced to move around sediment grains. The resulting spreading of a concentration front is called dispersion. Dispersion can either be longitudinal due to differences in travel times along flow lines and increases with increasing flow velocity or transverse when a chemical is carried to adjacent flow line by diffusion. Dispersion is described mathematically according to Fick's law like diffusion.

1.4 Thesis aims

Chemical pollution, and particularly the interaction of one particular constituent of this pollution, arsenic (As), with basaltic glass, a common aquifer constituent in geothermal areas, is the main research theme of this thesis. The interaction of As and basaltic glass will be measured and modelled by a series of laboratory experiments followed by sampling and measurements of geothermal wastewaters from the Nesjavellir geothermal

power plant, Iceland. Furthermore, the fate of As originating from a volcanic eruption will be studied.

Continental flood basalts cover an important fraction of the terrestrial surface (Jerram and Widdowson, 2005). Arsenic concentration in terrestrial basaltic rocks ranges from 0.18 to 113 mg kg^{-1}, with an average concentration of 2.3 mg kg^{-1} (Smedley and Kinniburgh, 2002). Examples include the Columbian river basalts in the US, the Deccan traps in India and the Siberian traps in Russia. Furthermore, the ocean floor is primarily composed of basalt (Ronov and Yaroshevsky, 1976). Geothermal activity is frequently associated with basalt that can either be glassy or crystalline in volcanic terrains (Mottl and Holland, 1978). Knowledge of As movement in basaltic environments, therefore, plays a key role in quantifying the global As cycle. Since Iceland is mainly composed of basaltic rocks where active seafloor spreading coincides with the occurrence of upwelling mantle plume resulting in intense volcanism (Schilling 1973), it constitutes a prime study area for understanding the role and movement of As in the environment. This geological situation leads to the widespread occurrence of high-temperature geothermal systems, some of which are currently utilized for power generation (Armannsson et al., 2005). Hydrothermal fluids, often As enriched (Wetang'ula and Snorrason, 2005), are pumped to the surface, where heat is extracted and electricity generated before these fluids are either pumped back into the crust through boreholes or released to adjacent surroundings. The subsequent fate of As in geothermal waters raised to the surface is not fully known and there is concern that As may be mobile in groundwater systems where basalt and basaltic glass are the main rock constituents (Arnorsson, 2003).

Aqueous and gaseous As in volcanic terrain can reach very elevated levels although the amount and partition of the As is highly dependent on the host magma and rocks. Although As levels in geothermal systems are generally low in basaltic environments, these basalts cover extensive proportion of the earth's crust and can as a consequence play an important role as source of As to the surface environment. The aims of this thesis are:

- To provide an overview of the mobility of arsenite, As(III) and arsenate, As(V) oxyanions in contact with basaltic glass surfaces by carrying out laboratory experiments under controlled pH, Eh and ionic strength conditions.

- To use the coefficients generated to predict As transport where high temperature geothermal water is released into the natural environment.
- Quantify the percentage of thioarsenates in high temperature geothermal water and estimate the effect of thioarsenate complexation on the mobility.
- To combine experimental and field results to describe As cycling in a glacial outburst flood (jökulhlaup) following a sub glacial basaltic eruption.

1.5 References

Aiuppa, A., Federico, C., Allard, P., Gurrieri, S. & Valenza, M. 2005, "Trace metal modeling of groundwater–gas–rock interactions in a volcanic aquifer: Mount Vesuvius, Southern Italy", *Chemical Geology,* vol. 216, no. 3-4, pp. 289-311.

Alfredsson, H.A., Hardarson, B.S. & Franzson, H. 2007, *Hola HK-31 Þrengslum, Hellisheiði - Jarðlög ummyndun og lekt (Hole HK-31, Þrengsli, Hellisheiði - Bedrock alteration and permeability)*, ÍSOR, Reykjavik.

Allison, G.B., Gee, G.W. & Tyler, S.W. 1994, "Vadose-zone techniques for estimating groundwater recharge in arid and semiarid regions.", *Soil Science Society of America Journal,* vol. 58, pp. 6-14.

Andreae, M.O. 1979, "Arsenic speciation in seawater in interstitial waters: the influence of biological-chemical interactions on the chemistry of a trace element", *Limnology and Oceanography,* vol. 24, pp. 440-452.

Appelo, C.A.J. & Postma, D. 2005, *Geochemistry, groundwater and pollution,* Second edn., A.A. Balkema publishers, Leiden, The Netherlands.

Arai, Y., Elzinga, E.J. & Sparks, D.L. 2001, "X-ray absorption spectroscopic investigation of arsenite and arsenate adsorption at the aluminum oxide-water interface", *Journal of colloid and interface science,* vol. 235, no. 1, pp. 80-88.

Arai, Y. & Sparks, D.L. 2002, "Residence time effects on arsenate surface speciation at the aluminum oxide-water interface", *Soil Science,* vol. 167, no. 5, pp. 303-314.

Arai, Y., Sparks, D.L. & Davis, J.A. 2005, "Arsenate adsorption mechanisms at the allophane - water interface", *Environmental science & technology,* vol. 39, no. 8, pp. 2537-2544.

Arai, Y., Sparks, D.L. & Davis, J.A. 2004, "Effects of dissolved carbonate on arsenate adsorption and surface speciation at the hematite-water interface", *Environmental science & technology,* vol. 38, no. 3, pp. 817-824.

Armannsson, H., Fridriksson, T. & Kristjansson, B.R. 2005, "CO2 emissions from geothermal power plants and natural geothermal activity in Iceland", *Geothermics*, vol. 34, pp. 286-296.

Arnorsson, S., Bjarnason, J.Ö., Giroud, N., Gunnarsson, I. & Stefansson, A. 2006, "Sampling and analysis of geothermal fluids", *Geofluids,* vol. 6, pp. 203-216.

Arnorsson, S., Eliasson, J. & Gudmundsson, B.T. 1999, *40 MW geothermal power plant at Námafjall. Assessment of environmental impact on groundwater and natural thermal manifestations*, Science Institute, University of Iceland, Reykjavik.

Arnorsson, S. 2003, "Arsenic in surface- and up to 90 degrees C ground waters in a basalt area, N-Iceland: processes controlling its mobility", *Applied Geochemistry,* vol. 18, no. 9, pp. 1297-1312.

Baas-Becking, L.G.M., Kaplan, I.R. & Moore, D. 1960, "Limits of the natural environment in terms of pH and oxydation-reduction potentials", *Journal of Geology,* vol. 68, pp. 243-284.

Bajracharya, K., Tran, Y.T. & Barry, D.A. 1996, "Cadmium adsorption at different pore water velocities", *Geoderma,* vol. 73, no. 3-4, pp. 197-216.

Bang, S., Johnson, M.D., Korfiatis, G.P. & Meng, X.G. 2005, "Chemical reactions between arsenic and zero-valent iron in water", *Water research,* vol. 39, no. 5, pp. 763-770.

Bang, S., Korfiatis, G.P. & Meng, X.G. 2005, "Removal of arsenic from water by zero-valent iron", *Journal of hazardous materials,* vol. 121, no. 1-3, pp. 61-67.

Batiza, R. & White, J.D.L. 2000, "Submarine lavas and hyaloclastite" in *Encylcopedia of volcanoes,* ed. Sigurdsson, H., Houghton, B., McNutt, S.R. & Stix, J., Academic Press, New York, pp. 361-381.

Batley, G.E. 1989, "Collection, preparation, and storage of samples for speciation analysis" in *Trace element speciation: Analytical Methods and problems*, ed. G.E. Batley, CRC Press, Boca Raton, pp. 1-24.

Bauer, W.H. & Onishi, H. 1978, "Arsenic" in *Handbook of Geochemistry*, ed. K.H. Wedepohl, Springer-Verlag, New York.

Beak, D.G., Wilkin, R.T., Ford, R.G. & Kelly, S.D. 2008, "Examination of arsenic speciation in sulfidic solutions using X-ray absorption spectroscopy", *Environmental science & technology,* vol. 42, no. 5, pp. 1643-1650.

B'Hymer, C. & Caruso, J.A. 2004, "Arsenic and its speciation analysis using high-performance liquid chromatography and inductively coupled plasma mass spectrometry", *Journal of Chromatography a,* vol. 1045, no. 1-2, pp. 1-13.

Biterna, M., Arditsoglou, A., Tsikouras, E. & Voutsa, D. 2007, "Arsenate removal by zero valent iron: Batch and column tests", *Journal of Hazardous Materials,* vol. 149, no. 3, pp. 548-552.

Brisbin, J.A., B'Hymer, C. & Caruso, J.A. 2002, "A gradient anion exchange chromatographic method for the speciation of arsenic in lobster tissue extracts", *Talanta,* vol. 58, no. 1, pp. 133-145.

Brookins, D.G. 1986, "Geochemical behavior of antimony, arsenic, cadmium and thallium: Eh ▪ pH diagrams for 25°C, 1-bar pressure", *Chemical Geology,* vol. 54, no. 3-4, pp. 271-278.

Buschmann, J., Kappeler, A., Lindauer, U., Kistler, D., Berg, M. & Sigg, L. 2006, "Arsenite and arsenate binding to dissolved humic acids: Influence of pH, type of humic acid, and aluminum", *Environmental science & technology,* vol. 40, no. 19, pp. 6015-6020.

Canfield, D.E., Olesen, C.A. & Cox, R.P. 2006, "Temperature and its control of isotope fractionation by a sulfate-reducing bacterium", *Geochimica et Cosmochimica Acta,* vol. 70, no. 3, pp. 548-561.

CCME 1995, "Protocol for the derivation of Canadian sediment quality guidelines for the protection of aquatic life", CCME EPC-98-E, Canadian Council of Ministers, Winnipeg.

Celorie, J.A., Woods, S.L., Vinson, T.S. & Istok, J.D. 1989, "A Comparison of Sorption Equilibrium Distribution Coefficients using Batch and Centrifugation Methods", *Journal of environmental quality,* vol. 18, no. 3, pp. 307-313.

Chakraborty, S., Wolthers, M., Chatterjee, D. & Charlet, L. 2007, "Adsorption of arsenite and arsenate onto muscovite and biotite mica", *Journal of colloid and interface science,* vol. 309, no. 2, pp. 392-401.

Chapin, R.M. 1914, "The reduction of arsenic acid to arsenious acid by thiosulfuric acid", *Journal of Agricultural Research,* vol. 1, pp. 515-517.

Charlet, L., Chakraborty, S., Varma, S., Tournassat, C., Wolthers, M., Chatterjee, D. & Ross, G.R. 2005, "Adsorption and heterogeneous reduction of arsenic at the phyllosilicate-water interface", *Advances in Arsenic Research,* vol. 915, pp. 41-+.

Charlet, L. & Polya, D.A. 2006, "Arsenic in shallow, reducing groundwaters in southern Asia: An environmental health disaster", *Elements,* vol. 2, no. 2, pp. 91-96.

Chen, H.W., Brindle, I.D. & Le, X.C. 1992, "Prereduction of Arsenic(v) to Arsenic(iii), Enhancement of the Signal, and Reduction of Interferences by L-Cysteine in the Determination of Arsenic by Hydride Generation", *Analytical Chemistry,* vol. 64, no. 6, pp. 667-672.

Cherry, J.A., Shaikh, A.U., Tallman, D.E. & Nicholson, R.V. 1979, "Arsenic Species as an Indicator of Redox Conditions in Groundwater", *Journal of Hydrology,* vol. 43, no. 1-4, pp. 373-392.

Cleverley, J.S., Benning, L.G. & Mountain, B.W. 2003, "Reaction path modelling in the As–S system: a case study for geothermal As transport", *Applied Geochemistry,* vol. 18, no. 9, pp. 1325-1345.

Corbisier, P., Ji, G., Nuyts, G., Mergeay, M. & Silver, S. 1993, "luxAB gene fusions with the arsenic and cadmium resistance operons of Staphylococcus aureus plasmid pI258", *FEMS Microbiology Letters,* vol. 110, no. 2, pp. 231-238.

Cotton, F.A. & Wilkinson, G. 1988, *Advanced inorganic chemistry, 5th edition,* John Wiley & Sons, New York.

Cox, K.G., Bell, J.D. & Pankhurst, R.J. *The interpretation of igneous rocks,* 6th edn., Cambridge University Press, Cambridge.

Dasgupta, P.K., Huang, H., Zhang, G. & Cobb, G.P. 2002, "Photometric measurement of trace As(III) and As(V) in drinking water", *Talanta,* vol. 58, no. 1, pp. 153-164.

Davis, A., Bellehumeur, T., Hunter, P., Hanna, B., Fennemore, G.G., Moomaw, C. & Schoen, S. 2006, "The nexus between groundwater modeling, pit lake chemogenesis and ecological risk from arsenic in the Getchell Main Pit, Nevada, USA", *Chemical Geology,* vol. 228, no. 1-3, pp. 175-196.

Davis, J.A., Coston, J.A., Kent, D.B. & Fuller, C.C. 1998, "Application of the surface complexation concept to complex mineral assemblages", *Environmental science & technology,* vol. 32, no. 19, pp. 2820-2828.

Debusschere, L., Demesmay, C. & Rocca, J.L. 2000, "Arsenic speciation by coupling capillary zone electrophoresis with mass spectrometry", *Chromatographia,* vol. 51, no. 5-6, pp. 262-268.

Ding, H., Wang, J.S., Dorsey, J.G. & Caruso, J.A. 1995, "Arsenic Speciation by Micellar Liquid-Chromatography with Inductively-Coupled Plasma-Mass Spectrometric Detection", *Journal of Chromatography a,* vol. 694, no. 2, pp. 425-431.

Dixit, S. & Hering, J.G. 2006, "Sorption of Fe(II) and As(III) on goethite in single- and dual-sorbate systems", *Chemical Geology,* vol. 228, no. 1-3, pp. 6-15.

Dzombak, D.A. & Morel, F.M.M. 1990, *Surface Complexation Modeling: Hydrous Ferric Oxide,* Wiley-Interscience.

Einarsson, P. 2008, "Plate boundaries, rifts and transforms in Iceland", *Jökull,* vol. 58, pp. 35-58.

Eiriksson, J. 2008, "Glaciation events in the Pliocene - Pleistocene volcanic succession of Iceland", *Jökull,* vol. 58, pp. 315-329.

Emett, M.T. & Khoe, G.H. 2001, "Photochemical oxidation of arsenic by oxygen and iron in acidic solutions", *Water Research,* vol. 35, pp. 649-656.

Ernst, R.E. & Buchan, K.L. 2003, "Recognizing Mantle Plumes in the Geological Record", *Annual Review of Earth & Planetary Sciences,* vol. 31, no. 1, pp. 469.

Farquhar, M.L., Charnock, J.M., Livens, F.R. & Vaughan, D.J. 2002, "Mechanisms of arsenic uptake from aqueous solution by interaction with goethite, lepidocrocite, mackinawite, and pyrite: An X-ray absorption spectroscopy study", *Environmental science & technology,* vol. 36, no. 8, pp. 1757-1762.

Feeney, R. & Kounaves, S.P. 2002, "Voltammetric measurement of arsenic in natural waters", *Talanta,* vol. 58, no. 1, pp. 23-31.

Ferguson, J.F. & Gavis, J. 1972, "A review of the arsenic cycle in natural waters", *Water Research,* vol. 6, no. 11, pp. 1259-1274.

Ficklin, W.H. 1983, "Separation of Arsenic(iii) and Arsenic(v) in Ground Waters by Ion-Exchange", *Talanta,* vol. 30, no. 5, pp. 371-373.

Fischer, R. V. & Schmincke, H.-U. 1984. *Pyroclastic rocks.* Springer Verlag, Berlin, 472 pp.

Flaathen, T.K. & Gislason, S.R. 2007, "The effect of volcanic eruptions on the chemistry of surface waters: The 1991 and 2000 eruptions of Mt. Hekla, Iceland", *Journal of Volcanology and Geothermal Research,* vol. 164, no. 4, pp. 293-316.

Flaathen, T.K., Gislason, S.R., Oelkers, E.H. & Sveinbjornsdottir, A.E. 2009, "Chemical evolution of the Mt. Hekla, Iceland, groundwaters: A natural analogue fro CO_2 sequestration in basaltic rocks" *Applied Geochemistry* vol. 24. No. 3, pp. 463-474

Flynn, H.C., McMahon, V., Diaz, G.C., Demergasso, C.S., Corbisier, P., Meharg, A.A. & Paton, G.I. 2002, "Assessment of bioavailable arsenic and copper in soils and sediments from the Antofagasta region of northern Chile", *Science of the Total Environment,* vol. 286, no. 1-3, pp. 51-59.

Freeman, M.C., Aggett, J. & O'Brien, G. 1986, "Microbial transformations of arsenic in Lake Ohakuri, New Zealand", *Water Research,* vol. 20, pp. 283-294.

Gallagher, P.A., Schewel, C.A., Wei, X. & Creed, J.T. 2001, "Speciation and preservation of inorganic arsenic in drinking water sources using EDTA with IC separation and ICP-MS detection", *Journal of Environmental Monitoring*, vol. 3, no.4, pp. 371-376.

Giles, C.H., Smith, D. & Huitson, A. 1974, "A general treatment and classification of the adsorption isotherm. I. Theoritical", *Journal of colloid and interface science,* vol. 47, pp. 755-765.

Giroud, N. 2008, *A chemical study of arsenic, boron and gases in high-temperature geothermal fluids in Iceland*, University of Iceland, Faculty of Science.

Gislason, S.R., Eiriksdottir, E.S., Stefansdottir, M.B. & Stefansson, A. 1999, *Vatnsrannsóknir í nágrenni iðnaðarsvæðisins á Grundartanga. Lokaskýrsla 15. júlí 1999*, Prepared for Norðurál HF and Íslenska Járnblendifélagið HF.

Gislason, S.R., Snorrason, A., Eiriksdottir, E.S., Sigfusson, B., Elefsen, S.O., Hardardottir, J., Gunnarsson, A., Hreinsson, E.O. & Torssander, P. 2004, *Efnasamsetning, rennsli og aurburður straumvatna á Suðurlandi, VIII (Chemical composition, discharge and suspended materials of rivers in South Iceland, VIII)*, Science Institute, University of Iceland, Reykjavik (in Icelandic).

Gislason, S.R., Eiriksdottir, E.S., Sigfusson, B., Elefsen, S.O. & Hardardottir, J. 2004, *Efnasamsetning og rennsli Skaftár; í septemberhlaupi 2002, sumarrennsli 2003 og í septemberhlaupi 2003 (Chemical composition and discharge of River Skaftá during two Jökulhlaups and summer discharge)*, Science Institute, University of Iceland, Reykjavik (in Icelandic).

Gislason, S.R., Gudmundsson, B.T. & Eiriksdottir, E.S. 1998, *Efnasamsetning Elliðaánna 1997 - 1998 (Chemistry of The Elliðaár river 1997-1998)*, Science Institute, University of Iceland, Reykjavik.

Gislason, S.R., Stefansdottir, M.B. & Eiriksdottir, E.S. 2000, *ARCTIS, Regional Investigation of Arctic Snow Chemistry: Results from the Icelandic Expeditions, 1997-1999.*, Science Institute, University of Iceland, Reykjavik.

Gislason, S.R., Snorrason, A., Kristmannsdottir, H.K., Sveinbjornsdottir, A.E., Torssander, P., Olafsson, J., Castet, S. & Dupre, B. 2002, "Effects of volcanic eruptions on the CO2 content of the atmosphere and the oceans: the 1996 eruption and flood within the Vatnajokull Glacier, Iceland", *Chemical Geology,* vol. 190, no. 1-4, pp. 181-205.

Gmelins, L. 1908, "As, Sb written by Fritz Ephraim" in *Gmelin-Kraut's handbuch der anorganishen chemie, Band III, Abteilung 2*, ed. F. Ephraim, Carl Whiter's Universitätbuchhandlung, Heidelberg.

Goldberg, S.R. 1992, "Use of surface complexation models in soil chemical systems", *Advances in Agronomy,* vol. 47, pp. 233-329.

Gong, Z., Lu, X., Ma, M., Watt, C. & Lee, X.C. 2002, "Arsenic speciation analysis", *Talanta,* vol. 58, no. 1, pp. 77-96.

Government News 1999, "Regulation on protection against water pollution No. 796", *Laws and ministrial gazette of Iceland, series B,* vol. 106, No. 785-810, pp. 2235-2253.

Guo, H., Stüben, D. & Berner, Z. 2007, "Adsorption of arsenic(III) and arsenic(V) from groundwater using natural siderite as the adsorbent", *Journal of Colloid and Interface Science,* vol. 315, no. 1, pp. 47-53.

Halter, W.E. & Pfeifer, H.R. 2001, "Arsenic(V) adsorption onto alpha-Al2O3 between 25 and 70 degrees C", *Applied Geochemistry,* vol. 16, no. 7-8, pp. 793-802.

Harvey, C.F., Swartz, C.H., Badruzzaman, A.B.M., Keon-Blute, N., Yu, W., Ali, M.A., Jay, J., Beckie, R., Niedan, V., Brabander, D., Oates, P.M., Ashfaque, K.N., Islam, S., Hemond, H.F. & Ahmed, M.F. 2002, "Arsenic mobility and groundwater extraction in Bangladesh", *Science,* vol. 298, no. 5598, pp. 1602-1606.

Heiken, G. & Wohletz, K. 1985. Volcanic Ash. University of California Press, Berkeley.

Ho, Y.S. & McKay, G. 1999, "Pseudo-second order model for sorption processes", *Process Biochemistry,* vol. 34, no. 5, pp. 451-465.

Hopenhayn, C. 2006, "Arsenic in drinking water: Impact on human health", *Elements,* vol. 2, no. 2, pp. 103-107.

Howard, A.G. & Hunt, L.E. 1993, "Coupled Photooxidation Hydride Aas Detector for the Hplc of Arsenic Compounds", *Analytical Chemistry,* vol. 65, no. 21, pp. 2995-2998.

Howard, A.G. & Salou, C. 1996, "Cysteine enhancement of the cryogenic trap hydride AAS determination of dissolved arsenic species", *Analytica Chimica Acta,* vol. 333, no. 1-2, pp. 89-96.

Hung, D.Q., Nekrassova, O. & Compton, R.G. 2004, "Analytical methods for inorganic arsenic in water: a review", *Talanta,* vol. 64, no. 2, pp. 269-277.

Jakobsson, S.P. & Gudmundsson, M.T. 2008, "Subglacial and intraglacial volcanic formations in Iceland", *Jökull,* vol. 58, pp. 179-196.

Jay, J.A., Blute, N.K., Hemond, H.F. & Durant, J.L. 2004, "Arsenic-sulfides confound anion exchange resin speciation of aqueous arsenic", *Water research,* vol. 38, no. 5, pp. 1155-1158.

Jensen, M.M., Thamdrup, B., Rysgaard, S., Holmer, M. & Fossing, H. 2003, "Rates and regulation of microbial iron reduction in sediments of the Baltic-North Sea transition", *Biogeochemistry,* vol. 65, no. 3, pp. 295-317.

Jeong, Y., Fan, M., Singh, S., Chuang, C., Saha, B. & Hans van Leeuwen, J. 2007, "Evaluation of iron oxide and aluminum oxide as potential arsenic(V) adsorbents", *Chemical Engineering and Processing: Process Intensification,* vol. 46, no. 10, pp. 1030-1039.

Jerram, D.A., Widdowson, M. 2005, "The anatomy of Continental Flood Basalt Provinces: geological constraints on the processes and products of flood volcanism", *Lithos*, vol. 79, pp. 385-405.

Jia, Y.F., Xu, L.Y., Fang, Z. & Demopoulos, G.P. 2006, "Observation of surface precipitation of arsenate on ferrihydrite", *Environmental science & technology,* vol. 40, no. 10, pp. 3248-3253.

Johannesson, H. & Saemundsson, K. 1998, *Jarðfræðikort af Íslandi 1:500.000. Bergrunnur (önnur útgáfa)- Geology Map of Iceland 1:500,000. Bedrock, (2nd edition)*, Icelandic Institute of Natural History, Reykjavik, Iceland.

Jones, J.G. 1969. Intraglacial volcanoes of the Laugarvatn region, south-west Iceland, I. *Quarterly J. Geol. Soc. London,* vol. 124, pp. 197-211.

Kjartansson, G. 1959, "The Moberg formation II" in *On the Geology and Geomorphology of Iceland*, ed. S. Thorarinsson, pp. 139-143.

Kristmannsdottir, H. & Armannsson, H. 2003, "Environmental aspects of geothermal energy utilization", *Geothermics,* vol. 32, no. 4-6, pp. 451-461.

Kuan, W.H., Lo, S.L., Chang, C.M. & Wang, M.K. 2000, "A geometric approach to determine adsorption and desorption kinetic constants", *Chemosphere,* vol. 41, no. 11, pp. 1741-1747.

Langmuir, D. 1997, *Aqueous environmental geochemistry,* Prentice-Hall, Inc, New Jersey, USA.

Langmuir, I. 1918, "The adsorption of gases on plane surfaces of glass, mica and platinum", *Journal of the American Chemical Society,* vol. 40, pp. 1361-1403.

Lien, H.L. & Wilkin, R.T. 2005, "High-level arsenite removal from groundwater by zero-valent iron", *Chemosphere,* vol. 59, no. 3, pp. 377-386.

Limousin, G., Gaudet, J.P., Charlet, L., Szenknect, S., Barthes, V. & Krimissa, M. 2007, "Sorption isotherms: A review on physical bases, modeling and measurement", *Applied Geochemistry,* vol. 22, no. 2, pp. 249-275.

Lin, T.F. & Wu, J.K. 2001, "Adsorption of arsenite and arsenate within activated alumina grains: Equilibrium and kinetics", *Water research,* vol. 35, no. 8, pp. 2049-2057.

Lin, Z. & Puls, R.W. 2000, "Adsorption, desorption and oxidation of arsenic affected by clay minerals and aging process", *Environmental Geology,* vol. 39, no. 7, pp. 753-759.

Lintschinger, J., Schramel, P., Hatalak-Rauscher, A., Wendler, I. & Michalke, B. 1998, "A new method for the analysis of arsenic species in urine by using HPLC-ICP-MS", *Fresenius Journal of Analytical Chemistry,* vol. 362, no. 3, pp. 313-318.

Loehr, T.M. & Plane, R.A. 1968, "Raman spectra and structure of arsenious acid and arsenite in aqueous solution.", *Journal of Inorganic Chemistry,* vol. 7, pp. 1708-1714.

Mandal, B.K. & Suzuki, K.T. 2002, "Arsenic round the world: a review", *Talanta,* vol. 58, no. 1, pp. 201-235.

Manning, B.A., Fendorf, S.E. & Goldberg, S. 1998, "Surface structures and stability of arsenic(III) on goethite: Spectroscopic evidence for inner-sphere complexes", *Environmental science & technology,* vol. 32, no. 16, pp. 2383-2388.

Manning, B.A. & Goldberg, S. 1997, "Adsorption and stability of arsenic(III) at the clay mineral-water interface", *Environmental science & technology,* vol. 31, no. 7, pp. 2005-2011.

Masscheleyn, P.H., Delaune, R.D. & Patrick, W.H. 1991, "A Hydride Generation Atomic-Absorption Technique for Arsenic Speciation", *Journal of environmental quality,* vol. 20, no. 1, pp. 96-100.

Masue, Y., Loeppert, R.H. & Kramer, T.A. 2007, "Arsenate and arsenite adsorption and desorption behavior on coprecipitated aluminum : iron hydroxides", *Environmental science & technology,* vol. 41, no. 3, pp. 837-842.

Mathews, W. H., 1947. ""Tuyas": Flat-topped volcanoes in northern British Columbia". *American Journal of Science*, vol. 245, pp. 560-570.

McCleskey, R.B., Nordstrom, D.K. & Maest, A.S. 2004, "Preservation of water samples for arsenic(III/V) determinations: an evaluation of the literature and new analytical results", *Applied Geochemistry,* vol. 19, no. 7, pp. 995-1009.

Mottl, M.J., Holland, H.D. 1978, "Chemical exchange during hydrothermal alteration of basalt by seawater-I. Experimental results for major and minor components of seawater", *Geochimica et Cosmochimica Acta*, vol. 42, pp. 1103-1115.

Mukhopadhyay, R., Rosen, B.P., Pung, L.T. & Silver, S. 2002, "Microbial arsenic: from geocycles to genes and enzymes", *FEMS microbiology reviews,* vol. 26, no. 3, pp. 311-325.

Munoz, E. & Palmero, S. 2005, "Analysis and speciation of arsenic by stripping potentiometry: a review", *Talanta,* vol. 65, no. 3, pp. 613-620.

Murali, V. & Aylmore, L.A.G. 1983, "Competetive adsorption during solute transport in soils: 1. Mathematical models", *Soil Science,* vol. 135, no. 3, pp. 143-150.

Nakazato, T., Taniguchi, T., Tao, H., Tominaga, M. & Miyazaki, A. 2000, "Ion-exclusion chromatography combined with ICP-MS and hydride generation-ICP-MS for the determination of arsenic species in biological matrices", *Journal of Analytical Atomic Spectrometry,* vol. 15, no. 12, pp. 1546-1552.

Nakazato, T., Tao, H., Taniguchi, T. & Isshiki, K. 2002, "Determination of arsenite, arsenate, and monomethylarsonic acid in seawater by ion-exclusion chromatography combined with inductively coupled plasma mass spectrometry using reaction cell and hydride generation techniques", *Talanta,* vol. 58, no. 1, pp. 121-132.

Naykki, T., Peramaki, P., Kujala, J. & Mikkonen, A. 2001, "Optimization of a flow injection hydride generation atomic absorption spectrometric method for the determination of arsenic, antimony and selenium in iron chloride", *Analytica Chimica Acta,* vol. 439, no. 2, pp. 229-238.

Neuhoff, P.S., Fridriksson, T., Arnorsson, S. & Bird, D.K. 1999, "Porosity evolution and mineral paragenesis during low-grade metamorphism of basaltic lavas at Teigarhorn, eastern Iceland", *American Journal of Science,* vol. 299, no. 6, pp. 467-501.

Newman, D.K., Ahmann, D. & Morel, F.M.M. 1998, "A brief review of microbial arsenate respiration", *Geomicrobiology Journal,* vol. 15, no. 4, pp. 255-268.

Nickson, R., McArthur, J., Burgess, W., Ahmed, K.M., Ravenscroft, P. & Rahman, M. 1998, "Arsenic poisoning of Bangladesh groundwater", *Nature,* vol. 395, no. 6700, pp. 338-338.

O'Day, P. 2006, "Chemistry and mineralogy of arsenic", *Elements,* vol. 2, no. 2, pp. 77-83.

Olafsson, J. 1992, "Chemical characteristics and trace-elements of Thingvallavatn", *Oikos,* vol. 64, pp. 151-161.

Olafsson, J. & Riley, J.P. 1978, "Geochemical studies on the thermal brine from Reykjanes (Iceland)", *Chemical Geology,* vol. 21, pp. 219-237.

Oliviera, V., Sarmiento, A.M., Gómez-Ariza, J.L., Nieto, J.M. & Sánchez-Rodas, D. 2005, "New preservation method for inorganic arsenic speciation in acid mine drainage samples", *Talanta*, vol. 69, no. 5, pp. 1182-1189.

O'Reilly, S.E., Strawn, D.G. & Sparks, D.L. 2001, "Residence time effects on arsenate adsorption", *Soil Science Society of America Journal,* vol. 65, no. 1, pp. 67-77.

Palmason, G. 1973, "Kinematics and heat flow in a volcanic rift zone with application to Iceland", *Geophysical Journal of the Royal Astronomical Society,* vol. 33, pp. 451-481.

Paton, G.I., Rattray, E.A.S., Campbell, C.D., Meussen, H., Cresser, M.S., Glover, L.A. & Killham, K. 1997, "Use of genetically modified microbial biosensors for soil ecotoxicity testing" in *Bioindicators of soil Health*, eds. C.S. Pankhurst, B. Doube & V. Gupta, CAB International, New York, pp. 397-418.

Planer-Friedrich, B., London, J., McCleskey, R.B., Nordstrom, D.K. & Wallschlager, D. 2007, "Thioarsenates in geothermal waters of yellowstone national park: Determination, preservation, and geochemical importance", *Environmental science & technology,* vol. 41, no. 15, pp. 5245-5251.

Pokrovski, G., Gout, R., Schott, J., Zotov, A. & Harrichoury, J.C. 1996, "Thermodynamic properties and stochiometry of As(III) hydroxide complexes at hydrothermal conditions", *Geochimica et Cosmochimica Acta,* vol. 60, no. 5, pp. 737-749.

Rasul, S.B., Munir, A.K.M., Hossain, Z.A., Khan, A.H., Alauddin, M. & Hussam, A. 2002, "Electrochemical measurement and speciation of inorganic arsenic in groundwater of Bangladesh", *Talanta,* vol. 58, no. 1, pp. 33-43.

Raven, K.P., Jain, A. & Loeppert, R.H. 1998, "Arsenite and arsenate adsorption on ferrihydrite: Kinetics, equilibrium, and adsorption envelopes", *Environmental science & technology,* vol. 32, no. 3, pp. 344-349.

REN21 2008, *Renewables 2007 Global Status Report*, Deutche Gesellschaft für Technische Zusammenarbeit (GTZ) GmbH, Paris: REN21 Secretariat and Waschington, DC: Worldwatch Institute.

Rochette, E.A., Bostick, B.C., Li, G.C. & Fendorf, S. 2000, "Kinetics of arsenate reduction by dissolved sulfide", *Environmental science & technology,* vol. 34, no. 22, pp. 4714-4720.

Ronov, A.B., Yaroshevsky, A.A. 1976, "New model of Earths crust chemical-structure", *Geokhimiya*, vol. 12, pp. 1763-1795.

Rubio, R., Padró, A., Albertí, J. & Rauret, G. 1993, "Determination of arsenic speciation by liquid chromatography—hydride generation inductively coupled plasma atomic emission spectrometry with on-line UV photooxidation", *Analytica Chimica Acta,* vol. 283, no. 1, pp. 160-166.

Sahai, N. & Sverjensky, D.A. 1997a, "Solvation and electrostatic model for specific electrolyte adsorption", *Geochimica et Cosmochimica Acta,* vol. 61, no. 14, pp. 2827-2848.

Sahai, N. & Sverjensky, D.A. 1997b, "Evaluation of internally consistent parameters for the triple-layer model by the systematic analysis of oxide surface titration data", *Geochimica et Cosmochimica Acta,* vol. 61, no. 14, pp. 2801-2826.

Salmassi, T.M., Venkateswaren, K., Satomi, M., Nealson, K.H., Newman, D.K. & Hering, J.G. 2002, "Oxidation of arsenite by Agrobacterium albertimagni, AOL15, sp nov., isolated from Hot Creek, California", *Geomicrobiology Journal,* vol. 19, no. 1, pp. 53-66.

Sathrugnan, K. & Hirata, S. 2004, "Determination of inorganic oxyanions of As and Se by HPLC-ICPMS", *Talanta,* vol. 64, no. 1, pp. 237-243.

Schilling, J.G. 1973, "Iceland mantle plume - geochemical study of Reykjanes Ridge", *Nature,* vol. 242, pp. 565-571.

Schweich, D. & Sardin, M. 1981, "Adsorption, partition, ion exchange and chemical reaction in batch reactors or in columns — A review", *Journal of Hydrology,* vol. 50, pp. 1-33.

Selim, H.M. & Ma, L. 2001, "Modeling nonlinear kinetic behaviour of copper adsorption-desorption in soil" in *Physical and chemical processes of water and solute transport/retention in soil.*, eds. H.M. Selim & D.L. Sparks, Soil Science Society of America, Madison, WI, pp. 189-212.

Selim, H.M. & Amacher, M.C. 1988, "A 2nd-Order Kinetic Approach for Modeling Solute Retention and Transport in Soils", *Water Resources Research,* vol. 24, no. 12, pp. 2061-2075.

Selim, H.M. & Zhang, H. 2007, "Arsenic adsorption in soils: Second-order and multireaction models", *Soil Science,* vol. 172, no. 6, pp. 444-458.

Sheppard, B.S., Shen, W.L., Caruso, J.A., Heitkemper, D.T. & Fricke, F.L. 1990, "Elimination of the Argon Chloride Interference on Arsenic Speciation in Inductively Coupled Plasma Mass-Spectrometry using Ion Chromatography", *Journal of Analytical Atomic Spectrometry,* vol. 5, no. 6, pp. 431-435.

Shiobara, Y., Ogra, Y. & Suzuki, K.T. 2001, "Animal species difference in the uptake of dimethylarsinous acid (DMA(III)) by red blood cells", *Chemical research in toxicology,* vol. 14, no. 10, pp. 1446-1452.

Sigurdsson, F. & Ingimarsson, J. 1990, "Lekt íslenskra jardefna", *Vatnið og Landið - Vatnafræðiráðstefna*, ed. G. Sigbjarnarson, Orkustofnun (in Icelandic), , pp. 121.

Singh, D.B., Prasad, G. & Rupainwar, D.C. 1996, "Adsorption technique for the treatment of As(V)-rich effluents", *Colloids and Surfaces A-Physicochemical and Engineering Aspects,* vol. 111, no. 1-2, pp. 49-56.

Smedley, P.L. & Kinniburgh, D.G. 2002, "A review of the source, behaviour and distribution of arsenic in natural waters", *Applied Geochemistry,* vol. 17, no. 5, pp. 517-568.

Smieja, J.A. & Wilkin, R.T. 2003, "Preservation of sulfidic waters containing dissolved As(III)", *Journal of Environmental Monitoring,* vol. 5, no. 6, pp. 913-916.

Sparks, D.L. & Rechcigl, J.E. 1982, "Comparison of Batch and Miscible Displacement Techniques to Describe Potassium Adsorption-Kinetics in Delaware Soils", *Soil Science Society of America Journal,* vol. 46, no. 4, pp. 875-877.

Sposito, G. 1984, *The surface chemistry of soils,* Oxford University Press, New York, USA.

Sracek, O., Bhattacharya, P., Jacks, G., Gustafsson, J.P. & von Bromssen, M. 2004, "Behavior of arsenic and geochemical modeling of arsenic enrichment in aqueous environments", *Applied Geochemistry,* vol. 19, no. 2, pp. 169-180.

Stauder, S., Raue, B. & Sacher, F. 2005, "Thioarsenates in sulfidic waters", *Environmental science & technology,* vol. 39, no. 16, pp. 5933-5939.

Stefansson, A. & Arnorsson, S. 2002, "Gas pressures and redox reactions in geothermal fluids in Iceland", *Chemical Geology,* vol. 190, no. 1-4, pp. 251-271.

Stroncik, N. A. and Schmincke, H.-U. 2002. Palagonite - a review. *International Journal of Earth Sciences*, vol. 91, pp. 680-697.

Stumm, W. & Morgan, J.J. 1996, *Aquatic Chemistry, Chemical Equilibria and Rates in Natural Waters,* 3rd edition edn, John Wiley & Sons, Inc., New York.

Symonds, R.B., Rose, W.I., Reed, M.K., Lichte, F.E. & Finnegan, D.L. 1987, "Volatilization, transport and sublimation of metallic and non-metallic elements in high temperature gases at Merapi Volcano, Indonesia", *Geochimica et Cosmochimica Acta,* vol. 51, pp. 2083-2101.

Taniguchi, T., Tao, H., Tominaga, M. & Miyazaki, A. 1999, "Sensitive determination of three arsenic species in water by ion exclusion chromatography-hydride generation inductively coupled plasma mass spectrometry", *Journal of Analytical Atomic Spectrometry,* vol. 14, no. 4, pp. 651-655.

Tao, H., Boyko, V.J. & Mclaren, J.W. 1993, "Improvements in the Signal-To-Background Ratio with Hydride Generation Inductively-Coupled Plasma-Atomic Emission-Spectrometry", *Spectrochimica Acta Part B-Atomic Spectroscopy,* vol. 48, no. 11, pp. 1339-1345.

Thorarinsson, S. 1944, "Tefrokronolgiska studier pa Island". *Geografiska Annaler,* vol. 26, pp. 1-217.

Tóth, J. 1994, "Thermodynamical Correctness of Gas/Solid Adsorption Isotherm Eq.s", *Journal of Colloid and Interface Science,* vol. 163, no. 2, pp. 299-302.

tuff. (2009). In Encyclopædia Britannica. Retrieved March 28, 2009, from Encyclopædia Britannica Online: http://www.britannica.com/EBchecked/topic/608481/tuff

Vaughan, D.J. 2006, "Arsenic", *Elements,* vol. 2, no. 2, pp. 71-75.

Vink, B.W. 1996, "Stability relations of antimony and arsenic compounds in the light of revised and extended Eh-pH diagrams", *Chemical Geology,* vol. 130, no. 1-2, pp. 21-30.

Voice, T.C., Rice, C.P. & Weber, W.J. 1983, "Effect of Solids Concentration on the Sorptive Partitioning of Hydrophobic Pollutants in Aquatic Systems", *Environmental science & technology,* vol. 17, no. 9, pp. 513-518.

volcanic glass. (2009). In Encyclopædia Britannica. Retrieved March 28, 2009, from Encyclopædia Britannica Online: http://www.britannica.com/EBchecked/topic/632062/volcanic-glass

Walker, G.P.L. 1960, "Zeolite zones and dike distribution in relation to the structure of the basalts of Eastern Iceland", *Journal of Geology,* vol. 68, pp. 515-527.

Webster, J.G. & Nordstrom, D.K. 2003, "Geothermal arsenic" in *Arsenic in Groundwater*, eds. A.H. Welch & K.G. Stollenwerk, Kluwer Academic Publishers, Boston, Massachusetts, pp. 101-125.

Wei, C. & Liu, J. 2007, "A new hydride generation system applied in determination of arsenic species with ion chromatography–hydride generation-atomic fluorescence spectrometry (IC–HG-AFS)", *Talanta,* vol. 73, no. 3, pp. 540-545.

Wetang'ula, G.N. & Snorrason, S.S. 2005, "Geothermal Wastewater Disposal: Chemical Stress Assessment Thingvallavatn - Iceland", *Proceedings World Geothermal Congress 2005*.

White, J. D.L. & Houghton, B., 2000. "Surtseyan and related phreatomagmatic eruptions". *Encyclopedia of volcanoes,* ed. Sigurdsson, H., Houghton, B., McNutt, S.R. & Stix, J., Academic Press, New York, pp. 495–511.

Wilkie, J.A. & Hering, J.G. 1998, "Rapid oxidation of geothermal arsenic(III) in streamwaters of the eastern Sierra Nevada", *Environmental science & technology,* vol. 32, no. 5, pp. 657-662.

Wilkin, R.T., Wallschlager, D. & Ford, R.G. 2003, "Speciation of arsenic in sulfidic waters", *Geochemical Transactions,* vol. 4, pp. 1-7.

World Health Organization 2004, *WHO, Guidelines for drinking water quality recommendations,* World Health Organization, Geneva, Switzerland.

Wu, J.Z. & Ho, P.C. 2004, "Speciation of inorganic and methylated arsenic compounds by capillary zone electrophoresis with indirect UV detection - Application to the analysis of alkali extracts of As2S2 (realgar) and As2S3 (orpiment)", *Journal of Chromatography a,* vol. 1026, no. 1-2, pp. 261-270.

Zhang, H. & Selim, H.M. 2005, "Kinetics of arsenate adsorption-desorption in soils", *Environmental science & technology,* vol. 39, no. 16, pp. 6101-6108.

2 Analytical techniques and experimental design

2.1 Materials

2.1.1 Basaltic glass

The solid material used throughout the experimental study was basaltic glass. It was obtained from the volcanic ash of Stapafell mountain, South-Western Iceland (Oelkers and Gislason, 2001). Preparation of the glass was carried out according to (Oelkers and Gislason, 2001). The glass was dried at ambient temperature and then further dried overnight in an oven at 50°C. Next the glass was mildly ground in a low density polyethylene (LDPE) bag with a plastic hammer in an attempt to induce minimum strain to the fresh surfaces. Subsequent dry sieving yielded primarily 125-250 μm size fraction. This fraction was ultrasonically cleaned, first in deionised water, then in acetone, by separating and discarding the ultra fine suspension at the end of each cleaning cycle which lasted for 10 min. Altogether five water and acetone cycles were carried out to remove fine particles. Finally the powders were dried overnight at 110°C. The rather complex preparation procedure ensured a large batch of rather homogenous material that was used throughout all experiments. The mild grounding in LDPE bags ensured minimum contamination during preparation and produced surfaces that were a result of gentle cracking of the material rather than being formed by a powerful grinder with resulting strain marks (and therefore ununiform surface). The repeated rinse cycles ensured a near complete removal of fine particles from the surfaces to be worked with. The specific surface area (1.533 m^2 g^{-1}) of the glass before the experiments was measured by the three-point BET method using Kr gas at University Paul Sabatier Toulouse. A Leo Supra 25 Field Emission Scanning Electron Microscope (FESEM) equipped with a Oxford Instruments Energy Dispersive Spectrometer (EDS) was used to characterise the glass surface. The chemical composition of the surface (Table 1) was measured with the FESEM-EDS and FESEM figures allowed visual estimation of the roughness of the surface (Figures 1a,b).

a

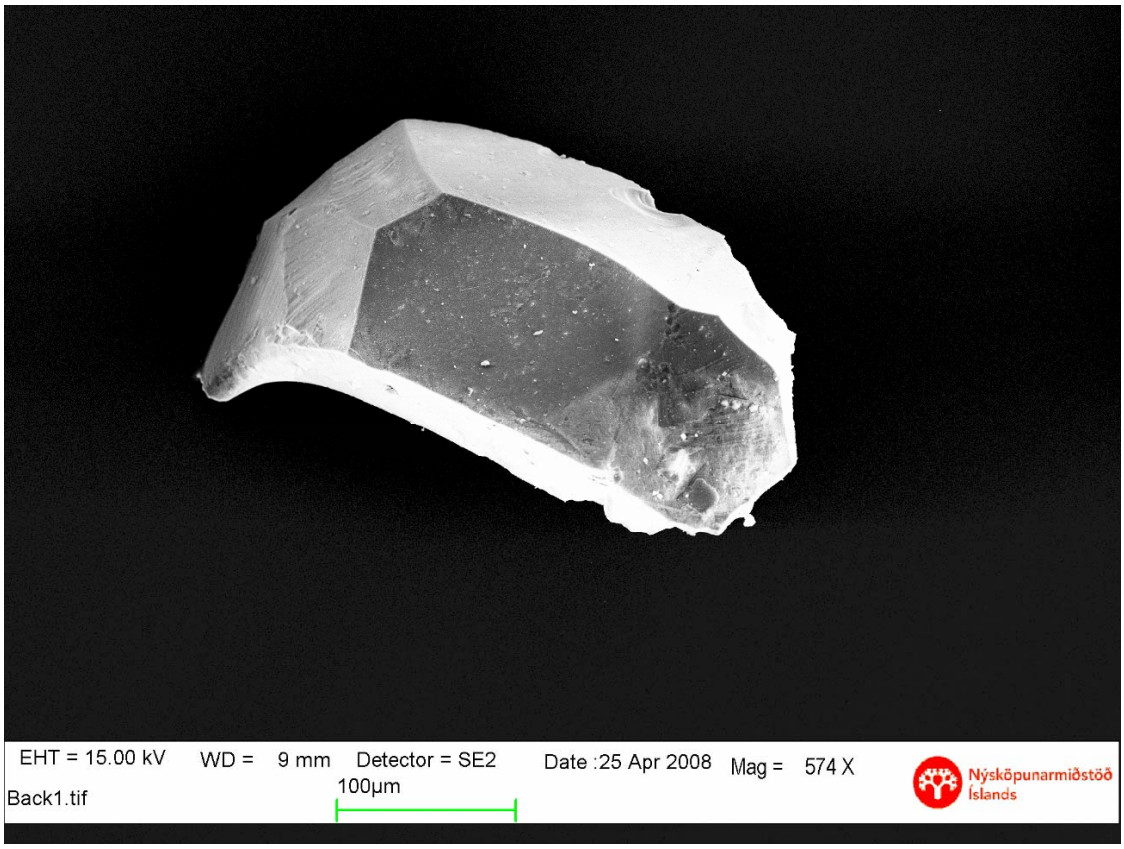

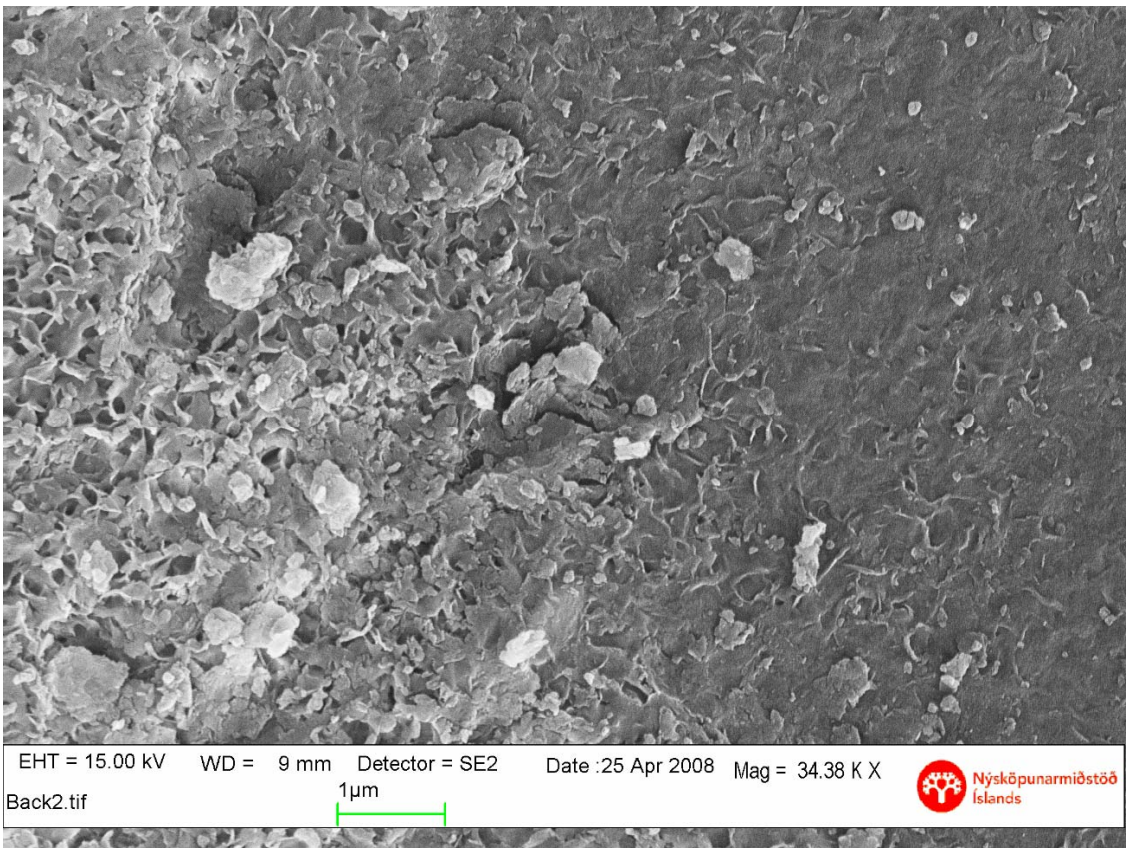

Figure 1 Field Emission Scanning Electron Microscope (FESEM) figures of basaltic glass used in the experiments. Figure a is a grain prior to the column experiments and figure b is a magnified section of figure a.

Table 1Atomic percentage of selected elements measured by FESEM-EDS on the surface of the basaltic glass prior (Stapafell) and after all column experiments (pH 3 to pH 10).

Sample	Si	Al	Fe	Ca	Mg	Na	Ti	O
Stapafell	16.8	5.92	3.28	4.18	3.59	1.17	0.37	64.7
pH 3	16.1	5.87	2.82	3.88	3.62	1.38	0.39	69.9
pH 6.3	16.1	5.68	3.11	3.97	3.75	1.39	0.43	68.6
pH 8	18.1	5.95	4.02	5.05	3.29	1.03	0.57	49.3
pH 9	15.4	6.43	2.79	3.22	3.36	1.21	0.40	74.7
pH 10	17.5	6.31	3.61	3.83	3.00	0.88	0.47	63.5

2.1.2 Laboratory reagents

The reagents sodium arsenite ($NaAsO_2$), sodium arsenate hydrated ($Na_2HAsO_4.7H_2O$), Sodium hydroxide (NaOH), trisodium citrate ($Na_3C_6H_5O_7$), hydrochloric acid (Analar) (HCl) and aqueous ammonia (Analar) (NH_4OH) were obtained from BDH Chemicals. Ascorbic acid ($C_6H_8O_6$), and potassium iodide (KI) were obtained from Acros organics and were both reagent grade**.** Sodium borohydride ($NaBH_4$) (puriss, p.a.) , Acid blue 9 ($C_{37}H_{34}Na_2N_2O_9S_3$) (grade: Standard Fluka) and phosphoric acid (H_3PO_4) (puriss, p.a.) were obtained from Sigma Aldrich Chemical Co. Nitric acid (Suprapure) (HNO_3) was obtained from Merck.

2.1.3 Field reagents

The reagents sodium arsenite ($NaAsO_2$), sodium arsenate hydrated ($Na_2HAsO_4{\cdot}7H_2O$) were obtained from BDH Chemicals. Ascorbic acid (reagent grade), potassium iodide (reagent grade) and sodium borohydride (puriss, p.a.) were obtained from Sigma Aldrich Chemical Co. Hydrochloric acid (suprapure) was obtained from Merck.

2.2 Methods

2.2.1 Static batch kinetic and isotherm studies

Stock solutions (60 mg l^{-1}) were prepared by weighing sodium arsenite and sodium arsenate daily into a 0.5 l volumetric flask and dissolve in DDI water for arsenite and arsenate solutions respectively. The column and batch experiments were carried out at with initial pH values (pH 3, 6.3, 8, 9 and 10) at ionic strength of 10 mM by varying concentrations of HCl, NH_4Cl and NH_4OH (Table 2). These solutions were purged for two hours with grade 5.0 N_2 gas (BOC gases, Aberdeen) before any As was added to them or before they came in contact with the basaltic glass.

Table 2 Composition of solutions used in the experiments performed in the present study.

pH (25°C)	HCl (mol L-1)	NH4Cl (mol L-1)	NH4OH (mol L-1)
3.00	0.00100	0.0090	
6.30	0.00010	0.0099	
8.02	0.00001	0.0095	0.0005
9.03		0.0065	0.0035
10.05		0.0015	0.0085

For kinetic experiments, 5 ml of stock solutions were pipetted into a 1 l volumetric flask and made up to volume with the desired pH solution. Solutions were then transferred to Duran bottles and inserted into a glove box as well as 50 ml centrifuge bottles containing 2 g of basaltic glass. The glove box was then closed and N_2 gas allowed purging through As solutions for 2 h to remove oxygen from solutions and the glove box itself. As solution (20 ml) was then dispensed with Eppendorff dispensers into a centrifuge bottle and closed. The samples were then shaken at 170 rpm at 30°C (±0.1°C) for 24, 8, 4, 1.5, 0.67, 0.2 and 0.1 hours on an incubated shaker (MaxQ mini, Barnstead International).

For Isotherm experiments, stock As solutions, desired pH solution and 50 ml centrifuge bottles containing 2 g of basaltic glass were inserted into a glove box and N_2 allowed purging through pH buffer solutions for 2h. Then stock solutions were pipetted into 20 ml volumetric flasks which were filled to mark with the pH solution to acquire desired concentrations. The samples were shaken at 170 rpm at 30°C (±0.1°C) during the 24 h incubation time. Following shaking period for both kinetic and isotherm experiments samples were centrifuged at 2100*g* for 5 m. Then 1 ml was pipetted from supernatant for total As analysis and 1 ml for arsenite analysis. Total As was determined in a Perkin Elmer FIAS 100 flow injection-hydride generation –interfaced with a Perkin Elmer AAnalyst 300 atomic absorption spectrophotometer (FIA-HG-AAS), after pre-reduction of an one ml aliquot of the sample with a 9 ml solution of 10% potassium iodide, 10% hydrochloric acid and 5% ascorbic acid. For analysis of arsenite, a HG-AAS method (Masscheleyn et al., 1991) was optimized for the FIA-HG-AAS system. An aliquot, 1 ml, was pipetted into a bottle containing 4 ml of DDI water and 5 ml of 0.4 M sodium citrate which had previously been adjusted to pH 5.0 with 4.0 M HCl. The sample was then analyzed within an hour. A series of test solutions were prepared from mixture of arsenite and arsenate standards to determine if any reduction of arsenate occurred during measurement (Figure 2).

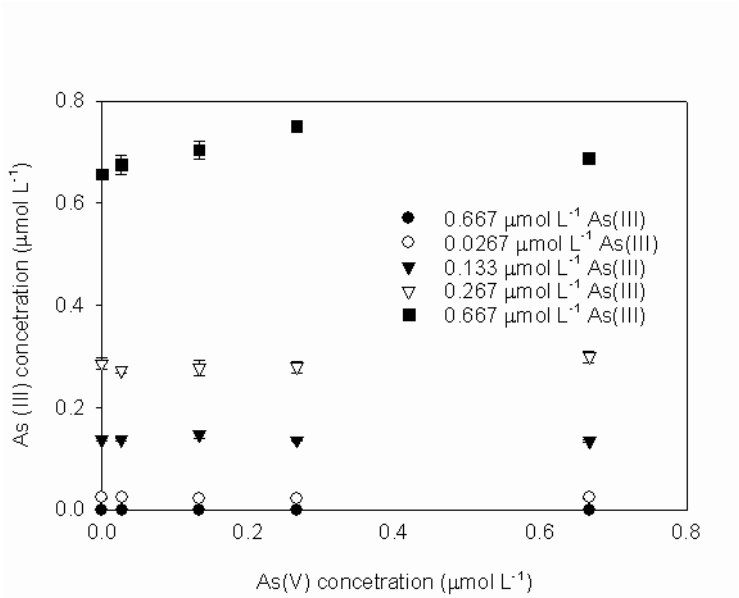

Figure 2 Addition of arsenate, As(V) to 0.2 M Na-citrate (pH 5.0) solutions containing As(III) did not increase the absorbance values measured in the HG-AAS therefore allowing estimation of arsenate by subtracting measured arsenite from measured As-total concentrations.

No reduction of arsenate was observed in the range of 0 to 0.67 µmol l^{-1} As which was the linear range of the HG-AAS. Cross validation of the method was determined on randomly selected samples by Arsenic species were separated by high performance liquid chromatography (HPLC), using a PRP X-100 anion exchange column (150 · 4.1 mm). The mobile phase was a 30 mM H_3PO_4 solution adjusted to pH 5.1 with aqueous NH_3. The HPLC was coupled to Agilent 7500 inductively coupled plasma mass spectrophotometer (ICP-MS) (Riekie et al., 2006) and the arsenite/arsenate speciation results concurred between the two techniques (Table 2). All batch experiments were carried out in triplicate.

2.2.2 **Column experiments:**

2.2.2.1 Column construction

Overview of the column experimental setup may be viewed in Figure 3a. The column was constructed from polytetrafluoroethylene (PTFE) with inner diameter of 1 cm, wall thickness of 1 cm, length 16 cm (Figure 3b). The column was closed in both ends with screw caps made from PTFE and a tight seal was provided by a silicone o-rings. Nylon meshes were placed at each end the column to contain the basaltic glass (Figure 3b).

Table 3 Speciation procedure in HG-AAS validated by HPLC-ICP-MS, all concentrations are in µmol l^{-1}.

Spiked solutions from method development:

	Spike conc.		HG-AAS measurement						HPLC-ICP-MS measurement					
	As(III)	As(V)	As(III)	S.E.	As(V)*	S.E.	As-Total	S.E.	As(III)	S.E.	As(V)	S.E.	As-total**	S.E.
Spike	0.133	0.000	0.137	0.002	0.000	-	0.136	0.002	0.141	0.009	<LOD	-	0.150	0.009
Spike	0.133	0.027	0.137	0.003	0.023	-	0.160	0.002	0.142	0.010	0.020	-	0.162	0.010
Spike	0.133	0.133	0.147	0.006	0.120	-	0.267	0.004	0.155	0.008	0.129	-	0.284	0.008
Spike	0.133	0.267	0.136	0.002	0.264	-	0.400	0.002	0.139	0.012	0.261	-	0.400	0.012
Spike	0.133	0.667	0.135	0.002	0.665	-	0.800	0.003	0.133	0.012	0.681	-	0.814	0.012

Samples from Langmuir isotherm experiments:

	Initial concentration													
pH	As(III)	As(V)	As(III)	S.E.	As(V)*	S.E.	As-Total	S.E.	As(III)	S.E.	As(V)	S.E.	As-total	S.E.
6.3	0.667	0	0.287	0.012	0.101	-	0.388	0.010	0.280	-	0.102	-	0.382	-
8	0.667	-	0.307	0.015	0.038	-	0.345	0.013	0.306	-	0.040	-	0.346	-
9	-	0.667	0.006	0.094	0.576	-	0.581	0.089	<LOD	-	0.576	-	0.576	-
10	-	0.667	0.233	0.011	0.414	-	0.647	0.012	0.228	-	0.410	-	0.644	-

* As(V) calculated by subtraction of As(III) from As-total in HG-AAS measurements

** As-total calculated as sum of As(III) and As(V)

2.2.2.2 Tubing

All three way valves were lined with PTFE (Hamilton, Switzerland). Majority of tubing for the column experiments was composed of PTFE (Hamilton, Switzerland) with the following exceptions:

1. The tubing between 3-way valves number 2 and 3 was composed from Norprene (Cole Parmer Masterflex L/S 14) which was compatible to the peristaltic pump head (Cole Parmer Masterflex).

2. The tubing from valve #4 to pH/Eh meters, from valve # 5 to valve #6 and from valve #5 to valve #7 was made from Tygon, which was compatible with the peristaltic pump head (Gilson).

The valves in the plumbing system had the following purposes:

1. Valve to switch between As solution and background eluting solution.

2. Valve to connect PTFE and Norprene tubing.

3. Valve to connect Norprene to PTFE tubing. The second purpose was to direct inlet solutions to waste. The solution was directed to waste when filling the tube from As bottle to valve #1. Once the tube had been filled with As solution, valve # 1 was switched to direct background solution into the system. Valve #3

was open to waste until all air and As solution had been ejected from the tubes between valves #1 and 3.

4. Valve to divide outlet solutions to pH/Eh meters and all other measuring devices respectively. The second purpose was to direct all air to waste when filling the column initially with background solution.

5. Valve to divide solution between spectrophotometer/fraction collector and HG-AAS respectively.

6. Valve to connect Tygon tubing to PTFE tubing.

7. Valve to connect Tygon tubing to PTFE tubing.

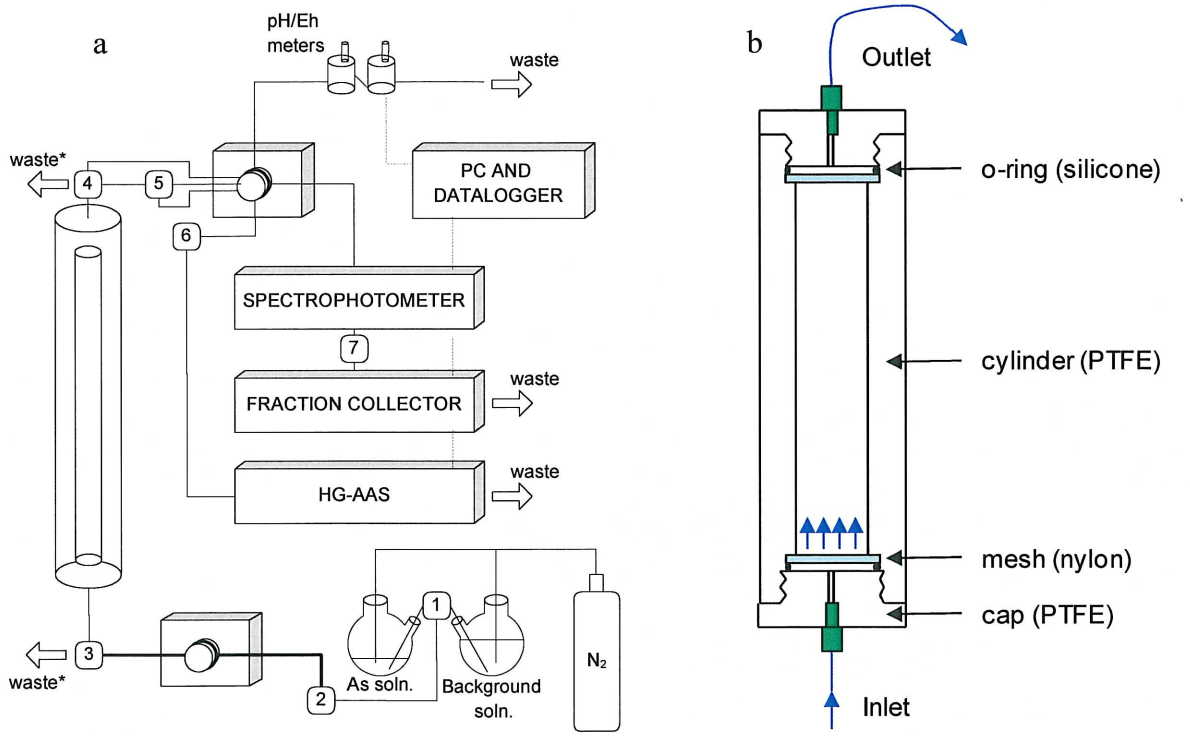

Figure 3 Experimental setup of column experiments. See text for explanations.

2.2.3 Characterisation of column conditions.

2.2.3.1 Methodology

A simplified experimental setup, which omitted the As solution, Spectrophotometer and HG-AAS systems was used to characterise the geochemical conditions in the column. Basaltic glass (16 g) was packed into a 16 cm long, 1 cm inner diameter PTFE column yielding porosity of 0.45. Background solution was pumped at 1 ml min^{-1} directly onto the column and the outlet solution was divided into two flow lines at valve #4, one for pH/Eh flow cells and the other directly to the fraction collector. The pH and Eh values were recorded every 3 minutes. Solutions were sampled at 0.5 ml min^{-1} in the fraction collector from time 0 until the end. Each sampling sequence consisted of the following:

1. Solution was sampled for 10 minutes yielding 5 ml into a 6 ml high density polyethylene (HDPE) vial for the analysis of fluoride and sulphate by Dionex ICS-2000 ion chromatograph (separation on a Ionpac AS-11 column and 23 mM KOH eluent).

2. Solution was sampled for 10 minutes yielding 5 ml into a 15 ml HDPE vial for analysis of Si, Na, K, Ca, Mg, Fe, Al, Sr, Mn, Ti, S, P, Li, Mo, Cl, Br and B by a Spectro Ciros Vision ICP -AES. The solution was filtered through 0.2 µm cellulose acetate (CA) membrane (Advantec) and acidified to pH<1 with concentrated HNO_3 (Merck, suprapure) prior to analysis.

3. Solution was sampled for 5 m yielding 2.5 ml into 15 ml HDPE auto sampler vial containing 0.25 ml of 5 M HCl for the analysis of ferrous and ferric iron (Fe(II) and Fe(III)) by Dionex ICS-3000 ion chromatograph (separation on a Ionpac CS5A column with Metpac PDCA eluent and Metpac post column reagent).

Three consecutive sampling cycles were carried out initially but thereafter a delay up to 8 hours towards the end of the experiment was placed between sampling cycles. A total of 1000 pore volumes (PV) were pumped through the columns prior to injection of As bearing solutions. After each experiment, the material from the column was dried in N_2 gas flow for 24 hours at ambient temperature prior to storage in air-tight container. The surface of the basaltic glass was then coated with gold and analysed by FESEM-EDS.

2.2.3.2 Chemical composition the basaltic glass surface and solution during As transport through columns

The chemical composition of the basaltic glass surface as determined by FESEM-EDS and is displayed in table 1. The surface of the basaltic glass prior to and after column experiments is displayed in figure 4. The chemical composition of the outlet solutions from the columns is tabulated in table 3.

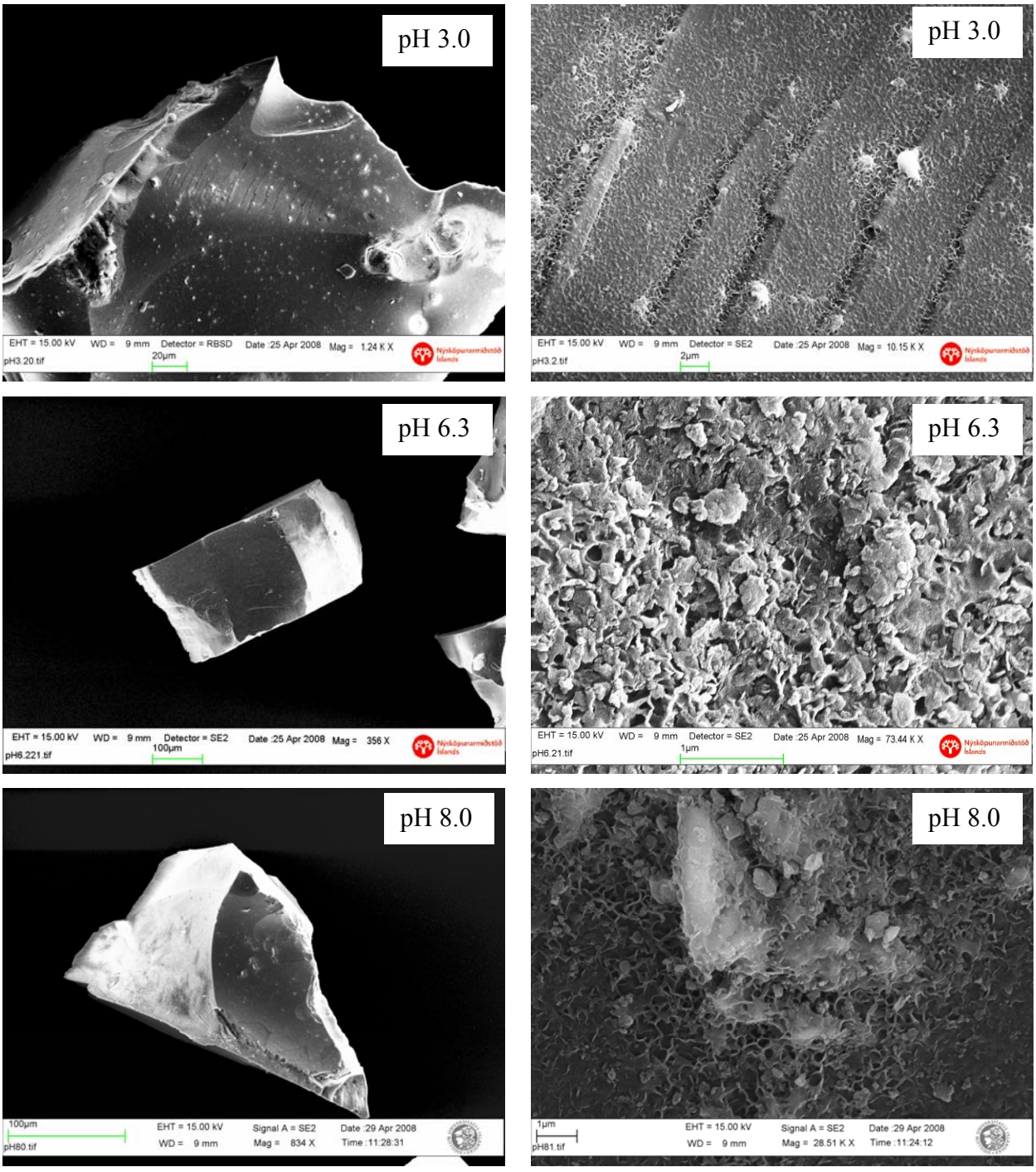

Figure 4 Basaltic glass after column experiments carried out at inlet pH 3, 6.3, 8.0, 9.0 and 10.0, respectively.

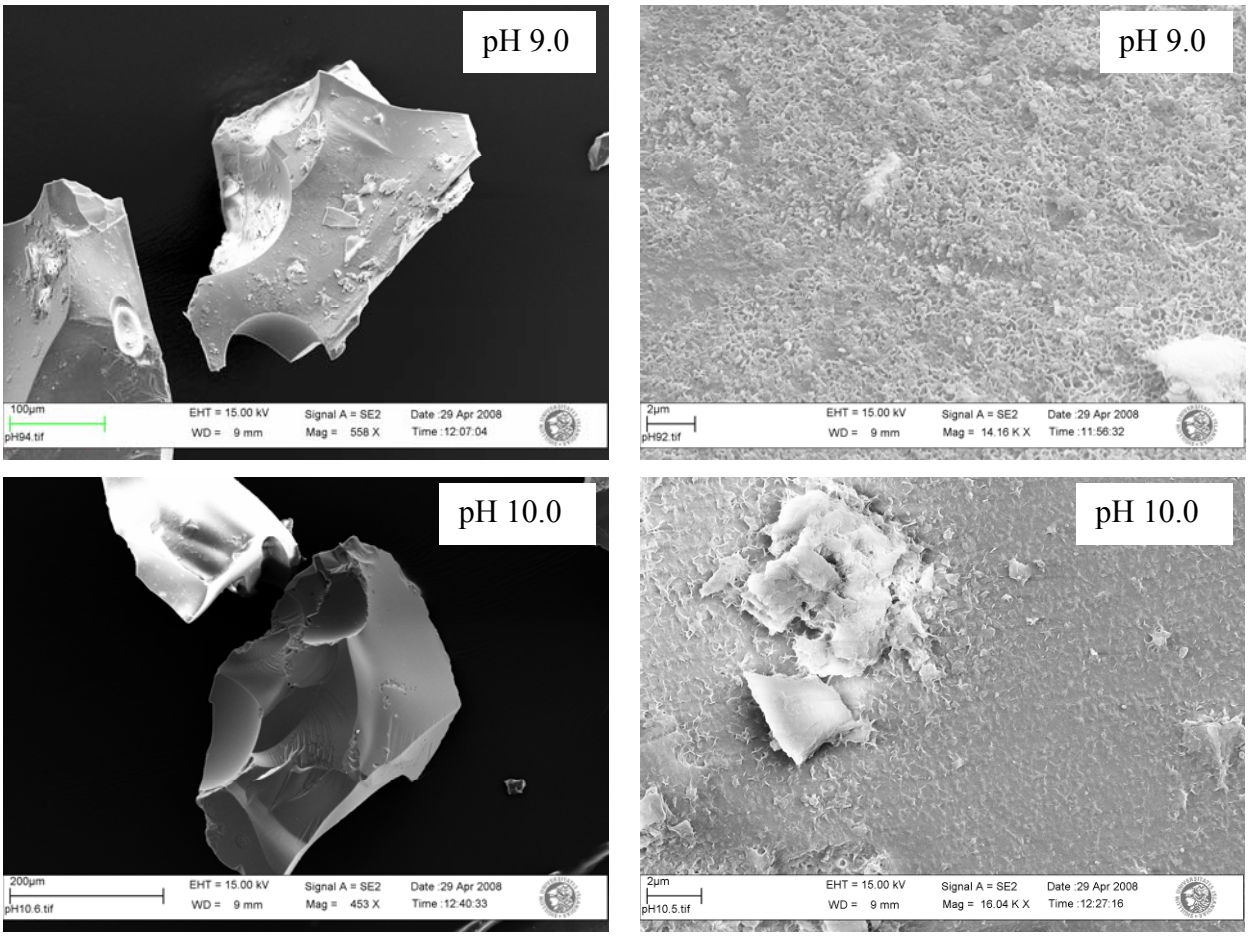

Figure 4. continued

Table 4 Column experiment (pH 3.0) solution outlet compositions prior to As injection.

Sample name	Pore volumes	pH	Eh mV	pe	F mM	Cl mM	SO_4^{2-} mM	Si mM	Na mM	K mM	Ca mM	Mg mM	Al mM	Sr mM	Mn mM	Ti mM	Fetot mM	Fe(II) mM	Fe(III) mM	Fe(III)/FeT %
20-02	2.62	5.09	234	3.96	3.42E-04	1.00E+01	3.91E-03	1.21E-01	3.58E-01	2.51E-01	1.62E+00	1.70E+00	1.29E-03	4.91E-03	5.45E-04	<LOD	6.39E-04	nd	no sample	nd
20-05	6.19	7.34	179	3.03	6.51E-04	1.00E+01	6.17E-04	1.89E-01	4.69E-02	1.20E-01	5.28E-01	3.80E-01	3.17E-03	1.83E-03	1.29E-04	8.30E-05	1.23E-03	1.16E-03	7.27E-05	6
20-08	9.76	7.27	184	3.12	3.70E-04	1.00E+01	1.56E-04	1.70E-01	1.89E-02	2.98E-02	3.54E-01	2.21E-01	2.19E-03	1.25E-03	1.15E-04	6.59E-05	1.07E-03	1.02E-03	5.24E-05	5
20-11	16.9	7.07	186	3.15	3.44E-04	1.00E+01	9.60E-05	1.74E-01	1.39E-02	1.47E-02	3.00E-01	1.85E-01	9.50E-03	1.06E-03	1.79E-04	4.08E-04	4.63E-03	4.58E-03	5.01E-05	1
20-14	24.0	6.85	191	3.24	5.20E-04	1.00E+01	2.35E-04	1.58E-01	1.08E-02	8.37E-03	2.63E-01	1.67E-01	3.81E-03	9.73E-04	1.24E-04	1.43E-04	2.08E-03	2.08E-03		nd
20-17	34.8	6.33	52	0.88	5.82E-04	1.00E+01	0.00E+00	1.57E-01	9.86E-03	5.98E-03	2.25E-01	1.45E-01	3.51E-03	1.32E-03	9.38E-03	1.06E-04	2.41E-02	1.90E-02	5.08E-03	21
20-20	52.6	4.18	323	5.48	<LOD	1.00E+01	4.09E-04	1.53E-01	1.23E-02	5.32E-03	1.07E-01	9.52E-02	1.62E-01	8.29E-04	3.30E-03	4.29E-05	5.01E-02	nd	no sample	nd
20-23	84.8	4.15	314	5.32	<LOD	1.00E+01	8.15E-04	1.58E-01	6.89E-03	5.28E-03	8.53E-02	8.86E-02	2.05E-01	3.30E-04	2.06E-03	8.01E-05	4.83E-02	4.13E-02	6.93E-03	14
20-26	145	4.19	315	5.34	<LOD	1.00E+01	9.04E-04	1.63E-01	8.19E-03	4.95E-03	8.16E-02	8.80E-02	2.14E-01	1.95E-04	1.76E-03	<LOD	4.79E-02	4.01E-02	7.73E-03	16
20-29	220	3.96	338	5.72	<LOD	1.00E+01	7.08E-04	1.78E-01	6.24E-03	4.31E-03	8.22E-02	8.97E-02	1.93E-01	1.51E-04	1.63E-03	<LOD	5.02E-02	4.34E-02	6.80E-03	14
20-32	295	3.79	365	6.19	<LOD	1.00E+01	2.54E-03	1.79E-01	1.40E-02	4.32E-03	8.52E-02	9.26E-02	1.67E-01	1.35E-04	1.59E-03	<LOD	5.17E-02	4.58E-02	5.91E-03	11
20-35	370	3.67	382	6.47	<LOD	1.00E+01	9.52E-04	1.91E-01	1.38E-02	3.77E-03	8.71E-02	1.04E-01	1.61E-01	1.52E-04	1.75E-03	<LOD	6.04E-02	5.79E-02	2.50E-03	4
20-38	445	3.70	391	6.63	<LOD	1.00E+01	9.31E-04	1.76E-01	7.44E-03	4.19E-03	8.44E-02	9.19E-02	1.39E-01	1.11E-04	1.49E-03	<LOD	5.34E-02	4.46E-02	8.84E-03	17
20-41	520	3.64	405	6.86	<LOD	1.00E+01	1.39E-03	1.78E-01	8.89E-03	4.57E-03	8.40E-02	9.25E-02	1.31E-01	1.05E-04	1.44E-03	<LOD	5.43E-02	4.52E-02	9.05E-03	17
no icp sample	595	3.56	415	7.03	<LOD	nd	1.00E-03	nd	nd	nd	nd	nd	nd	nd	nd	nd	nd	nd	nd	nd
20-47	670	3.64	420	7.12	<LOD	1.00E+01	1.39E-03	1.96E-01	1.11E-02	4.41E-03	8.76E-02	1.04E-01	1.33E-01	1.24E-04	1.63E-03	<LOD	6.36E-02	5.45E-02	9.10E-03	14
20-50	745	3.54	408	6.92	<LOD	1.00E+01	4.61E-04	1.78E-01	<LOD	3.74E-03	8.29E-02	9.00E-02	1.20E-01	9.22E-05	1.35E-03	8.06E-05	5.49E-02	nd	no sample	nd
20-53	820	3.52	431	7.30	<LOD	1.00E+01	1.03E-03	1.63E-01	<LOD	<LOD	7.75E-02	8.36E-02	1.11E-01	8.35E-05	1.22E-03	7.05E-05	5.22E-02	5.02E-02	2.00E-03	4
20-56	895	3.55	431	7.31	<LOD	1.00E+01	8.88E-04	1.66E-01	<LOD	<LOD	7.80E-02	8.38E-02	1.09E-01	8.24E-05	1.18E-03	5.19E-05	5.28E-02	5.12E-02	1.60E-03	3
20-59	970	3.52	429	7.27	<LOD	1.00E+01	6.61E-04	1.91E-01	<LOD	3.17E-03	8.18E-02	8.85E-02	1.02E-01	8.78E-05	1.25E-03	8.84E-05	5.63E-02	5.48E-02	1.51E-03	3
20-62	1170	nd	nd	nd	<LOD	1.00E+01	<LOD	1.99E-01	<LOD	3.08E-03	7.40E-02	8.11E-02	9.78E-02	7.66E-05	1.05E-03	4.79E-05	5.14E-02	nd	no sample	nd
20-65	1245	nd	nd	nd	<LOD	1.00E+01	<LOD	1.95E-01	<LOD	<LOD	7.73E-02	8.52E-02	1.01E-01	7.77E-05	1.12E-03	8.65E-05	5.35E-02	nd	no sample	nd

Table 5 Column experiment (pH 6.3) solution outlet compositions prior to As injection.

Sample name	Pore volumes	pH	Eh mV	pe	F mM	Cl mM	SO_4^{2-} mM	Si mM	Na mM	K mM	Ca mM	Mg mM	Al mM	Sr mM	Mn mM	Ti mM	Fetot mM	Fe(II) mM	Fe(III) mM	Fe(III)/FeT %
22-02	3	7.20	221	3.74	5.38E-02	9.99E+00	7.49E-03	5.95E-02	2.40E-01	#VALUE!	1.39E+00	1.28E+00	2.40E-03	4.23E-03	4.42E-04	1.16E-04	1.38E-03	0.00E+00	1.38E-03	100
22-05	6	7.44	214	3.62	5.38E-02	9.99E+00	7.49E-03	4.15E-02	4.62E-02	9.43E-02	4.04E-01	2.32E-01	2.97E-03	1.40E-03	1.30E-04	1.76E-04	1.48E-03	0.00E+00	1.48E-03	100
22-08	10	7.55	218	3.69	4.12E-04	9.99E+00	3.38E-04	3.56E-02	4.51E-02	2.06E-02	2.63E-01	1.41E-01	2.39E-03	9.29E-04	9.46E-05	1.20E-04	9.43E-04	8.66E-05	8.56E-04	91
22-11	17	7.31	236	4.00	4.34E-04	9.99E+00	3.01E-04	2.82E-02	4.19E-02	6.24E-03	1.54E-01	7.80E-02	2.08E-03	5.94E-04	7.67E-05	1.13E-04	8.11E-04	1.14E-04	6.97E-04	86
22-14	24	7.31	230	3.90	4.84E-04	9.99E+00	3.00E-04	2.48E-02	3.98E-02	2.85E-03	1.09E-01	5.50E-02	1.84E-03	4.51E-04	6.33E-05	1.02E-04	8.23E-04	0.00E+00	8.23E-04	100
22-17	35	7.13	243	4.12	3.86E-04	9.99E+00	2.61E-04	2.29E-02	4.33E-02	2.12E-03	7.44E-02	3.71E-02	3.40E-03	3.34E-04	6.56E-05	1.30E-04	1.81E-03	0.00E+00	1.81E-03	100
22-20	53	7.05	238	4.04	4.16E-04	9.99E+00	2.38E-04	2.40E-02	3.18E-02	1.30E-03	4.95E-02	2.53E-02	2.15E-03	2.50E-04	4.81E-05	1.38E-04	9.58E-04	0.00E+00	9.58E-04	100
22-23	85	6.92	254	4.31	4.09E-04	9.99E+00	2.22E-04	1.83E-02	2.85E-02	7.48E-04	3.04E-02	1.59E-02	2.68E-03	1.79E-04	5.48E-05	1.70E-04	1.28E-03	1.27E-04	1.15E-03	90
22-26	146	6.91	262	4.45	4.27E-04	9.99E+00	2.42E-04	1.54E-02	2.68E-02	9.72E-04	1.57E-02	8.55E-03	1.53E-03	1.15E-04	3.91E-05	9.76E-05	8.16E-04	0.00E+00	8.16E-04	100
22-29	221	6.69	259	4.39	4.00E-04	9.99E+00	1.78E-04	1.17E-02	2.02E-02	1.11E-03	8.18E-03	4.77E-03	3.69E-04	8.33E-05	4.41E-05	2.56E-05	9.49E-04	0.00E+00	9.49E-04	100
22-32	296	6.72	255	4.32	3.95E-04	9.99E+00	1.97E-04	9.46E-03	2.80E-02	<LOD	5.37E-03	3.48E-03	4.32E-04	6.50E-05	2.50E-05	1.75E-05	1.43E-04	6.00E-05	8.28E-05	58
22-35	371	6.61	256	4.34	4.09E-04	9.99E+00	2.02E-04	8.94E-03	1.71E-02	<LOD	3.78E-03	2.30E-03	2.76E-04	5.21E-05	2.95E-05	1.69E-05	1.20E-04	0.00E+00	1.20E-04	100
22-38	446	6.65	255	4.32	3.97E-04	9.99E+00	2.46E-04	9.17E-03	3.47E-02	<LOD	2.62E-03	1.80E-03	2.42E-04	4.42E-05	2.56E-05	<LOD	1.22E-04	0.00E+00	1.22E-04	100
22-41	521	6.72	258	4.38	1.65E-04	9.99E+00	3.23E-04	9.18E-03	5.48E-02	6.99E-04	2.26E-03	1.62E-03	2.57E-04	3.91E-05	3.33E-05	1.42E-05	1.48E-04	nd	no sample	nd
22-44	596	6.53	263	4.45	1.79E-04	9.99E+00	1.40E-04	4.48E-02	6.06E-02	1.06E-03	1.09E-02	1.12E-02	1.26E-02	4.38E-05	1.88E-04	8.56E-04	6.56E-03	nd	no sample	nd
22-47	671	6.68	250	4.23	1.55E-04	9.99E+00	9.40E-05	1.50E-02	4.65E-02	1.01E-02	1.68E-03	2.15E-03	3.21E-04	3.06E-05	6.91E-05	1.63E-05	1.39E-04	nd	no sample	nd
22-50	746	6.52	258	4.38	3.87E-04	9.99E+00	1.81E-04	7.77E-03	2.88E-02	4.76E-04	1.87E-03	1.39E-03	5.87E-04	2.79E-05	3.41E-05	2.02E-05	1.66E-04	nd	no sample	nd
no icp sample	821	6.47	257	4.35	<LOD	nd	<LOD	nd	nd	nd	nd	nd	nd	nd	nd	nd	nd	nd	nd	nd
no icp sample	896	6.51	259	4.39	<LOD	nd	<LOD	nd	nd	nd	nd	nd	nd	nd	nd	nd	nd	nd	nd	nd
22-59	971	6.41	255	4.32	4.27E-04	9.99E+00	1.73E-04	7.75E-03	2.88E-02	8.70E-04	1.04E-03	7.66E-04	2.03E-04	2.18E-05	2.90E-05	2.64E-05	7.04E-04	7.04E-04		5

Table 6 Column experiment (pH 8.0) solution outlet compositions prior to As injection.

Sample name	Pore volumes	pH	Eh mV	pe	F mM	Cl mM	SO_4^{2-} mM	Si mM	Na mM	K mM	Ca mM	Mg mM	Al mM	Sr mM	Mn mM	Ti mM	Fetot mM	Fe(II) mM	Fe(III) mM	Fe(III)/FeT %
23-02	3	7.47	205	3.47	0.00E+00	9.50E+00	5.86E-03	7.74E-02	1.32E-01	<LOD	1.04E+00	6.87E-01	3.82E-03	3.11E-03	2.38E-04	1.99E-04	1.51E-03	0.00E+00	1.51E-03	100
23-05	6	8.23	168	2.85	5.53E-04	9.50E+00	1.99E-03	5.16E-02	5.40E-03	6.14E-02	3.57E-01	1.99E-01	4.57E-03	1.15E-03	1.00E-04	1.76E-04	1.34E-03	2.33E-04	1.11E-03	83
23-08	10	8.24	166	2.81	5.08E-04	9.50E+00	1.64E-03	4.28E-02	<LOD	1.39E-02	2.08E-01	1.12E-01	3.87E-03	7.36E-04	5.91E-05	1.56E-04	1.35E-03	0.00E+00	1.35E-03	100
23-11	17	8.21	179	3.03	5.13E-04	9.50E+00	1.07E-03	3.03E-02	<LOD	4.68E-03	1.18E-01	6.05E-02	3.90E-03	4.49E-04	4.05E-05	1.45E-04	1.04E-03	0.00E+00	1.04E-03	100
23-14	24	8.28	172	2.91	4.99E-04	9.50E+00	9.68E-04	2.65E-02	<LOD	2.20E-03	8.20E-02	4.09E-02	4.26E-03	3.34E-04	4.06E-05	1.45E-04	1.41E-03	0.00E+00	1.41E-03	100
23-17	35	8.21	178	3.02	5.21E-04	9.50E+00	9.38E-04	2.16E-02	4.25E-03	3.50E-03	5.75E-02	2.68E-02	4.48E-03	2.44E-04	6.31E-05	1.37E-04	1.21E-03	1.77E-04	1.03E-03	85
23-20	53	8.28	179	3.03	4.90E-04	9.50E+00	8.14E-04	1.91E-02	4.60E-03	<LOD	3.73E-02	1.76E-02	4.82E-03	1.71E-04	3.43E-05	1.41E-04	1.06E-03	5.64E-05	1.01E-03	95
23-23	85	8.27	188	3.19	4.97E-04	9.50E+00	6.75E-04	1.50E-02	7.13E-04	<LOD	2.02E-02	1.07E-02	4.68E-03	1.12E-04	2.27E-05	1.03E-04	7.86E-04	2.49E-05	7.61E-04	97
23-26	145	8.24	184	3.11	5.59E-04	9.50E+00	1.13E-03	1.31E-02	4.24E-03	<LOD	1.13E-02	5.83E-03	3.70E-03	7.01E-05	1.41E-05	3.38E-05	2.64E-04	nd	nd	-
23-29	220	8.13	185	3.13	5.85E-04	9.50E+00	6.28E-04	1.28E-02	6.34E-04	<LOD	7.34E-03	4.17E-03	3.76E-03	5.07E-05	1.26E-05	3.55E-05	3.15E-04	nd	nd	-
23-32	295	8.27	191	3.24	5.35E-04	9.50E+00	5.95E-04	1.31E-02	<LOD	<LOD	4.64E-03	3.65E-03	3.61E-03	3.88E-05	<LOD	4.13E-05	3.34E-04	nd	nd	-
23-35	370	8.17	189	3.20	6.16E-04	9.50E+00	1.12E-03	1.09E-02	4.36E-03	<LOD	1.14E-02	2.53E-03	3.07E-03	3.51E-05	<LOD	<LOD	1.25E-04	0.00E+00	1.25E-04	100
23-38	445	8.21	190	3.22	7.80E-05	9.50E+00	2.17E-04	1.08E-02	4.84E-04	<LOD	3.43E-03	1.86E-03	3.02E-03	2.72E-05	<LOD	<LOD	7.75E-05	0.00E+00	7.75E-05	100
23-41	520	8.27	189	3.20	5.21E-04	9.50E+00	5.65E-04	9.17E-03	<LOD	<LOD	2.14E-03	1.53E-03	2.70E-03	2.30E-05	<LOD	<LOD	1.35E-04	0.00E+00	1.35E-04	100
23-44	595	8.17	183	3.09	6.13E-04	9.50E+00	6.79E-04	1.02E-02	<LOD	<LOD	1.72E-03	1.30E-03	3.08E-03	2.04E-05	<LOD	<LOD	3.36E-04	0.00E+00	3.36E-04	100
23-47	670	8.15	180	3.05	5.81E-04	9.50E+00	6.71E-04	9.59E-03	5.04E-04	<LOD	1.52E-03	1.22E-03	2.89E-03	2.03E-05	2.19E-05	<LOD	6.55E-05	0.00E+00	6.55E-05	100
23-50	745	8.19	185	3.13	<LOD	9.50E+00	6.71E-04	1.10E-02	<LOD	1.06E-02	1.32E-03	2.45E-03	2.70E-03	1.71E-05	3.63E-05	<LOD	9.19E-04	0.00E+00	9.19E-04	100
23-53	820	8.26	185	3.13	<LOD	9.50E+00	6.63E-04	9.34E-03	<LOD	<LOD	1.14E-03	9.72E-04	2.75E-03	1.56E-05	<LOD	<LOD	4.50E-05	0.00E+00	4.50E-05	100
23-56	895	8.15	185	3.14	<LOD	9.50E+00	6.54E-04	8.88E-03	<LOD	<LOD	9.61E-04	8.75E-04	2.55E-03	1.47E-05	<LOD	<LOD	3.48E-05	0.00E+00	3.48E-05	100
23-59	970	8.11	183	3.11	7.68E-04	9.50E+00	5.88E-04	9.55E-03	<LOD	<LOD	7.88E-04	7.43E-04	2.60E-03	1.35E-05	<LOD	<LOD	1.16E-04	0.00E+00	1.16E-04	100

Table 7 Column experiment (pH 9.0) solution outlet compositions prior to As injection.

Sample name	Pore volumes	pH	Eh mV	pe	F mM	Cl mM	SO_4^{2-} mM	Si mM	Na mM	K mM	Ca mM	Mg mM	Al mM	Sr mM	Mn mM	Ti mM	Fetot mM	Fe(II) mM	Fe(III) mM	Fe(III)/FeT %
24-2	3	9.45	113	1.91	2.25E-03	6.50E+00	1.26E-02	2.70E-01	1.19E-01	1.82E-01	7.63E-01	7.76E-01	6.28E-03	1.98E-03	2.13E-05	4.61E-05	5.48E-04	0.00E+00	5.48E-04	100
24-5	6	9.36	116	1.96	5.33E-04	6.50E+00	4.18E-03	1.07E-01	1.19E-02	1.15E-01	3.73E-01	3.17E-01	9.42E-03	1.06E-03	2.10E-05	1.05E-04	7.21E-04	4.52E-04	2.68E-04	37
24-8	10	9.32	124	2.09	5.32E-04	6.50E+00	2.77E-03	6.93E-02	4.72E-03	3.51E-02	2.29E-01	1.77E-01	9.23E-03	6.78E-04	1.96E-05	1.07E-04	8.07E-04	0.00E+00	8.07E-04	100
no icp sample	17	9.34	129	2.19	5.77E-04	nd	1.63E-03	nd	nd	nd	nd	nd	nd	nd	nd	nd	nd	nd	nd	100
24-14	24	9.27	137	2.32	5.23E-04	6.50E+00	1.32E-03	4.11E-02	1.04E-03	2.95E-03	8.95E-02	5.85E-02	1.06E-02	2.97E-04	3.22E-05	8.85E-05	7.63E-04	0.00E+00	7.63E-04	100
24-17	35	9.34	132	2.24	5.26E-04	6.50E+00	1.06E-03	3.60E-02	1.04E-03	<LOD	6.29E-02	3.91E-02	1.14E-02	2.21E-04	3.39E-05	8.89E-05	6.62E-04	0.00E+00	6.62E-04	100
24-20	53	9.18	129	2.19	4.51E-04	6.50E+00	5.74E-04	3.17E-02	7.76E-04	<LOD	4.32E-02	2.43E-02	1.02E-02	1.56E-04	1.92E-05	8.66E-05	6.80E-04	nd	no sample	nd
24-23	85	9.20	141	2.39	5.43E-04	6.50E+00	5.04E-04	2.80E-02	4.37E-03	<LOD	3.27E-02	1.51E-02	9.67E-03	1.11E-04	1.64E-05	8.40E-05	6.17E-04	3.77E-05	5.79E-04	94
24-26	145	9.31	132	2.23	5.11E-04	6.50E+00	5.00E-04	2.56E-02	<LOD	<LOD	1.61E-02	8.80E-03	8.93E-03	7.15E-05	<LOD	5.01E-05	5.71E-04	0.00E+00	5.71E-04	100
24-29	220	9.01	152	2.58	7.38E-04	6.50E+00	5.17E-04	2.34E-02	<LOD	<LOD	9.45E-03	5.63E-03	8.37E-03	4.97E-05	<LOD	5.15E-05	4.23E-04	0.00E+00	4.23E-04	100
24-32	295	9.10	157	2.67	5.80E-04	6.50E+00	5.26E-04	2.09E-02	<LOD	<LOD	6.68E-03	4.05E-03	7.53E-03	3.81E-05	<LOD	3.19E-05	3.16E-04	0.00E+00	3.16E-04	100
24-35	370	9.10	155	2.63	5.63E-04	6.50E+00	6.10E-04	2.18E-02	<LOD	<LOD	6.94E-03	3.27E-03	8.09E-03	3.30E-05	<LOD	<LOD	1.71E-04	4.16E-06	1.67E-04	98
24-38	445	9.20	155	2.63	4.81E-04	6.50E+00	4.67E-04	2.08E-02	<LOD	<LOD	6.02E-03	2.75E-03	6.98E-03	2.86E-05	<LOD	<LOD	2.09E-04	0.00E+00	2.09E-04	100
24-41	520	9.28	151	2.56	7.04E-04	6.50E+00	5.23E-04	1.96E-02	<LOD	<LOD	3.79E-03	2.46E-03	7.50E-03	2.50E-05	<LOD	3.61E-05	3.01E-04	0.00E+00	3.01E-04	100
24-44	595	9.18	154	2.61	6.05E-04	6.50E+00	4.35E-04	2.03E-02	<LOD	<LOD	8.73E-03	2.25E-03	7.42E-03	2.50E-05	<LOD	3.19E-05	4.86E-04	9.38E-05	3.93E-04	81
24-47	670	9.32	161	2.73	6.30E-04	6.50E+00	2.23E-04	1.93E-02	<LOD	<LOD	2.92E-03	1.96E-03	6.22E-03	2.17E-05	2.36E-05	2.83E-05	2.90E-04	0.00E+00	2.90E-04	100
24-50	745	9.09	150	2.55	6.00E-04	6.50E+00	3.78E-04	2.03E-02	<LOD	<LOD	2.46E-03	1.75E-03	6.88E-03	1.93E-05	8.16E-06	<LOD	1.85E-04	5.61E-05	1.29E-04	70
24-53	820	9.10	151	2.55	7.51E-04	6.50E+00	4.33E-04	1.96E-02	<LOD	<LOD	2.53E-03	1.62E-03	6.83E-03	1.78E-05	8.04E-06	3.22E-05	2.23E-03	0.00E+00	2.23E-03	100
24-56	895	9.14	156	2.64	6.04E-04	6.50E+00	4.37E-04	1.74E-02	4.50E-04	<LOD	2.11E-03	1.62E-03	6.58E-03	1.69E-05	<LOD	<LOD	2.28E-04	0.00E+00	2.28E-04	100
24-59	970	9.14	157	2.65	6.81E-04	6.50E+00	6.43E-04	1.80E-02	<LOD	<LOD	1.90E-03	1.27E-03	7.24E-03	1.50E-05	<LOD	<LOD	1.50E-04	2.93E-05	1.20E-04	80

Table 8 Column experiment (pH 10.0) solution outlet compositions prior to As injection.

Sample name	Pore volumes	pH	Eh mV	pe	F mM	Cl mM	SO_4^{2-} mM	Si mM	Na mM	K mM	Ca mM	Mg mM	Al mM	Sr mM	Mn mM	Ti mM	Fetot mM	Fe(II) mM	Fe(III) mM	Fe(III)/FeT %
21-02	3	9.77	86	1.46	4.80E-03	1.50E+00	5.96E-03	4.06E-01	6.85E-01	2.84E-02	2.36E-01	6.70E-02	1.45E-02	1.51E-04	9.36E-05	5.85E-04	4.90E-03	4.68E-03	2.13E-04	4
21-05	6	9.91	86	1.46	1.00E-04	1.50E+00	1.04E-03	2.22E-01	4.56E-02	4.78E-02	1.69E-01	1.28E-01	8.30E-03	2.77E-04	<LOD	1.99E-04	9.03E-04	8.56E-04	4.73E-05	5
21-08	10	9.88	80	1.35	1.13E-02	1.50E+00	7.55E-04	1.75E-01	1.59E-02	4.82E-02	1.60E-01	1.21E-01	8.41E-03	2.82E-04	<LOD	2.64E-04	1.47E-03	1.42E-03	4.87E-05	3
21-11	17	9.91	72	1.22	1.00E-04	1.50E+00	1.46E-04	1.41E-01	2.86E-02	5.20E-02	1.05E-01	8.22E-02	8.67E-03	2.09E-04	<LOD	2.34E-04	6.50E-04	5.89E-04	6.14E-05	9
21-14	24	9.87	82	1.39	2.50E-03	1.50E+00	4.57E-04	1.58E-01	<LOD	3.64E-02	7.55E-02	6.10E-02	1.14E-02	1.55E-04	<LOD	2.20E-04	6.85E-04	4.20E-04	2.65E-04	39
21-17	35	9.86	89	1.51	1.97E-02	1.50E+00	7.09E-04	1.13E-01	<LOD	1.26E-02	5.50E-02	4.44E-02	1.73E-02	1.12E-04	<LOD	3.07E-04	9.32E-04	9.08E-04	2.40E-05	3
21-20	53	9.78	82	1.38	3.80E-03	1.50E+00	<LOD	1.01E-01	<LOD	<LOD	3.91E-02	3.11E-02	1.59E-02	7.97E-05	<LOD	3.02E-04	8.08E-04	7.33E-04	7.49E-05	9
21-23	85	9.77	99	1.68	3.70E-03	1.50E+00	<LOD	9.48E-02	<LOD	<LOD	2.72E-02	2.09E-02	1.73E-02	5.29E-05	<LOD	2.86E-04	6.42E-04	5.12E-04	1.29E-04	20
21-26	145	9.77	99	1.68	2.20E-03	1.50E+00	<LOD	9.72E-02	<LOD	<LOD	1.74E-02	1.50E-02	2.16E-02	2.94E-05	<LOD	3.52E-04	6.26E-04	5.77E-04	4.87E-05	8
21-29	220	9.76	91	1.54	1.00E-03	1.50E+00	<LOD	9.06E-02	<LOD	2.22E-03	1.37E-02	9.20E-03	1.74E-02	2.36E-05	<LOD	3.56E-04	7.08E-04	6.65E-04	4.29E-05	6
21-32	295	9.60	123	2.08	5.24E-02	1.50E+00	2.12E-03	8.38E-02	<LOD	<LOD	1.16E-02	8.30E-03	1.69E-02	1.38E-05	<LOD	4.28E-04	1.54E-03	1.43E-03	1.12E-04	7
21-35	370	9.53	102	1.74	4.70E-03	1.50E+00	0.00E+00	7.87E-02	<LOD	<LOD	8.98E-03	5.96E-03	1.46E-02	<LOD	<LOD	3.40E-04	8.05E-04	7.62E-04	4.25E-05	5
21-38	445	9.47	113	1.91	1.59E-02	1.50E+00	3.45E-04	7.49E-02	<LOD	1.80E-03	4.32E-02	6.82E-03	1.79E-02	1.48E-05	<LOD	4.83E-04	2.00E-03	1.95E-03	5.77E-05	3
no icp sample	520	9.44	109	1.85	1.20E-03	nd	6.00E-06	nd	nd	nd	nd	nd	nd	nd	nd	nd	nd	nd	nd	nd
21-43	595	9.40	111	1.88	0.00E+00	1.50E+00	0.00E+00	6.75E-02	<LOD	<LOD	7.33E-03	3.64E-03	1.41E-02	<LOD	#VALUE!	4.01E-04	9.13E-04	8.89E-04	2.41E-05	3
21-46	670	9.53	108	1.82	2.00E-03	1.50E+00	3.60E-05	6.25E-02	<LOD	5.70E-03	9.56E-03	4.02E-03	1.43E-02	<LOD	7.94E-04	2.70E-04	1.32E-03	1.29E-03	3.08E-05	2
21-49	745	9.49	103	1.75	<LOD	1.50E+00	<LOD	6.51E-02	<LOD	4.03E-03	1.07E-02	3.58E-03	1.31E-02	<LOD	6.87E-05	5.05E-04	1.30E-03	1.27E-03	2.79E-05	2
no icp sample	820	9.44	111	1.88	<LOD	nd	<LOD	nd	nd	nd	nd	nd	nd	nd	nd	nd	nd	nd	nd	nd
21-55	895	9.47	114	1.93	7.00E-04	1.50E+00	2.50E-05	6.33E-02	<LOD	<LOD	6.24E-03	2.79E-03	1.20E-02	<LOD	<LOD	5.14E-04	1.29E-03	1.05E-03	2.40E-04	19
21-58	970	9.35	120	2.03	5.00E-04	1.50E+00	1.19E-04	5.78E-02	<LOD	5.92E-03	8.39E-03	2.82E-03	1.14E-02	<LOD	<LOD	5.71E-04	1.44E-03	1.42E-03	1.85E-05	1

2.2.4 Column experiments for arsenic transport

Basaltic glass (16 g) was packed into a 16 cm long, 1 cm inner diameter PTFE column yielding porosity of 0.45 which was measured by saturating the column with DI water and measure the weight (Figure 2a). Arsenic containing solution was prepared by pipetting 5 ml of 60 mg l^{-1} stock solution into volumetric flask, adding 20 mg of Acid blue 9 which acted as a conservative tracer (Mon et al., 2006) into a 0.5 l volumetric flask and fill to mark with an ammonium chloride solution. Nitrogen gas was purged through the buffers for two hours prior to pumping them onto the column. A peristaltic pump (Cole-Parmer Masterflex) pumped buffer solution at 1 ml min^{-1} to base of column. At stable pH and Eh conditions 4 pore volumes of As containing solution were injected into the column. Finally the column was eluted with 25 pore volumes of As free solution. Outflow of the column was divided to three flow lines were following steps were taken:

1. Continuous pH and Eh measurement by electrodes (Cole Parmer) in flow through cells. The pH/Eh signal was read by Eutech pH 200 series and subsequently recorded by a Campbell CR10X data logger.

2. A conservative tracer was measured online in a flow through cell by Sterilin Instruments Colorimeter. The solution was then pumped onwards to a Thermo Jarrell Ash fraction collector which sampled solutions for total As analysis.

3. Arsenite was measured continuously by Perkin Elmer AAnalyst 300 HG-AAS. For the arsenite measurement, the outlet of experiment (flow rate 0.33 ml min^{-1}) was mixed with 0.2 M Na-citrate (adjusted to pH 5.0 with 4 M HCl) carrier solution (flow rate 0.9 ml min^{-1}) and the mixture subsequently mixed with 1% Na-borohydride and pumped into the HG-AAS allowing for continuous measurement of arsenite and the absorbance value recorded every 1 to 3 minutes. The method was validated by pumping 4 µmol l^{-1} arsenite and arsenate solution directly into the measurement system and the absorbance observed. No increase in absorbance was observed when arsenate was used indicating that reduction was sufficiently limited to conclude that all absorbance in the measurement was due to AsH_3 generated

from arsenite. The total As was analyzed after each experiment in the same way as described in isotherm experiment section above.

2.2.5 **Modeling**

All geochemical modeling was carried out the computer program PHREEQC-2 (Parkhurst and Appelo, 1999) versions 2.11 to 2.15 with the database wateq4f.dat (23rd August 2005) and a graphical interface by V.E.A. Post. The program is based on equilibrium chemistry of aqueous solutions interacting with minerals, gases, solid solutions, exchangers and sorption surfaces, but also includes the capability to model kinetic reactions with rate equations that are completely user-specified in the form of Basic statements. A 1D transport algorithm comprises dispersion, diffusion and various options for dual porosity media. An extensible chemical data base allows application of the reaction, transport and inverse modeling capabilities to almost any chemical reaction that is recognized to influence rain-, soil-, ground-, and surface water quality (Parkhurst and Appelo, 1999).

As mentioned in the introduction As sorption is kinetically controlled (Arai et al., 2004, Arai et al., 2005, O'Reilly et al., 2001). The ability of PHREEQC-2 to implement user defined kinetically controlled reactions made it the preferred choice for this research. The user's guide to PHREEQC-2 gives a general indication of the programs capabilities:

In batch-reaction calculations, PHREEQC-2 is oriented toward system equilibrium rather than just aqueous equilibrium. For a purely equilibrium calculation, all of the moles of each element in the system are distributed among the aqueous phase, pure phases, solid solutions, gas phase, exchange sites, and surface sites to attain system equilibrium. Non-equilibrium reactions can also be modelled, including aqueous-phase mixing, user-specified changes in the elemental totals of the system, kinetically controlled solid-liquid heterogeneous reactions, and to a limited extent kinetically controlled aqueous homogeneous reactions. Kinetically controlled reactions can be defined in a general way by using an embedded Basic interpreter. Rate expressions written in the Basic language are included in the input file, and the program uses the Basic interpreter to calculate rates. Batch reactions allow any combination of solution (or mixture of solutions), gas phase, and assemblages to be brought together, any irreversible reactions are added, and the resulting system is brought to equilibrium. If kinetic reactions are defined, then the kinetic reactions are integrated with an automatic

time-stepping algorithm and system equilibrium is calculated after each time step. The capability to define multiple solutions and multiple assemblages combined with the capability to determine the stable phase assemblage provides a framework for 1D transport modeling. PHREEQC-2 provides a numerically efficient method for simulating the movement of solutions through a column or 1D flow path with or without the effects of dispersion. The initial composition of the aqueous, gas, and solid phases within the column are specified and the changes in composition due to advection and dispersion (Appelo and Postma, 1993) coupled with reversible and irreversible chemical reactions within the column can be modelled.

Any modeling calculations in PHREEQC-2 are carried out by composing a so called input file. This file holds for this research's purposes data blocks that are described in chapters 3 to 5 of this thesis. A full description of the program is provided by Parkhurst and Appelo (1999). Examples are provided for each data block if necessary. All text that follows a # sign is for explanation only and is not read by the computer program.

2.2.5.1 Kinetics

A kinetic data block defines the amount and stoichiometry of a kinetic reactant. The duration of reaction steps is furthermore defined here.

Table 9 Definition of basaltic glass in a batch reactor

```
KINETICS 1
BG_Stapafell    #name of kinetic reactant
-formula  Si 1.000 Ti 0.024 Al 0.358 Fe0.188 Mg 0.281 Ca 0.264 Na 0.079 K0.008 P0.004 O3.380
    1 # during one kinetic step the elements are released in these ratios
-m 0.03 #moles of reactant in each kinetic cell.  Each time step, this changes as reactions proceed
 -m0      0.03 # inital moles of kinetic reactant in each cell
-step 86400 in 1440 steps  #Duration of reaction, 86400 seconds in 1440 steps.  This would describe
    a closed batch reaction that occurs over 24 hours and each reaction step is allowed to proceed for
    60 seconds.
```

Table 10 Definition of a surface that is created when As is sorbed

```
KINETICS 1
  Sorb_pseudo2ndorder_arsenic # name of kinetic reactant
  -formula  As   1 # During kinetic steps the  elements change according to the numbers
  -m0    0 #initial moles of Sorb_arsenic (no arsenic is sorbed and therefore the reactant sorb_arsenic
    is not available initially
  -tol 1e-8 # tolerance for calculations
```

2.2.5.2 Rates

A rate expression describes either the process of basaltic glass dissolution or the sorption process of As on the basaltic glass surface.

Table 11 Description of bulk basaltic glass dissolution (Gislason, Oelkers 2003).

```
RATES

BG_Stapafell# name of rate expression that describes the change for kinetics data block with same
    name
-start
10 A0 = 12000    #cm2 g-1 Specific surface area of basaltic glass in each kinetic cell (1 gram of glass)
20 area = (M/M0)^(2/3)*A0    #describes the change in surface area as reaction proceeds
30 EA = 25500  # Activation energy or reaction J mole-1
40 AA = 2.512e-006 # rate constant mole Si cm-2 sec-1 (Gislason and Oelkers, 2003)
50 sr_BG = SR("Stapafell")# Saturation ratio of basaltic glass is dependent of the saturation ratio of the
    phase "Stapafell"  which is the leached layer of basaltic glass.
60 if (M<=0) then goto 200 #if all BG Stapafell has dissolved then go directly to end of calculation
70 R = 8.3144         #Universal gas constant )J mole-1 K-1=
80 T = 298.15       #Temperature (K)
90 rate_const = AA*EXP(-EA/(R*T)) # rate constant for the reaction
100 DF = ((ACT("H+")^3)/(ACT("Al+3")))^(1/3) # driving force for the reaction
110 BF = (1-sr_BG) # braking force of the reaction
120  rate = area*rate_const*DF*BF #overall rate of reaction
130 moles = rate*TIME # change in moles during each reaction step
200 SAVE moles
-end
```

Table 12 Description of two models describing As sorption onto basaltic glass

```
#Model 1.  Pseudo second order model (Ho, Mckay 1999)
RATES
Sorb_pseudo2ndorder_arsenic # name of rate expression that describes the change for kinetics data
    block with same name

-start
10 k = 240 #kg mol-1 sek-1, Empirical constant derived from kinetic batch experiment.  This coefficient
    needs to be scaled according to the difference in fluid rock ratio between the experiment where it
    was derived from and the system that is to be modelled.
20 ct = tot("As")#mol kgw #definition of the concentration of As at each reaction step
30 qmax = 5.05e-6 #moles kg-1.  Maximum adsorption according Langmuir isotherm fitted to batch
    experiment.  This coefficient also needs to be scaled according to fluid rock ratio.
40 KL = 8.7e4 # mole l-1.  Langmuir constant derived from batch isotherm experiment.
50 qe = (qmax *KL* ct) /(1+(KL * ct))# Langmuir eq. to describe the equilibrium concentration at each
    reaction step
60 dif = qe – m # this line is only to define the difference between equilibrium concentration and the
    amount of As sorbed (m) at the surface of the glass.
70  rate_forward = -k * (dif)^2 #Pseudo second order model (Ho and McKay, 1999) describing
    adsorption.
80 if dif < 0 then rate_forward = -rate_forward # this section is inserted to describe desorption.  This
    means that As desorbs from the surface if the concentration on the surface exceeds the equilibrium
    sorption concentration.  This occurs when As-free solution is introduced into a system that had
    previously reacted with As-solutions.
90 moles = rate_forward   *time
```

```
100 SAVE moles
-end

#Model 2.  Dynamic Langmuir kinetic model (Langmuir, 1908)
Sorb_dynamic_langmuir_arsenic
-start
10 k_forward = 1.15   #l mol-1 s-1
20 ct =tot("As") #mol kgw-1
30 if ct <1e-9 then goto 70
40 KL = 54100#69400 # l mol-1   Derived from Langmuir isotherm experiment and used to calculate kd
    after ka has been found, that is KL =ka/kd
50 qmax = 2.21e-5#*20# mol l-1  Derived from Langmuir isotherm experiment
60 k_backward = 0.0000213 # s-1
70 theta =m/qmax   #unit less ratio
#Langmuir kinetic model
80 rate = (-k_forward *tot("As")*(1- theta) +(k_backward * theta))*qmax
90 moles = rate * time
100 SAVE moles
-end
```

2.2.5.3 Surface

Used for surface complexation modeling. Surface complex reactions can be inserted into the database. The surface is then described by the keyword Surface.

Table 13 Surface data block for a HFO surface

```
SURFACE 1

-sites DENSITY # Site density is used to describe the surface
Hfo_wOH 3.8     600     0.217# A HFO surface with weak sites.  3.8 sites nm-2, specific surface area is
    600 m2 g-1 and mass of the surfaces reactant is 0.217 g.

end
```

2.2.5.4 Transport.

A description of the transport process in a column experiment, this section describes the size and boundary conditions of the column, the flow conditions and the time duration of each kinetic step. The time step described under *transport* overrides the time definition in *kinetics* data block.

Table 14 Transport data block for 16 cm column that has been divided into four parts.

```
TRANSPORT
-cells 4 # number of cells that column is composed of
-length 0.04 m #length of cells in meters
-shifts 4000 #one thousand pore volumes displaced since one pore volume is 4 shifts
-disp 0.014 # dispersivity of material calculated from a breakthrough curve of a conservative tracer
-diffc 0 #assume no diffusion
-time 120 seconds # each reaction is allowed to proceed for 120 seconds
```

```
-punch_c  4 # record the results from the final cell of column (outlet) after each reaction step.  These
    results will be shown on graph or punched into a data file.
```

2.2.5.5 User_graph.

A data block to construct a graph of the data as modeling is carried out.

Table 15 USER_GRAPH data block to show concentration in a column along a horizontal distance

```
USER_GRAPH
 -heading pv/ 1_m_cell
 -axis_scale x_axis 0 4
 -axis_scale y_axis 0 1
 -axis_titles PV c/c0
 -chart_title
 -initial_solutions false  01
 -plot_concentration_vs x
-start
10 graph_x dist
 20 graph_y tot("As")
-end
```

Table 16 USER_GRAPH data block to show outlet concentration of a column as reactions proceed

```
USER_GRAPH
-heading pv/ Arsenite
 -axis_scale x_axis 0 30 5 1 #The graph will show 30 pore volumes (PV) and place a label every  5 PV
    and place a tick every PV
 -axis_scale y_axis 0 1
 -axis_titles PV c/c0
-initial_solutions false  01 #Do not plot before transport initiates
 -plot_csv_file C:\As3pH3.csv # The program plots experimental data for fast comparison with
    modelled results
 -plot_concentration_vs time
 -start
 10 graph_x (step_no +0.5)/ cell_no
 20 graph_y  tot("As") / 4e-6 # this gives C/Co since the concentration of inlet solution was 4 µmole l-1
-end
```

2.2.6 Field measurements

2.2.6.1 Field sampling

Samples were pumped directly from respective source (well, spring or stream) by a peristaltic pump (Cole Parmer Masterflex E/S portable sampler) through a High Density Polyethylene (HDPE) cooling loop followed by a 0.2 µm cellulose acetate (CA) filter (Advantec MFS) enclosed in a HDPE housing. Samples from wells were extracted 2 m below the water table. All bottles were pre-rinsed with filtered water prior to sample

collection. Sample for As and anion speciation was directed into a 10 ml gas tight syringe and injected into a Dionex ICS-2000 anion exchange chromatograph (AEC) coupled to a PSAnalytical hydride-generation atomic fluorescence spectrophotometer (HG-AFS) immediately on sampling as the analytical equipment was field deployed. Then sample was directed through the cooling loop into a pH/Eh flow cell and pH and Eh recorded respectively (Cole Parmer combination gel filled electrode for pH and Pt-electrode for Eh with Eutech pH200 displays). Temperature of the pH/Eh flow-cell was set as close to 25°C by adjusting the sample flow rate through the cooling loop. Then 60 ml for total carbonate carbon (TCC) was pumped into an amber glass bottle and filled completely before being sealed with an air tight cap. Sample was then pumped into a 50 ml HDPE bottle and 0.5-7.5 ml of sample pipetted to a 15 ml HDPE bottle for determination of H_2S. The remainder in the 50 ml bottle was preserved to 1% 6 N HCl for the determination of ferric and ferrous iron. Another 50 ml HDPE bottle was filled for total As measurement and sample pH increased to >10 by the addition of 1.0 N NaOH followed by the addition of 0.5 mL of 30% H_2O_2. After 30 min, HCl was used to acidify sample to pH<2 (Beak et al., 2008). After that, 50 ml HDPE bottle was filled and acidified to 0.5% by concentrated $HNO_3$for the analysis of major constituents and selected minor constituents. Finally, sample for further As-speciation analysis was pumped into two 15 ml HDPE bottles which were immediately frozen in dry-ice.

2.2.6.2 Analytical methods from field measurements

Major and some minor constituents were measured on by Spectro Ciros Vision Inductively Coupled Plasma Atomic Emission Spectrometer (ICP-AES).

Arsenic species (arsenite, arsenate, mono-, di-, tri- and tetrathioarsenate) and the anions F^-, Cl^-, SO_4^{2-}, $S_2O_3^{2-}$ were separated according to Planer-Friedrich et al. (2007). Briefly a Dionex ICS-2000 with self generated eluent cartridge separated and detected, anionic species and the HG-AFS detected species that contained As (Table 17). The As concentration for each individual species was quantified with HG-AFS as opposed to ICP-MS, as the instrumentation was field deployed. Total As was measured by HG-AFS according to (PSAnalytical, 1997). Total carbonic carbon was measured by AEC according to (Stefansson et al.,2007). Iron speciation was carried out with Metpac^{TM} PCDA eluent on a Dionex ICS-3000 according to Dionex technical note 10 (Dionex). Alterations to the method were: a 1 ml injection loop was used to increase sensitivity and 4-(2-pyridylazo) resorcinol (PAR) was halved to 60 µg l^{-1}. Total As was analysed

in HNO_3 acidified samples from Reykjavik Energy archives, covering the time period1991-2008 and few samples sampled prior to 1990. The method was according to (PSAnalytical, 1997).

Table 17 Instrumental setup for the detection of arsenic oxy- and thioanions by AEC-HG-AFS. The speciation procedure was adopted from Planer-Friedrich et al. (2007).

Anion Exchange Chromatography (AEC) separation		
Instrument	**DIONEX ICS-2000**	
Column	IonPac AS-16/AG-16 4-mm (10-32) (Dionex, Sunnyvale, CA)	
Eluent Gradient	KOH, Automated eluent generation at 1 ml/min 0 → 7 min 20 mmol/l 7 → 17 min 20 → 100 mmol/l 17 → 25 min 100 mmol/l 25 → 28 min 100 → 20 mmol/l	
Sample volume	100 µl	
Typical retention times	arsenite	271 s
	arsenate	693 s
	monothioarsenite	777 s
	dithioarsenite	861 s
	trithioarsenite	948 s
	tetrathioarsenite	1039 s
Supression	ASRS-Ultra 4-mm (Dionex, Sunnyvale, CA) 300 mA current, 5 ml min-1 water, (external mode)	
Hydride Generation Atomic Fluoresence Spectroscopy (HG-AFS) detection		
Instrument	**PSAnalytical Millenium Excalibur**	
Reductant	12,5% HCl, red-red tubing, pump 50% 0.7% $NaBH_4$ in 0.1 M NaOH, grey-grey tubing, pump 100%	
Carrier gas	Ar (5.0 grade), flow rate 300 ml/min	
Gas / liquid separator	Type ME Gas/liquid separator	
Air dryer	Permapure dryer system Dryer gas, Ar, flow rate 2.5 l/min	
Lamp	Boosted discharge hollow cathode lamp (BDHCL) Primary current 27.5 mA Boost current 35.0 mA	

2.3 References

Arai, Y., Sparks, D.L. & Davis, J.A. 2005, "Arsenate adsorption mechanisms at the allophane - water interface", *Environmental science & technology,* vol. 39, no. 8, pp. 2537-2544.

Arai, Y., Sparks, D.L. & Davis, J.A. 2004, "Effects of dissolved carbonate on arsenate adsorption and surface speciation at the hematite-water interface", *Environmental science & technology,* vol. 38, no. 3, pp. 817-824.

Beak, D.G., Wilkin, R.T., Ford, R.G. & Kelly, S.D. 2008, "Examination of arsenic speciation in sulfidic solutions using X-ray absorption spectroscopy", *Environmental science & technology,* vol. 42, no. 5, pp. 1643-1650.

Dionex
Determination of Transition Metals by Ion Chromatography, Dionex.

Masscheleyn, P.H., Delaune, R.D. & Patrick, W.H. 1991, "A Hydride Generation Atomic-Absorption Technique for Arsenic Speciation", *Journal of environmental quality,* vol. 20, no. 1, pp. 96-100.

Mon, J., Flury, M. & Harsh, J.B. 2006, "Sorption of four triarylmethane dyes in a sandy soil determined by batch and column experiments", *Geoderma,* vol. 133, no. 3-4, pp. 217-224.

Oelkers, E.H. & Gislason, S.R. 2001, "The mechanism, rates and consequences of basaltic glass dissolution: I. An experimental study of the dissolution rates of basaltic glass as a function of aqueous Al, Si and oxalic acid concentration at 25 degrees C and pH=3 and 11.", *Geochimica et Cosmochimica Acta,* vol. 65, no. 21, pp. 3671-3681.

O'Reilly, S.E., Strawn, D.G. & Sparks, D.L. 2001, "Residence time effects on arsenate adsorption", *Soil Science Society of America Journal,* vol. 65, no. 1, pp. 67-77.

Parkhurst, D.L., Appelo, C.A.J. 1999, *User's guide to PHREEQC (Version 2)- A computer program for speciation, batch-reaction, one-dimensional transport, and inverse geochemical calculations*, US Geological Survey.

PSAnalytical 1997, *PSA Application note no. 11. Millennium Excalibur method for arsenic in drinking, surface, ground, saline and industrial and domestic waste waters*, PSAnalytical, Orpington, UK.

Riekie, G.J., Williams, P.N., Raab, A. & Meharg, A.A. 2006, "The potential for kelp manufacture to lead to arsenic pollution of remote Scottish islands", *Chemosphere,* vol. 65, no. 2, pp. 332-342.

Stefansson, A., Gunnarsson, I. & Giroud, N. 2007, "New methods for the direct determination of dissolved inorganic, organic and total carbon in natural waters by Reagent-Free™ Ion Chromatography and inductively coupled plasma atomic emission spectrometry", *Analytica Chimica Acta,* vol. 582, no. 1, pp. 69-74.

3 Regulation of Arsenic mobility on basaltic glass surfaces by speciation and pH.

Bergur Sigfusson[1,2], Andrew A. Meharg[1] and Sigurdur R. Gislason[2]

1) School of Biological Sciences, University of Aberdeen, AB243UU, Aberdeen, UK

2) Institute of Earth Sciences, University of Iceland, 101 Reykjavik, Iceland

Corresponding author: Bergur@raunvis.hi.is (Bergur Sigfusson)

Environmental Science and Technology, 2008, 42(23), pp. 8816-8821.

Description of work of individual authors:
Bergur Sigfusson designed and built all the experimental apparatus exept the analytical instruments, sampled and analysed all samples, wrote the manuscript, constructed the geochemical models and corresponded to the journal.
Andrew A. Meharg advised mainly on the writing of the manuscript and the development of analytical methods for speciation.
Sigurdur R. Gislason advised mainly on the writing of the manuscript and design of the experimental columns.
Other contributors are thanked in the acknowledgements.

Abstract

The importance of geothermal energy as a source for electricity generation and district heating has increased over recent decades. Arsenic can be a significant constituent of the geothermal fluids pumped to the surface during power generation. Dissolved As exists in different oxidation states, mainly as As(III) and As(V), and the charge of individual species varies with pH. Basaltic glass is one of the most important rock types in many high-temperature geothermal fields. Static batch and dynamic column experiments were combined to generate and validate sorption coefficients for As(III) and As(V) in contact with basaltic glass at pH 3 to 10. Validation was carried out by two empirical kinetic models and a surface complexation model (SCM). The SCM provided a better fit to the experimental column data than kinetic models at high pH values. However in certain circumstances an adequate estimation of As transport in the column could not be attained without incorporation of kinetic reactions. The varying mobility with pH was due to the combined effects of the variable charge of the basaltic glass with the pH point of zero charge at 6.8 and the individual As species as pH shifted, respectively. The mobility of As(III) decreased with increasing pH. The opposite was true for As(V), being nearly immobile at pH 3 to being highly mobile at pH 10. Incorporation of appropriate sorption constants, based on the measured pH and Eh of geothermal fluids, into regional groundwater-flow models should allow prediction of the As(III) and As(V) transport from geothermal systems to adjacent drinking water sources and ecosystems.

3.1 Introduction

Arsenic is released from soil and geothermal environments into ground waters through natural processes and anthropogenic activities *(1,2,3)*. There are many pathways for As to threaten human health via polluted ground- or surface waters *(2,4)*. Speciation of As is the most important factor controlling its toxicity, bioavailability and mobility, depending mainly on the environmental parameters such as pH and redox potential *(2)*. Arsenic is mostly present in aqueous environments in +III and +V oxidation states as arsenite and arsenate oxyanions and their hydrolysis species, respectively (Fig. 1) *(2,5)* with minor amount of methyl and dimethyl As compounds being detected in some systems (6). As(V) forms the negatively charged oxyanions $H_2AsO_4^-$ and $HAsO_4^{-2}$ at pH values above 2 and 7, respectively, while As (III) forms the uncharged oxyanion H_3AsO_3 at a pH up to around 9 (pKa= 9.2) *(7)*. Recently the importance of thioarsenates in sulfidic geothermal waters has been reported as it has been found to be as high as 83% dissolved As under alkaline conditions *(8)*.

The aqueous redox reactions of As are slow without some form of catalyst *(9)*. Oxidation of As(III) is frequently facilitated by reduction of Fe(III), and the reduction of As(V) by oxidation of sulfides *(10)* with redox processes accelerated by up to 5 orders of magnitude in geothermal waters by microbial activity *(11)*. Knowledge of the kinetics of redox reactions between the individual As species can therefore play an important role when quantifying sorption processes and As transfer. The variable charges of the As species and the interacting surfaces lead to variable adsorption and retention of the respective species relative to groundwater flow. Accurate determination of the speciation of As in natural water is therefore fundamental to predict its transport in the environment.

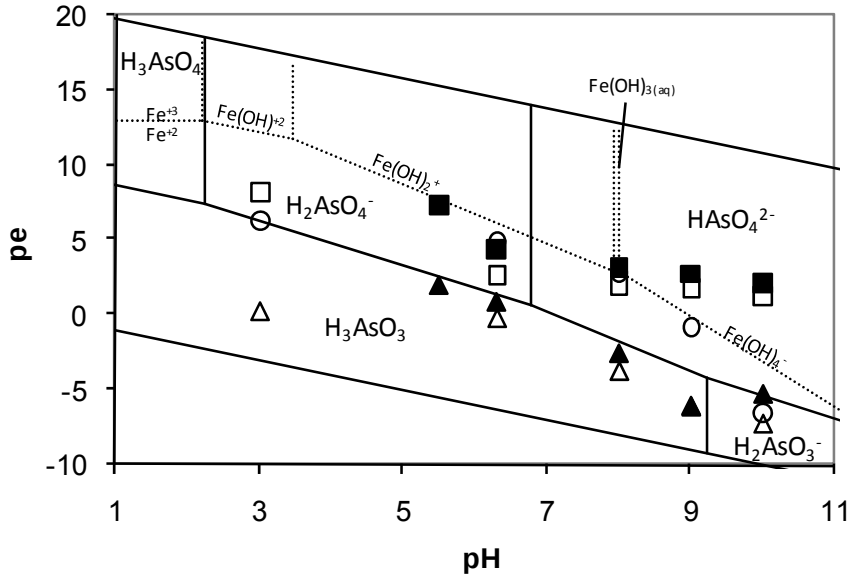

Figure 1 Thermodynamic system of As oxyanion species in water (7). Superimposed are Fe species with $Fe(OH)_3$(s) under saturated. The As species have anticipated increased mobility in basaltic glass media in the following order: $H_2AsO_4^-$<H_3AsO_4≈H_3AsO_3<H_2AsO_3-<$HAsO_4^{2-}$. Open symbols represent conditions in column experiments, closed symbols represent batch experiments. Squares represent measured pe, circles are pe calculated from Fe(II)/Fe(III) redox couple, and triangles are pe calculated from As(III)/As(V) redox couple.

Continental flood basalts cover an important fraction of the terrestrial surface *(12)*. Arsenic concentration in terrestrial basaltic rocks ranges from 0.18 to 113 mg kg^{-1}, with an average concentration of 2.3 mg kg^{-1} *(2)*. Examples include the Columbian river basalts in the US, the Deccan traps in India and the Siberian traps in Russia. Furthermore, the ocean floor is primarily composed of basalt *(13)*. Geothermal activity is frequently associated with basalt that can either be glassy or crystalline in volcanic terrains *(14)*. Knowledge of As movement in basaltic environments, therefore, plays a key role in quantifying the global As cycle. Since Iceland is mainly composed of basaltic rocks where active seafloor spreading coincides with the occurrence of upwelling mantle plume resulting in intense volcanism *(15)*, it constitutes a prime study area for understanding the role and movement of As in the environment. This geological situation leads to the widespread occurrence of high-temperature geothermal systems, some of which are currently utilized for power generation *(16)*. Hydrothermal fluids, often As enriched *(17)*, are pumped to the surface, where heat is extracted and electricity generated before these fluids are either pumped back into the crust through boreholes or released to adjacent surroundings. The subsequent fate of arsenic in

geothermal waters raised to the surface is not fully known and there is concern that arsenic may be mobile in groundwater systems where basalt and basaltic glass are the main rock constituents *(18)*.

The surface sites of basaltic glass can be considered as >SOH (where >S signifies any –OH binding atom at the surface site) that can either accept proton represented by the reaction:

$$> SOH + H^{+}_{(aq)} \leftrightarrow > SOH^{+}_{2} \qquad \text{Eq. 1}$$

associated with the intrinsic equilibrium constant $K_{S,1}$ or donate proton to the solution represented by the reaction:

$$> SOH \leftrightarrow > SO^{-} + H^{+}_{(aq)} \qquad \text{Eq. 2}$$

associated with the equilibrium constant $K_{S,2}$. The equilibrium constants $K_{S,1}$ and $K_{S,2}$ differ between the respective surface sites and consequently the point of zero charge of the surface site mixture. The chemical composition of the basaltic glass is primarily Si with lesser amounts of Al and Fe on a molar basis with Si and Al, and to a lesser extent Fe(III), as the network forming elements, and with Fe(II) occupying the space within the network *(19)*. Therefore, the surface may be assumed to consist primarily of silanol sites followed by aluminol sites and to a lesser extent amorphous Fe(III) hydroxide sites.

Mobility of key As species in thermodynamic equilibrium in groundwater conditions in contact with basaltic glass with a point of zero charge at pH 6.8 *(20)* can be predicted by studying Fig. 1*(7)*. Under reduced conditions the main As(III) species has -1 charge above 9.2 and is, therefore, repelled from the surface. Below pH 9.2 the species is uncharged and should, therefore, have some degree of mobility. At oxidized conditions at pH levels below 2, the dominant As(V) species is uncharged and should have high mobility. Between pH 2 and 6.8 the charges of the main species and surface sites are opposite and As(V) should be immobile at pH 3, but increasingly mobile as the pH rises and the positive charge on the surface is decreased. Above pH 6.8 the dominant As(V) species is -2 charged and is, therefore, repelled from the surface sites.

Adsorption of As(III) was predicted to be small on am-SiO_2 *(21)*. Increased adsorption of As(III) on surface sites of illite, ferrihydrite, goethite and am-$Al(OH)_3$, respectively, was observed from pH 4 to 9; however, adsorption declined on ferrihydrite, goethite, am-$Al(OH)_3$ above pH 9 *(22, 23, 24, 25)* a finding that corresponds closely to the first pKa (9.2) of H_3AsO_3. Adsorption of As(V) was

predicted to be small on am-SiO_2 *(21)*. Arsenic(V) was decreasingly sorbed on ferrihydrite *(23)* and am-$Al(OH)_3$ *(25)* as pH increased from 3 to 10.

The goal of this study was to predict the transfer of As oxyanions through basaltic glass media, a significant constituent of aquifers in geothermal areas and continental flood basalt areas. The main objectives were to (i) determine the rate and extent of As(III) and As(V) adsorption on the basaltic glass surface at pH 3 to 10, and (ii) predict whether and how As(III) and As(V) will move from high-temperature geothermal waters into shallow groundwater environments.

3.2 Experimental section

3.2.1 Materials and Chemicals

The chemical reagents used in this study were of reagent grade. The reagents $NaAsO_2$, $Na_2HAsO_4.7H_20$, NaOH and $Na_3C_6H_5O_7$ (Trisodium citrate) were obtained from BDH Chemicals. Ascorbic acid, and KI were obtained from Acros organics**.** $NaBH_4$ and $C_{37}H_{34}Na_2N_2O_9S_3$ (Acid Blue 9) were obtained from Sigma Aldrich Chemical Co.

The basaltic glass used in experiments was obtained from the volcanic ash of Stapafell mountain, southwestern Iceland *(19)*. Preparation of the glass was carried out according to (25) except that the 125-250 μm size fraction was used in the current contribution. The specific surface area (1.533 $m^2\ g^{-1}$) of the glass was measured by the three-point BET method using Kr gas.

3.2.2 Test solutions

Initial column and batch experiments solutions were adjusted to pH values of 3, 6.3, 8, 9 and 10 and ionic strength of 10 mM by varying concentrations of HCl, NH_4Cl and NH_4OH *(19)* (Table S1). These solutions were purged for two hours with grade 5.0 N_2 gas (BOC gases, Aberdeen) and all batch experiments were prepared and carried out in a N_2 filled glove box. Detailed description of the experimental procedures can be found in the SI.

3.2.3 Batch kinetic/equilibrium experiments.

Stock As solutions (60 mg L^{-1}) were prepared by weighing $NaAsO_2$ and $Na_2HAsO_4.7H_2O$ daily into a 0.5 L volumetric flask and dissolved in DDI water for As(III) and As(V) solutions, respectively.

For kinetic experiments, 20 ml of 4 μM As(III) and As(V) solutions of desired pH were dispensed into 50 mL centrifuge bottles containing 2g of basaltic glass. The samples were then shaken at 170 rpm at 30°C (±0.1°C) for 24, 8, 4, 1.5, 0.67, 0.2 and 0.1 hours on an incubated shaker (MaxQ mini, Barnstead International).

For isotherm experiments, solutions of desired pH with As concentrations of 0.667, 1.33, 4.00, 8.01 and 16.0 μmol L^{-1}, respectively, were dispensed into 50 mL centrifuge bottles containing 2 g of basaltic glass. The samples were shaken at 170 rpm at 30°C (±0.1°C) for 24h. All solutions were analyzed for As(III) by an optimized HG-AAS method *(26)* for FIA-HG-AAS and total As with FIA-HG-AAS. The As(III) method was cross validated on randomly selected samples with HPLC-ICP-MS *(27)* and the As(III)/As(V) speciation results concurred between the two techniques (Table S2). All As analyses were compared against the SLRS-4 Certified Reference Material. All experiments were carried out in triplicate.

3.2.4 **Column experiments**

Basaltic glass (16 g) was packed into a 16 cm long, 1 cm inner diameter PTFE column providing a porosity of 0.45 (Fig. S2). An As containing solution was prepared by pipetting 5 ml of 60 mg/L stock solution into a volumetric flask, adding 20 mg of Acid blue 9 that acted as a conservative tracer *(28)* into a 0.5 L volumetric flask and filling to the mark with solution of desired pH. Nitrogen gas was purged through the inlet solutions for two hours before pumping them onto the column. A peristaltic pump (Cole-Parmer Masterflex) pumped 1000 PV of inlet solution at 1 mL min^{-1} into the base of the column. During this period, chemical composition, pH and Eh were monitored At stable outlet pH conditions of 3.0, 6.4, 8.1, 9.1 and 9.5(±0.1) for initial the pH 3, 6.3, 8, 9 and 10 values, respectively, 4 pore volumes of As containing the inlet solution were injected into the column. Finally, the column was eluted with 25 pore volumes of As-free inlet solution. A detailed description of the measurement procedure of the outlet solutions may be found in the SI. The low amount of sulfate (<0.6 μg L^{-1}) and absence of sulfide in the outlet solutions due to the low concentration of sulfur (S) in the basaltic glass ensured a minimum effect of As-S species during the experimental procedure.

3.3 Results and discussion

3.3.1 Redox state of experiments

The discrepancy between the measured pe with a platinum electrode and the calculated pe from measured redox couples As(III)/As(V) and Fe(II)/Fe(III) indicated a lack of system redox equilibrium, which has been attributed to the slow conversion between the two oxidation states *(9)*. Arsenic(V) as the initial species in the experiments, was never reduced to As(III). In the batch experiments As(III) was partially oxidized to As(V) and nearly reached equilibrium at pH 10 (Fig. 1, Table S4). In the column experiments, As(III) was not oxidized (Fig. 1) and the Fe redox couple indicated the dominance of Fe(II) oxidation to $Fe^{III}(OH)_2^+$(aq), $Fe^{III}(OH)_3$ (aq), $Fe^{III}(OH)_4^-$ except at pH 3 and 10 where Fe^{+2} was the dominant species.

3.3.2 Batch adsorption experiments

In the batch experiments, the pH increased within hours from pH 3 to pH 5.5. Batch experiments carried out at an initial pH 3 value will therefore be referred to as pH 5.5 from this point on and cannot be used to predict As transport in columns at pH 3. The pH shift could have been the result of initial fast basaltic glass dissolution at pH 3 *(29)* leading to increased pH and subsequent formation of am-Al and am-Fe(III) hydroxides that would adsorb the As(III) in solution at pH 5.5 and generate the discrepancy between experimental and modelled results at pH 3 (5.5). The column experiments, however were carried out at pH 3.0 due to the pre-experimental extended flushing period that was characterized by an initial fast rise to pH 6, which was then followed by a stepwise drop in pH values to pH 3.0 with the surface Si:Al:Fe chemical composition not differing from the fresh basaltic glass (Table S3, Fig. S3).

The kinetics of adsorption was analyzed according to the second order kinetic model *(30)* and a dynamic Langmuir kinetic model *(31)*. The pseudo second order model was represented as:

$$\frac{dq_t}{dt} = k(q_e - q_t)^2 \qquad \text{Eq. 3}$$

where t is time, k is the rate constant of sorption (kg sec mol^{-1}), q_e is the amount of soluted As adsorbed at equilibrium (mol kg^{-1}) and q_t is the amount of As sorbed on the surface at any given time (mol kg^{-1}). Derivation of the second order kinetic constants may be found in the SI.

The dynamic Langmuir kinetic model was represented as:

$$\frac{dq}{dt} = k_a(C_0 - q_m\Theta)(1-\Theta) - k_d\Theta \qquad \text{Eq. 4}$$

where k_a is the first order constant for adsorption, C_0 is the initial solute concentration (mol L^{-1}), q_m is the maximum amount of adsorbate (mol kg^{-1}) (derived from experimental data described in the next section), θ is the fraction of covered surface and k_d is the first order rate constant for desorption. The kinetic Langmuir constants were derived by a method described in the supplementary information section SI. The constants from kinetic experiments are tabulated in Table S5. The pseudo-second-order model showed better fit to the data than the dynamic Langmuir model (Figs. 2a,b). The Langmuir model could not simulate the fast initial sorption rate; hence the deviation from the initial data points in Figs. 2a and 2b. This deviation was also evident for the pseudo second order model when the rate constant for the overall sorption (k) was used (Figs. 2a,b).

The equilibrium adsorption isotherm data at varying pH were analyzed using the Langmuir adsorption expression:

$$q_e = \frac{q_m K_L Ce}{1 + K_L C_t} \qquad \text{Eq. 5}$$

where q_e (mol kg^{-1}) is the amount of adsorbed As at equilibrium, q_m (mol kg^{-1}) is the maximum adsorption capacity corresponding to complete monolayer coverage, C_e (mol L^{-1}) is the equilibrium solute (As) concentration, K_L is the Langmuir constant related to the energy of sorption (L mol^{-1}) and C_t is As concentration As in solution at time t. The Langmuir parameters were obtained by nonlinear least-squares regression analysis on experimental data using the computer program Excel (Microsoft) (Figs. 2c,d) and are summarized in Table S5.

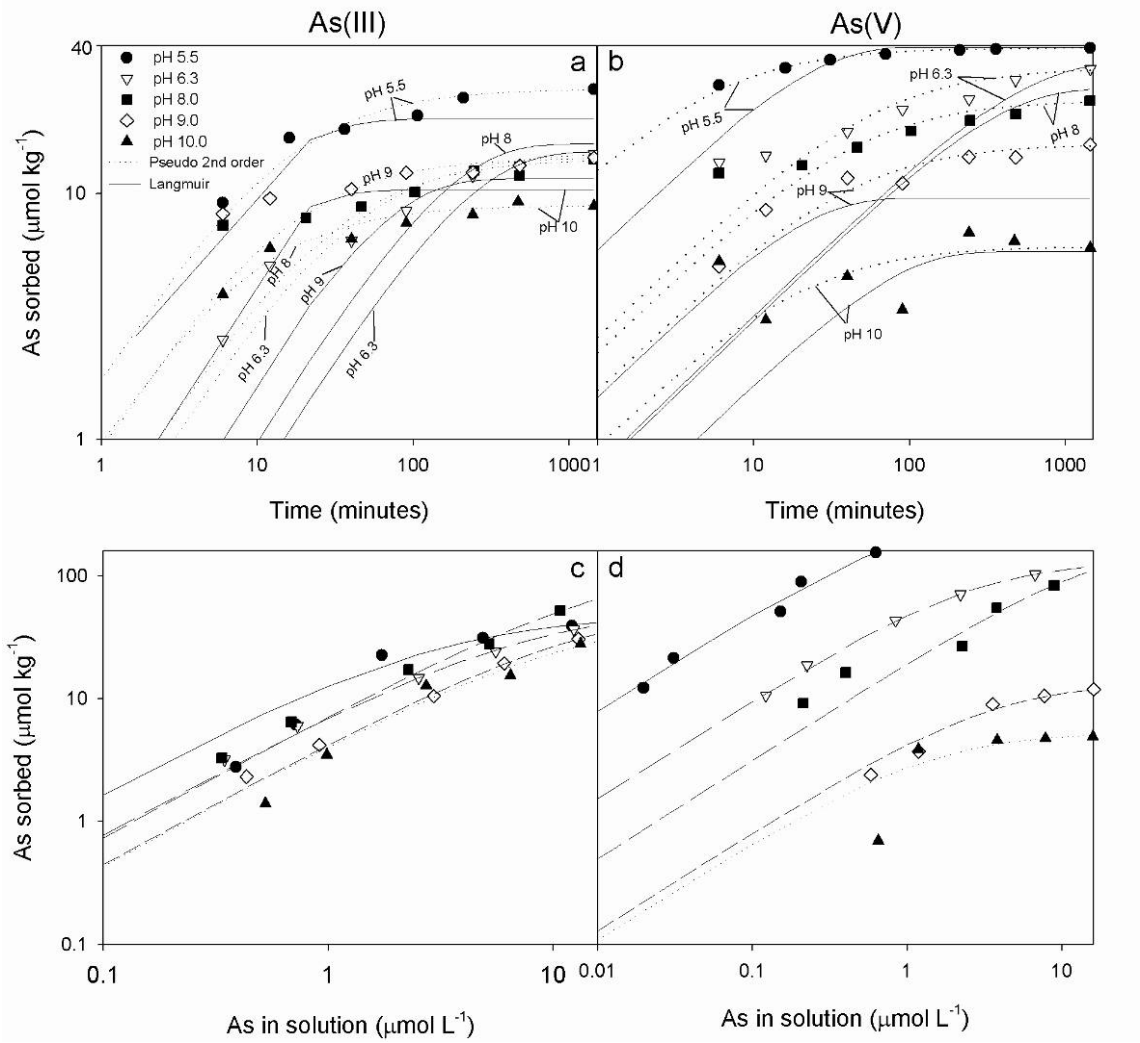

Figure 2 Kinetic adsorption experiments of 4 μmol L^{-1} As(III) and As(V) (b) and adsorption isotherm experiments for As(III) (c) and As(V) (d) onto basaltic glass. A complete sorption was 40 μmol kg^{-1}. Fit to the pseudo-second- order model (dotted lines) and dynamic Langmuir model (solid lines) respectively on Figs. a and b. Fit to Langmuir isotherm model is represented as incremented lines on Figs. c and d. Adsorbent dose 2g 20 mL^{-1}, ionic strength 0.01 M, temperature 30°C.

The equilibrium adsorption data were further analyzed with the generalized two layer model *(32)* incorporated into PHREEQC-2 (33). The surface in the surface complexation model (SCM) was considered to be a mechanical mixture of silanol, aluminol and amorphous Fe sites (34) in ratios equivalent to the Si, Al and Fe(III) ratios of the basaltic glass and surface site density as 1 μmol g^{-1} (Table S6). With this methodology, $\log_{ks,1}$, $\log_{ks,2}$ (5.56, -7.89, respectively) from eq.s 1 and 2 were calculated based on a consistent database for a triple layer model *(21,34).* The intrinsic equilibrium constants for H_3AsO_3 and H_3AsO_4 adsorption reactions were estimated from isotherm experiments by iteratively optimizing experimental curves to the SCM by minimizing

the differences between calculated and experimental adsorption data. Two surface reactions were assigned for As(III), formation of the bidentate inner sphere complex and the monodentate outer sphere complex *(35)* and two bidentate inner sphere complexes and one monodentate inner sphere complex for As(V) *(36)*, respectively. By using the SCM, the effect of varying Cl^- concentrations in the solution could be estimated and incorporated into the model (Table S6) and competitive sorption was diminishing except at pH 3 where Cl-surface complexes formed.

3.3.2.1 As(III)

For all pH treatments (except pH 6.3 treatment), sorption sites were saturated with As(III) within 8 h with less than 40% As(III) sorption (Fig 2a). The initial sorption rate for As(III) was fastest at pH 5.5 (28 nmol sec^{-1} kg^{-1}) and slowest at pH 6.3 and 8 (5 and 6 nmol sec^{-1} kg^{-1} respectively), but then increased again toward pH 10 (15 nmol sec^{-1} kg^{-1}) (Table S5, Fig. 2a). The minimum and maximum equilibrium adsorption of As(III) was calculated as 49.3 and 145 μmol kg^{-1} at pH 5.5 and pH 8 respectively by the Langmuir isotherm (Table S5). The small difference detected in the maximum adsorption capacity of As(III) between pH treatments was due to the charge of the As(III) species. The As(III) occurred mainly as H_3AsO_3 up to pH 8 , but as $H_2AsO_3^-$ with a percentage of 37% and 85% of the As(III) at pH 9 and 10, respectively (Table S4). Furthermore, a stronger negative surface charge of the glass at pH 10 explained the lower adsorption than at pH 9 (Figs. 1 and 2, Tables S4 and S5). The SCM predicted batch adsorption well over the whole pH range (Fig. 2c,d). Chloride competed with As(III) below pH 6.3 and as a consequence As(III) had limited sorption on the basaltic glass surface. The predicted increased deviation from the batch experimental data at low pH resulted in an enhanced fit to the experimental column data as will be discussed below.

3.3.2.2 As(V)

Sorption sites were saturated with As(V) within 8 h at pH 5.5, 9 and 10, whereas, adsorption was not completed at the end of experiment at pH 6.3 and 8 (Fig. 2b). The initial sorption rate was highest (99 nmol sec^{-1} kg^{-1}) for As(V) at pH 5.5 but lowered toward 1.3 nmol sec^{-1} kg^{-1} at pH 10 (Fig. 2b, Table S5). The minimum and maximum equilibrium adsorption of As(V) was calculated as 442 and 2.33 μmol kg^{-1} at pH 5.5 and pH 10 respectively by the Langmuir isotherm (Table S5).The predominant As(V)

species at pH 5.5 was $H_2AsO_4^-$ which was strongly attracted to the high positive surface charge of the glass (Fig. 1,Table S4). As the pH increased the surface charge decreased and was close to zero at pH 6.3 and pH 8, resulting in a small difference in the maximum calculated adsorbance of As(V). The surface charge of the glass was increasingly negative at pH 9, resulting in a low adsorbance potential of negatively charged $HAsO_4^{2-}$ species (Table S4). Very limited adsorption was measured (Fig. 2d) and calculated (Table S5) at pH 10 due to the strong repulsion of the $HAsO_4^{2-}$ from the negatively charged surface (Fig. 2, Table S4).

3.3.3 **Arsenic transfer through columns**

Movement of As through experimental columns was modelled by the geochemical program PHREEQC-2 *(33)* by i) combining the pseudo-second order kinetic model (eq.3) with the Langmuir isotherm eq. (eq. 8). The combination of eq. 3 and eq. 8 was necessary since the sorption rate depends on the equilibrium sorption concentration (q_e in eq. 3), which in turn depends on the As solution concentration (C_t in eq. 8). Substituting eq. 8 for q_e in eq. 3 therefore gives:

$$\frac{dq_t}{dt} = k((\frac{q_m K_L C_t}{1+K_L C_t}) - q_t)^2 \qquad \text{Eq. 6}$$

Modeling was further carried out by using ii) the dynamic Langmuir kinetic model (eq. 7), and finally iii) by surface complexation modeling (SCM). The models generated were then validated by a series of column experiments where the inlet solution contained the respective As species at 4 μmol L^{-1} along with a conservative tracer (Figs. 3 and S4). Recovery of As at the outlet of columns was estimated by integrating the area under the elution curves in Figs. 3 and S4. In the column experiments, As species were always retarded compared to the conservative tracer except for As(V) at pH 10 (Fig. 2). The experimental data were successfully modeled by kinetic approaches in 7 out of 10 systems with either kinetic models, but there was considerable discrepancy for As(III) at pH 3 (due to the pH shift to 5.5) and 6.3 and for As(V) at pH 8 (Fig. S4). The SCM modeled high pH experimental conditions successfully (Figs. 3 and S4), indicating that the dominant reactions reached equilibrium sufficiently quickly as the SCM used was an equilibrium based model. For As(III) inadequate fit by the SCM at pH 6.3-8 and for as As(V) at pH 8 was due to slow surface reactions that did not reach equilibrium in the column which is in agreement with As(V) adsorption rates onto aluminum oxide *(37)*.

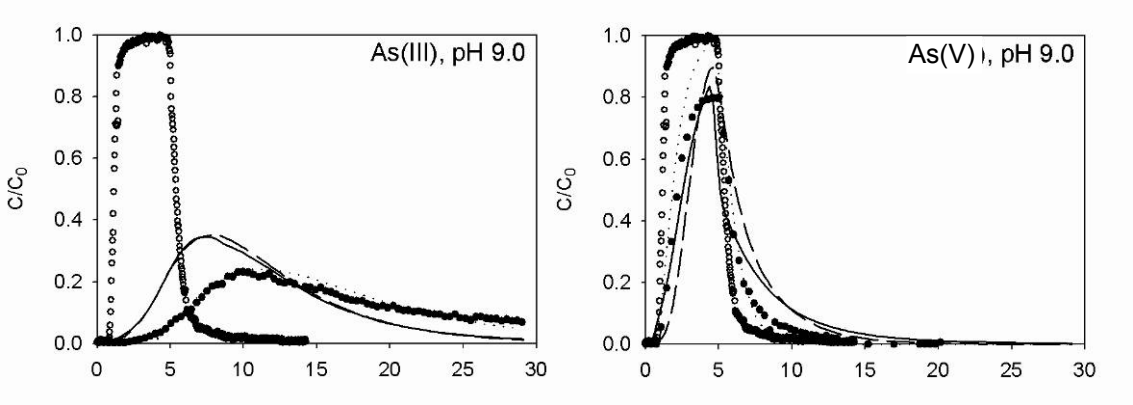

Figure 3 Transport of As(III) and As(V) through basaltic glass columns at pH 9. Four pore volumes of solution containing 4 µmol L^{-1} As and 40 mg L^{-1} Acid blue 9, a conservative tracer, were injected onto column and then eluted with 25 pore volumes of As free solution of the same pH and ionic strength. Filled circles are experimental data points, open circles are conservative tracer, hatched lines give results from pseudo-second-order and solid lines dynamic Langmuir kinetic models, respectively, dotted lines indicate the SCM model. Results from other pH values may be found in the SI.

3.3.3.1 As(III)

The maximum adsorption of As(III), as with many oxyanions, occurs around its first pKa (pH 9.2) on surfaces such as ferrihydrite (pH 8-10, *(23)*), am-$Al(OH)_3$ (pH 7-9,*(25)*) and coprecipated Al:Fe hydroxides (pH 8-9, *(38)*). At pH 9 and 10, 90% of As(III) was recovered from the outlet of the column and less than 2% of the available surface sites (q_m) in the column were occupied with As after elution (Table S7). Both kinetic models provided excellent fit for As(III) at pH 10 but a slightly weaker fit at pH 9 (Figs. 3 and S4). At pH 8, the dynamic Langmuir model simulated data well but a less strong fit was generated by the pseudo-second-order model. At pH 8, 68% of the injected As(III) was recovered from the column´s surface sites, which were 2% occupied (Table S7.) All As(III) was recovered from the pH 3 experiment, though least from the pH 8 (68%) experiment where the available surface sites for sorption (q_m = 145 µmol kg^{-1}) of As(III) were most abundant. However, As(III) showed the highest retardation at pH 9 followed by 10, then 8≈6.3, and at pH 3 the retardation was limited, results which are in agreement with the fastest initial adsorption rates measured at pH 9 and 10 (Figs. 3 and S4, Table S5). At pH 10 the solubility of am-$Al(OH)_3$ and Fe(III)-hydroxides are higher than at pH 6-9 *(39)*, allowing more fluctuations in pH and solute concentrations before the hydroxides start precipitating. The shift from pH 3 to 5.5 in batch experiments may have led to a formation of am-Al and am-Fe(III) hydroxides that

would adsorb the As(III) in solution at pH 5.5 and generate the discrepancy between the experimental and modeled results at pH 3 (5.5). The SCM did not allow for surface precipitation and assumed constant ratio of different sorption sites at different pH levels (Fig. S3 and Table S3) and modeled the As(III) sorption at pH 3 sufficiently when the chloride sorption reaction was taken into account (Fig. S4).

3.3.3.2 As(V)

All measured and modeled data for As(V) showed consistently similar trends from slow and incomplete sorption at pH 10 to fast and extensive sorption at pH 3 (Figs. 1, 2 and 3,Table S5). At pH 9 and 10, 95% of As(V) was recovered from the outlet of the column and 11.8 and 38.6% of available surface sites (q_m) were occupied by As after elution, respectively (Table S7). The adsorption rates (h, k and k_a) and capacity (q_m) were smallest at these pH levels (Table S5). Both kinetic models successfully described column experimental data at pH 9 and 10 (Figs. 3 and S4). At pH 8 neither kinetic models described the column data successfully (Fig. S4) where 55% of As(V) was recovered while occupying less than 2% of the columns adsorption capacity (q_m = 145 μmol kg^{-1}) (Tables S5,S7). Both kinetic models described experimental data for As(V) well at pH 3 and 6.3. The difference in pH at 5.5 in the batch experiments and pH 3 in the column experiments was not sufficient to show discrepancy between the data and the kinetic models as the basaltic glass surface sites were very far from being saturated (0.0 and 0.6 %) and nearly no As(V) (1% and 1%) was recovered from the column outlets at pH 3 or 6.3, respectively (Table S7). On the contrary, 95 % of As(V) was recovered at both pH 9 and 10 with 11.8 and 38.6% of sorption sites being occupied, respectively, indicating a large shift in sorption capacity as pH is shifted within the system.

3.4 Implication for regional groundwater flow models

During recent years, injection of spent geothermal wastewaters has received increased attention, although many geothermal power plants still release wastewater from discharging boreholes and production water at the surface or in shallow boreholes. The injection reduces declining pressures and extends the sustainability of the geothermal system (40). Injection furthermore prevents release of unwanted chemicals in elevated concentrations into the surface environment.

An important part in successful and sustainable utilization of geothermal energy lies in constructing models to predict thermal energy- and groundwater flow in the respective area. These models allow the prediction of movement of wastewater from the geothermal power plants. The current study highlights the importance of accurate definition of geochemical characteristics of the aquifers and the pollutant carrying water. An accurate prediction of As movement from geothermal power plant effluents to the surrounding environments relies on the knowledge of: i) the surface characteristics and hydraulic conductivity of the aquifer, ii) the speciation of As in the geothermal effluent and iii) the ability of the aquifer and geothermal water to maintain or alter the speciation of As when it moves through the aquifer. Arsenic in high-temperature geothermal water is primarily As(III) *(41)* or on thioarsenate forms that can transform to As(III) and As(V) under atmospheric conditions *(8)*. Results generated in the current contribution can be applied to wastewater from discharging boreholes and to those released into shallow groundwater and suggest that alkaline geothermal waters in basaltic environment should be maintained in a reduced condition before shallow injection to prevent oxidation of As(III) to As(V), which is very mobile under alkaline conditions (Figs. 1, 2 and 3). In contrast, acid geothermal waters should be oxidized before injection into the ground due to the high sorption capacity of basaltic glass for As(V) at low pH provided that the adsorption rate of As(V) is faster than the reduction rate of As(V) to As(III) and all As(V) can be removed from the solution before the pH of the system is elevated due to weathering of the aquifer rocks. For decisions regarding injection into deep aquifers at higher temperatures further research needs to be carried out as the thermodynamic properties of arsenic species alter significantly as temperature increases (42). Finally, further study is needed to take into account the importance of thioarsenic species in sulfidic geothermal water (8).

3.5 Acknowledgements

Bergur Sigfusson would like to thank Rannveig Guicharnaud for valuable discussions and constructive criticism during this work. Thanks to Tony Appelo and Jón Örn Bjarnason for help in the modeling work, to Sigurdur Markus Hafsteinsson for the SEM figures and to Eric Oelkers for the BET analyses. This study was supported by the Icelandic Research Fund 050204033, Reykjavik Energy and the Icelandic Graduate Research Fund.

3.6 Supporting information available

Supporting information with validation of the speciation analyses, figure of the experimental column setup and coefficients generated in the current contribution are available. In addition, the chemical composition of all solutions and the basaltic glass surface is also provided as well as the reactions used in the SCM and their equilibrium constants.

This information is available free of charge via the Internet at http://pubs.acs.org

3.7 Literature Cited

(1) Rice, K. C.; Conko, K. M.; Hornberger, G. M. Anthropogenic sources of arsenic and copper to sediments in a suburban lake, Northern Virginia. *Environ. Sci. Technol.* **2002**, *36*, 4962-4967.

(2) Smedley, P. L.; Kinniburgh, D. G. A review of the source, behaviour and distribution of arsenic in natural waters. *Appl. Geochem.* **2002**, *17*, 517-568.

(3) Nimick, D. A.; Moore, J. N.; Dalby, C. E.; Savka, M. W. The fate of geothermal arsenic in the Madison and Missouri Rivers, Montana and Wyoming. *Water Resour. Res.* **1988**, *34*, 3051-3067.

(4) Mandal, B. K.; Suzuki, K. T. Arsenic round the world: a review. *Talanta* **2002**, *58*, 201-235.

(5) Ferguson, J. F.; Gavis, J. A. A review of the arsenic cycle in natural waters. *Water res.* **1972,** 6, 1259-1274.

(6) Hung, D. Q., Nekrassova, O., Compton, R. G. Analytical methods for inorganic arsenic in water : a review. *Talanta* **2004**, *64*, 269-277.

(7) Wolery, T. J. EQ3/6, A software package for geochemical modeling of aqueous systems. **1992.** Lawrence Livermore National Laboratory

(8) Planer-Friedrich, B., London, J., McCleskey, R. B., Nordstrom, D. K., Wallschlager, D. Thioarsenates in geothermal waters of Yellowstone national park: Determination, preservation and geochemical importance. *Environ. Sci. Technol.* **2007**, *41*, 5245-5251.

(9) Gmelin, L.. Arsenic. *Gmelin-Kraut's Handbuch der anorganischen Chemie. System nummer 17.* **1952**. Verlag Cemie, Weinheim.

(10) Cherry, J. A.; Shaikh, A. U.; Tallman, D. E.; Nicholson, R. V. Arsenic species as an indicator of redox conditions in groundwater. *J. Hydrol.* **1979**, *43*, 373-392.

(11) Nordstrom, D. K, Ball, J. W., McCleskey, R. B. Oxidation reactions for reduced Fe, As, and S in thermal outflows of Yellowstone National park: biotic or abiotic? In: Wanty and Seal II (editors). Water rock interaction. Proceedings of the 11th international symposium on water-rock interaction, WRI-11 **2004.** Saratoga springs, New York. Balkema.

(12) Jerram, D. A.; Widdowson, M. The anatomy of Contintal Flood Basalt Provinces: geological constraints on the processes and products of flood volcanism. *Lithos* **2005**, *79*, 385-405.

(13) Ronov, A. B.; Yaroshevsky, A. A. New Model of Earths Crust Chemical-Structure. *Geokhimiya* **1976**, *12*, 1763-1795.

(14) Mottl, M. J.; Holland, H. D. Chemical exchange during hydrothermal alteration of basalt by seawater-I. Experimental results for major and minor components of seawater. *Geochim. Cosmochim. Acta* **1978**, *42*, 1103-1115.
(15) Schilling, J. G. Iceland mantle plume – Geochemical study of Reykjanes Ridge. *Nature* **1973**, *242*, 565-571.
(16) Armannsson, H.; Fridriksson, T.; Kristjansson, B. R. CO2 emissions from geothermal power plants and natural geothermal activity in Iceland. *Geothermics* **2005,** *34*, 286-296.
(17) Wetang'ula, G. N.; Snorrason S. S. Geothermal wastewater disposal: Chemical stress assessment Thingvallavatn – Iceland. *Proceedings World Geothermal Congress*, **2005.**
(18) Arnorsson, S. Arsenic in surface- and up to 90°C ground waters in a basalt area, N-Iceland: processes controlling its mobility. *Appl. Geochem.* **2003**, *18*, 1297-1312.
(19) Oelkers, E. H.; Gislason, S. R. The mechanism, rates and consequences of basaltic glass dissolution: I. An experimental study of the dissolution rates of basaltic glass as a function of aqueous Al, Si and oxalic acid concentration at 25(deg)C and pH = 3 and 11. *Geochim. Cosmochim. Acta* **2001**, *65*, 3671-3681.
(20) Guy, C., Schott, J. Multisite surface reaction versus transport control during hydrolysis of a complex oxide. *Chem. Geol.* **1989**, *78*, 181-204.
(21) Sahai, N.; Sverjensky, D. A. Solvation and electrostatic model for specific electrolyte adsorption. *Geochim. Cosmochim. Acta* **1997**, *61*, 2827-2848.
(22) Manning, B. A.; Goldberg. S. Adsorption and Stability of Arsenic(III) at the clay mineral-water interface. *Environ. Sci. Technol.* **1997**, *31*, 2005-2011.
(23) Raven, K. P.; Jain, A.; Loeppert, R. H. Arsenite and arsenate adsorption on ferrihydrite: Kinetics, equilibrium and adsorption envelopes. *Environ. Sci. Technol.* **1998**, *32*, 344-349.
(24) Manning, B. A.; Fendorf, S. E.; Goldberg. S. Surface structures and stability of arsenic(III) on goethite: Spectroscopic evidence for inner-sphere complexes. *Environ. Sci. Technol.* **1998**, *32*, 2383-2388.
(25) Arai, Y.; Elzinga, E. J.; Sparks, D. L. X-ray adsorption spectroscopic investigation of arsenite and arsenate adsorption at the aluminum oxide-water interface. *J. Colloid Interface Sci.* **2001**, *235*, 80-88.
(26) Masscheleyn. P. H.; Delaune, R. D.; Patrick, W. H. A Hydride generation atomic-absorption technique for arsenic speciation. *J. Env. Qual.* **1991**, *20*, 96-100.
(27) Williams, P. N.; Price, A. H.; Raab, A.; Hossain, S. A.; Feldmann, J.; Meharg, A. A. Variation in arsenic speciation and concentration in paddy rice related to dietary exposure. *Environ. Sci. Technol.* **2005,** *39*, 5531-5540.
(28) Mon, J., Flury, M., Harsh, J. B. Sorption of four triarylmethane dyes in a sandy soil determined by batch and column experiments. *Geoderma* **2006**, *133*, 217-224.
(29) Gislason. S. R.; Oelkers, E. H. Mechanism, rates, and consequences of basaltic glass dissolution: II. An experimental study of the dissolution rates of basaltic glass as a function of pH and temperature. *Geochim. Cosmochim. Acta.* **2003**, *67*, 3817-3832.
(30) Ho, Y. S., McKay, G. Pseudo-second order model for sorption processes. *Process Biochem.* **1999**, *24*, 451-465.
(31) Langmuir, I. The adsorption of gases on plane surfaces of glass, mica and platinum. *J. Am. Chem. Soc.* **1918**, 1361-1403.
(32) Dzombak, D. A.; Morel, F. M. M. *Surface Complexation Modeling: Hydrous Ferric Oxide*; John Wiley & Sons: New York, 1990.

(33) Parkhurst, D. L.; Appelo, C. A. H. User's guide to PHREEQC (Version 2)−A computer program for speciation, batch-reaction, one-dimensional transport, and inverse geochemical calculations, U. S. G. S. Wat. Res. Inv. Report **1999**, 99-4259.
(34) Sahai, N.; Sverjensky, D. A. Evaluation of internally consistent parameters for the triple-layer model by systematic analysis of oxide surface titration data. *Geochim. Cosmochim. Acta* **1997**, 61, 2801-2826.
(35) Sverjensky, D. A.; Fukushi, K. A predictive model (ETLM) for As(III) adsorption and surface speciation on oxides consistent with spectroscopic data. *Geochim. Cosmochim. Acta* **2006**, 70, 3778-3802.
(36) Fukushi, K.; Sverjensky, D. A. A predictive model (ETLM) for arsenate adsorption and surface speciation on oxides consistent with spectroscopic and theoretical molecular evidence. *Geochim. Cosmochim. Acta* **2007**, 71, 3717-3745.
(37) Arai, Y.; Sparks, D. L. Residence time effects on arsenate surface speciation at the aluminum oxide-water interface. *Soil Sci.* **2002**, 167, 303-314.
(38) Masue, Y.; Loeppert, R. H.; Kramer, T. A. Arsenate and arsenite adsorption and desorption behavior on coprecipated aluminium:iron hydroxides. *Environ. Sci. Technol.* **2007**, *41*, 837-842.
(39) Lindsay, W. L. *Chemical Equilibria in Soils*; John Wiley & Sons: New York, 1979.
(40) Majer, E. L.; Peterson, J. E. The impact of injection on seismicity at The Geysers, California Geothermal Field, *Int. J. Rock Mech. Min. Sci.* **2007**, *44*, 1079-1090.
(41) Yokohama, T.; Takahashi, Y.; Tarutani, T. Simultaneous determination of arsenic and arsenious acids in geothermal water. *Chem. Geol.* **1993**, 103, 103-111.
(42) Halter, W.E.; Pfeifer, H.R. Arsenic(V) adsorption onto alpha-Al_2O_3 between 25 and 70 degrees C. *Appl. Geochem.* **2001**, 16, 793-802.

Supporting information

Regulation of arsenic mobility on basaltic glass surfaces by speciation and pH

Bergur Sigfusson[1,2], Andrew A. Meharg[1] and Sigurdur R. Gislason[2]*

1) *School of Biological Sciences, University of Aberdeen, AB243UU, Aberdeen, UK*
2) *Institute of Earth Sciences, University of Iceland, 101 Reykjavik, Iceland*

* *To whom the correspondence should be addressed. Tel: +354 516-6991. Email: bergur@raunvis.hi.is (Bergur Sigfusson).*

12 pages, Text S1-S4, 7 tables, 4 figures

S1 Introduction. The supporting information includes four figures and seven tables and a description of method to generate values of ka and kd in the dynamic Langmuir kinetic model. The first figure displays results from development of As(III) measurements (Fig. S1). The second figure displays the experimental column setup (Fig. S2). The third figure is SEM pictures of the basaltic glass (Fig. S3). The fourth figure shows results from column experiments at pH values from 3 to 10. The first table lists the composition of the starting and inlet solutions in batch and dynamic experiments respectively (Table S1). The second table displays results from cross validation between two measuring procedures, HG-AAS and HPLC-ICP-MS (Table S2). The third table tabulates the ratio of Si, Al and Fe on the basaltic glass surface according to SEM/EDS measurements (Table S3). The fourth table tabulates the speciation of As species at the end of batch experiments (Table S4). The fifth table displays all kinetic and equilibrium coefficients derived from current experimental data (Table S5). The sixth table displays all surface reactions used in the SCM (Table S6). Finally the seventh table, lists recovery results of As from column experiment outlets (Table S7).

S2 Solutions. The column and batch experiments were carried out at with initial pH values (pH 3, 6.3, 8, 9 and 10) at ionic strength of 10 mM by varying concentrations of HCl, NH_4Cl and NH_4OH (Table S1). These solutions were purged for two hours with

grade 5.0 N_2 gas (BOC gases, Aberdeen) before any As was added to them or before they came in contact with the basaltic glass.

S3 Validation of analytical method. Cross validation of the HG-AAS method was determined with solutions spiked with known amounts of As(III) and As(V) stock solutions respectively. An aliquot of these solutions was then mixed (50:50 V/V) with 0.4 M Na-citrate buffer (pH 5.5) and measured within an hour in HG-AAS (Fig. S1, Table S2). Another aliquot of the same spike was measured within one day in HPLC-ICP-MS *(27)*. Furthermore randomly selected samples from batch experiments were analyzed by HPLC-ICP-MS *(27)* and the As(III)/As(V) speciation results concurred between the two techniques (Table S2). Briefly the HPCL speciation was carried out on an Hamilton columns consisting of a pre column (11.2 mm, 12-20µm) and a PRP-X100 10-µm anion-exchange column (150 x 4.1 mm). Injection volume of 100 µL were injected manually into a HP1100 HPLC system (Agilent Technologies) with a mobile phase consisting of 6.66 mM ammonium hydrophosphate ($NH_4H_2PO_4$) and 6.66 mM ammonium nitrate (NH_4NO_3), adjusted to pH 6.2 with ammonia.

S4 Surface reactions. Table S6 tabulates surface reactions included to simulate column experiments in Phreeqc-2. The surface area and available surface sites in on the basaltic glass in the SCM were adjusted to 7e-7 moles g^{-1} and 0.15 m^2 g^{-1} by comparing experimental and modeled results for As(III) at pH 9.

Adsorption constants for the dynamic Langmuir kinetic model were derived in the following way.

The dynamic Langmuir kinetic equation is:

$$\frac{d\Theta}{dt} = k_a(c_0 - q_{\max}\Theta)(1-\Theta) - k_d\Theta \qquad \text{Eq. S1}$$

Where k_a is adsorption constant (mol kg^{-1}), C_0 is the initial solution composition (mol L^{-1}), q_{max} is the maximum sorption (mol kg^{-1}) derived from Langmuir Isotherm model and k_d is the desorption constant (s^{-1}). First we multiply out the parenthesis:

$$\frac{d\Theta}{dt} = k_a c_0 - k_a c_0\Theta - k_a q_{\max}\Theta - k_a q_{\max}\Theta^2 - k_d\Theta \qquad \text{Eq. S2}$$

and rearrange:

$$\frac{d\Theta}{dt} = k_a q_{\max}\Theta^2 - \Theta(k_a q_{\max} + k_a c_0 + k_d) + k_a c_0 \qquad \text{Eq. S3}$$

The eq. is a "variables separable" and is solved by:

$$\int k_a q_{\max} dt = \int \frac{d\Theta}{\Theta^2 - \Theta\left(1 + \frac{c_0}{q_{\max}} + \frac{k_d}{k_a q_{\max}}\right) + \frac{c_0}{q_{\max}}_0} \qquad \text{Eq. S4}$$

Call the zero-roots of the quadratic in the denominator r_1 and r_2. The discriminator of the quadratic is given by:

$$D = \left(1 + \frac{c_0}{q_{\max}} + \frac{k_d}{k_a q_{\max}}\right)^2 - 4\frac{c_0}{q_{\max}} \qquad \text{Eq. S5}$$

Wish to determine whether D > 0 or D z 0.

Rearrange:

$$D = 1 + \frac{2c_0}{q_{\max}} + \frac{c_0^2}{q_{\max}^2} + \frac{2k_d}{k_a q_{\max}}\left(1 + \frac{c_0}{q_{\max}}\right) + \frac{k_d^2}{k_a^2 q_{\max}^2} - 4\frac{c_0}{q_{\max}} \qquad \text{Eq. S6}$$

And:

$$D = 1 - \frac{2c_0}{q_{\max}} + \frac{c_0^2}{q_{\max}^2} + \frac{2k_d}{k_a q_{\max}}\left(1 + \frac{c_0}{q_{\max}}\right) + \frac{k_d^2}{k_a^2 q_{\max}^2} \qquad \text{Eq. S7}$$

Now subtract and add $4k_d c_0 \big/ k_a q_{\max}^2$:

$$D = 1 - \frac{2c_0}{q_{\max}} + \frac{c_0^2}{q_{\max}^2} + \frac{2k_d}{k_a q_{\max}}\left(1 - \frac{c_0}{q_{\max}}\right) + \frac{k_d^2}{k_a^2 q_{\max}^2} + \frac{4k_d c_o}{k_a q_{\max}^2} \qquad \text{Eq. S8}$$

Which becomes:

$$D = \left(1 - \frac{c_0}{q_{\max}} + \frac{k_d}{k_a q_{\max}}\right)^2 + \frac{4k_d c_o}{k_a q_{\max}^2} \qquad \text{Eq. S9}$$

D is clearly >0. Thus the quadratic has two real roots and can be factored, thus: $(\Theta - r_1)(\Theta - r_2)$ where:

$$r_1 = \frac{1}{2}\left(1 + \frac{c_0}{q_{\max}} + \frac{k_d}{k_a q_{\max}}\right) + \frac{1}{2}\sqrt{D} \qquad \text{Eq. S10}$$

and:

$$r_2 = \frac{1}{2}\left(1 + \frac{c_0}{q_{\max}} + \frac{k_d}{k_a q_{\max}}\right) - \frac{1}{2}\sqrt{D} \qquad \text{Eq. S11}$$

Now we can decompose eq. 4 into partial fractions:

$$\int k_a q_{\max} dt = \int \frac{d\Theta}{(\Theta - r_1)(\Theta - r_2)} \qquad \text{Eq. S12}$$

or:

$$\int k_a q_{\max} dt = \frac{1}{(r_1 - r_2)} \int \frac{d\Theta}{(\Theta - r_1)} - \frac{1}{(r_1 - r_2)} \int \frac{d\Theta}{(\Theta - r_2)} \qquad \text{Eq. S13}$$

Now $r_1 - r_2$ equals $\sqrt{D}$ and integration at boundary conditions t = 0 to t =t with the eq.:

$$k_a q_{\max} t \int_{t=0}^{t} \frac{1}{\sqrt{D}} \ln(\Theta - r_1) - \frac{1}{\sqrt{D}} \ln(\Theta - r_2) + C' \int_{\Theta=0}^{\Theta} \qquad \text{Eq. S14}$$

And then integrate at boundary conditions θ = 0 to θ = θ:

$$\sqrt{D} k_a q_{\max} t = \ln \frac{(\Theta - r_1)}{(\Theta - r_2)} + C' \int_{\Theta=0}^{\Theta} \qquad \text{Eq. S15}$$

Which gives:

$$e^{\sqrt{D} k_a q_{\max} t} = \frac{r_2}{r_1} \left(\frac{\Theta - r_1}{\Theta - r_2} \right) \qquad \text{Eq. S16}$$

or:

$$\frac{\Theta - r_2}{\Theta - r_1} = \frac{r_2}{r_1} e^{-\sqrt{D} k_a q_{\max} t} \qquad \text{Eq. S17}$$

Eq. 17 can thus be fitted to experimental data by iteration by varying k_a only. The k_d constant is later calculated by dividing ka by K_L derived from sorption isotherm data since:

$$K_L = \frac{k_a}{k_d} \qquad \text{Eq. S18}$$

Table S1 Composition of solutions used in the experiments performed in the present study

pH (25°C)	HCl (mol L-1)	NH4Cl (mol L-1)	NH4OH (mol L-1)
3.00	0.00100	0.0090	
6.30	0.00010	0.0099	
8.02	0.00001	0.0095	0.0005
9.03		0.0065	0.0035
10.05		0.0015	0.0085

Table S2 Speciation procedure in HG-AAS validated by HPLC-ICP-MS, all concentrations are in µmol l^{-1}.

Spiked solutions from method development:

	Spike conc.		HG-AAS measurement						HPLC-ICP-MS measurement					
	As(III)	As(V)	As(III)	S.E.	As(V)*	S.E.	As-Total	S.E.	As(III)	S.E.	As(V)	S.E.	As-total**	S.E.
Spike	0.133	0.000	0.137	0.002	0.000	-	0.136	0.002	0.141	0.009	<LOD	-	0.150	0.009
Spike	0.133	0.027	0.137	0.003	0.023	-	0.160	0.002	0.142	0.010	0.020	-	0.162	0.010
Spike	0.133	0.133	0.147	0.006	0.120	-	0.267	0.004	0.155	0.008	0.129	-	0.284	0.008
Spike	0.133	0.267	0.136	0.002	0.264	-	0.400	0.002	0.139	0.012	0.261	-	0.400	0.012
Spike	0.133	0.667	0.135	0.002	0.665	-	0.800	0.003	0.133	0.012	0.681	-	0.814	0.012

Samples from Langmuir isotherm experiments:

	Initial concentration													
pH	As(III)	As(V)	As(III)	S.E.	As(V)*	S.E.	As-Total	S.E.	As(III)	S.E.	As(V)	S.E.	As-total	S.E.
6.3	0.667	0	0.287	0.012	0.101	-	0.388	0.010	0.280	-	0.102	-	0.382	-
8	0.667	-	0.307	0.015	0.038	-	0.345	0.013	0.306	-	0.040	-	0.346	-
9	-	0.667	0.006	0.094	0.576	-	0.581	0.089	<LOD	-	0.576	-	0.576	-
10	-	0.667	0.233	0.011	0.414	-	0.647	0.012	0.228	-	0.410	-	0.644	-

* As(V) calculated by subtraction of As(III) from As-total in HG-AAS measurements

** As-total calculated as sum of As(III) and As(V)

Table S3 Ratio of Al,Si and Fe on basaltic glass surface prior and after column experiments.

Sample	*Al*	*Si*	*Fe*
Fresh material	0.23	0.65	0.13
column experiments:			
3	0.24	0.65	0.11
6.3	0.23	0.65	0.13
8	0.21	0.65	0.14
9	0.26	0.63	0.11
10	0.23	0.64	0.13
mean of leachec	0.23	0.64	0.13
SE	0.01	0.00	0.01

Table S4 Measured oxidation states of As at end of batch isotherm experiments and calculation of species assuming thermodynamic equilibrium.

		As (III) experiments:				*As(V) experiments:*					
pH*	Surface charge C m^{-2}	measured oxidation state (%)		Partition of As(III) species		measured oxidation state (%)		Partition of As(V) species			
		As(III)	As(V)	H_3AsO_3	$H_2AsO_3^-$	As(III)	As(V)	H_3AsO_4	$H_2AsO_4^-$	$HAsO_4^{2-}$	AsO_4^{-3}
5.5	+0.3	91	9	100	0	0	100	0	100	0	0
6.3	0	86	14	100	0	0	100	0	72	28	0
8.0	0	98	2	94	6	0	100	0	5	95	0
9.0	-0.5	100	0	63	37	0	100	0	0.5	99	0.5
10.0	-5	60	40	15	85	0	100	0	0	97	3

* pH in all experiments were within 0.1 pH value from reported value

Table S5 Pseudo second order kinetic, Langmuir kinetic and isotherm coefficients for As(III) and As(V) derived from static batch experiments at pH 5.5-10. Ionic strength, 0.01 M; Adsorbent dose 100 g L-1; Temperature, 30°C; Initial As concentration in kinetic experiments was 4 µM and 0.67-16 µM in isotherm experiments respectively.

	Pseudo second order model			*Langmuir kinetic*		*Langmuir Isotherm*	
pH	h*	k	qe	ka	kd	KL	qmax
	mol sec kg^{-1}	kg sec mol^{-1}	mol kg^{-1}	L mol^{-1} s-1	s^{-1}	L mol^{-1}	mol kg^{-1}
As(III)							
5.5	2.80±0.12E-08	40.7±1.2	2.62±0.13e-5	69.8±8.8	2.0±0.2e-4	3.48±1.33e5	4.93±0.69e-5
6.3	5.06±0.08E-09	22.7±0.3	1.49±0.04e-5	4.86±0.80	3.6±0.4e-5	1.36±0.15e5	5.81±0.31e-5
8	6.22±0.80E-09	30.9±2.1	1.42±0.07e-5	2.82±0.18	5.5±0.4e-5	5.12±2.20e4	1.45±0.44e-4
9	1.36±0.02E-08	69.0±2.7	1.41±0.06e-5	10.0±0.11	1.4±0.2e-4	6.94±0.77e4	6.49±0.44e-5
10	1.51±0.04E-08	187±9.1	0.90±0.09e-5	36.0±4.2	4.1±0.5e-4	8.70±5.14e4	5.05±1.67e-5
As(V)							
5.5	9.86±0.09E-08	65.8±0.4	3.87±0.40e-5	16.6±0.15	1.9±0.1e-5	8.61±5.19e5	4.42±1.87e-4
6.3	6.61±0.09E-09	7.89±0.3	2.89±0.11e-5	2.10±0.09	5.6±0.2e-6	3.78±0.16e5	1.29±0.02e-4
8	5.18±0.04E-09	16.6±0.2	1.77±0.14e-5	1.15±0.14	2.1±0.2e-5	5.41±0.45e5	2.21±1.33e-4
9	2.98±0.01E-09	36.4±0.1	9.04±0.77e-6	103±9.6	3.5±0.4e-4	2.93±0.94e5	7.61±0.85e-6
10	1.31±0.02E-09	363±7.0	1.90±0.08e-6	42.0±0.33	5.4±0.5e-4	7.73±5.86e5	2.33±0.46e-6

* All values are mean+/- one sigma of the curve fitting

Table S6 Reactions used in the SCM model. Log K values were calculated based on the approximation that the basaltic glass surface was a mixture of Si (65%), Al (22.5%) and Fe (12.5%) surfaces and as a consequence having silanol, aluminol and goethite sites in identical fractions.

Reaction	log K	Ref.
Silanol-OH + H^+ = Silanol-OH_2^+	-0.7	(34)
Silanol-OH = Silanol-O- + H^+	-7.7	(34)
Aluminol-OH + H^+ = Aluminol-OH_2^+	5.5	(34)
Aluminol-OH = Aluminol-O- + H^+	-11.5	(34)
Goethite-OH + H^+ = Goethite-OH_2^+	6.3	(34)
Goethite-OH = Goethite-O- + H^+	-11.9	(34)
Glass-OH + H^+ = Glass-OH_2^+	5.52	*
Glass-OH = Glass-O- + H^+	-7.88	*
2Glass-OH + H_3AsO_3 = $(Glass\text{-}O)_2AsOH$ +$2H_2O$	4.7	*
Glass-OH + H_3AsO_3 = Glass-H_4AsO_4	2.78	*
Glass-OH + H_3AsO_4 = Glass-$OAsO_3^{-2}$ + $2H_+$ + H_2O	-2.4	*
2Glass-OH + H_3AsO_4 = $(Glass\text{-}O)_2AsO_2^-$ + H^+ + $2H_2O$	2.3	*
2Glass-OH + H_3AsO_4 = $(Glass\text{-}O)_2AsOOH$ + $2H_2O$	4.3	*
Glass-OH + Cl^- + H^+ = Glass-OH_2Cl	1.56	*

Table S7 Recovery of As from outlet of column experiments.

	% of inlet recovered		% of q_m occupied	
pH	AsIII	AsV	AsIII	AsV
3	100	1	0.0	0.0
6.3	92	1	1.2	0.6
8	68	55	2.0	1.3
9	90	95	1.4	11.8
10	90	95	1.8	38.6

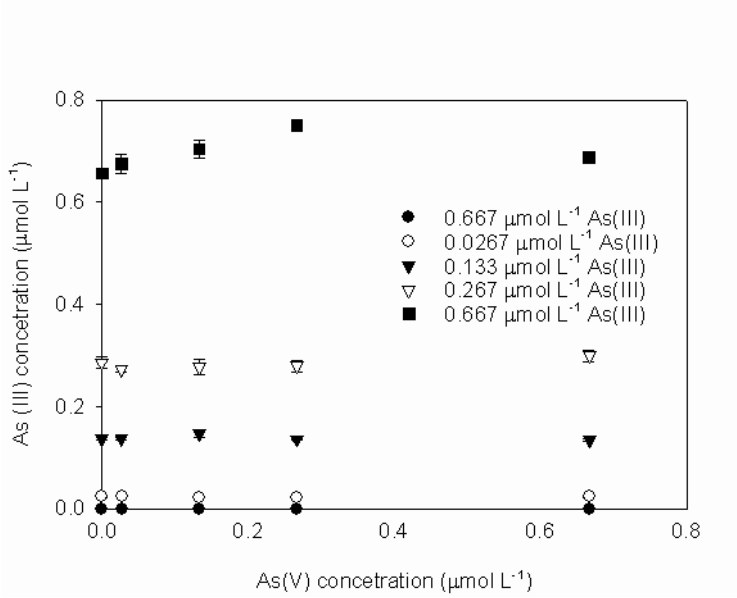

Figure S1 Addition of As(V) to 0.2 M Na-citrate (pH 5.0) solutions containing As(III) did not increase the absorbance values measure in HG-AAS therefore allowing estimation of As(V) by subtracting measured As(III) from measured As-total concentrations.

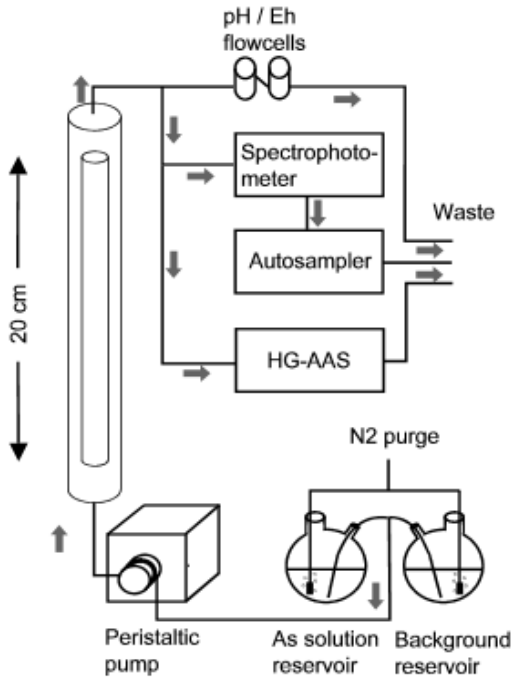

Figure S2 Experimental setup. One thousand pore volumes (PV) of solution from the background reservoir were pumped through the column before 4 PV of As solution was injected followed by 25 PV of background solution. The outflow was divided to 3 lines where pH, Eh, a conservative tracer and As(III) were measured continuously and samples for total As analysis were collected by a fraction collector.

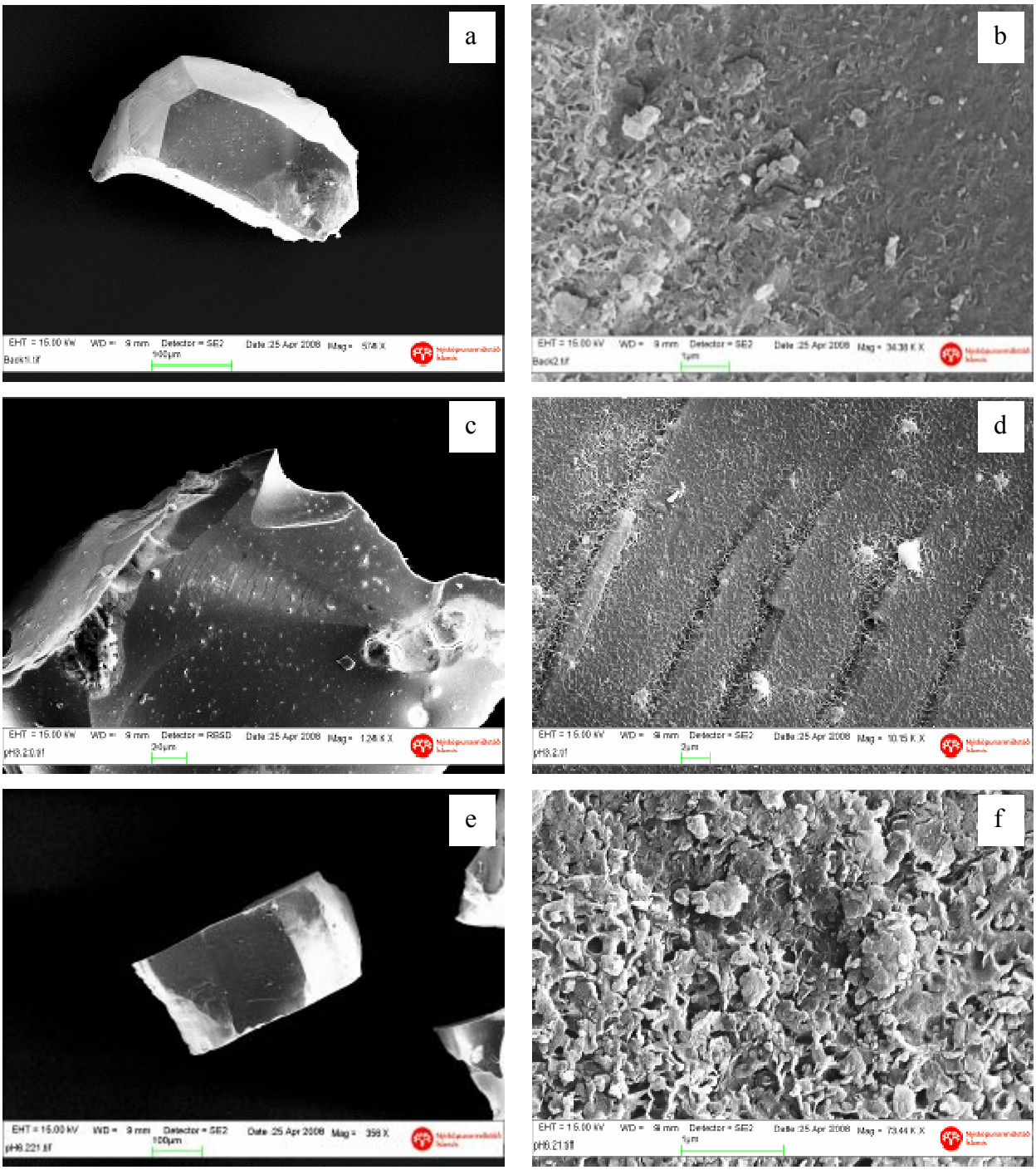

Figure S3 Fresh basaltic glass (a,b) and basaltic glass after column experiments carried out at inlet pH 3(c,d), 6.3(e,f), 8(g,h), 9(i,j) and 10(k,l), respectively.

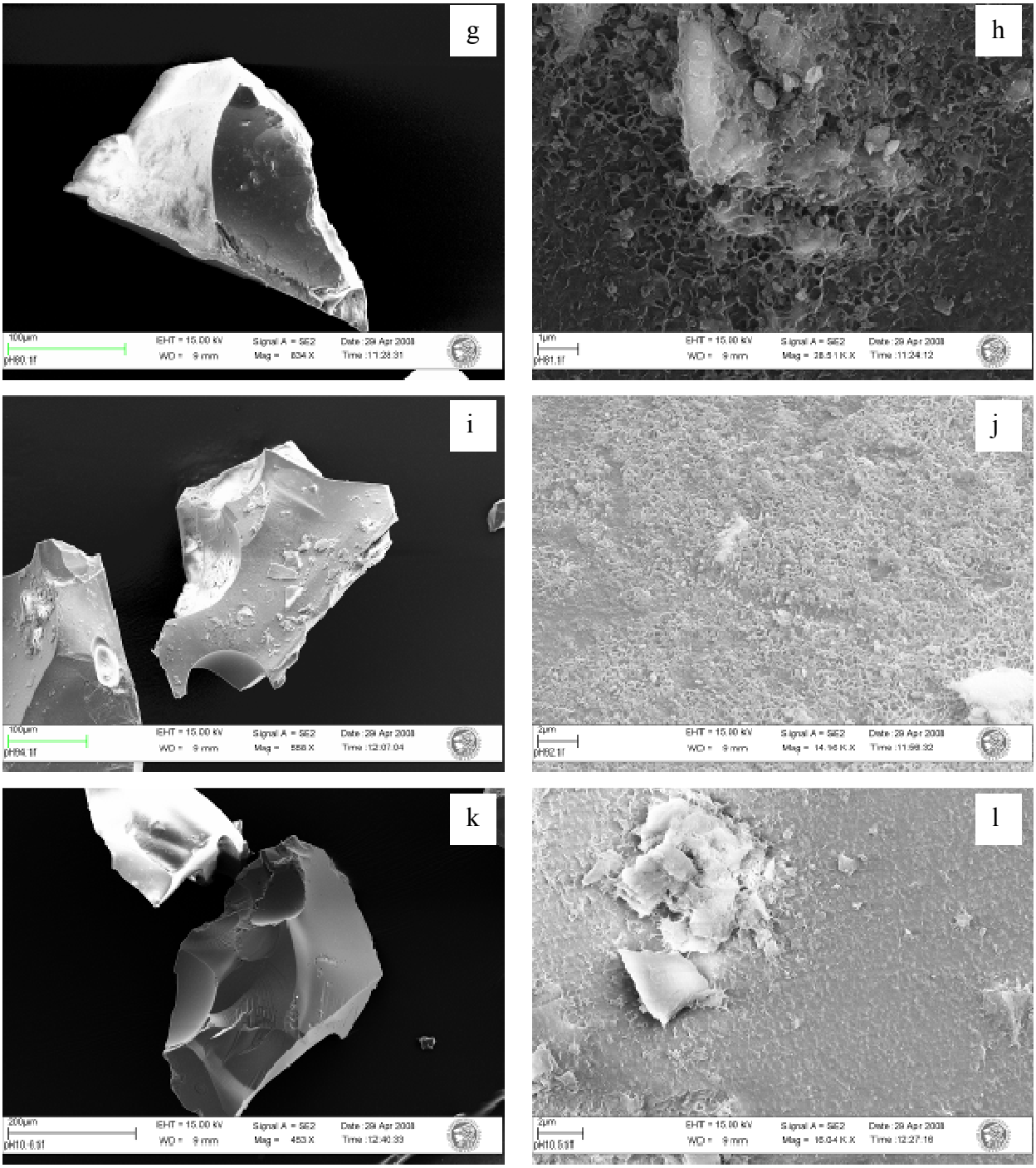

Figure S3 continued.

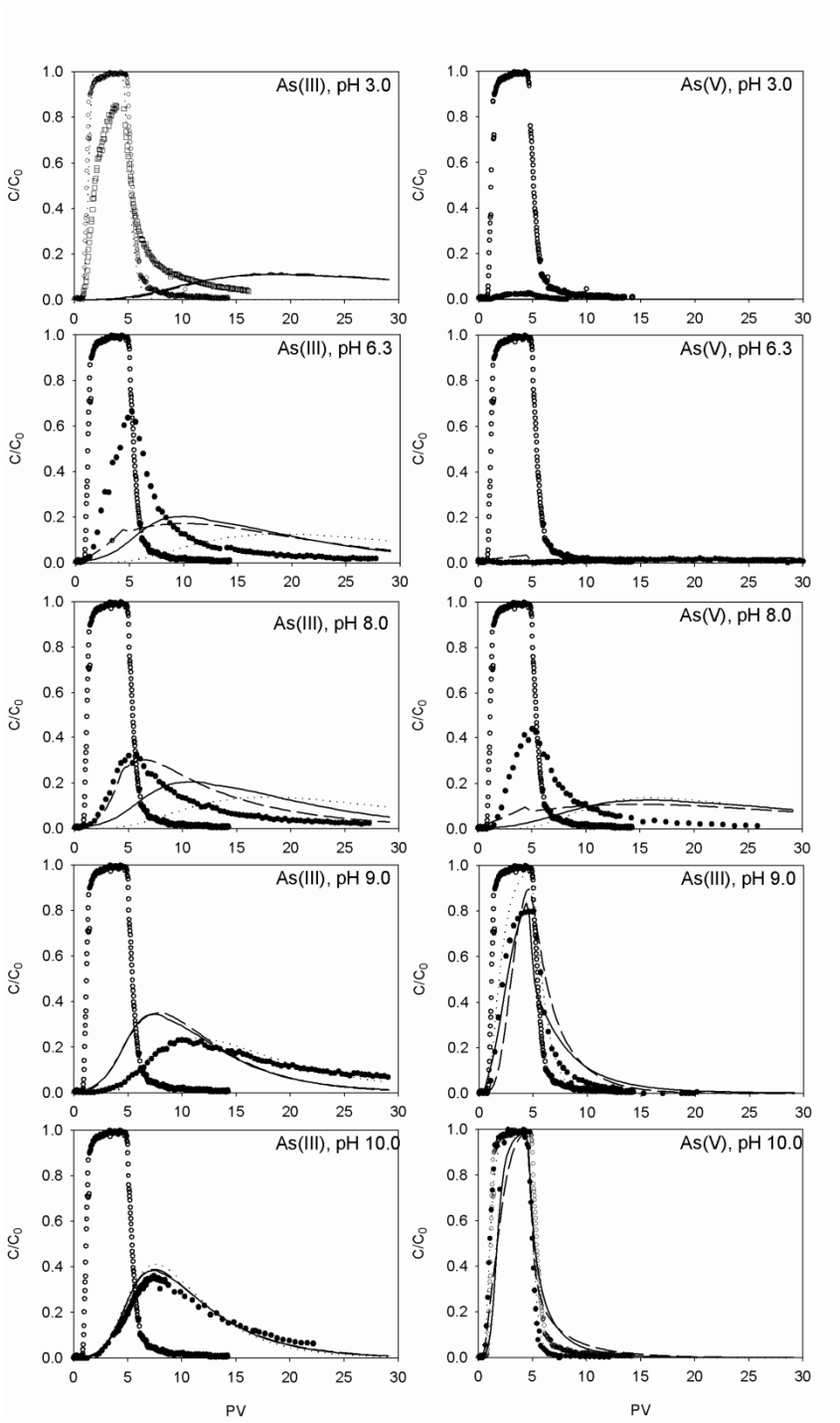

Figure S4 Transport of As(III) and As(V) through basaltic glass columns at pH 3-10. Four pore volumes of solution containing 4 µmol L^{-1} As and 40 mg L^{-1} Acid blue 9, a conservative tracer, were injected onto column and then eluted with 25 pore volumes of As free solution of the same pH and ionic strength. Filled circles are experimental data points, open circles are conservative tracer, hatched lines give results from pseudo-second-order and solid lines dynamic Langmuir kinetic models, respectively, dotted lines indicate the SCM model.

4 A field and reactive transport model study of Arsenic in basaltic rock aquifer:

Bergur Sigfusson[1,2], Sigurdur R. Gislason[2] and Andrew A. Meharg[1]*

1) School of Biological Sciences, University of Aberdeen, AB243UU, Aberdeen, UK
2) Institute of Earth Sciences, University of Iceland, 101 Reykjavik, Iceland
*Present address, Reykjavik Energy, Baejarhals 1, 110 Reykjavik, Iceland

Corresponding author: bergur.sigfusson@or.is (Bergur Sigfusson)
In preparation for submission to Applied Geochemistry.

Contribution of individual authors:
Bergur Sigfusson assembled all analytical apparatus for field deployment, sampled and analysed all samples, wrote the manuscript and constructed the geochemical models.

Sigurdur R. Gislason advised mainly on the writing of the manuscript and provided input on discussions on analysis of As in sulphidic waters.
Andrew A. Meharg advised mainly on the writing of the manuscript and provided input on discussions on analysis of As in sulphidic waters.

Other contributors are thanked in the acknowledgements.

Abstract

The use of geothermal energy as a source for electricity and district heating has increased over recent decades. Dissolved arsenic (As) can be an important constituent of the geothermal fluids brought to the Earth's surface. Here we present the field application of laboratory measured adsorption coefficients of aquatic As species on basaltic glass surfaces (Sigfusson et al., 2008). The mobility of As species in the basaltic aquifer in the Nesjavellir geothermal system was modelled by the one dimensional (1 D) reactive transport model PHREEQC-2 (Appelo and Postma, 1999), constrained by a long time series of field measurements of chemical composition of geothermal effluent fluids, pH, Eh and sometimes Fe- and As-dissolved species measurements. Di-, tri- and tetrathioarsenic species ($As(OH)S_2^{2-}$,AsS_3H^{2-} ,AsS_3^{3-} and $As(SH)_4$) were the dominant form of dissolved As in geothermal waters exiting the power plant but converted to some extent to arsenite (H_3AsO_3) and arsenate ($HAsO_4^{2-}$) oxyanions coinciding with rapid oxidation of sulphide (S_2^-) to thiosulphide ($S_2O_3^{2-}$) and finally to sulphate (SO_4^{2-}) during surface runoff before feeding into a basaltic lava field.

A continuous 25 year data set monitoring groundwater chemistry along a traverse of warm springs on the Lake Thingvallavatn shoreline allowed calibration of the 1D model. Furthermore, a series of ground water wells located in the basaltic lava field, provided access along the line of flow of the geothermal effluent waters towards the lake. The conservative ion, chloride (Cl^-), moved through the basaltic lava field (4100 m) in less than10 years but As was retarded considerably due to surface reactions and has entered a groundwater well 850 m down the flow path as arsenate in accordance to prediction by the 1D model. The 1D model predicted a complete breakthrough of arsenate in the year 2100 while arsenite will be retained for about 1000 years. Due to increased deep well injection of geothermal effluents, adsorption to the basalt surfaces and dilution from ground waters, As concentrations in springs discharging into Lake Thingvallavatn will not reach those of the inlet concentrations during the years 1990-2006.

4.1 Introduction

Geothermal areas frequently produce spring and stream waters with elevated arsenic (As) concentrations (Webster and Nordstrom, 2003). Utilisation of geothermal areas can increase the discharge of geothermal waters towards the surface with associated heavy metal contamination (Olafsson, 1992; Baba and Armannsson, 2006; Gallup, 2007; Aksoy et al., 2009). Re-injection of spent geothermal fluids to deep aquifers is rapidly increasing around the world and is recommended as the standard procedure to avoid adverse impacts of geothermal utilisation (Baba and Armannsson, 2006).

Arsenic is believed to primarily enter crustal fluids during crystallising of deep plutons as hot volatile-rich magmatic fluids escape from the plutons and segregate into vapour and brine resulting in formation of porphyry-style and epithermal ore deposits and fumaroles activity in volcanic areas (Goldschmidt, 1954; Ballantyne and Moore 1988). Arsenic concentrations in volcanic gases sampled between 400 and 900°C often range between 1-10 ppm of the vapour condensates (Mambo, Yoshida & Matsuo 1991) corresponding to As enrichment in the gas phase between 100 and 1000 with respect to the magma body suggesting an important transfer of As into the hydrosphere and atmosphere during magma degassing and volcanic eruptions (Pokrovski et al., 2002). Arsenic preferentially concentrates into the liquid aqueous phase in water dominated active hydrothermal systems below 350°C (Ballantyne and Moore, 1988). Arsenic mainly occurs as As(III) hydroxide, primarily as $As(OH)_3$ aqueous species and to lesser extent, the sulphide $H_{0-3}As_{1-3}S_{3-6}$, species in natural hydrothermal solutions depending on temperature, pH and H_2S content (Akinfiev et al., 1992; Helz et al., 1995; Pokrovski et al., 1996). According to dissolution experiments, As occurs to a large extent on a soluble form in intermediate and silicic volcanics in New Zealand, probably as salts on mineral grain surfaces (Ellis and Mahon, 1964). The ratio of As to Cl in solution in deep aquifers in Iceland is similar to that of tholeiitic basalts indicating the As may be leached congruently from the rock surfaces as meteoric water reacts with those rocks in high-temperature geothermal systems (Giroud, 2008) or at lower depths in colder environments (Arnorsson, 2003).

Although arsenate is relatively mobile in surface waters and as a mixture of arsenite and arsenate in shallow ground waters in basaltic terrain (Arnorsson, 2003), it may not be considered as conservative as Cl^- and boron (B) in hydrothermal solutions in Iceland (Giroud, 2008). It may be incorporated into secondary sulphide minerals such as pyrite

(FeS_2), realgar (As_2S_2) and orpiment (As_2S_3) (Cleverley et al., 2003) depending on $H_2S_{(aq)}$ concentrations. As the hydrothermal solutions rise towards the surface and mix with cold ground waters at shallow levels the As may be effectively removed from the solution by coprecipitation with or adsorption onto ferric hydroxides (Giroud, 2008; Arnorsson, 2003) or sorbed on basaltic glass surfaces (Sigfusson et al., 2008).

Hydrothermal fluids may rise towards the surface with limited interaction with cold ground waters, either naturally in the form of springs and fumaroles or through discharging boreholes utilised for geothermal power production. Recent advances in analytical techniques have made possible direct determination of thioarsenic species in geothermal waters either in the field (this study) or in the laboratory after preservation (Wallschlager and Roehl, 2001, Stauder et al., 2005, Planer-Friedrich et al., 2007). As the discharged waters from a sulphidic hot spring flowed on the surface, thioarsenates preferably transformed into arsenite with less thioarsenates transforming stepwise by ligand exchange to arsenate and finally the arsenite oxidised to arsenate as all thioarsenates and H_2S had disappeared (Planer-Friedrich et al., 2007).

The As contained in alkaline sulphidic solutions can occur either mainly as thioarsenate or thioarsenite according to a chromatographic method (Wilkin et al., 2003; Stauder et al., 2005; Planer-Friedrich et al., 2007) whereas Beak et al. (2008) have pointed out that the chromatographic methods cannot independently determine the oxidation state of As and peaks generated by thioarsenates may also be explained by thioarsenite species. In any case, the thioarsenic species, incorporating the As on either oxidation state, brake down under oxidised conditions at the surface in a series of kinetically controlled reactions (Planer-Friedrich et al., 2007). Therefore, the chemical composition of the water and the reaction time at the Earth's surface determine the As speciation in the geothermal water once it runs on the surface or seeps back into the bedrock. An accurate quantification of the individual species may as a consequence, be detrimental on As transport prediction with geochemical modeling.

The transport of As in shallow groundwater aquifers has been studied extensively due to its toxicity e.g. Charlet et al. (2007). The reduced form of arsenic, arsenite (As(III)) is generally considered more toxic than the oxidised form, arsenate (As(V)) (Ferguson and Gavis, 1972). The harmfulness of arsenite is based on its reaction with SH-groups of proteins (Squibb and Fowler, 1983) and, therefore, Stauder et al. (2005) suggested the toxicity of As could be decreased by formation of thioarsenates (addition of SH-groups to As) from arsenite in sulphidic environments. The mobility of these As

species depends on the chemical characteristics of the species themselves as well as the surface properties of the aquifer matrix. The surface of the aquifer in this contribution is primarily composed of basaltic glass. Sigfusson et al. (2008) measured sorption processes of arsenite and arsenate on basaltic glass and reported decreasing mobility of arsenite as pH increased from pH 3 to 10 whereas arsenate was immobile at pH 3 and highly mobile at pH 10. Stauder et al. (2005) predicted that thioarsenates should be less mobile than arsenite and arsenate on soil materials such as pyrite and goethite due to the shift from neutral to weak anionic form to a strong anionic As complex as a result of thioarsenates. This would be the case under acidic conditions whereas the thioarsenates should be more mobile at alkaline conditions as encountered in the high-temperature geothermal fluids in the current contribution.

The aim of this study was to predict the transport of As in a basaltic aquifer within the Nesjavellir geothermal system in SW Iceland. To this end, laboratory measured adsorption coefficients of aquatic As species on basaltic glass surfaces were incorporated into the one dimensional (1 D) reactive transport model PHREEQC-2 (Parkhurst and Appelo 1999) constrained by 25 year long time series of field measurements of chemical composition of geothermal effluent fluids and ground waters, pH, Eh and sometimes Fe- and As-dissolved species measurements.

4.2 Geological setting and power production

4.2.1 Geological setting

The Nesjavellir geothermal power plant is a so called co-generation power plant, producing both 88°C hot water by heat exchange and electricity. It lies in the eastern rim of the Hengill central volcano complex in south western Iceland (Fig. 1). The Hengill central volcano complex is the northernmost complex of the Western volcanic rift zone of Iceland that extends from the tip of Reykjanes peninsula which then submerges to form the Mid Atlantic ridge (MAR). To the north of the Hengill central volcano, Lake Thingvallavatn fills a tectonic graben associated with west north-westward tectonic movement of the North American plate and the Hreppar micro plate which separates the North American and Eurasian plates in the area (Einarsson, 2008). The lake is primarily spring fed by shallow aquifers to the north and supports a relatively high productivity ecosystem for its latitude (Jonasson, 1992). The Nesjavellir

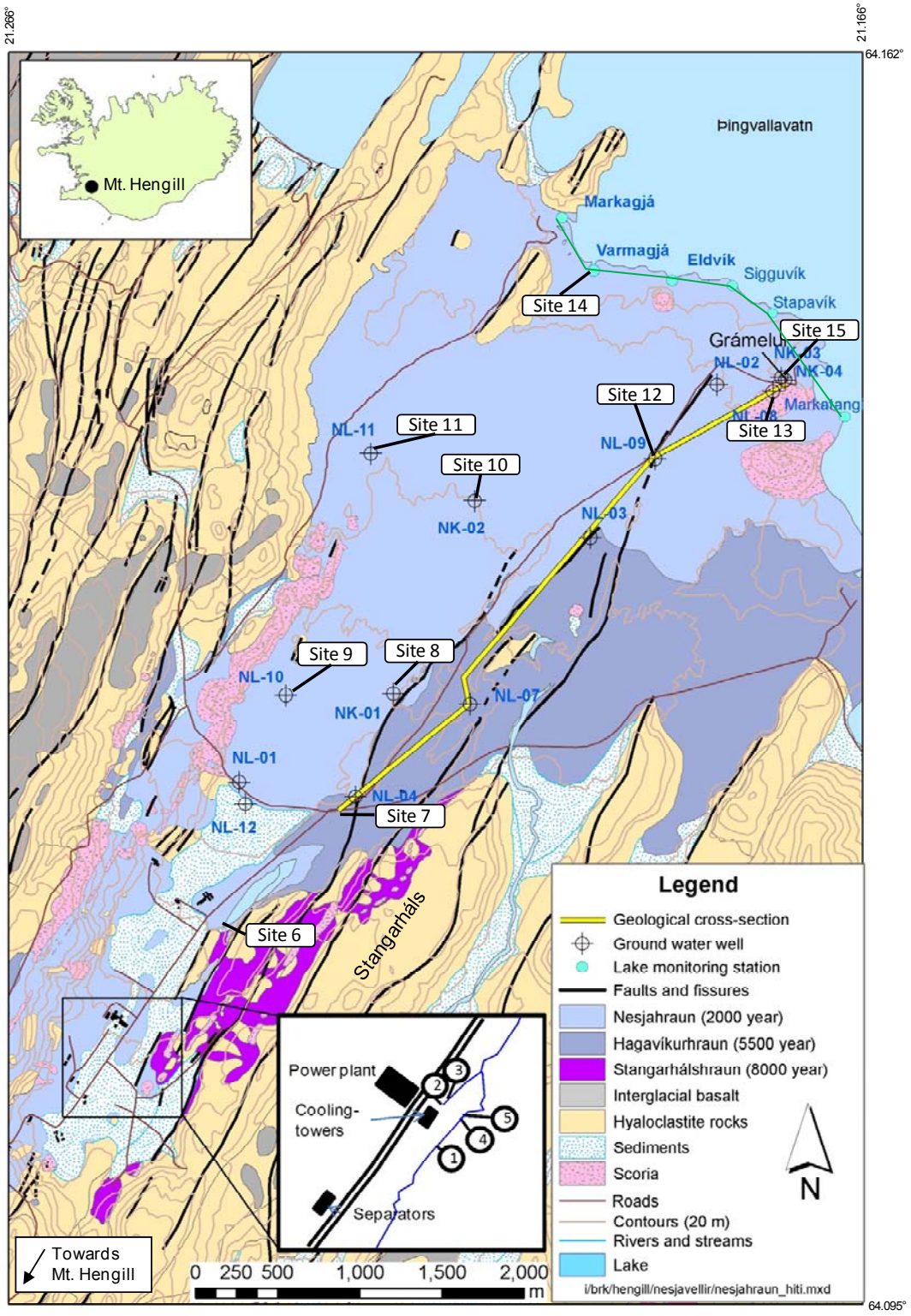

Figure 1 Location of sampling sites, the geological cross section and the 1D model path. Green line near the shore depicts the transverse in figure 3. Modified from Hafstað et al. (2007).

power plant lies in the Nesjavellir graben extending from Hengill central volcano to Lake Thingvallavatn (Fig. 1). The bedrock topography is characterised by predominantly basaltic lavas formed at interglacial intervals or predominantly

hyaloclastite ridges which are mostly basaltic glass, formed sub glacially during glacial intervals (Tomasson and Saemundsson, 1967). The area is one of the most active volcanic areas in Iceland. On the surface, Holocene lavas of variable age have flowed from eruption sites in the vicinity and extended far into the lake. Of the surface lavas, Stangarhólshraun is the oldest and erupted in early Holocene (8 ka) from a crater row extending from westerly parts of Stangarháls toward the lake in NE-SV (Figs.1 and 2a). The lava flows in this area are of AA type with thick glassy scoria at the base and top of the lava flows facilitating fast groundwater flow at the base of the lavas. The lava is partially covered by the younger Hagavíkurhraun (5.5 ka) erupted from a crater row to the east of the Nesjavellir graben and flowed over the graben (Figs. 1 and 2a,)). The lava is composed of oxidized scoria at the top and base of the flow while the centre of the flow is more dense and crystalline. The youngest lava, Nesjahraun (2 ka), erupted near the Hagavíkurhraun and covers a large portion of the older lavas as shown in Figs.

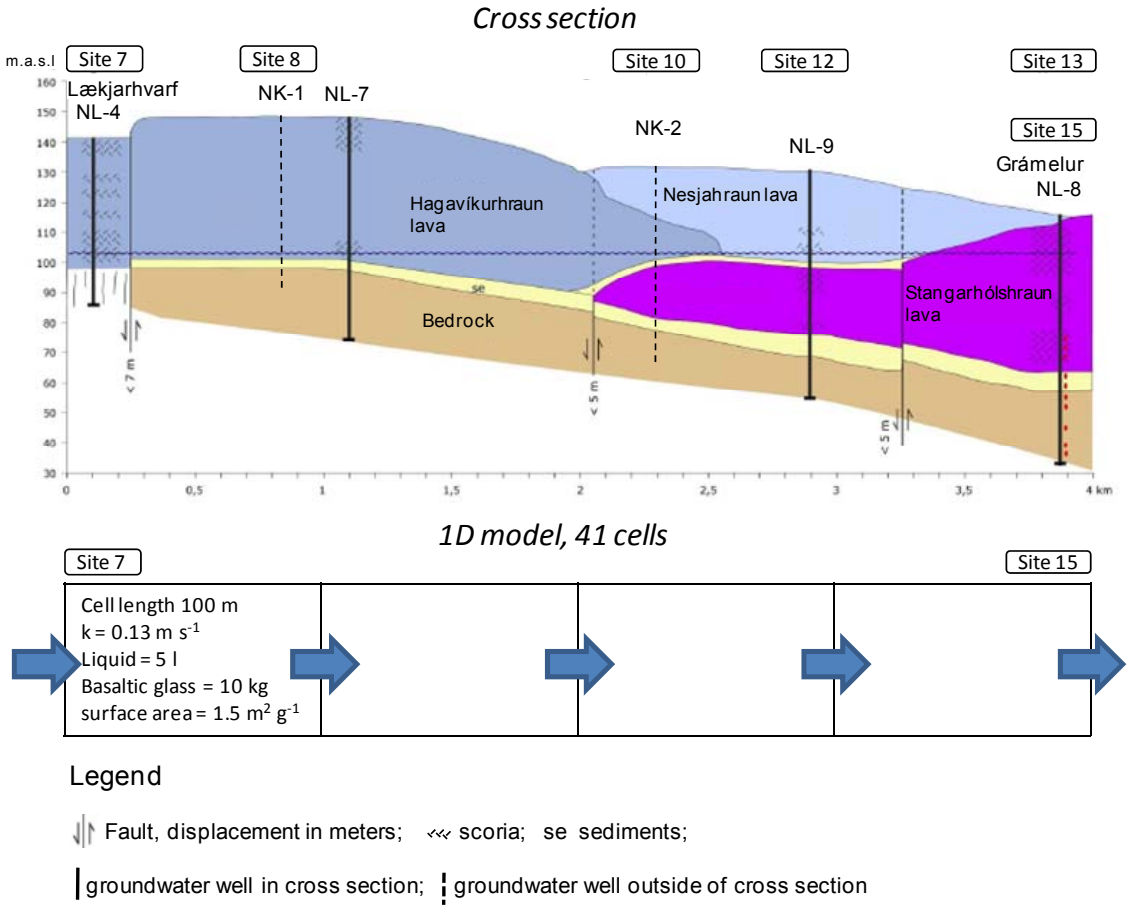

Figure 2a. Geological cross section of the modelled area (modified from Hafstað et. al, 2007). Geographical location of the cross section is displayed as yellow line in Fig. 1. Fig. 2b. The 1D model for water flow from Lækjarhvarf (Site 7) to Grámelur (site 13) corresponding to the cross-section in Fig. 2a.

1 and 2a (Saemundsson, 1995). The lava primarily covers the eastern parts of the Nesjavellir graben between the power plant and Lake Thingvallavatn and extends 1 km into the lake to 40 m depth. A series of tectonic events occurred between the eruptions of the two youngest lavas leaving series of faults in the Nesjavellir graben (Fig. 2a). The subsided area formed in these tectonic events was later filled with the Nesjahraun lava (Saemundsson, 1995). The Holocene lavas overlie the hyaloclastite rock formation consisting of basalt of variable crystallinity such as tuff, breccias, pillow lavas, and pillow fragments and glacial till can also be found in the bedrock (Hafstað et al., 2007) (Fig. 2a). Figure. 2a represents lateral transect extending along the main groundwater flow path. Figure 2b depicts the proposed mass balance scheme for the As transport as described later.

4.2.2 Power production at the Nesjavellir site.

The power plant was commissioned in September 1990. Initially, 4 wells were connected to the production line. Prior to the electrical power production in 1998, the 198°C geothermal fluid was separated by gravity into its water and gas phase. The hot steam was used to heat the 4°C ground water from the Grámelur (site 13 in Figure 1) to 88°C. This low dissolved solid 88°C heated water was then used for municipal district heating.

The brine was boiled down to atmospheric pressure and disposed of in the nearby Nesjavallalækur brook as shown in Fig. 1. Further downstream, this brook forms the pond Lækjarhvarf, which entirely drains into the subsurface. The separated steam phase was conducted to the power house where it was used for the heat exchange. The condensed steam produced during the heat exchange was disposed of into shallow wells adjacent to the power plant.

The geothermal power plant was redesigned to a co-generation plant for both hot water and electricity production in the summer of 1998. From then on, heat exchangers harnessed the energy of the high dissolved solid geothermal waters, while the steam was conducted to two turbine units for electricity production. Following 1998, increasing amounts of cold ground water were needed for municipal heating, which lead to dramatic increase in discharge from the Grámelur pumping station. The separated water phase was disposed of into the brook Nesjavallalækur, but since 2004 an increasing amount (initially 40 l s^{-1}) of separator water has been disposed of into 800 m deep wells near the power plant. In the beginning of 2009, 190 l s^{-1} were disposed of into the wells

along with large proportion of the condensate while the remaining 50 l s^{-1} are disposed of into the Nesjavallalækur brook.

4.3 Fluid geochemistry

4.3.1 Sampling sites

Samples for detailed chemical analysis were collected at 13 sites near the Nesjavellir power plant in March 2008 (Figure 1 and Table 1). Furthermore, the research Department of Reykjavík Energy has sampled the water at Nesjavallalækur and Lækjarhvarf (Sites 1 and 7, respectively), at Grámelur (Site 15) and the shoreline of Thingvallavatn biannually since 1983 (Figs. 1 and 3a,b,c and d).

4.3.2 Sampling methodology

Samples were pumped directly from respective source (borehole, spring or stream) by a peristaltic pump (Cole Parmer Masterflex E/S portable sampler) through a High Density Polyethylene (HDPE) cooling loop followed by a 0.2 μm cellulose acetate (CA) filter (Advantec MFS) enclosed in a HDPE housing. Samples from boreholes were extracted 2 m below the water table. All bottles were pre-rinsed with filtered water prior to sample collection. Sample for As and anion speciation was directed into a 10 ml gas tight syringe and injected into a Dionex ICS-2000 ion chromatograph (IC) coupled to a PSAnalytical hydride-generation atomic fluorescence spectrophotometer (HG-AFS) immediately on sampling as the analytical equipment was field deployed. An example chromatogram may be found in Fig. 4. Then sample was directed through the cooling loop into a pH/Eh flow cell and pH and Eh recorded respectively (Cole Parmer combination gel filled electrode for pH and Pt-electrode for Eh with Eutech pH200 displays). Temperature of the pH/Eh flow-cell was set as close to 25°C by adjusting the sample flow rate through the cooling loop. Then 60 ml for total carbonate carbon (TCC)

Table 1 Chemical composition of geothermal effluent, river and groundwaters

	location	distance along flowpath meters	Temp °C	pH	Eh mV	T pH/Eh °C	As total µM	Σas speciation µM	As(III) µM	As(V) µM	Monothio Arsenic µM	Dithio Arsenic µM	Trithio Arsenic µM	Tetrathio Arsenic µM	Fe^{3+} uM IC	Fe^{2+} uM IC
Site 1	Nesjavallalækur	-1620	20,8	8,75	nd	24	nd	nd	nd	nd	nd	nd	nd	nd	nd	nd
Site 2	Heated groundwater	-1600	17.7	8.03	89	17.7	0.077	0.074	<0.013	0.074	<0.013	<0.013	<0.013	<0.013	0.115	0.103
Site 3	Condensate	-1600	36.7	6.86	-209	24.9	0.093	0.129	0.092	0.036	<0.013	<0.013	<0.013	<0.013	0.194	0.118
Site 4	Outlet	-1600	65.55	9.00	-234	25.8	2.556	2.327	0.290	<0.013	<0.013	0.992	0.752	0.294	0.790	0.000
Site 5	Outlet+Brook	-1600	42	8.8	-185	25.5	2.008	1.874	0.228	0.024	<0.013	0.770	0.612	0.240	4.550	
Site 6	Brook	-1100	29.4	8.82	-68	24.4	1.064	1.148	0.047	0.102	0.067	0.448	0.486	<0.013	0.594	0.780
Site 7	Lækjarhvarf	0	22	8.64	23	22.5	0.882	0.839	<0.013	0.013*	0.013*	0.397	0.442	<0.013	2.263	0.236
Site 8	NK1	850	28.4	9.01	76	25.1	0.031	0.031	<0.013	0.031	<0.013	<0.013	<0.013	<0.013	0.182	0.036
Site 9	NL 10	870	24	8.38	59	23.8	<0.0013	<0.013	<0.013	<0.013	<0.013	<0.013	<0.013	<0.013	1.553	0.476
Site 10	NK 2	2100	31.6	7.60	115	24.3	<0.0013	<0.013	<0.013	<0.013	<0.013	<0.013	<0.013	<0.013	0.094	0.000
Site 11	NL11	2200	22	8.64	64	21.8	<0.0013	<0.013	<0.013	<0.013	<0.013	<0.013	<0.013	<0.013	0.101	0.000
Site 12	NL9	3000	11.4	7.60	96	11.4	0.0035	<0.013	<0.013	<0.013	<0.013	<0.013	<0.013	<0.013	0.927	0.000
Site 13	NL 8	3900	22.8	7.80	132	22.2	0.0026	<0.013	<0.013	<0.013	<0.013	<0.013	<0.013	<0.013	1.159	0.000
Site 14	Varmagjá	4100	30	7.53	84	25.2	0.0066	<0.013	<0.013	<0.013	<0.013	<0.013	<0.013	<0.013	1.514	0.000
Site 15	Grámelur, 1991	4100	5	7.71	nd	25	0.0020	nd	nd	nd	nd	nd	nd	nd	1.004	nd
Site 15	Grámelur, 2007	4100	22	7.00	nd	22	0.0020	nd	nd	nd	nd	nd	nd	nd	1.600	nd

Location	HS^- mM titration	SO_4^{2-} mM AEC	$S_2O_3^{2-}$ mM AEC	S total mM ICP	CO_3^{2-} mM AEC	F mM AEC	Cl mM AEC	Si mM ICP	Na mM ICP	K mM ICP	Ca mM ICP	Mg mM ICP	Al µM ICP	Mn µM ICP	B µM ICP
Site 1	0.0007	0.514	nd	nd	1.34	0.038	1.918	2.31	1.19	0.088	0.329	0.156	<0.04	<0.036	<0.7
Site 2	<0.00008	0.168	0.000	0.156	1.45	0.009	0.463	0.792	0.864	0.071	0.236	0.206	5.57	<0.036	9.34
Site 3	0.187	0.110	0.013	0.469	0.687	0.005	0.270	0.424	0.491	0.040	0.134	0.115	3.04	0.017	6.82
Site 4	1.04	0.173	0.113	0.160	0.484	0.063	4.04	12.3	6.99	0.801	0.010	0.002	69.7	0.014	172
Site 5	0.310	0.332	0.114	0.382	0.553	0.046	3.29	8.56	5.24	0.584	0.218	0.102	46.4	0.226	125
Site 6	0.013	0.334	0.057	0.498	1.16	0.020	1.32	4.29	2.92	0.302	0.303	0.183	24.4	0.439	60.8
Site 7	<0.00008	0.486	0.119	0.645	0.826	0.033	2.24	5.77	3.71	0.395	0.206	0.113	32.3	0.382	83.8
Site 8	<0.00008	0.210	0.000	0.161	0.434	0.011	0.864	0.845	1.56	0.151	0.160	0.090	5.49	0.071	22.9
Site 9	<0.00008	0.239	0.000	0.224	0.580	0.007	0.216	0.460	0.653	0.041	0.234	0.234	<0.04	0.067	1.62
Site 10	<0.00008	0.002	0.000	0.007	0.196	0.007	1.17	0.037	0.587	0.046	0.357	0.074	<0.04	0.102	5.42
Site 11	<0.00008	0.002	0.000	0.002	0.960	0.013	0.261	0.011	1.046	0.068	0.110	0.344	<0.04	0.231	0.788
Site 12	<0.00008	0.164	0.001	0.108	0.718	0.005	0.269	0.433	0.551	0.045	0.251	0.254	0.332	0.047	1.69
Site 13	<0.00008	0.169	0.000	0.141	0.719	0.007	0.324	0.515	0.581	0.041	0.275	0.298	0.764	0.041	3.06
Site 14	<0.00008	0.302	0.000	0.283	1.24	0.012	0.395	1.10	1.04	0.111	0.351	0.248	0.577	<0.036	8.47
Site 15	<0.00008	0.085	nd	nd	0.70	0.005	0.264	0.39	0.46	0.027	0.219	0.217	2.480	nd	nd
Site 15	<0.00008	0.504	0.000	0.504	0.64	0.007	0.460	0.94	1.00	0.093	0.240	0.204	5.930	0.050	11.10

were pumped into an amber glass bottle and filled completely before being sealed

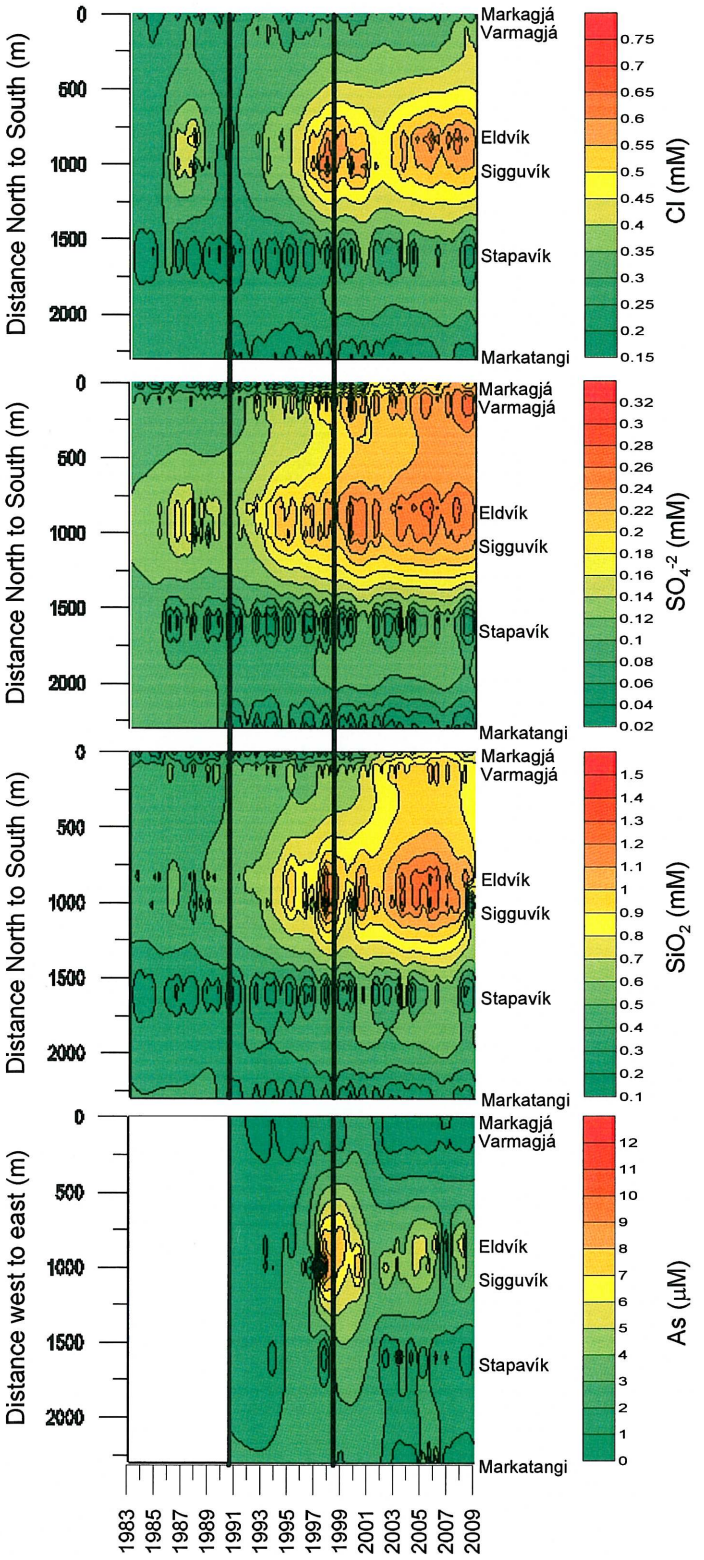

Figure 3 Measured Cl, SO_4, SiO_2 and As concentrations from the springs along Lake Thingvallavatn shoreline from 1983 to December 2008. Sampling locations are displayed in Fig. 1. Black line in 1990 marks commission of the powerplant, black line in 1998 marks the expansion of the power plant to electricity generation. All samples were collected by the research department of Reykjavik Energy, which also analysed Cl^-, SO_4^{-2} and SiO_2 concentrations. Arsenic concentrations were measured from archived samples.

with an air tight cap. Sample was then pumped into a 50 ml HDPE bottle and 0.5-7.5 ml of sample pipetted to a 15 ml HDPE bottle for determination of H_2S. The remainder in the 50 ml bottle was preserved to 1% 6 N HCl for the determination of ferric and ferrous iron. Another 50 ml HDPE bottle was filled and sample pH raised to >10 by the addition of 1.0 N NaOH followed by the addition of 0.5 mL of 30% H_2O_2. After 30 min, HCl was used to acidify sample to pH<2 (Beak et al., 2008). After that, 50 ml HDPE bottle was filled and acidified to 0.5% by concentrated $HNO_3$for the analysis of major constituents and selected minor constituents. Finally, sample for further As-speciation analysis was pumped into two 15 ml HDPE bottles which were immediately frozen in dry-ice.

4.3.3 **Analytical methods**

Major and some minor constituents were measured on by Spectro Ciros Vision Inductively Coupled Plasma Atomic Emission Spectrometer (ICP-AES). Arsenic species, arsenite (H_3AsO_3) , arsenate ($HAsO_3^{2-}$), mono-, di-, tri- and tetrathioarsenate, ($As(OH)_2(SH)$, $As(OH)_2S^-$, $As(OH)S_2^{2-}$,AsS_3H^{2-} ,AsS_3^{3-} and $As(SH)_4$) and the anions F^-, Cl^-, SO_4^{2-}, $S_2O_3^{2-}$ were separated according to Planer-Friedrich et al. (2007). Briefly A Dionex ICS-2000 with self generated AEC separated and detected, anionic species and the HG-AFS detected species that contained As (Table 2). The As concentration for each individual species was quantified with HG-AFS as opposed to ICP-MS, as the instrumentation was field deployed. Total As was measured by HG-AFS according to (PSAnalytical 1997). Total carbonic carbon was measured by AEC according to (Stefansson et al., 2007). DOC was measured by persulphate UV-oxidation followed by infrared detection of generated CO_2 (LABTOC-Pollution and Process Monitoring). Iron speciation was carried out with Metpac^{TM} PCDA eluent on a Dionex ICS-3000 according to Dionex technical note 10 (Dionex). Alterations to the method were: a 1 ml injection loop was used to increase sensitivity and 4-(2-pyridylazo) resorcinol (PAR) was halved to 60 μg l^{-1}. Total As was analysed in HNO_3 acidified samples from Reykjavik Energy archives, covering the time period1991-2008 and few samples sampled prior to 1990. The method was according to (PSAnalytical, 1997).

Table 2 Instrumental setup for the detection of arsenic oxy- and thioanions by AEC-HG-AFS. Speciation procedure was adapted from Planer-Friedrich et al. (2007).

Anion Exchange Chromatography (AEC) separation		
Instrument	**DIONEX ICS-2000**	
Column	IonPac AS-16/AG-16 4-mm (10-32) (Dionex, Sunnyvale, CA)	
Eluent	KOH, Automated eluent generation at 1 ml/min	
Gradient	0 → 7 min 20 mmol/l 7 → 17 min 20 → 100 mmol/l 17 → 25 min 100 mmol/l 25 → 28 min 100 → 20 mmol/l	
Sample volume	100 µl	
Typical retention times	arsenite	271 s
	arsenate	693 s
	monothioarsenite	777 s
	dithioarsenite	861 s
	trithioarsenite	948 s
	tetrathioarsenite	1039 s
Supression	ASRS-Ultra 4-mm (Dionex, Sunnyvale, CA) 300 mA current, 5 ml min-1 water, (external mode)	
Hydride Generation Atomic Fluoresence Spectroscopy (HG-AFS) detection		
Instrument	**PSAnalytical Millenium Excalibur**	
Reductant	12,5% HCl, red-red tubing, pump 50% 0.7% $NaBH_4$ in 0.1 M NaOH, grey-grey tubing, pump 100%	
Carrier gas	Ar (5.0 grade), flow rate 300 ml/min	
Gas / liquid separator	Type ME Gas/liquid separator	
Air dryer	Permapure dryer system Dryer gas, Ar, flow rate 2.5 l/min	
Lamp	Boosted discharge hollow cathode lamp (BDHCL) Primary current 27.5 mA Boost current 35.0 mA	

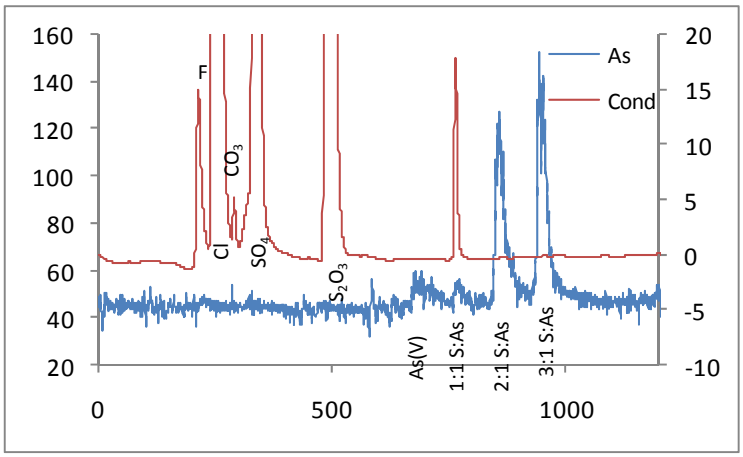

Figure 4 Sample chromatogram for arsenic and anion speciation from water measured at site 6 less than one minute after sampling

4.3.4 Thermodynamic data

Results from chemical analysis were inserted into the computer code PHREEQC-2 (Appelo and Postma, 1999) where speciation calculations were carried out. The wateq4f.dat (with PHREEQC-2 version 2.15) was amended with equilibrium constants for thioarsenite from Wilkin et al. (2003).

4.3.5 Fluid composition

Results from aqueous chemical analysis are given in Table 1. The temperature and pH of the geothermal outlet brine at Site 4 was 65.5°C and 9.00 (measured at 25 °C) respectively and had lowered to 22°C and pH 8.64 at Site 7 were surface water disappeared under the lava. Similarly the Eh shifted from -234 to +22. Ferric iron was the dominant iron species in the groundwater wells whereas more ferrous iron was detected in some surface waters.

The pH drop in the brook is a consequence of H_2S oxidation to SO_4^{2-} (Table 1), silica polymerization (Gunnarsson and Arnorsson, 2008) and dilution with surface runoff as indicated by the Cl^-/B ratio of these waters (Fig. 5). The mixed Nesjavallalækur (Site 5) was a 2:1 mixture of the outlet water (Site 4) and Nesjavallalækur (Site 1) based on Cl^- concentrations. The high carbon concentration at Site 6 was due to surface runoff from Site 2 (heated groundwater rich in carbonate (1.45 mM)) which mixed with the Nesjavallalækur brook to achieve a carbonate concentration of (1.16 mM).

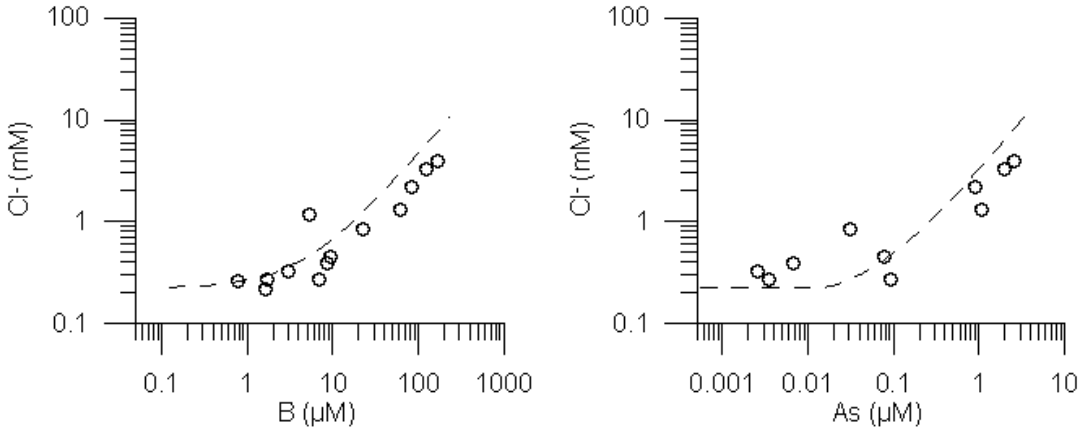

Figure 5. The relationship of B and total As with the conservative ion Cl^-. Measured Cl, B and As concentrations represented at dots. Dashed line represents the reaction path for basalt leaching by the local precipitation.

Arnorsson and Andresdottir (1995) showed that chlorine/boron (Cl/B) ratio of geothermal waters could be explained by leaching of basaltic rocks and that both components were highly conservative in solution. Giroud (2008) used the same ratio and furthermore the Cl^-/As ratio of Icelandic geothermal waters to show less mobility of As. Figure 5 displays the Cl^-/B and Cl^-/As ratios of all samples in the current contribution and it may be inferred that those waters are products of leaching of basaltic rock with local precipitation. The outlet of the power plant has the highest Cl^- and B concentrations while the NL-11 water from the flank of the rift valley (Fig. 1) has the lowest concentrations and most samples lie on a line between those two end members. The Cl^-/As ratio on the other hand shows depletion of As compared to simple leaching of basalt indicating retention of As compared to Cl^- and B in the groundwater flow but Cl^- concentration increased in Varmagjá (site 14), Eldvík and Sigguvík (Fig. 1) shortly after the commission of the power plant whereas the total As peak was slightly retained (Figs. 3 and 7a,d). The sharp increase of As in Eldvík and Sigguvík in 1998 after the expansion of the power plant was presumably due to limited preferential flow through crevasses which was maintained to some extent throughout the study period. The same As increase was not observed in Varmagjá or Grámelur (Figs. 6c,d), which lie in the course of the main streams of the ground water flow in the lava field (Kjaran and Myer 2005).

4.3.6 Arsenic speciation of surface and ground waters

Heated ground water (Site 2) is mainly directed directly into shallow wells at the power plant but some fraction enters the Nesjavellir Brook as is evident from the high carbon concentration in site 6. The water at Site 2 had small amount of arsenate (mainly as $HAs^{V}O_4^{2-}$). Site 3 is a condensed steam which is also mainly directed into wells but at the time of sampling a small proportion of this water entered the Nesjavellir Brook. The main As-species was arsenite ($H_3As^{III}O_3$) with less arsenate ($H_2As^{V}O_4^-$ and $HAs^{V}O_4^{2-}$) and no thioarsenites were detected. Current instrumental setup could not distinguish between thioarsenites and thioarsenates, but the thioarsenite species $As(OH)_2(SH)$, $As(OH)_2S^-$, $As(OH)S_2^{2-}$,AsS_3H^{2-} ,AsS_3^{3-} and $As(SH)_4^-$ proposed by Wilkin et al. (2003) were used in all calculations (Fig. 5). At the power plant outlet (Site 4) the abundance of As-species in the separator water decreased from the thioarsenite species As:S 1:2>1:3>1:4 followed by the arsenite species (Table 1). The power plant effluent was immediately mixed at Site 5 with surface runoff of the Nesjavallalækur (Site 1) were the HS^- concentration decreased from 1 mM in the outlet to 0.3 mM in the mixture associated with a ~25% dilution of the conservative components Cl^-, B, F^- and Na. At Site 5, the thioarsenite species were still the most important As-species (Table 1). The brook flowed approximately 500 meters before the next sampling Site 6 (Figure 1). At Site 6, HS^- had decreased from 0.3 mM to 0.01 mM without significant increase in $S_2O_3^{2-}$ and SO_4^{2-} (Table 1) whereas the total As concentration had lowered. The tetra-thioarsenite was no longer detected and monothioarsenite had formed as well as arsenate (Fig. 7, Table 1). At Site 7 (the surface inlet solution for the groundwater model) the HS^- had decreased to 0.002 mM with associated increase in $S_2O_3^{2-}$ and SO_4^{2-} and a small decrease in total As concentration, of which dithio- and trithioarsenite were the only detected species (Table 1). The concentration of As dropped markedly from the surface waters to the ground waters and no thioarsenite species were detected in groundwater wells (Sites 8-13), the spring (Site 14) in Thingvallavatn and Grámelur (Site 15) and arsenate was the only species detected at these sites (Fig. 7).

The occurrence of thioarsenite species down the brook flow-path was clearly kinetically controlled. According to thermodynamic calculations the thioarsenites should be the dominant species in the outlet and the mixture at Site 5, however, down the flow path at Sites 6 and 7 the dominant species should be arsenite due to the low concentration of HS^- (Wilkin et al., 2003) (Fig. 5). Speciation calculations in

PHREEQC-2 highlighted the sluggishness of the thioarsenites breakdown although no thioarsenites were detected in the shallow groundwater wells down-flow from site 7 representing the termination of the Brook. The residence time of the groundwater was counted in days to months (Table 3) compared to hours in the brook.

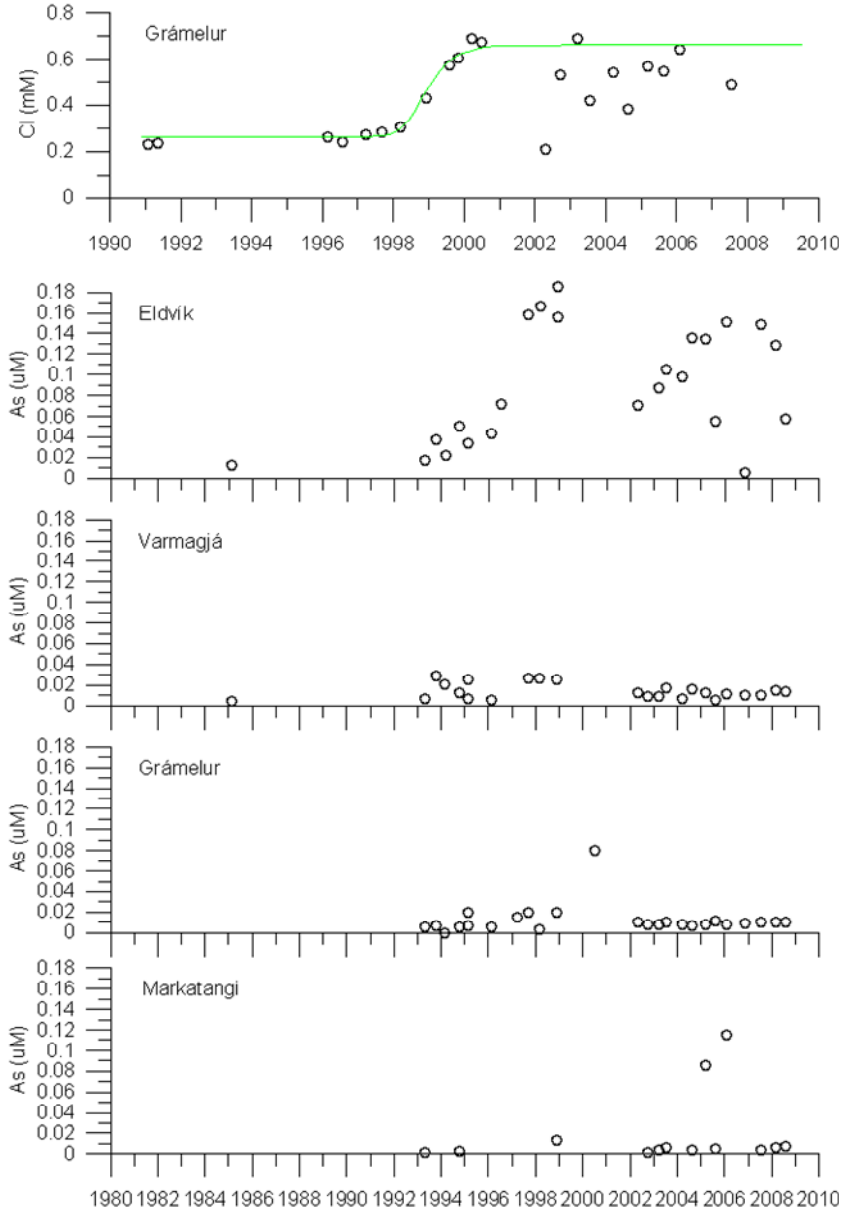

Figure 6 Calibration of the groundwater model assuming Cl acted as conservative (a). Lækjarhvarf water was mixed to pristine ground water from Grámelur. This mixture flowed through the model and the duration of each time shift in the transport model was iterated until the modelled curve corresponded to the data prior to 2000. After 2000, the Cl data from Grámelur displayed increased scatter due to extensive pumping from the groundwater system leading increased influx of surface rain and melt-waters along with geothermal water (Werner and Wallquist, 2008). Figs. b,c and d represent measured total As concentrations at the shoreline of lake Thingvallavatn and Grámelur.

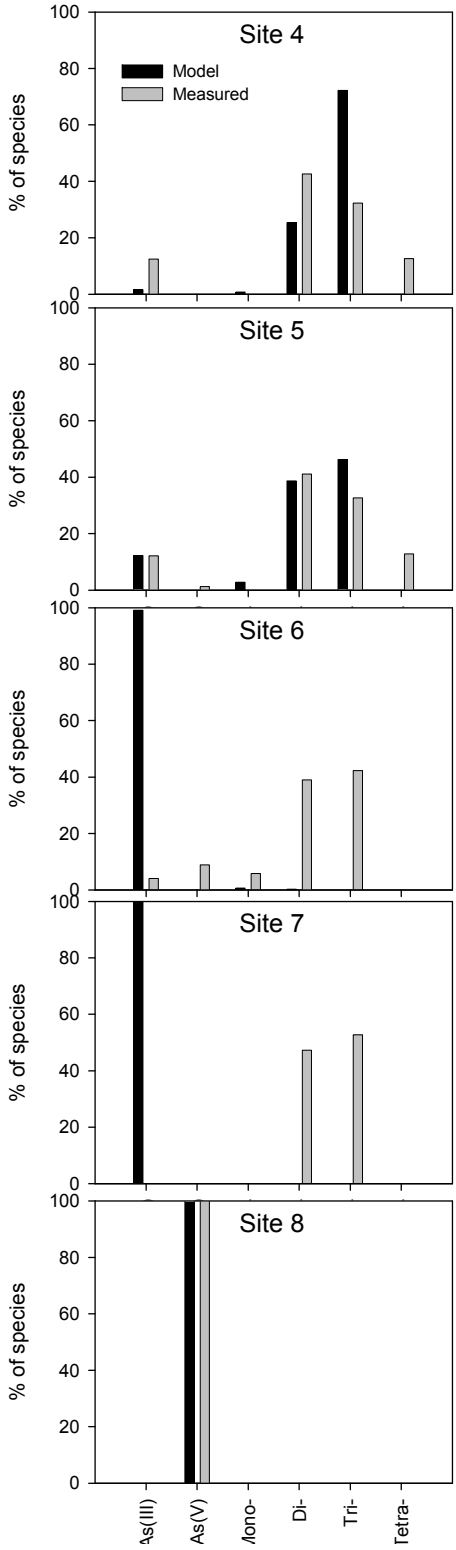

Figure 7 Modelled and measured As speciation from 5 samples at Nesjavellir. Sites 4-7 are surface waters at increasing distance from the power-plant outlet and display elevated discrepancy between the modelled and measured results downstream indicating kinetic control of the thioarsenic degradation. Site 8 is well-water 800 meters downstream of site 7.

4.4 Groundwater flow model

A mass balance scheme, as proposed by Werner and Wallquist (2008) for the fate of CO_2 in the groundwater system, was used in the present study to determine input and fate of As in the groundwater system (Figure 2b). The system boundary was chosen to frame the disappearance of the geothermal wastewater at Laekjarhvarf (site 7, Figs.1,2a) to the Grámelur pumping station (site 15, Figs. 1,2a) close to the shoreline of Lake Thingvallavatn. Groundwater flow rate was calibrated against changes in measured chloride concentrations in the Grámelur pumping station (outlet water) during the time period 1996 to 2008 (Fig. 5). The following assumptions were made:

1. Chloride acted as a conservative ion in the groundwater (Gislason and Eugster, 1987; Arnorsson and Andresdottir, 1995).
2. The water pumped up in Grámelur during the years 1991-1997 was assumed to be "pristine" ground waters without the influence of anthropogenic geothermal effluents from the power plant (Figs 3a and 5a).
3. The water pumped up in Grámelur from 1998 onwards had increasing effluent signature (Cl^- concentration) with a complete breakthrough of the effluents in July 2000 (Fig. 5a). As a result, one pore volume in the system was replaced in 3320 days (9 years and 36 days).
4. The inlet solution for the reactive transport modeling was produced by mixing Lækjarhvarf and pristine Grámelur waters in 1:4 ratio to produce the chloride concentrations measured at Grámelur after one PV had been replaced in the system.

Once boundary conditions for the groundwater flow had been established a 4100 m 1D column was defined by a series of forty one 100 m long cells as shown in Fig. 2b. The column was a scaled up column from Sigfusson et al. (2008) maintaining identical physical characteristics such as specific surface area, solid/solution ratio and dispersivity. All cells had the same physical properties (Table 3). A prediction of As movement was then carried out based on adsorption coefficients generated from laboratory experiments on the interaction between basaltic glass and dissolved arsenite and arsenate (Table 3) (Sigfusson et al., 2008) into the one dimensional (1D) reactive transport model PHREEQC-2 (Parkhurst and Appelo, 1999) (Fig. 8). According to

Table 3 Properties of the 1D transport model in PHREEQC-2

Column properties		
Number of cells	41	
Cell Length	100	m
Liquid in each cell	5	liters
hydraulic conductivity, K	5.86E-04	m s^{-1}
dispersivity	14	m
=> Column timestep	7000000	s
=> one Pore Volume (PV)	79722.22	hours
=> shifts in each year	5	shifts

Solution composition

	Background	Lækjarhvarf	Input mixture	
pH	7.71	8.64	8.62	
pe	1.54	0.38	1.1	
HS-	0	0.002	0	mmol l^{-1}
SO42-	0.085	0.486	0.165	mmol l^{-1}
CO32-	0.699	0.862	0.73	mmol l^{-1}
F	0.005	0.033	0.011	mmol l^{-1}
Cl	0.264	2.243	0.66	mmol l^{-1}
Si	0.389	5.77	1.467	mmol l^{-1}
Na	0.454	3.712	1.108	mmol l^{-1}
K	0.0274	0.395	0.101	mmol l^{-1}
Ca	0.219	0.206	0.217	mmol l^{-1}
Mg	0.217	0.113	0.196	mmol l^{-1}
As	0	0.882	0.1765	µmol l^{-1}
Fe(2)	0	236	72.3	µmol l^{-1}
Fe(3)	1000	2263	1300	µmol l^{-1}
Al	2.48	32.2	8.43	µmol l^{-1}
B		83	16.6	µmol l^{-1}

Basaltic glass:

Mass in each cell	10	kg
Specific surface area	1.5	m^2 g^{-1}
Surface sites	4	sites nm^{-2}

Arsenic surface reactions on BG (Sigfusson, et. al., 2008)

Reaction	log K (25°C)
As(III)	
$2Glass\text{-}OH + H_3AsO_3 = (Glass\text{-}O)_2AsOH + 2H_2O$	4.7
$Glass\text{-}OH + H_3AsO_3 = Glass\text{-}H_4AsO_4$	2.78
As(V)	
$Glass\text{-}OH + H_3AsO_4 = Glass\text{-}OAsO_3^{-2} + 2H_+ + H_2O$	-2.4
$2Glass\text{-}OH + H_3AsO_4 = (Glass\text{-}O)_2AsO_2^- + H^+ + 2H_2O$	2.3
$2Glass\text{-}OH + H_3AsO_4 = (Glass\text{-}O)_2AsOOH + 2H_2O$	4.3

thermodynamic calculations and measurements showed that all As in the ground waters was on the arsenate (As(V)) form. However, since As is anticipated to exist as arsenite in geothermal waters which are immediately disposed of into the ground after utilisation without flowing on the surface, predictions were made for arsenite by blocking (increasing the logK for arsenate reduction to 100) the oxidation of the arsenite from the inlet solution in the model. At the pH conditions encountered in the model (pH 8.5 – 8.6) arsenate in Grámelur would be close to that of the inlet mixture towards the year 2100 whereas arsenite bound more strongly to the basaltic glass surface and would still be very low (Fig. 8a). Predicted traverse of the groundwater system for the year 2009 indicated the concentration of arsenate in well NK-1(site 8) should be 0.09μM compared to the measured concentration of 0.031 μM (Table 1). The heterogeneity of the aquifer is clear from these figures and shows that some part of the effluent waters travels through crevasses with limited contact to the aquifer matrix (Figs. 5b-e and 8b) although the As was always retained compared to Cl^- (Figs. 7a,d).Two sets of calculations were done for traverses of the years 2050 and 2100, one assuming continued disposal of all effluents into Lækjarhvarf (dashed lines) and the other assuming a complete disposal of effluents into deep wells (Figs. 8c and d). Continued injection of geothermal wastewater would result in saturation of the aquifer matrix surface soon after the year 2100 with the arsenate concentration at the lake shoreline as high as the concentration in the inlet mixture. Disposal of the effluents into deep wells is a clear advantage since the As peak from the 20 year seepage period commencing in 1990 would smear out resulting in lower eluted concentrations at the lake shoreline as may be inferred from comparing the arsenate peaks in Figs. 8c and d. The arsenate already adsorbed at the proximal end of the column, will elute slowly into the groundwater over but the concentrations will always be low as opposed continued effluent seepage into Lækjarhvarf.

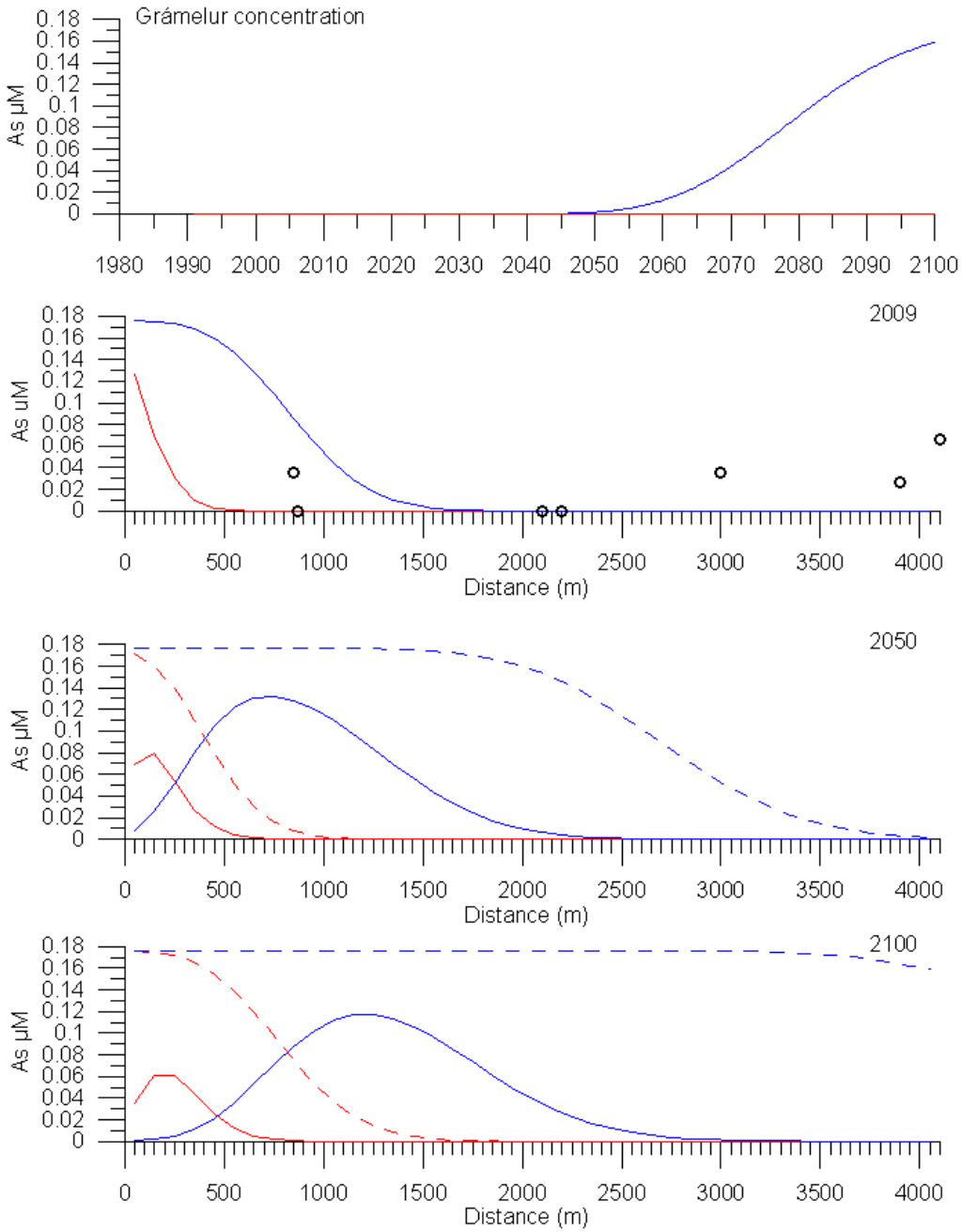

Figure 8 Predicted breakthrough of arsenite and arsenate at Grámelur pumping station if all effluent water would have been disposed off into Lækjarhvarf (a). Predicted traverse of arsenite (red curve) and arsenate (blue curve) in January 2009, circles represent total As measurements (b). Predicted traverse of arsenite (red) and arsenate (blue) in the year 2050 assuming all effluent water is disposed off into Lækjarhvarf (dashed lines) and assuming all effluent water is disposed off into deep wells after 2010 (lines) (c). Predicted traverse of arsenite and arsenate in the year 2100 assuming all effluent water is disposed off into Lækjarhvarf (dashed lines) and assuming all effluent water is disposed off into deep wells after 2010 (lines) (d).

4.5 Conclusion

The Nesjavellir geothermal power plant has been in operation since 1990. During this time increased proportion of the separator water has been directed into deep wells. Prior to deep well injection, majority of the effluent waters with elevated Si, Cl^-, SO_4^{2-} and As concentrations seeped into a lava field in a proximity to the power plant. These effluent waters mixed with the ground water and flowed trough faults and crevasses and as matrix flow towards Lake Thingvallavatn. The As in the geothermal effluents existed primarily as thioarsenic species with decreasing S:As ratios as the water flowed from the source. Although dithioarsenic and trithiorsenic were the main As species in the seepage water to the lava field, arsenate was the only As species measured in the ground waters towards Lake Thingvallavatn. Two scenarios for groundwater movement modeling were assumed, i) continued seepage of all separator waters into the lava field and ii), discharge of all separator water into deep wells after the year 2010. Geochemical modeling predicted a complete breakthrough of arsenate into the lake soon after the 2100 while arsenite breakthrough would take about 900 years assuming all effluents would seep into the lava field. Increased proportion of deep well injection will lead to increasingly retained discharge of arsenate from the lava field compared to dissolved conservative compounds and the eluted arsenate concentration always be much lower than that of the seepage phase in Lækjarhvarf.

4.6 Acknowledgements

This study was supported by the Icelandic Research Fund 050204033, Reykjavik Energy, Institute of Earth Sciences - University of Iceland and the Icelandic Governmental fund for Graduate Education. Gretar Ívarsson, Gestur Gíslason and Einar Gunnlaugsson sampled most of the Reykjavik Energy samples together with Einar Örn Þrastarson who also provided help with field work. Bjarni Reyr Kristjánsson at Reykjavik Energy and Gunnlaugur Einarsson at Iceland Geosurvey provided the map in Fig. 1.

4.7 References

Akinfiev, N.N., Zotov, A.V. & Nikonorov, A.P. 1992, "Thermodynamic Analysis of Equilibria in the System As(iii)-S(ii)-O-H", *Geokhimiya,* , no. 5, pp. 721-734.

Aksoy, N., Simsek, C. & Gunduz, O. 2009, "Groundwater contamination mechanism in a geothermal field: A case study of Balcova, Turkey", *Journal of contaminant hydrology,* vol. 103, no. 1-2, pp. 13-28.

Arnorsson, S. 2003, "Arsenic in surface- and up to 90 degrees C ground waters in a basalt area, N-Iceland: processes controlling its mobility", *Applied Geochemistry,* vol. 18, no. 9, pp. 1297-1312.

Arnorsson, S. & Andresdottir, A. 1995, "Processes controlling the distribution of boron and chlorine in natural waters in Iceland", *Geochimica et Cosmochimica Acta,* vol. 59, no. 20, pp. 4125-4146.

Baba, A. & Armannsson, H. 2006, "Environmental impact of the utilization of geothermal areas", *Energy Sources Part B-Economics Planning and Policy,* vol. 1, no. 3, pp. 267-278.

Ballantyne, J.M. & Moore, J.N. 1988, "Arsenic geochemistry in geothermal systems", *Geochimica et Cosmochimica Acta,* vol. 52, no. 2, pp. 475-483.

Beak, D.G., Wilkin, R.T., Ford, R.G. & Kelly, S.D. 2008, "Examination of arsenic speciation in sulfidic solutions using X-ray absorption spectroscopy", *Environmental science & technology,* vol. 42, no. 5, pp. 1643-1650.

Charlet, L., Chakraborty, S., Appelo, C.A.J., Roman-Ross, G., Nath, B., Ansari, A.A., Lanson, M., Chatterjee, D. & Mallik, S.B. 2007, "Chemodynamics of an arsenic "hotspot" in a West Bengal aquifer: A field and reactive transport modeling study", *Applied Geochemistry,* vol. 22, no. 7, pp. 1273-1292.

Cleverley, J.S., Benning, L.G. & Mountain, B.W. 2003, "Reaction path modelling in the As–S system: a case study for geothermal As transport", *Applied Geochemistry,* vol. 18, no. 9, pp. 1325-1345.

Dionex *Determination of Transition Metals by Ion Chromatography*, Dionex.

Einarsson, P. 2008, "Plate boundaries, rifts and transforms in Iceland", *Jökull,* vol. 58, pp. 35-58.

Ellis, A.J. & Mahon, W.A.J. 1964, "Natural hydrothermal systems and experimental hot water/rock interactions", *Geochimica et Cosmochimica Acta,* vol. 28, pp. 1323-1357.

Ferguson, J.F. & Gavis, J. 1972, "A review of the arsenic cycle in natural waters", *Water Research,* vol. 6, no. 11, pp. 1259-1274.

Gallup, D.L. 2007, "Treatment of geothermal waters for production of industrial, agricultural or drinking water", *Geothermics,* vol. 36, no. 5, pp. 473-483.

Giroud, N. 2009 *A chemical study of arsenic, boron and gases in high-temperature geothermal fluids in Iceland*. PhD thesis, University of Iceland, Faculty of Science.

Gislason S.R. & Eugster H.P. 1987, "Meteoric water-basalt interactions: II. A field study in NE Iceland", *Geochimica et Cosmochimica Acta*, vol. 51, pp. 2841-2855.Goldschmidt, V.M. 1954, *Geochemistry,* , Oxford.

Gunnarsson, I. & Arnorsson, S. 2008, *Hraði kísilfjölliðunar í háhitavatni (Silica polimerization rate in high temperature fluids)*, Jarðvísindastofnun Háskólans, Reykjavík.

Hafstað, T.H., Vilmundardottir, E.G. & Kristjansson, B.R. 2007, *Nesjavellir - Rannsóknarborholur á affallssvæði virkjunarinnar (Nesjavellir - Research boreholes of the seepage area of the power plant)*, ISOR, Reykjavik (In Icelandic).

Helz, G.R., Tossell, J.A., Charnock, J.M., Pattrick, R.A.D., Vaughan, D.J. & David Garner, C. 1995, "Oligomerization in As (III) sulfide solutions: Theoretical constraints and spectroscopic evidence", *Geochimica et Cosmochimica Acta,* vol. 59, no. 22, pp. 4591-4604.

Jonasson, P.M. 1992, "The Ecosystem of Thingvallavatn: a synthesis", *Oikos*, vol. 64, no. 1-2, pp. 405-434.

Kjaran, S.P. & Myer, E.C. 2005, *Nesjavellir - Árleg endurskoðun á grunnvatnslíknai fyrir árið 2003.*, Vatnaskil, Unnið fyrir Orkuveitu Reykjavíkur- Prepared for Reykjavik Energy.

Mambo, V.S., Yoshida, M. & Matsuo, S. 1991, "Partition of arsenic and phosphorus between volcanic gases and rock. Part I: analytical data and magmatic conditions of Mt. Usu, Japan", *Journal of Volcanology and Geothermal Research,* vol. 46, no. 1-2, pp. 37-47.

Olafsson, J. 1992, "Chemical characteristics and trace-elements of Thingvallavatn", *Oikos,* vol. 64, pp. 151-161.

Parkhurst, D.L., Appelo, C.A.J. 1999, *User's guide to PHREEQC (Version 2)- A computer program for speciation, batch-reaction, one-dimensional transport, and inverse geochemical calculations*, US Geological Survey.

Planer-Friedrich, B., London, J., McCleskey, R.B., Nordstrom, D.K. & Wallschlager, D. 2007, "Thioarsenates in geothermal waters of yellowstone national park: Determination, preservation, and geochemical importance", *Environmental science & technology,* vol. 41, no. 15, pp. 5245-5251.

Pokrovski, G., Gout, R., Schott, J., Zotov, A. & Harrichoury, J.C. 1996, "Thermodynamic properties and stochiometry of As(III) hydroxide complexes at hydrothermal conditions", *Geochimica et Cosmochimica Acta,* vol. 60, no. 5, pp. 737-749.

Pokrovski, G.S., Zakirov, I.V., Roux, J., Testemale, D., Hazemann, J., Bychkov, A.Y.u. & Golikova, G.V. 2002, "Experimental study of arsenic speciation in vapor phase to 500°C: implications for As transport and fractionation in low-density crustal fluids and volcanic gases", *Geochimica et Cosmochimica Acta,* vol. 66, no. 19, pp. 3453-3480.

PSAnalytical 1997, *PSA Application note no. 11. Millenium excalibur method for arsenic in drinking, surface, ground, saline and industrial and domestic waste waters*, PSAnalytical, Orpington, UK.

Saemundsson, K. 1995, *Hengill, jarðfræðikort (berggrunnur); Hengill, geology map (Bedrock)*, Orkustofnun, Reykjavik (In Icelandic).

Sigfusson, B., Meharg, A.A. & Gislason, S.R. 2008, "Regulation of Arsenic Mobility on Basaltic Class Surfaces by Speciation and pH", *Environmental science & technology,* vol. 42, no. 23, pp. 8816-8821.

Squibb, K.S. & Fowler, B.A. 1983, "The toxicity of arsenic and its compounds" in *Biological and environmental effects of arsenic*, ed. B.A. Fowler, Elsevier, Amsterdam, pp. 233-269.

Stauder, S., Raue, B. & Sacher, F. 2005, "Thioarsenates in sulfidic waters", *Environmental science & technology,* vol. 39, no. 16, pp. 5933-5939.

Stefansson, A., Gunnarsson, I. & Giroud, N. 2007, "New methods for the direct determination of dissolved inorganic, organic and total carbon in natural waters by Reagent-Free™ Ion Chromatography and inductively coupled plasma atomic emission spectrometry", *Analytica Chimica Acta,* vol. 582, no. 1, pp. 69-74.

Tomasson, J. & Saemundsson, K. 1967, *Borholur á Nesjavöllum: Með jarðfræðilegum inngangi (Borholes on Nesjavellir: With geological introduction)*, Raforkumálastjóri (Jarðhitadeild), Reykjavik (In Icelandic).

Wallschlager, D. & Roehl, R. 2001, "Determination of inorganic selenium speciation in waters by ion chromatography-inductively coupled plasma-mass spectrometry using eluant elimination with a membrane suppressor", *Journal of Analytical Atomic Spectrometry*, pp. 922.

Webster, J.G. & Nordstrom, D.K. 2003, "Geothermal arsenic" in *Arsenic in Groundwater*, eds. A.H. Welch & K.G. Stollenwerk, Kluwer Academic Publishers, Boston, Massachusetts, pp. 101-125.

Werner, M. & Wallquist, L. 2008, *Long-term CO_2 injection into basalt at Nesjavellir, Iceland*, Reykjavik Energy/ ETH Zurich.

Wilkin, R.T., Wallschlager, D. & Ford, R.G. 2003, "Speciation of arsenic in sulfidic waters", *Geochemical Transactions,* vol. 4, pp. 1-7.

5. The Grímsvötn 2004 eruption and glacial flood – a geochemical modeling study of the fate of Arsenic during tephra/floodwater interactions and subsequent floodwater/ seawater interactions.

Bergur Sigfusson[1,2], Sigurdur R. Gislason[2], Rannveig Guicharnaud[3], Jorunn Hardardottir[4], Peter Torssander[5] and Andrew A. Meharg[1]*

1) School of Biological Sciences, University of Aberdeen, AB243UU, Aberdeen, UK
2) Institute of Earth Sciences, University of Iceland, 101 Reykjavik, Iceland
3) Agricultural University of Iceland, 112 Reykjavik, Iceland
4) Icelandic Met Office. 150 Reykjavik, Iceland
5) Department of Geology and Geochemistry, Stockholm University, SE 106-91, Sweden

*Present address, Reykjavik Energy, Baejarhals 1, 110 Reykjavik, Iceland

Corresponding author: bergur.sigfusson@or.is (Bergur Sigfusson)

In preparation for submission to Journal of Volcanology and geothermal research.

Contribution of individual authors:

Bergur Sigfusson sampled all samples except two and prepared all samples for further analysis wrote the manuscript and constructed the geochemical models.
Sigurdur R. Gislason sampled the two final samples, advised mainly on the writing of the manuscript and discussed the modeling procedure in detail.
Rannveig Guicharnaud, sampled all samples except two, carried out some analysis and provided discussions on the manuscript throughout.
Jorunn Hardardottir analysed suspended sediments and provided discussions on that subject.
Peter Torssander analysed the sulphur isotopes and provided discussions on that subject.
Andrew A. Meharg advised mainly on the writing of the manuscript and provided feedback on the modeling procedure.
Other contributors are thanked in the acknowledgements.

Abstract

The November 2004 eruption within the Vatnajökull Glacier, Iceland, provided an opportunity to study elemental fluxes from volcanic eruptions into the environment. On 28th October, Lake Grímsvötn started draining sub glacially with the floodwater entering River Skeiðará 50 km south of the lake. Following four days draining of Lake Grímsvötn with subsequently increasing discharge in River Skeiðará an eruption started at 21:50 GMT on 1st November 2004 forming an eruption column up to 12-14 km. This vigorous stage continued until the morning of 3rd November with continuous plume rising to 9 km. Maximum discharge of the glacial flood rose from 50 m^3 sec^{-1} base flow to 3,300 m^3 sec^{-1} on 2 November at 16:40. The volume of the actual flood peak was 0.45 km^3 and further 0.35 km^3 of floodwater discharged until 7th of December as new melt water due to the eruption was generated. A distinct change in the floodwater chemistry was observed between 8:20 and 12:15 on 2 November where dissolved $S_2O_3^{2-}$ and Hg were first detected with corresponding peak flux of Na, Cl, B and V. Further change occurred between 12:15 and 19:15 where all other elemental fluxes peaked with concurrent decrease in δ34S values from 7.5‰ to 3.5‰. According to geochemical modeling by PHREEQC-2, lowering of pH due to magma gases during the eruption led to rapid tephra dissolution with corresponding change in flood water chemistry. Geochemical modeling of floodwater/seawater mixing indicated localised decrease in dissolved arsenic (As) and sulphur (S) due to adsorption on the suspended floodwater materials. As the floodwater was diluted the As desorbed and limited effect of the floodwater was predicted after thousand fold dilution.

5.1 Introduction

Volcanic eruptions represent an important natural source of various elements to the atmosphere and shallow aqueous systems (Nriagu, 1989). Acids, metal salts and adsorbed gases on tephra (airborne volcanic particulate matter) and volcanic glass are highly soluble and dissolve rapidly in contact with water (Frogner et al., 2001; Flaathen and Gislason, 2008; Jones and Gislason 2008). During sub glacial eruptions, large proportion of volcanic glass does not become airborne and may be transported from the eruption site with the melt water generated during the eruption resulting in intense water rock and water magma interactions (Gislason et al., 2002). The November 2004 eruption within the Vatnajökull Glacier, Iceland, provides an opportunity to study elemental fluxes from volcanic eruptions into the environment (Figure 1). The eruption followed a glacial flood being monitored on site and therefore provided the opportunity to sample a near complete dataset throughout the eruption period. Aqueous and suspended samples were gathered and treated only 14 h after being brought to the Earth's surface.

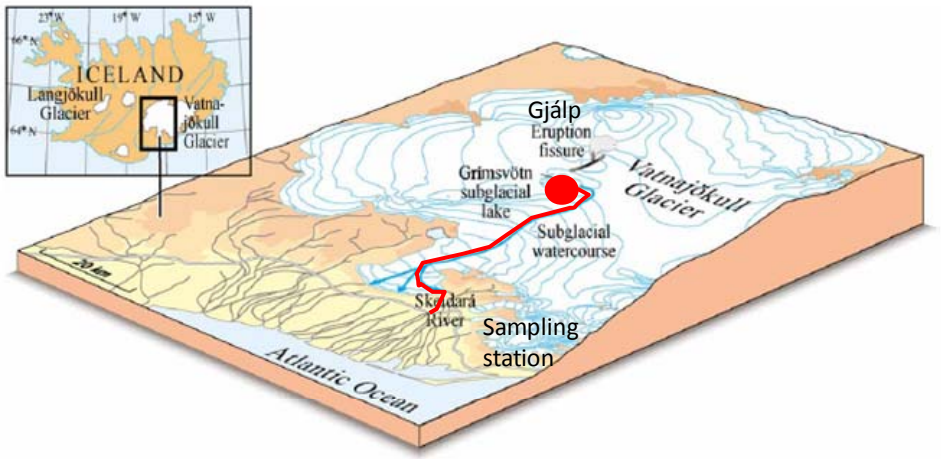

Figure 1 Location of the 2004 eruption site and the flood path in Vatnajökull glacier. Modified from Gislason et al. (2002).

Soluble salts from pristine volcanic glass will dissolve rapidly in aqueous environments releasing anions such as chloride, fluoride, (Frogner et al, 2001) and metals such as Al, Fe, Mn, As, Cd, Pb, Zn and U (Flaathen and Gislason, 2007). Arsenic (As) is believed to primarily enter crustal fluids during crystallising of deep plutons as hot volatile-rich magmatic fluids escape from the plutons and segregate into vapour and brine resulting in formation of porphyry-style and epithermal ore deposits and fumaroles activity in volcanic areas (Goldschmidt, 1954; Ballantyne and Moore, 1988). Arsenic

concentrations in volcanic gases sampled between 400 and 900°C often range between 1-10 ppm of the vapour condensates (Mambo et al., 1991) corresponding to As enrichment in the gas phase between 100 and 1000 with respect to the magma body suggesting an important transfer of As into the hydrosphere and atmosphere during magma degassing and volcanic eruptions (Pokrovski et al., 2002). Arsenic preferentially concentrates into the liquid aqueous phase in water dominated active hydrothermal systems below 350°C (Ballantyne and Moore, 1988). Arsenic mainly occurs as As(III) hydroxide, primarily as $As(OH)_3$ aqueous species and to lesser extent, the sulphide $H_{0-3}As_{1-3}S_{3-6}$, species in natural hydrothermal solutions depending on temperature, pH and H_2S content (Akinfiev et al, 1992; Helz et al., 1995; Pokrovski et al., 1996).

Suspended materials constitute large proportion of the floodwaters leaving sub glacial eruption sites (Gislason et al., 2002; Hardardottir et al., 2004; Stefansdottir and Gislason, 2005) and these materials may provide a potential adsorption sites for the dissolved constituents. As the conditions of the floodwaters are altered, such as when entering the ocean these constituents may be desorbed form the suspended materials, forming temporary sources of nutrients and metals to the ocean (Stefansdottir and Gislason, 2005) similarly to when airborne tephra lands on the ocean surface (Jones and Gislason, 2008).

The objectives of this study were to estimate volcanic tephra dissolution immediately after its formation on the Earth's surface and predict the release of selected metals to the environment following short term interactions between tephra, volcanic gases, glacial melt waters and the ocean. To this end, fresh tephra, floodwater and suspended materials were collected during the 2004 Grímsvötn eruption. Experimental data on surface complexation and basaltic glass dissolution were used to model the dominant reactions.

5.2 The 2004 eruption

On 28th October, Lake Grímsvötn started draining sub glacially according to increasing tremor on seismometers (Vogfjörd et al., 2005) with the floodwater entering River Skeiðará 50 km south of the lake as detected by elevated river conductivity measurements on 29th of October (Hardardottir et al., 2004) (Figure 1). Following 4 d draining of Lake Grímsvötn with subsequently increasing discharge in River Skeiðará from 50 $m^3 s^{-1}$ base flow to 1435 $m^3 s^{-1}$ at 16:00 (Hardardottir et al., 2004) an eruption started at 21:50 GMT on 1st of November 2004 (Gislason et al., 2002) forming an

eruption column up to 10km (Oddsson, 2007) (Figure 2a). The flood peak reached 3300 m^3 s^{-1} at 16:40 on 2nd of November (Hardardottir et al., 2004). The vigorous stage of eruption continued until the morning of 3 November with continuous plume rising to 9 km. On 4th of November the volcanic activity had greatly reduced and limited explosive activity generating a 3-4 km high plume was observed in the cauldron produced by the eruption (Oddsson, 2007). On 5th of November a steam plume rose to 500 m while on 6th of November no activity was recorded.

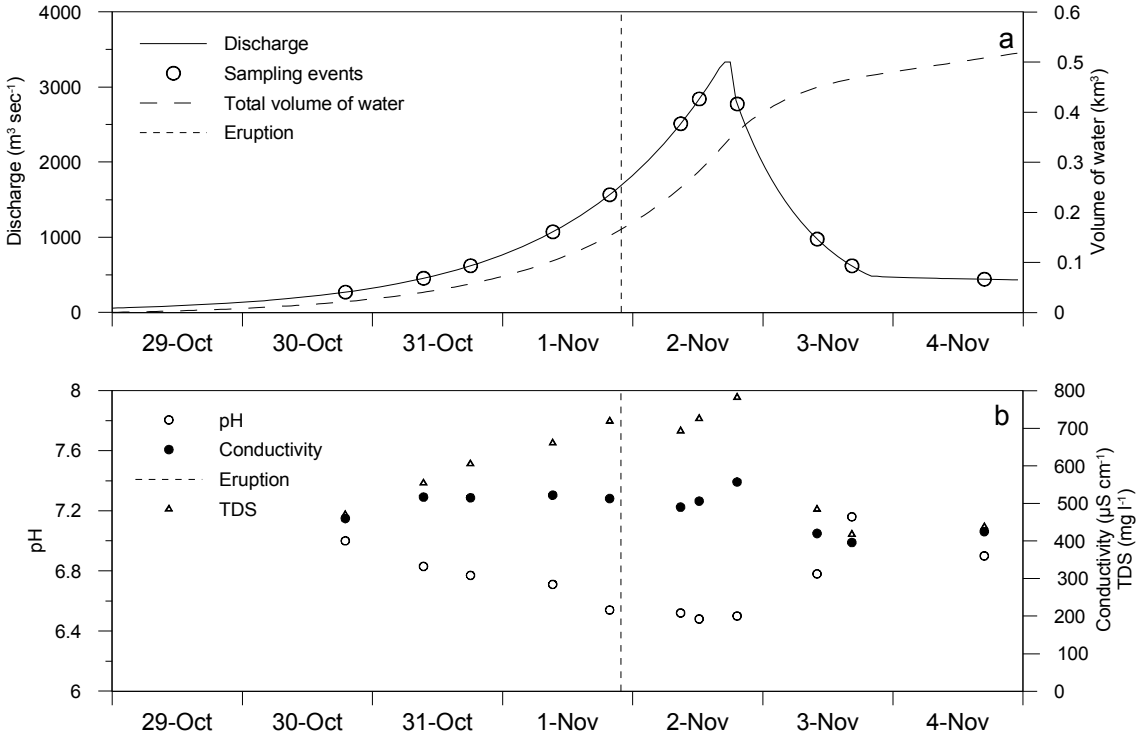

Figure 2 (a) Flood discharge and total volume of floodwater until November 4th. The eruption began on 1st of November at 21:50 (hatched line). Further 0.2 km^3 were discharged until December 7th as new melt water was generated in the caldera. (b) pH, conductivity and total dissolved solids (TDS) in the floodwater.

The estimated volume of ice melted during the 33 h eruption was 0.1 km^3 when 150 -200 m thick ice sheet was melted (Oddsson, 2007). All of the erupted magma fragmented into tephra with total mass being $5.2\pm1.0\cdot10^{10}$ kg (Oddsson, 2007). Of the total mass $2.7\cdot10^{10}$ kg remained within the ice cauldron formed in the eruption and the rest was carried by the eruption plume into the atmosphere or was carried with the floodwater to the ocean.

About 95% of the total mass outside the ice cauldron was deposited in an 800 km^2 area and only 2% ($5.4\cdot10^8$ kg) of the total tephra mass deposited outside the Vatnajökull Glacier (Oddsson, 2007). The total discharge of the flood peak itself was 0.45 km3 (Figure 2a) carrying $4\cdot10^9$ kg of suspended materials towards the Skeiðará

Sandur plain (Hardardottir et al., 2004). The total dissolved solids flux in the flood was $3.27 \cdot 10^8$ kg (Figure 2b).

5.3 Methods

A sampling campaign of River Skeiðará was carried out during the glacial flood event and subsequent eruption from 30 October - 4 November. During this period water and river suspended matter samples were collected for detailed chemical analyses and discharge was measured.

5.3.1 Sampling of tephra

Tephra fallout was sampled into a HDPE bag directly from the snow 50 m from the eruption cauldron on 4 November. The sample was stored in a coolbox and transferred to -18°C the same day prior to being freeze dried freeze-dried for 24 h at − 40 °C and 3 PSI pressure.

5.3.2 Sampling of river water

5.3.2.1 Suspended materials

For particle size distribution determination and mineral analysis suspended materials were collected into four 250 ml glass bottles with a S49 sampler (Guy and Norman, 1970) attached to a winch which lowered and lifted the sampler to and from the river bottom at a constant rate (Hardardottir et al., 2003).

For elemental analysis of selected samples, two 30 l HDPE containers were filled with the aid of a plastic bucket. Following the flood event, the samples were transferred to the laboratory and filtered using a Sartorius®, tangential filtration unit and a Hydrosart® 0.2 μm filtration cartridge. The remaining slurry was centrifuged for 10 min at 15 °C at 10 000 rpm, the remaining solids were freeze-dried for 24 h at − 40 °C and 3 PSI pressure and stored in a desiccators until analysed.

5.3.2.2 Dissolved constituents

Sampling methodology followed to large extent that applied to the floodwaters of the 1996 Vatnajökull eruption (Gislason et al., 2002).

The first river sample (04V001) was collected from the westernmost section of the bridge crossing River Skeiðará (Figure 1) adjacent to the river monitoring station. All

other samples (04V002-11) were collected from the next section of the bridge to the East in order to collect water from the main flood channel. The samples were collected in a plastic bucket and transferred to one 5 l and one 10 l High Density Polyethylene (HDPE) containers. The containers were filled entirely before being closed. The containers were rinsed 3 times with the sample water prior to filling. The temperature of the water was measured directly in the river by a thermistor (±0.1°C). The containers were transferred to the laboratory and were prepared within 15 min from sampling. Samples from the five litre container were pumped by a peristaltic pump (Cole Parmer Masterflex Portable Sampler) through silicone tubing to a Sartorius Polytetrafluoroethylene (PTFE) in line filter holder with Cellulose Acetate (CA) membrane (142mm diameter, 0.2µm pore size). One l of sample water was pumped through the filtration unit prior to sample collection and all the air in the unit was expelled through an air valve.

Samples for dissolved oxygen determination were filtered into a 50 ml Erlenmeyer flask and the oxygen fixed according to the Winkler method (Grasshoff, 1983). Then, sample for H_2S measurement was filtrated into a 50 ml Erlenmeyer flask and measured immediately by titration (Archer. 1955). Thereafter, 60 ml were filtered into an amber glass bottle and pH and conductivity measured. Filtration proceeded concurrently to the pH measurement and 250 ml were filtered into an amber glass bottle with specially designed caps to prevent air bubbles in the bottles for alkalinity titration. After that, 1 l of water was filtered from the 10 l container into a HDPE bottle for the determination of sulphur isotopes. Then, 200 ml were filtered into a HDPE bottle for the determination of anions and 20 ml were filtered into a HDPE bottle and frozen (-18°C) immediately for the determination of thiosulphate ($S_2O_3^{2-}$). Finally, 125 ml were filtered into a pre-acid washed (1 M HCl) HDPE bottle for the determination of major and trace elements. The 125 ml bottle was acidified immediately with 1 ml of Suprapure® nitric acid (HNO_3). Depending on the suspended material load, 1-3 filters were needed for each sample and sampling, filtration, treatment and measurements described above took less than 2 h.

5.3.3 Analytical methods

5.3.3.1 Suspended materials

The concentration and the grain size distribution of the suspended particulate matter and total dissolved solids were measured at the Hydrological Service of the National Energy (Hardardottir et al., 2004). The grain size of the suspended fraction was determined using sieving for material coarser than 63 μm and the sediment settling method for the size fraction finer than 63 μm.

The specific surface area of the suspended material was measured by the three-point BET method using Kr gas at University Paul Sabatier Toulouse.

The geometric specific surface area A_{geo} was calculated using (Brantley et al., 1999; Gautier et al., 2001):

$$A_{geo} = \frac{6}{\rho d_{eff}} \qquad \text{Equation 1}$$

where ρ is the glass density and d_{eff} is the effective particle diameter. The number 6 is based on the assumption that grains have a regular and smooth spherical shape. Assuming a homogeneous particle distribution, d_{eff} can be obtained from (Tester et al., 1994):

$$d_{eff} = \frac{d_{max} - d_{min}}{\ln\left(\frac{d_{max}}{d_{min}}\right)} \qquad \text{Equation 2}$$

where d_{max} and d_{min} refer to the maximum and minimum particle size of each size fraction measured. The d_{eff} for each size fraction was calculated and the A_{geo} calculated as the sum of specific surface area contributed by each size fraction.

Elemental analysis was carried out on both fresh tephra and the suspended matter by Analytica, Sweden. The samples measured at Analytica were digested in three different ways depending on which elements were to be analysed: 1) HNO_3 + HF; 2) $LiBO_2$-fusion; 3) Aqua Regia + 0.1 ml HF. The major elements were analysed by ICP-AES, the trace elements either by ICP-AES or ICP-MS. Fluorine in the samples was not analysed but to allow for comparison of waters discharged before and after flow peak it

was estimated to be 100 mg/kg based on the Georoc database on Icelandic volcanic rocks by the Max-Planck Gesellschaft. Chlorine concentration was estimated to be 180 mg/kg based on data from Sigvaldason and Oskarsson (1976).

5.3.3.2 Dissolved constituents

Major and trace elements were determined from the acidified samples by Analytica, Sweden. The major elements were determined by Inductively Coupled Plasma Atomic Emission Spectrometry (ICP-AES) and trace elements by ICP- Sector Mass Spectrometry (SMS), also referred to as high resolution ICP-MS. Mercury was determined by cold vapour - Atomic Fluorescence Spectrometry (AFS). The anions fluoride (F^-), chloride (Cl^-), sulphate (SO_4^{2-}) and thiosulphate ($S_2O_3^{2-}$) were measured at the Institute of Earth Sciences, University of Iceland by Anion Exchange Chromatography (AEC) with a Dionex ICS-2000. Sulphur isotope measurements were done at the University of Stockholm, Sweden. Dissolved sulphate was converted to $BaSO_4$ for sulphur isotopic analyses (Mörth et al. 2005). The $BaSO_4$ was mixed with an equal amount of V_2O_5 and reacted in an online elemental analyzer (EA) converting the BaSO4 to SO_2(g), which was then analyzed in a continuous flow isotope ratio mass spectrometer (CF-IRMS; Finnigan Delta+). The sulphur isotope composition was defined as a deviation in ‰ of the ratio $^{34}S/^{32}S$ between a sample and a standard, expressed in the conventional δ34S notation relative to the Canon Diablo Troilite (V-CDT). The accuracy of the measurements based on standard measurements was better than 0.2‰ for all samples.

5.3.4 Discharge measurements and dissolved flux calculations

The flood discharge was assessed by measuring water velocities and cross sections of the river channels. The water velocities were measured on the surface only as is custom in flood events. A 100 kg weight was lowered into the river to measure the depth of the river. In total, eight discharge measurements were carried out and an exponential function was fitted to the data except for the time span between the last two discharge measurements where melt water due to the eruption was presumably flowing to the river (Hardardottir et al., 2004). A multiplication of calculated discharge and measured concentration allowed estimation of elemental fluxes at the time of sampling. The total fluxes of individual elements were then calculated by numerical integration over the duration of the flood using the trapezoidal rule.

5.3.5 Relative mobility calculations

Relative mobility of selected elements was calculated in relation to Na. The calculation was carried out in three ways, a) The total flux of an element was divided by the total flux of Na in the flood. This value was divided by the element/Na ratio of the fresh tephra. b) The total flux of an element was divided by the total flux of Na in the flood. This value was divided by the mean element/Na ratio of the suspended samples V07 and V08. c) Finally the concentration of element was divided by the concentration of Na in water samples V07 and V08 respectively and the value divided by the element/Na ratio of the fresh tephra.

5.3.6 Model calculations

All geochemical modeling was carried out by PHREEQC-2 v2.15.0 (Parkhurst and Appelo, 1999). Two sets of calculations were done, firstly, tephra dissolution in geothermal water in the presence of additional volcanic gas from the eruption and secondly, the fate of adsorbed materials on the suspended matter once the floodwater entered the ocean was modelled.

5.3.6.1 Tephra dissolution in the flood path

No experimental data exists on the dissolution rate of the volcanic tephra generated in the Grímsvötn 2004 eruption. Therefore due to their similar chemical composition the primary phase used in the simulation calculations was basaltic glass from Stapafell, SW Iceland (Oelkers and Gislason, 2001). The dissolution kinetics of Stapafell basaltic glass were measured far from equilibrium at temperatures ranging from 6 to 300°C at pH 1 to 11 (Gislason and Oelkers, 2003). The rate law in terms of surface area describing the dissolution of basaltic glass is given by:

$$r_+ = ke^{\left(\frac{-E_A}{RT}\right)}\left(\frac{a^3_{H_+}}{a_{Al^{3+}}}\right)^{1/3}\left(1-Q/K\right) \qquad \text{Equation 3}$$

Where r_+ is the dissolution rate of basaltic glass in moles A is the surface area in $cm^2\ g^{-1}$, k is the rate constant ($10^{-5.6}$ moles $cm^{-2}\ s^{-1}$) and E_A represents the activation energy (25.5 kJ mol^{-1}) (Gislason and Oelkers, 2003). The specific surface area can then be chosen for the calculations depending on the data available. In the present contribution BET surface area and geometric surface area based on particle size analysis were available

and used in all calculations as representatives for minimum and maximum specific surface area, respectively. The surface area varies as reactions progress according to:

$$A_n = \frac{(m_n / m_0)^{2/3} A_0}{V} \qquad \text{Equation 4}$$

where A_n and A_0 are the present and initial surface area ($cm^2\ g^{-1}$) at each reaction step, respectively, m_n and m_0 are the present and initial moles of the mineral, respectively, and V is the volume of the modelled system in litres.

As described by Oelkers and Gislason (2001) the initial dissolution of basaltic glass was characterised by preferential release of Na^+, K^+, Ca^{2+} and Mg^{2+} through cation proton exchange. Upon progressive dissolution a leached surface layer strongly enriched in Si, Al and Fe is produced. The thickness of this layer increases until the diffusion rates of the alkali and alkaline earth elements equals the dissolution rate of the leached layer itself. The time to reach this stoichiometric dissolution is rapid (a few h). Therefore the long term dissolution rates of basalt and the leached layer are equal and the dissolution front is the interface between the leached layer and the solution. As a consequence, the saturation state of the leached layer with respect to the solution determines the effects of basaltic glass saturation on the rate expression (Daux et al., 1997; Oelkers and Gislason, 2001). The equilibrium constant for the hydrated leached layer given by the reaction:

$$SiAl_{0.36}O_2(OH)_{1.08} + 1.08H^+ + 0.92H_2O = H_4SiO_4 + 0.36Al^{3+} \qquad \text{Equation 5}$$

was estimated to be log K = 0.05 at 25°C (Gislason and Oelkers, 2003).

The very short residence time from the eruption source to sampling, only 14 h, provided an opportunity to carry out geochemical modeling of the interactions between fresh tephra, geothermal water, glacial melt water and volcanic gases. The following conditions were set for the modeling which was carried out by PHREEQC-2 v2.15.0 (Parkhurst and Appelo, 1999):

1. Input solution was a one litre mixture of i) geothermal water sampled at the first stages of the flood prior to the eruption (sample 04V002) and ii) glacier melt water represented by the 1996-1997 winter precipitation on Vatnajökull Glacier (Gislason et al. 2002). The geothermal water was the dominant component for modeling of the flood peak while glacier water was increasingly introduced as the eruption progressed.

2. The solid material amount was assumed to be 11 grams which was around the estimated concentration in the flood peak.
3. Geometric surface area (2600 cm^2 g^{-1}) and BET surface area (12,300 m^2 g^{-1}) were used in calculations and the effect of these end member values on the reactions was studied.
4. The mixture was treated like a one litre batch reactor that was transferred from the eruption site towards the sampling site in 14 h in 140 steps, which corresponded to the delay time between the beginning of the eruption and the sampling time of water exhibiting distinct change measured in sulphur isotope ratio.
5. Calculations were done at temperatures from 0-50°C until best fit to the measured data were achieved (2°C).
6. Hydrous Ferric oxide (HFO) surface was used as a proxy for the surface based on comparisons of a surface complexation on HFO and basaltic glass (Sigfusson et al., 2008). This was done to allow for competitive sorption of anions on the surface of which database for volcanic glass does not exist. The flood waters were supersaturated with respect to HFO throughout the flood according to the PHREEQC-2 calculations.
7. Carbon dioxide (CO_2) was equilibrated with the system at the start of reactions to generate the dissolved inorganic carbon concentrations measured at the bridge.
8. Chloride was added into the system in the form of hydrogen chloride ($HCl_{(g)}$) to achieve the chloride concentrations measured in the volcanic water.
9. Sulfur was added to the system in the form of sulphur dioxide ($SO_{2(g)}$) to achieve sulphur concentrations measured in the volcanic water. The sulphur speciation data from Lawrence Livermore National Laboratory (LLNL) database (version 2335 2007-10-19), which comes with PHREEQC-2 was used to calculate all sulphur reactions.
10. The following phases were allowed to precipitate reversibly in the system: allophane, imogolite, amorphous iron hydroxide, amorphous aluminium hydroxide, magnesite, calcite, siderite, dolomite, Ca-Mg carbonate, chlorite, celadonite, Fe-celadonite, Ca-Mg-Fe smectite (Stefansson, 2008) and moganite (Gislason et al., 1997).

5.3.6.2 The fate of adsorbed materials on the suspended matter in seawater.

For floodwater/seawater, modeling was carried out by PHREEQC-2 v2.15.0 (Parkhurst and Appelo, 1999) assuming the floodwater to be in equilibrium with Hydrous Ferric oxide (HFO) surface. Results from flood path calculations were not used for the seawater mixing, but rather the measured chemical composition of floodwaters sampled at the bridge. HFO surface was mixed with seawater (Bruland, 1983) in floodwater/seawater ratios between 0.1 and 100,000 and equilibrium attained in the solution and on the solid surfaces.

5.4 Results and discussion

The results for the suspended materials collected at Skeiðará Bridge and fresh tephra collected at the eruption site are displayed in Table 1. The results for discharge, suspended load and for chemical composition of flood samples are displayed in Table 2. The charge balance based on the main ionic species for the floodwater samples 04V001-5 varied between 0 and -1.1% whereas samples 6 and 7 displayed -1.9 and -2.2% difference followed by samples 8 to 11 that had -4 to -7% charge balance. The increasing negative charge balance corresponded to the appearance of $HS_2O_3^-$ in the waters. The charge balance of samples 8-11 converged to zero if 10-15% of the total sulphur was defined as the SO_4^{2-} species instead of the IC - measured values in Table 2. This indicates some degradation of sulphur species to SO_4^{2-} in the untreated sample bottle prior to IC analysis.

5.4.1 The volcanic ash on the Vatnajökull glacier

About 50% of the erupted tephra was forced through the melt water at the eruption site and dispersed aerially (Oddsson, 2007). Analysis of ice and snow of which fresh tephra lands on can indicate the existence of soluble salts on the tephra grains (Gislason et al., 2002). No ice in contact with tephra was collected during the 2004 eruption however, data from recent Gjálp eruption in 1996 indicated the tephra ejected through the melt water did not contain a significant amount of acid producing volcanic aerosols (Gislason et al., 2002). These soluble salts were primarily washed away in the melt water and to lesser extent in the eruption column.

Table 1 Chemical composition of suspended materials collected at Skeiðará Bridge and fresh tephra.

	Suspended solids (mg/l)	A_{geo} (m^2/g)	A_{BET} (m^2/g) Surface area	Error	SiO_2 %	Al_2O_3 %	CaO %	Fe_2O_3 %	K_2O %	MgO %	MnO %	Na_2O %	P_2O_5 %	TiO_2 %	Sum %
04V002	4678	3.41	26.22	0.044	47.4	13.7	8.81	13.9	0.422	5.62	0.198	2.35	0.268	2.41	95.1
04V005	3564	3.53	19.09	0.122	47.5	13.6	9.27	13.9	0.402	5.84	0.201	2.43	0.258	2.43	95.8
04V007	11712	2.75	8.25	0.053	46.9	13.4	9.47	13.8	0.412	5.90	0.201	2.43	0.254	2.42	95.2
04V008	10444	3.63	12.37	0.047	47.9	13.5	9.26	14.3	0.433	5.91	0.205	2.43	0.277	2.54	96.8
04V009	3895	3.46	12.20	0.067	47.5	13.3	8.62	14.5	0.435	5.59	0.203	2.36	0.289	2.56	95.4
Fresh tephra					49.5	13.6	9.76	15.0	0.534	5.55	0.218	2.88	0.312	2.84	100.2

	As mg/kg	B mg/kg	Cd mg/kg	Co mg/kg	Cr mg/kg	Cu mg/kg	Hg mg/kg	Mo mg/kg	Ni mg/kg	Pb mg/kg	S mg/kg	Sr mg/kg	V mg/kg
04V002	0.335	2.68	0.151	47.4	119	138	0.0103	0.667	49.8	1.26	1030	218	363
04V005	0.445	3.08	0.137	52.1	132	129	0.0101	0.705	52.7	1.05	957	218	414
04V007	0.385	2.8	0.144	52.1	137	127	0.0067	0.722	53.3	1.06	949	217	369
04V008	0.332	3.46	0.153	52.7	104	131	0.0136	0.766	50	1.07	1580	219	386
04V009	0.337	2.99	0.18	52.6	108	142	0.0282	0.767	49.3	1.5	1430	215	378
Fresh tephra	0.288	2.21	0.155	49.7	76.5	97.1	<0.005	0.971	36.2	1.18	855	238	472

5.4.2 Conditions at the eruption site

The ice that melted at the eruption site and in the flow path within the Vatnajökull glacier was primarily purified snow (Gislason et al., 2002). Thus the dissolved constituents in the floodwater were primarily of magmatic, geothermal and rock origin. They were not brought in with the rain and snow. Prior to the eruption the floodwaters constituents were of geothermal and rock origin. However as the eruption commenced a flux of CO_2, S, Cl and F from magma was introduced to the system and a distinct shift in the δ34S values was measured in floodwaters along with elevated levels of Hg (Table 2). According to the concentration of these anions, the pH of melted ice in contact with the volcanic gases may have reached as low as pH 2. The presence of geothermal water in the lake however buffered the system and the pH only lowered to 6.2 from 7 according to PHREEQC-2 calculations.

Table 2 Information on water samples from River Skeiðará during the flood

Sample	Si	Na	K	Ca	Mg	Al	Fe	Mn	Sr	V	As	Ba	Cd	Co	Cr	Cu	Ni	Pb	Zn	Hg	Mo	Ti
	mmol l^{-1}	mmol l^{-1}	mmol l^{-1}	mmol l^{-1}	mmol l^{-1}	µmol l^{-1}	µmol l^{-1}	µmol l^{-1}	µmol l^{-1}	µmol l^{-1}	nmol l^{-1}	nmol l^{-1}	nmol l^{-1}	nmol l^{-1}	nmol l^{-1}	nmol l^{-1}	nmol l^{-1}	nmol l^{-1}	nmol l^{-1}	nmol l^{-1}	nmol l^{-1}	nmol l^{-1}
04V001	0.616	1.23	0.025	1.35	0.366	0.151	0.19	2.44	0.441	0.080	<0.67	0.90	0.061	9.08	0.302	3.43	46.5	0.26	11.2	<0.010	3.86	14.7
04V002	0.730	1.46	0.032	1.43	0.400	0.198	0.51	3.02	0.488	0.073	1.17	0.96	0.047	12.3	0.267	2.93	50.9	0.30	8.35	<0.010	3.21	19.1
04V003	0.790	1.60	0.036	1.46	0.416	0.715	0.95	3.31	0.509	0.078	0.72	1.12	0.060	15.4	0.544	3.86	55.2	0.32	14.7	<0.010	2.97	67.3
04V004	0.862	1.78	0.041	1.46	0.424	1.39	1.88	3.75	0.517	0.074	0.84	1.39	0.061	16.4	1.01	3.68	52.1	0.29	17.0	<0.010	2.94	131
04V005	0.915	1.91	0.048	1.44	0.432	1.23	2.04	4.13	0.543	0.073	1.90	1.35	0.055	19.6	0.785	2.64	56.2	0.28	20.6	<0.010	2.74	103
04V006	0.840	1.79	0.047	1.31	0.391	2.11	2.29	3.59	0.478	0.071	1.62	1.50	0.055	16.4	1.11	4.72	48.2	0.24	20.6	<0.010	2.68	187
04V007	0.851	1.81	0.042	1.34	0.398	0.608	1.48	3.66	0.492	0.076	0.94	1.16	0.058	18.0	0.531	3.65	51.1	0.17	39.0	0.014	2.85	56.0
04V008	0.830	1.80	0.048	1.49	0.432	1.25	11.0	6.66	0.633	0.065	2.11	1.52	0.103	28.2	0.608	73.3	61.0	0.16	30.9	0.018	3.21	109
04V009	0.598	1.27	0.033	1.17	0.339	0.217	5.96	5.04	0.495	0.034	1.90	0.98	0.093	19.2	0.287	112	49.6	0.07	16.1	0.011	3.11	15.9
04V010	0.552	1.19	0.031	1.12	0.318	0.149	1.64	4.22	0.447	0.030	2.18	0.81	0.068	14.0	<0.192	98.4	40.2	<0.048	9.37	0.015	2.78	6.22
04V011	0.580	1.21	0.034	1.13	0.344	0.156	7.29	4.97	0.478	0.026	1.95	0.93	0.108	18.6	0.317	142	53.3	<0.048	22.9	0.031	3.04	6.77

Sample	Date	Discharge	Water temperature	Air temperature	pH	Conductivity	T (°C) /pH, cond.	TDS	DIC	Alk	DOC	O2	Cl	S	H2SuM	SO_4	S_2O_3	$\delta^{34}S$	F	B	NH_4-N	NO_3-N	PO_4-P
		m^3 s^{-1}	°C	°C		µS/cm		mg l^{-1}	mmol l^{-1}	meq l^{-1}	mmol l^{-1}	mmol l^{-1}	mmol l^{-1}	mmol l^{-1}	µmol l^{-1}	mmol l^{-1}	mmol l^{-1}	‰	µmol l^{-1}	µmol l^{-1}	µmol l^{-1}	µmol l^{-1}	µmol l^{-1}
04V001	30.10.04 19:00	270	1.3	1.0	7.00	460	14.9	470	5.30	4.20	0.009	0.30	0.204	0.165	0.40	0.182	<0.001	5.96	4.81	7.28	3.79	0.87	0.29
04V002	31.10.04 09:25	454	1.2	1.0	6.83	517	11.6	554	6.37	4.50	0.010	0.29	0.243	0.187	0.00	0.207	<0.001	6.35	5.15	9.99	1.15	1.39	0.31
04V003	31.10.04 18:05	620	0.2	1.2	6.77	515	10.3	605	7.05	4.73	0.034	0.25	0.266	0.197	0.00	0.221	<0.001	6.82	5.71	10.5	1.47	2.04	0.37
04V004	01.11.04 09:15	1072	0.6	2.7	6.71	522	9.6	661	7.80	4.96	0.019	0.18	0.290	0.208	0.00	0.232	<0.001	7.18	6.04	12.5	2.43	0.59	0.31
04V005	01.11.04 19:45	1566	1.4	8.6	6.54	513	15.3	719	8.66	4.94	<0.0083	0.24	0.297	0.218	0.00	0.232	<0.001	7.56	6.72	12.9	0.59	0.41	0.17
04V006	02.11.04 08:50	2511	1.7	6.0	6.52	490	14.6	693	8.49	4.72	0.032	0.26	0.286	0.193	0.00	0.220	<0.001	7.84	6.60	11.7	2.60	0.67	1.12
04V007	02.11.04 12:15	2841	1	5.8	6.48	506	15.1	726	8.96	4.80	0.009	0.26	0.289	0.214	0.00	0.239	0.001	7.55	6.61	12.0	0.80	0.43	0.30
04V008	02.11.04 19:15	2774	1.8	6.2	6.50	557	13.3	782	8.08	4.35	<0.0083	0.23	0.260	1.304	0.00	0.646	0.650	3.27	10.8	11.5	0.37	1.25	0.24
04V009	03.11.04 10:00	976	1.5	6.1	6.78	420	12.0	485	4.14	2.83	<0.0083	0.33	0.181	1.132	0.12	0.879	0.249	3.49	13.1	6.65	0.28	1.45	0.07
04V010	03.11.04 16:25	619	1.7	4.2	7.16	396	11.5	418	3.29	2.75	<0.0083	0.18	0.176	1.045	0.08	0.730	0.314	3.44	12.9	6.71	0.40	1.58	0.00
04V011	04.11.04 16:50	441	0.7	2.0	6.90	425	15.9	438	3.17	2.39	0.013	0.35	0.253	1.266	0.93	0.688	0.576	3.89	17.4	5.95	1.82	1.50	0.00

5.4.3 Chemistry of fresh tephra, the suspended materials and the floodwaters

5.4.3.1 Solids

The specific surface area and chemical composition of solids is tabulated in Table 1. All major elements except Mg were slightly elevated in the tephra compared to samples 8 and 9 which were sampled from the river after the volcanic influenced water had arrived to the sampling site (Table 1). This suggests that most of the suspended materials in the flood were older material and/or that the new tephra leached rapidly in the flood water. The sum of the major elements differed between the suspended materials (mean 95.7%) and fresh tephra (100.2%) indicating considerable contribution of suspended materials eroded from the flood channel as in the Gjálp 1996 eruption (Stefansdottir and Gislason, 2005) and hydration of the tephra in the flood channel during transport to the flood plain (Table 1). Results from PHREEQC-2 calculations in section 4.5 below further indicated that 1 to 4% of the tephra mass was leached to the floodwater using geometric surface area or BET surface area, respectively. On the contrary to major elements, the semi volatile and volatile elements As, B, Hg and S were elevated in the suspended materials compared to the tephra (table 1). These elements all originate in magma gases (Bauer and Onishi 1978; Mambo et al.,1991; Bagnato et al., 2009) and can be transported with steam in geothermal systems (Bauer and Onishi, 1978, Giroud, 2008; Bragason and Yngvadottir, 2009). As the magma gases and steam entered the cauldron high amounts of available surface was available (Table 1) to adsorb these elements but metals may often be adsorbed or coprecipated in the volcanic environment (Cleverley et al., 2003)

5.4.3.2 Aqueous chemistry

The temperature of the floodwater, as measured at the bridge, did not exceed 2°C and the maximum dissolved oxygen in the water was between 40 and 70% of air saturation at the sampling temperature which was always higher than 1°C (Table 1). A trace of H_2S was measured in some samples although the distinct smell was never observed. The partial pressure of CO_2 in the samples at the sampling temperature calculated with Phreeqc-2 based on pH temperature and chemical analysis was always higher than in the atmosphere. Thus, once the water emerged from the base of the glacier, there was a flux of CO_2 from the water and conversely influx of heat and O_2 to the water.

The flood path shown in figure 1 may be considered to behave like a 50 km chromatographic column although part of the solid phase in this case travels with the mobile phase. The bedrock surface of the flood path though perhaps has enough surface area to separate some of the ions. Figure 3 displays the flux of selected elements at the time of sampling and figure 4 displays the relative mobility of selected elements to Na. Table 3 tabulates predicted surface reactions of the dominant anionic species in the floodwater. The maximum flux of B, Cl, As, Si and Na was observed in the water sampled at 12:15 on 2 Nov whereas the maximum flux of F, S_{total} and P was observed in the next sample at 19:15. Boron, As and Si form large oxyanions as do P and S which peaked later. The relative mobility of the total elemental flux vs. the fresh tephra indicated that B was the most mobile element followed by Cl, S, F and then As and Si being much less mobile (Figure 4a).

Table 3 Surface complexation reactions used in PHREEQC-2 calculations

Species	Surface reaction of the dominant aqueous species	log K	Reference
Borate	Hfo_wOH + H_3BO_3 = Hfo_wH_2BO_3 + H_2O	0.62	1
Chloride	Hfo_wOH + Cl^- + H^+ = Hfo_wOH_2Cl	2.24	1
Silicate	Hfo_wOH + H_4SiO_4 = Hfo_wOSi$(OH)_3$ + H_2O	4.28	2
Arsenite	Hfo_wOH + H_3AsO_3 = Hfo_wH_2AsO_3 + H_2O	5.41	1
Sulphate	Hfo_wOH + SO_4^{2-} + H^+ = Hfo_wSO_4^- + H_2O	7.78	1
	Hfo_wOH + SO_4^{2-} = Hfo_wOHSO_4^{2-}	0.78	1
Fluoride	Hfo_wOH + F^- + H^+ = Hfo_wF + H2O	8.7	1
	Hfo_wOH + F^- = Hfo_wOHF^-	1.6	1
Arsenate	Hfo_wOH + H_2AsO_4- + H^+ = Hfo_wH_2AsO_4 + H_2O	10.95	1
	Hfo_wOH + $H_2AsO_4^-$ = Hfo_wHAsO_4^- + H_2O	5.15	1
	Hfo_wOH + $H_2AsO_4^-$ = Hfo_wOHAsO_4^{3-} + $2H^+$	-7.78	1
Bicarbonate	Hfo_wOH + HCO_3^- = Hfo_wCO_3^- + H_2O	2.23	3
	Hfo_wOH + HCO_3^- + H^+ = Hfo_wHCO_3^- + H2O	10.29	3
Phosphate	Hfo_wOH + $H_2PO_4^-$ + H^+ = Hfo_wH_2PO4 + H_2O	11.76	1
	Hfo_wOH + $H_2PO_4^-$ = Hfo_wHPO4$^-$ + H_2O	5.86	1
	Hfo_wOH + $H_2PO_4^-$ = Hfo_wPO_4^{2-} + H^+ + H_2O	-1.80	1

1 Dzombak, Morel 1990
2 Swendlund, Webster 1999
3 Van Geen et al.

The elements, B (as borate, H_3BO_3) Cl (as chloride, Cl^-), As (as arsenite, H_3AsO_3, Si (as silicate, H_4SiO_4) , S (as sulphate, SO_4^{2-}) and P (as phosphate $H_2PO_4^-$) probably all form

surface complexes (Table 3) on the tephra surface and may be delayed in the flood path. The results of the flux calculations are shown in Table 4.

Table 4 Dissolved flood fluxes

	Moles	Tonnes		Moles	Tonnes		Moles	Tonnes		Moles	Tonnes
TDS		3.27×10^{5}	S_2O_3	1.03×10^{8}	6.60×10^{3}	NO_3	4.60×10^{5}	6.45	Mo	1.46×10^{3}	1.14×10^{-1}
DIC as CO_2	1.05×10^{9}	4.61×10^{4}	K	2.08×10^{7}	8.13×10^{2}	Sr	2.61×10^{5}	2.29×10^{1}	As	8.05×10^{2}	6.03×10^{-2}
Na	8.30×10^{8}	1.91×10^{4}	B	5.35×10^{6}	5.79×10^{1}	PO_4	1.72×10^{5}	5.33	Ba	6.34×10^{2}	8.71×10^{-2}
Ca	6.76×10^{8}	2.72×10^{4}	DOC	5.28×10^{6}	6.34×10^{1}	Ti	4.53×10^{4}	2.17	Cr	3.18×10^{1}	6.99×10^{-3}
Si	3.93×10^{8}	1.10×10^{4}	F	4.31×10^{6}	8.19×10^{1}	V	3.18×10^{4}	1.62	Pb	9.60×10^{1}	1.99×10^{-2}
S	3.05×10^{8}	9.77×10^{3}	Mn	2.24×10^{6}	1.23×10^{2}	Ni	2.63×10^{4}	1.54	Cd	3.59×10^{1}	4.04×10^{-3}
SO_4	2.08×10^{8}	6.68×10^{3}	Fe	2.13×10^{6}	1.19×10^{2}	Cu	1.93×10^{4}	1.23	Hg	4.30	8.63×10^{-4}
Mg	1.98×10^{8}	4.82×10^{3}	NH_4	5.83×10^{5}	8.16	Zn	1.12×10^{4}	0.73			
Cl	1.30×10^{8}	4.60×10^{3}	Al	5.16×10^{5}	1.39×10^{1}	Co	9.62×10^{3}	0.57			

5.4.4 **Sulphur isotopes**

The δ34S values of the floodwaters ranged from +3.27 to +7.84 ‰ (table 2).The principal gas in equilibrium with basaltic magma at low pressure and high temperature is SO_2 (Gerlach and Nordlie, 1975). Rapid degassing of SO_2 from a finite magma reservoir decreases the sulphur concentration and the δ34S isotope composition of the magma, if the magma is reduced. Conversely, the δ34S value of the magma increases during degassing if the magma is oxidised (Sakai et al., 1982). Icelandic rocks generally range from -2 ‰ to 0 ‰ (Torssander, 1989) due to degassing at reduced conditions and as a consequence, the degassing SO_2 gas is enriched in heavier S relative to the melt. Gislason et al. (2002) assumed the δ34S of SO_2 gas entering the melt water in Gjálp 1996 eruption to be 1.8 ‰. The decrease of δ34S values during the flood event strongly indicates flow of new light SO_2 gas into the melt water.

A disproportion of SO_2 in water produces bisulphide, sulphide and elemental sulphur (Kusakabe et al., 2000) according to the following reactions:

$$3SO_2 + 3H_2O = 2HSO_4^- + S_0 + 2H^+ \qquad \text{Equation 6}$$

Or

$$4SO_2 + 3H_2O = 3HSO_4^- + H_2S + 3H^+ \qquad \text{Equation 7}$$

Elemental sulphur is stable under relatively oxidised conditions, low temperatures and high total sulphur concentrations whereas sulphide forms at reduced conditions, high temperatures and low sulphur concentrations (Kusakabe et al., 2000). The SO_2 disproportionation reaction is rapid at high temperatures (Kusakabe et al., 2000) but did not proceed entirely in the eruption water as high proportion of the sulphur was the

intermediate product thiosulphate (Table 2) which was present for up to 50 h under experimental conditions (Kusakabe et al., 2000).

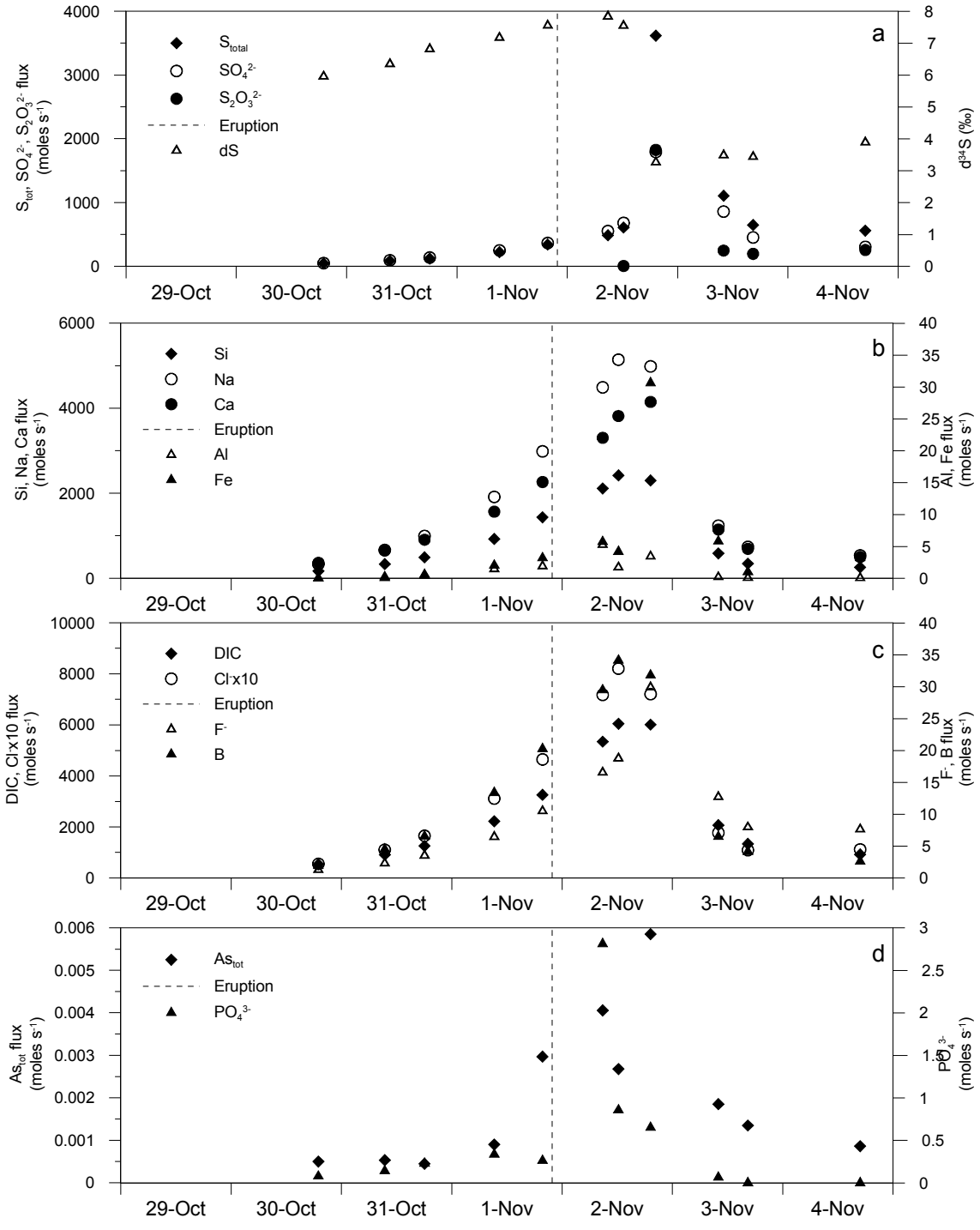

Figure 3 Elemental fluxes with the floodwater. The eruption began on 1. November at 21:50 (hatched line). The Si, Na, DIC, Cl, B and PO_4 had highest fluxes before the flood water peak whereas Ca, F, S and As had highest fluxes after the flood water peak.

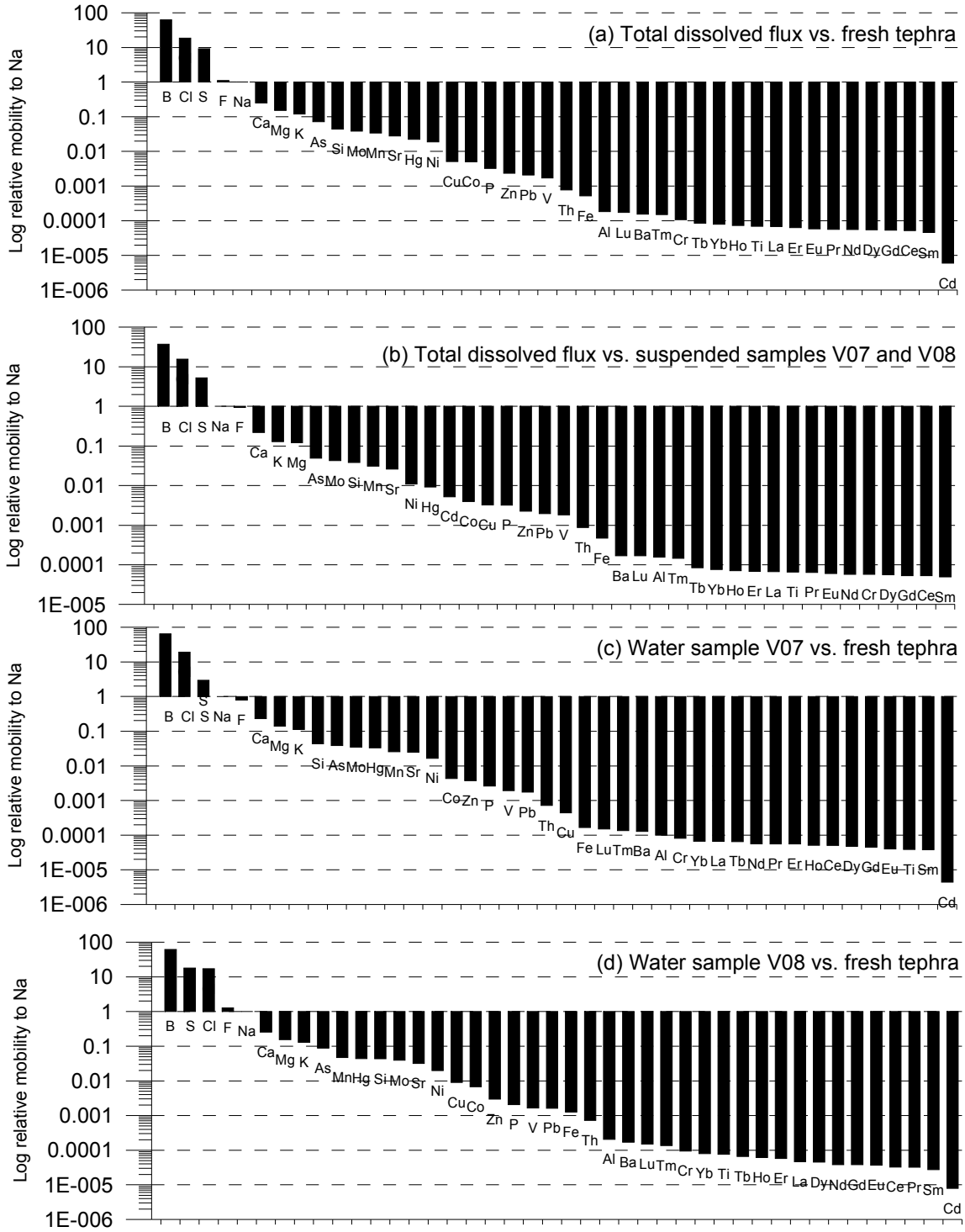

Figure 4 Relative mobility of selected elements to Na. (a) The total flux compared to fresh tephra. (b) The total flux compared to suspended samples V07 and V08 sampled around the discharge maximum. (c) The water sample V07 compared to fresh tephra. (d) The water sample V08 compared to fresh tephra.

5.4.5 Reaction path modeling in the flood path

5.4.5.1 Surface complexation

Hydrated volcanic glass may be considered as a mechanical mixture SiO_2, Al_2O_3 and FeO oxides in that order. The 3 most abundant surface sites contributing to the surface of volcanic glass are Si-OH, Al-OH and Fe-OH sites in that order. Furthermore, the equilibrium constants for As(III) adsorption onto Fe-OH are higher than for sorption onto Si-OH and Al-OH sites (Sahai and Sverjensky, 1997; Sverjensky and Fukushi, 2006) and order of magnitudes higher for arsenate (Fukushi and Sverjensky, 2007). Therefore, the contribution of Fe-OH sites to the sorption was dominant as was observed by comparing modelled results from As sorption onto HFO (Figures 5a and 5b) with As sorption onto basaltic glass (Figures 5c and 5d) when the number of active surface sites have been equalled and the only difference being the equilibrium constants for association/dissociation surface reactions and the As sorption reactions. Although the system may not have reached equilibrium, when equilibrium constants for the surface reactions were used to predict mobility, borate should have been most mobile, followed by chloride, silicate, arsenite, sulphate, fluoride, arsenite, bicarbonate and finally phosphate. The chemistry of the sulphur is further complicated since the speciation varied according to its source as will be discussed in next section. Arsenic may be considered to have been on the arsenite form (As(III)) in the flood path due to its rapid appearance peak in the flood, the low oxygen saturation of the water and the short reaction time. In fact, As is primarily measured on the arsenite form in geothermal waters in Iceland (Chapter 4, this thesis). The oxidised form arsenate should have been retained more according to experimental data on basaltic glass surfaces (Sigfusson et al., 2008).

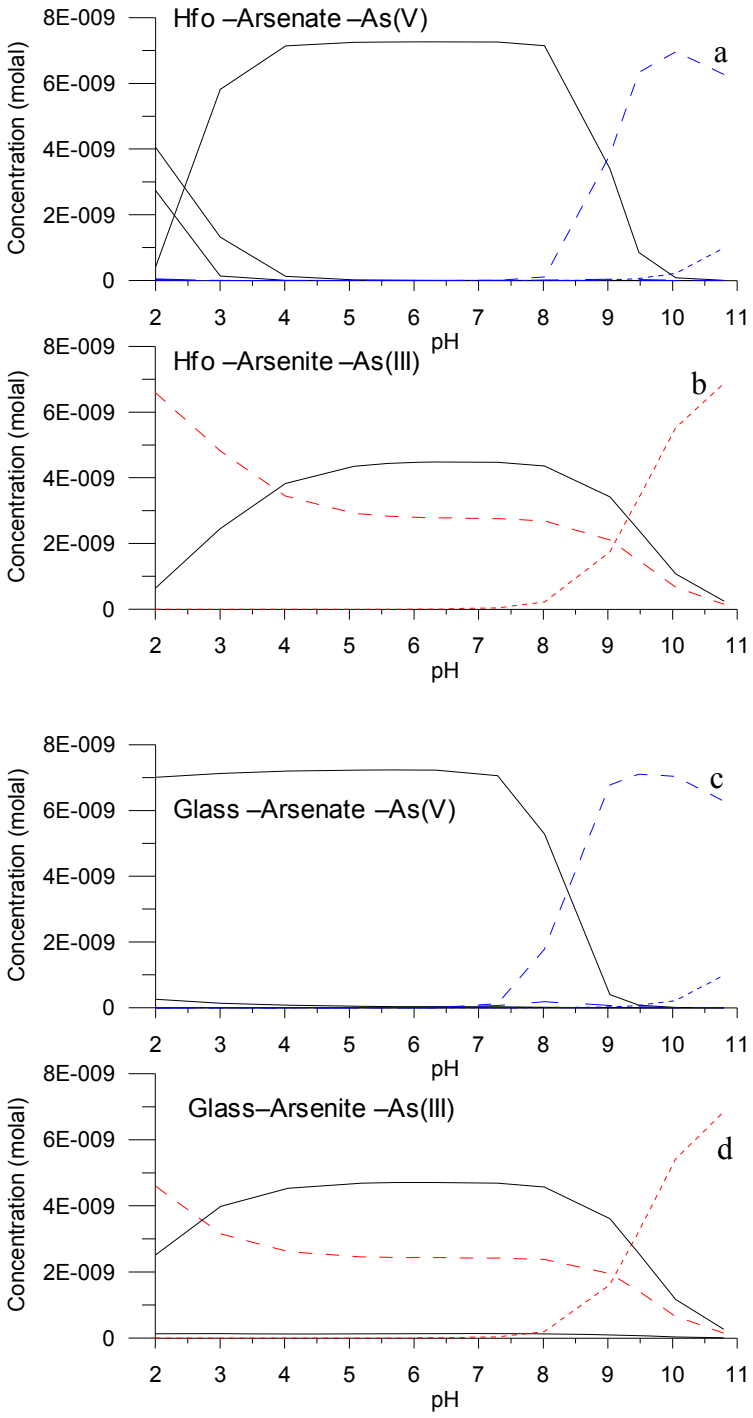

Figure 5 Results of model calculations when Hydrous Ferric Oxide (HFO) was used to represent all the surface (2.17mg in 1 litre water 10 g of Basaltic glass in 1 litre of water) (a and b) . Same calculations when basaltic glass represented all of the surface (10 g in 1 litre water). Hfo was used to represent the surface of the tephra in all simulations to allow for incorporation of competitive surface reactions of other ions.

5.4.5.2 Constraint of temperature

The mean temperature in the flood path was estimated by adjusting the temperature for geothermal water/volcanic gas/tephra interactions between 0 and 50°C. Fifty degrees led to rapid dissolution rates of the tephra and a high pH rise as a consequence. On the contrary 0°C, led to slow dissolution rates. After few test runs, the temperature was set to 2°C due to sufficient pH rise of the floodwaters to measured values (Figure 6a,b). This was estimated to be the mean temperature in the flood path whereas published data have estimated that the temperature leaving Grímsvötn in the Gjálp eruption was 8°C (Gudmundsson et al., 1997) and measured temperature at the bridge was between 0.2 and 1.8 °C at air temperatures between 1 and 8.6°C (table 2). The glacial outburst flood following the Gjálp eruption had very different characteristics to the 2004 eruption in a way that melt water flowed continuously for 5 weeks into Lake Grímsvötn prior to the glacial flood out of the lakes. No published heat and mass balance calculations exists on the estimation of floodwater temperatures leaving Grímsvötn in the 2004 eruption. The modeling, however, demonstrates that the products from chemical reactions in the flood path may help constrain the heat flux of eruption and flood.

5.4.5.3 Tephra dissolution in the flood path

The aim of the modeling exercise of the flood path water was to be able to end up with a pH close to the measured value at the bridge and by the means of dissolving tephra according to experimentally derived data (Gislason and Oelkers, 2003) and adding a known amount of volcanic gases based on chemical analyses at the bridge to adjust the major element concentration measured. This first attempt successfully reproduced the pH value if the specific surface area is larger than geometric but smaller than BET surface area. Further, allowing moganite to precipitate in the solution fixed the Si concentration while the modelled total dissolution of tephra corresponded roughly to the sum of measured oxides in the suspend matter collected at the bridge (Table 1). The modeling also demonstrated that the most of the silicate, sulphur and bicarbonate was partitioned in the solution compared to surface (Figures 6a, 6b, 6c and 7a, 7b, 7c) The same applied to fluoride (Figures 6e and 7e) whereas phosphate was primarily on the surface of the suspended materials (Figures 6d and 7d). Arsenic was primarily in solution which corresponds to measured values (Figures 6f and 7f).

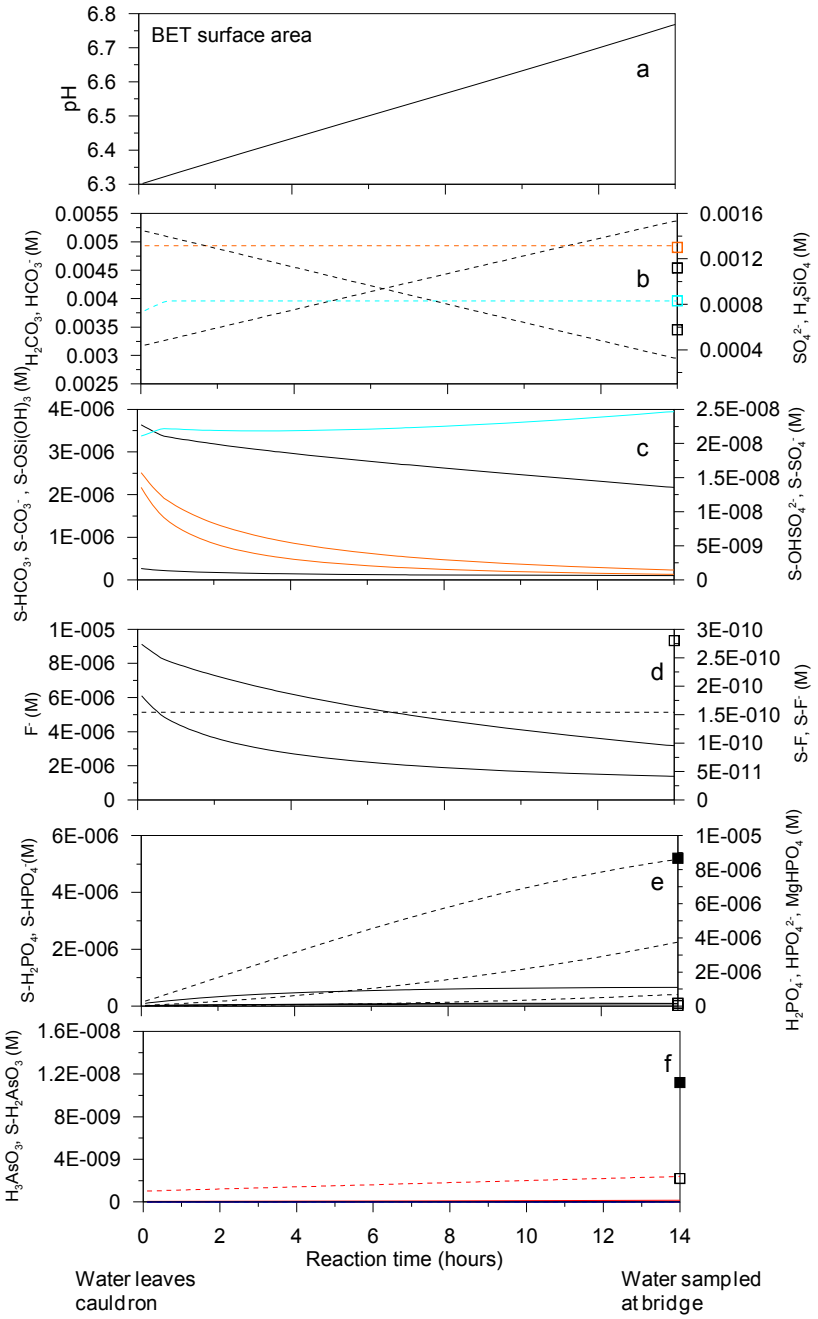

Figure 6. The eruption floodwater flowed for 14 hours before sampling at Skeiðará Bridge. The eruption water was simulated by dissolving 10 grams of fresh tephra with specific BET surface area of 12.6 m^2 g^{-1} in 1 litre of floodwater prior to eruption (02V002 in Table 2) for the period of 14 hours . Dashed lines represent aqueous species concentrations, but solid lines surface species concentrations in (mol/kg). Open symbols on the right y-axes represent measured aqueous concentrations (Table 2) and closed symbols sorbed concentrations. Other sources such as volcanic gases were needed in addition to dissolution of tephra, adsorption and desorption to account for measured DIC, Cl^-, SO_4^{2-} and F^- whereas excess dissolution and adsorption of P was predicted. Elevated arsenic concentrations in the floodwater peak could be explained by dissolution of tephra only. Black lines represent carbon species, blue lines silicon species and orange lines sulphur species in the combined figure.

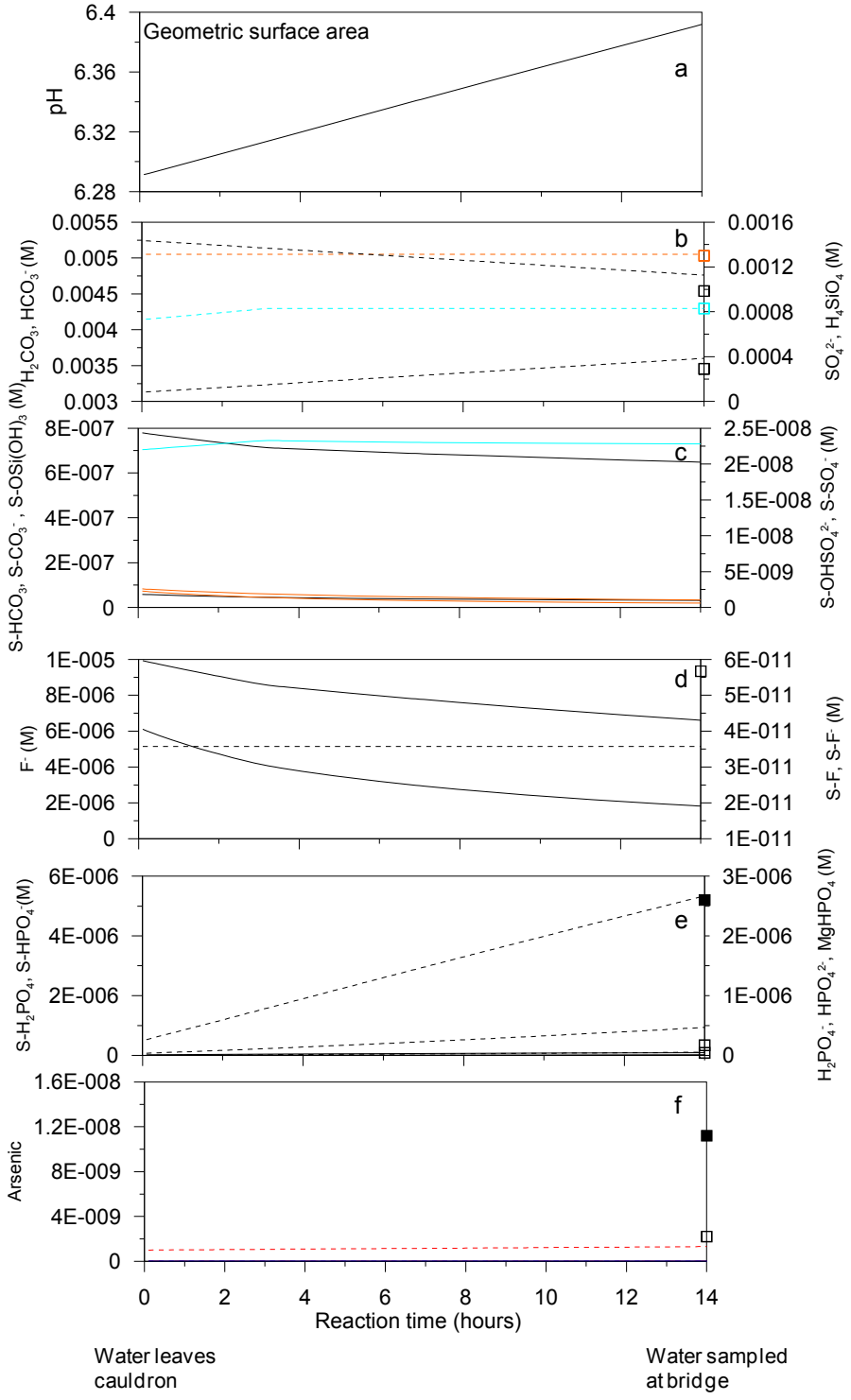

Figure 7 Same simulation as in figure 6 assuming specific geometric surface area of 2.3 $m^2 g^{-1}$. Elevated As concentrations in the floodwater peak could not be explained by dissolution of tephra only. The actual reactive surface area was presumably between geometric and BET surface area. Black lines represent carbon species, blue lines silicon species and orange lines sulphur species in the combined figure.

5.4.6 **Mixing of floodwaters and seawater**

Figure 8 displays the predicted fate of selected elements when the floodwater prior to eruption entered the ocean at 25°C. Figure 9 displays the predicted fate of selected elements when the volcanic floodwater sampled during the flood peak entered the ocean. The fate of selected elements was predicted during this mixing and is primarily dependent on the chemical composition and pH of the mixture as well. The pH of the mixture shifted from 6.7 and 6.2 to 8.2 for geothermal and volcanic floodwaters, respectively. The aqueous species of all elements were always in much higher concentrations than adsorbed species except for As when BET surface area was used and as a consequence the predicted impact of the floodwaters was higher. The high adsorbed arsenate concentration in floodwater/seawater mixtures of ~1:5 to ~1:100 where the majority of the As was from the seawater but available surface was still sufficient to complex the arsenic. As the seawater ratio increased the surface was saturated and higher proportion was dissolved in the seawater and the effects of the floodwaters were negligible. The floodwater also diluted the S and P concentrations locally in the ocean but the effects were much more due to dilution rather than surface complexation (Figures 7 and 8). After extensive dilution all adsorbed S and P had been desorbed again indicating the localised effect of such small eruptions, a P deficiency only occurs after small mixing but increased mixing minimises sorbed P (Figures 8 and 9). The Si, C and F in the floodwaters were conversely diluted very rapidly by the ocean due to mixing and limited surface reactions occurred. Simple mixing calculations assumed no floodwater effect would be measured within 10% analytical error after 40 fold dilution with seawater. The was no difference between mixing geothermal floodwater with seawater on one hand and volcanic floodwater with seawater on the other hand, after the floodwater/seawater ratio had exceeded 1:1000 (Figures 8 and 9) Therefore the effect of the floodwater on the ocean are localised in such a small eruption.

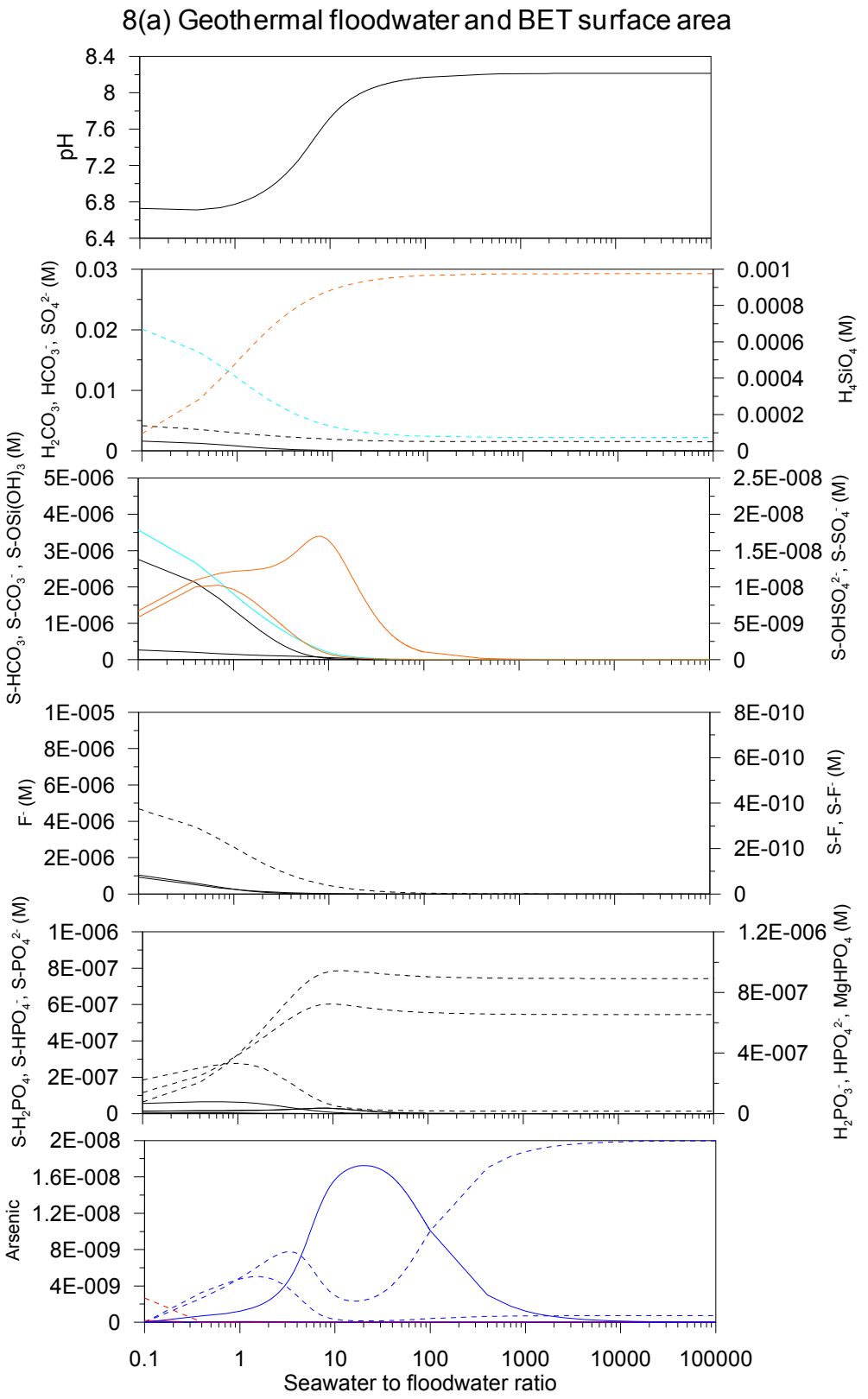

Figure 8 Mixing of geothermal floodwater and seawater <u>prior</u> to the eruption. Initially, the suspended materials in the floodwater adsorbed SO_4^{2-} and As from the seawater. Following a continued dilution of the floodwaters with increasing pH values in the mixture, all ions desorbed substantially to the ocean. Figure 8a uses BET surface area and Figure 8b geometric surface area.

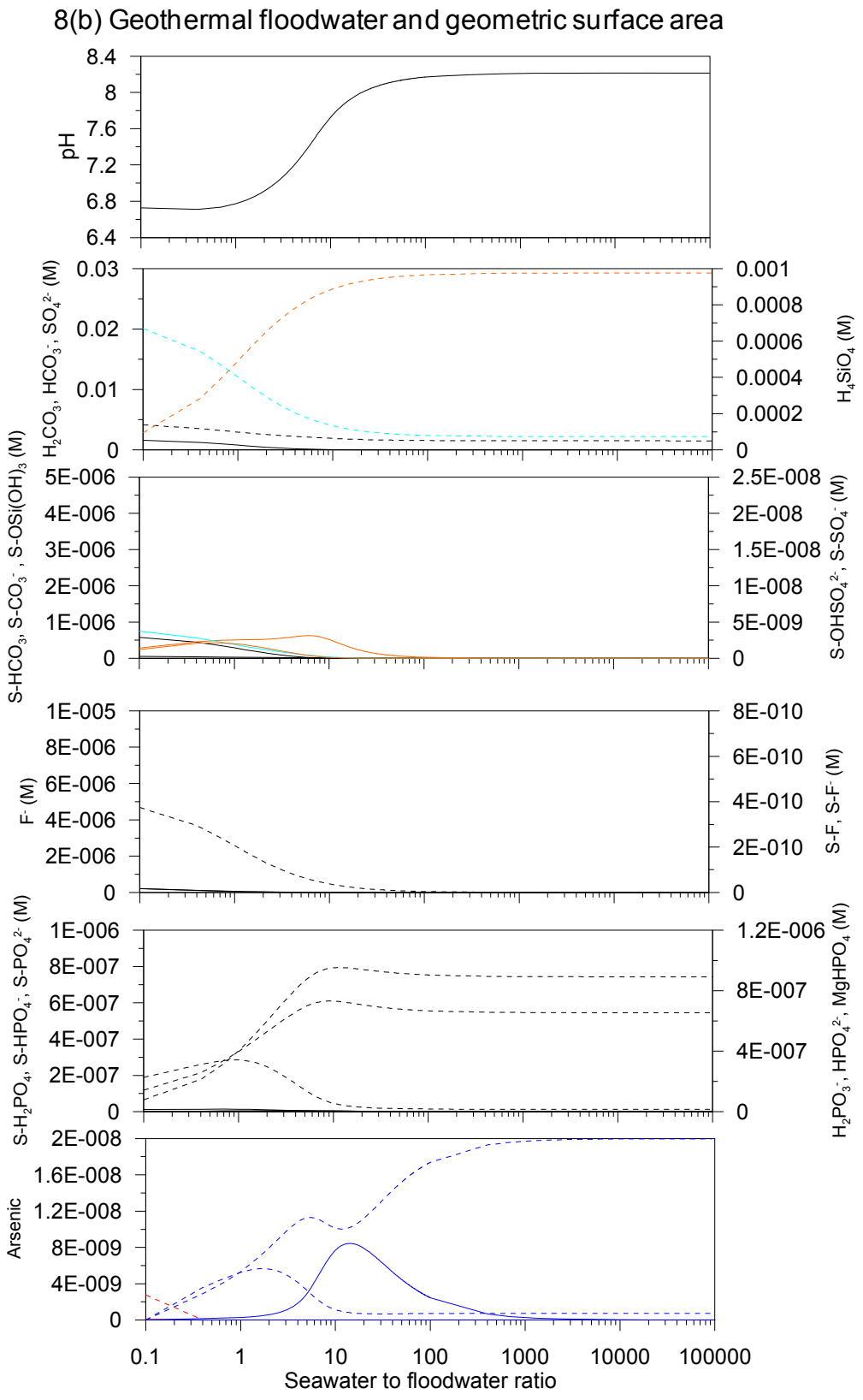
8(b) Geothermal floodwater and geometric surface area
pH
8.4
8
7.6
7.2
6.8
6.4
H2CO3, HCO3-, SO4 2- (M)
0.03
0.02
0.01
0
H4SiO4 (M)
0.001
0.0008
0.0006
0.0004
0.0002
0
S-HCO3, S-CO3-, S-OSi(OH)3 (M)
5E-006
4E-006
3E-006
2E-006
1E-006
0
S-OHSO4 2-, S-SO4- (M)
2.5E-008
2E-008
1.5E-008
1E-008
5E-009
0
F- (M)
1E-005
8E-006
6E-006
4E-006
2E-006
0
S-F, S-F- (M)
8E-010
6E-010
4E-010
2E-010
0
S-H2PO4, S-HPO4-, S-PO4 2- (M)
1E-006
8E-007
6E-007
4E-007
2E-007
0
H2PO3-, HPO4 2-, MgHPO4 (M)
1.2E-006
8E-007
4E-007
0
Arsenic
2E-008
1.6E-008
1.2E-008
8E-009
4E-009
0
0.1
1
10
100
1000
10000
100000
Seawater to floodwater ratio

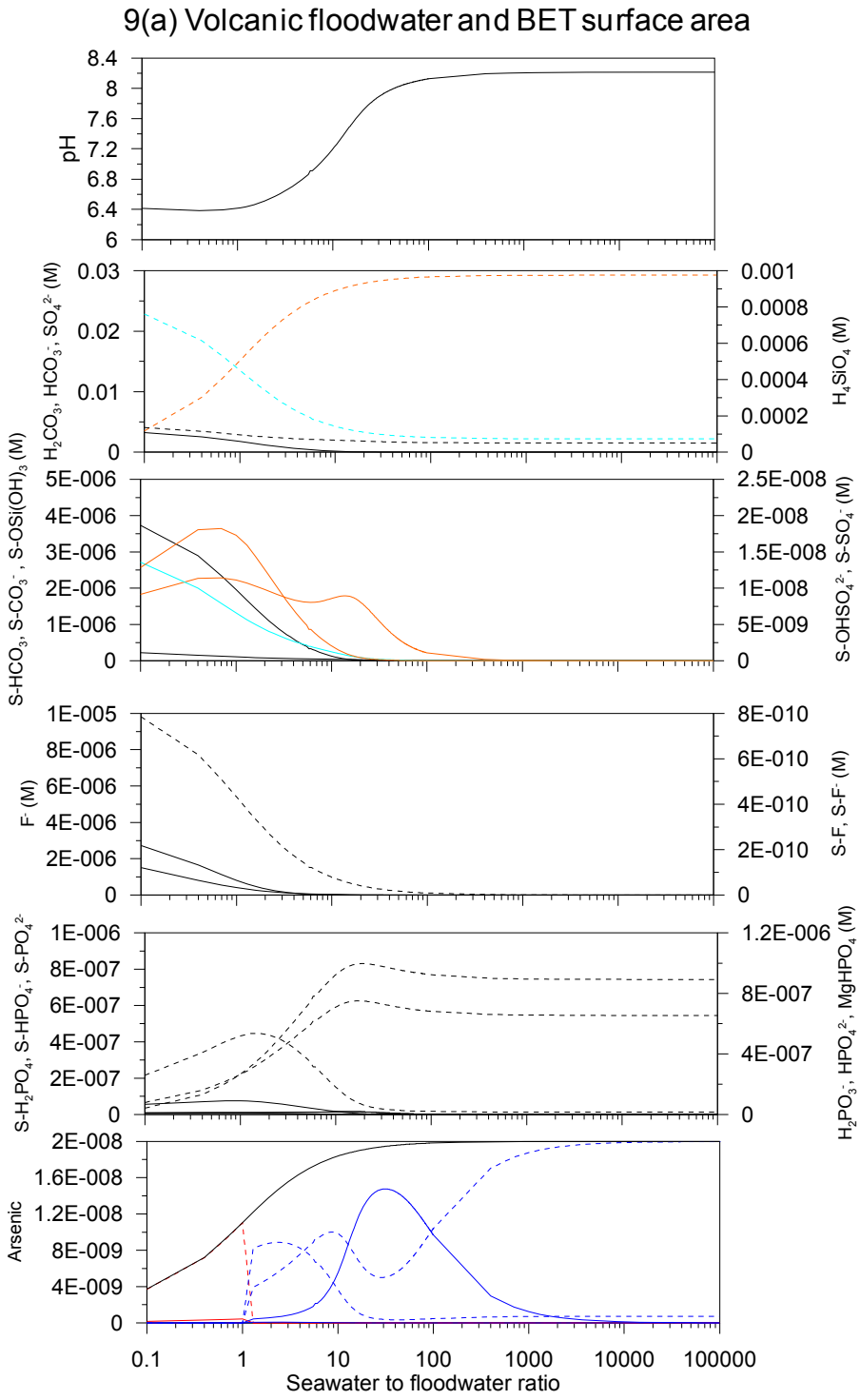

Figure 9 Mixing of floodwater and seawater during the volcanic eruption. Initially, the suspended materials in the floodwater adsorbed SO_4^{2-} and As from the seawater. Following a continued dilution of the floodwaters with increasing pH values in the mixture, all ions desorbed substantially to the ocean. Black line on the As diagram represents As concentration by mixing between the two waters with no surface complexation. Otherwise the same colours apply as in Figure 8. Figure 9a assumes BET surface area and Figure 9b geometric surface area.

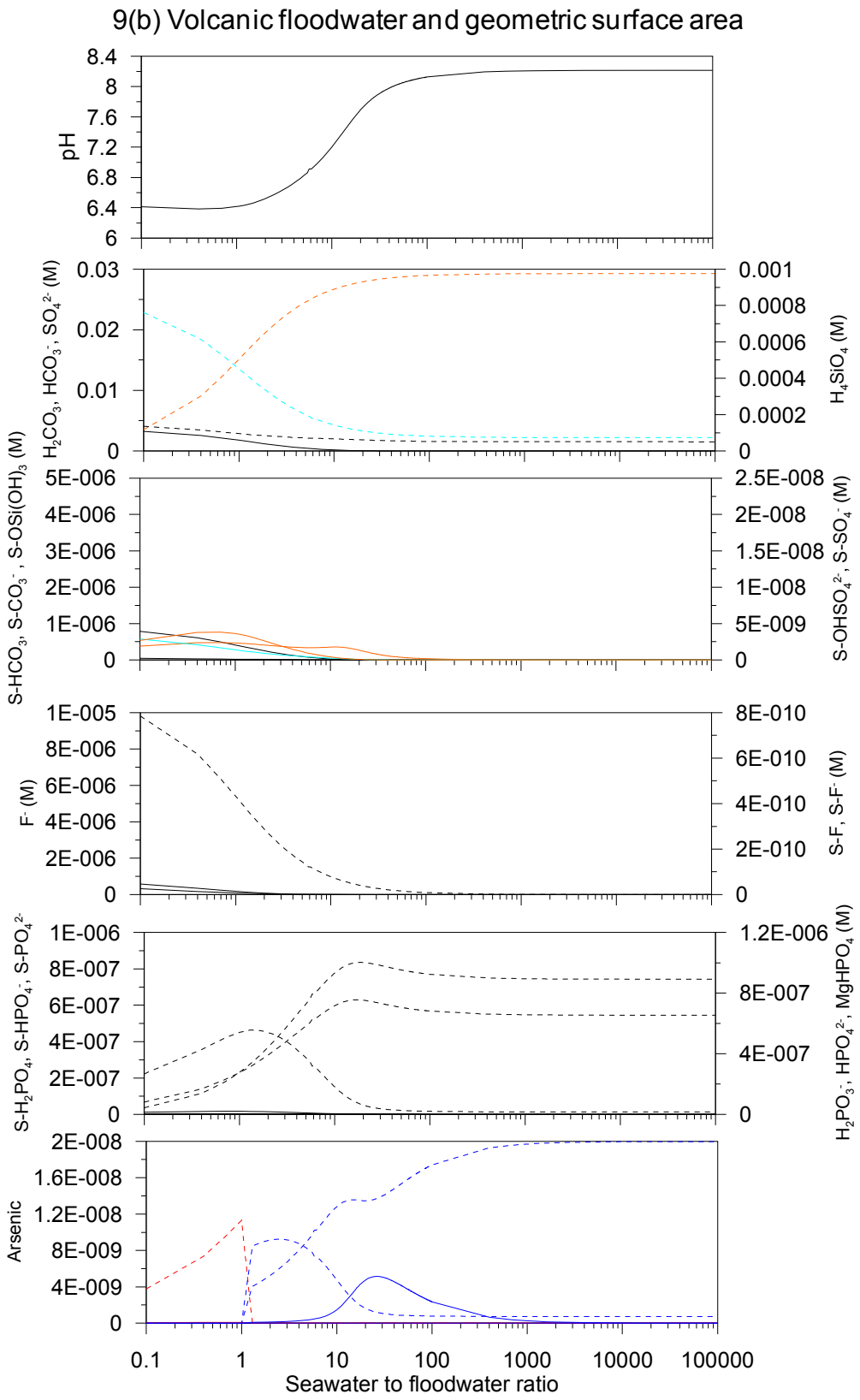

5.5 Conclusions

A continuous monitoring network detected signs of glacial flooding event from the Mt. Grímsfjall volcano in Vatnajökull glacier. As a consequence a sampling campaign could

be launched prior to initiation of the November 2004 eruption of Grímsvötn. Floodwater and suspended material samples were sampled less than 14 h after the tephra entered the Earth's surface providing unique opportunity to study volcano glacier interactions. The melt water flowed sub glacially for 50 km and there was evidence the sub glacial tunnel may have acted as a natural ion chromatograph. Geothermal melt water in Lake Grímsvötn buffered volcanic gases emitted in the eruption, therefore slowing down dissolution of the tephra. The As dissolved from the tephra in the eruption was adsorbed to the suspended materials in the flooding event. Once entering the ocean, the suspended materials probably caused local decrease in aqueous As concentrations. Upon prolonged dilution of the floodwater by seawater the As was desorbed from the surface and the floodwater chemical signals were not predicted to be measurable once they had been diluted thousand times by sea water. The selection which surface area measurement to use highly influences predicted effects of floodwaters entering the ocean.

5.6 References

Akinfiev, N.N., Zotov, A.V. & Nikonorov, A.P. 1992, "Thermodynamic Analysis of Equilibria in the System As(iii)-S(ii)-O-H", *Geokhimiya,* , no. 5, pp. 721-734.

Archer, E.E. 1955, "The determination of small amounts of sulphate by reduction to hydrogen sulphide, and titration with mercury or cadmium salts with dithizone as an indicator", *Analyst,* vol. 81, pp. 181-182.

Bagnato, E., Aiuppa, A., Parello, F., D'Alessandro, W., Allard, P. & Calabrese, S. 2009, "Mercury concentration, speciation and budget in volcanic aquifers: Italy and Guadeloupe (Lesser Antilles)", *Journal of Volcanology and Geothermal Research,* vol. 179, no. 1-2, pp. 96-106.

Ballantyne, J.M. & Moore, J.N. 1988, "Arsenic geochemistry in geothermal systems", *Geochimica et Cosmochimica Acta,* vol. 52, no. 2, pp. 475-483.

Bauer, W.H. & Onishi, H. 1978, "Arsenic" in *Handbook of Geochemistry*, ed. K.H. Wedepohl, Springer-Verlag, New York.

Bragason, A. & Yngvadottir, E. 2009, *Rannsóknir á mosa við jarðvarmavirkjun Orkuveitu Reykjavíkur á Hellisheiði (Research on moss around the Hellisheiði Geothermal powereplant)*, Efla Consltants, Reykjavik (in Icelandic).

Brantley, S.L., White, A.F. & Hodson, M. 1999, "Surface area of primary silicate minerals" in *Growth, dissolution and pattern formation in geosystems*, eds. B. Jamtveit & P. Meakin, Kluwer Academic Publishers, USA, pp. 291-326.

Bruland, K.W. 1983, "Trace elements in sea water" in *Chemical Oceanography*, eds. J.P. Riley & R. Chester, Academic Press, London, pp. 157-220.

Cleverley, J.S., Benning, L.G. & Mountain, B.W. 2003, "Reaction path modelling in the As–S system: a case study for geothermal As transport", *Applied Geochemistry,* vol. 18, no. 9, pp. 1325-1345.

Daux V., Guy C., Advocat T., Crovisier J. & Stille M. 1997, “Kinetic aspects of basaltic glass dissolution at 90°C: Role of silicon and aluminum”, *Chemical Geology,* vol. 142, pp. 109–128.

Flaathen, T.K. & Gislason, S.R. 2007, "The effect of volcanic eruptions on the chemistry of surface waters: The 1991 and 2000 eruptions of Mt. Hekla, Iceland", *Journal of Volcanology and Geothermal Research,* vol. 164, no. 4, pp. 293-316.

Frogner, P., Gislason, S.R. & Oskarsson, N. 2001, "Fertilizing potential of volcanic ash in ocean surface water", *Geology,* vol. 29, no. 6, pp. 487-490.

Fukushi, K. & Sverjensky, D.A. 2007, "A predictive model (ETLM) for arsenate adsorption and surface speciation on oxides consistent with spectroscopic and theoretical molecular evidence", *Geochimica et Cosmochimica Acta,* vol. 71, no. 15, pp. 3717-3745.

Gautier, J., Oelkers, E.H. & Schott, J. 2001, "Are quartz dissolution rates proportional to B.E.T. surface areas?", *Geochimica et Cosmochimica Acta,* vol. 65, no. 7, pp. 1059-1070.

Gerlach, T.M. & Nordlie, B.E. 1975, "The C-O-H-S gaseous system, Part II: temperature, atomic composition, and moleculat equilibria in volcanic gases", *American Journal of Science,* vol. 275, pp. 377-394.

Giroud, N. 2008. *A chemical study of arsenic, boron and gases in high-temperature geothermal fluids in Iceland*. PhD thesis University of Iceland, Faculty of Science.

Gislason, S.R. & Oelkers, E.H. 2003, "Mechanism, rates, and consequences of basaltic glass dissolution: II. An experimental study of the dissolution rates of basaltic glass as a function of pH and temperature", *Geochimica et Cosmochimica Acta,* vol. 67, no. 20, pp. 3817-3832.

Gislason, S.R., Heaney, P.J., Oelkers, E.H. & Schott, J. 1997, "Kinetic and thermodynamic properties of moganite, a novel silica polymorph", *Geochimica et Cosmochimica Acta,* vol. 61, no. 6, pp. 1193-1204.

Gislason, S.R., Snorrason, A., Kristmannsdottir, H.K., Sveinbjornsdottir, A.E., Torsander, P., Olafsson, J., Castet, S. & Dupre, B. 2002, "Effects of volcanic eruptions on the CO2 content of the atmosphere and the oceans: the 1996 eruption and flood within the Vatnajokull Glacier, Iceland", *Chemical Geology,* vol. 190, no. 1-4, pp. 181-205.

Goldschmidt, V.M. 1954, *Geochemistry,* , Oxford.

Grasshoff, K. 1983, "Determination of oxygen" in *Methods of seawater analysis. Second, revised and extended edition.*, eds. K. Grasshoff, M. Ehrhardt & K. Kremling, 2nd edn, Verlag Chemie, New York, USA, pp. 1-419.

Gudmundsson, M.T., Sigurdsson, F. & Björnsson, H. 1997, "Ice-volcano interaction of the 1996 Gjálp subglacial eruption, Vatnajökull, Iceland", *Nature,* vol. 389, pp. 954-957.

Guy, H.P. & Norman, V.W. 1970, *Techniques of Water-Resources Investigations of the United States Geological Survey. Field Methods for Measurement of Fluvial Sediment 3 (C2)*, United States Government Printing Office, Washington, DC.

Hardardottir, J., Gunnarsson, A. & Thorlaksdottir, S.B. 2003, *Mælingar á rennsli, svifaur og skridaur í Jökulsá á Dal árid 2002.*, Orkustofnun (in Icelandic).

Hardardottir, J., Sigfusson, B., Jonsson, P., Gislason, S.R., Sigurdsson, G. & Elefsen, S.O. 2004, *Nidurstodur rennslis-, aurburdar- og efnamaelinga i Skeiðarárhlaupi haustid 2004*, Orkustofnun (in Icelandic), Reykjavik.

Helz, G.R., Tossell, J.A., Charnock, J.M., Pattrick, R.A.D., Vaughan, D.J. & David Garner, C. 1995, "Oligomerization in As (III) sulfide solutions: Theoretical

constraints and spectroscopic evidence", *Geochimica et Cosmochimica Acta,* vol. 59, no. 22, pp. 4591-4604.

Jones, M.T. & Gislason, S.R. 2008, "Rapid releases of metal salts and nutrients following the deposition of volcanic ash into aqueous environments", *Geochimica et Cosmochimica Acta,* vol. 72, no. 15, pp. 3661-3680.

Kusakabe, M., Komoda, Y., Takano, B. & Abiko, T. 2000, "Sulfur isotopic effects in the disproportionation reaction of sulfur dioxide in hydrothermal fluids: implications for the δ34S variations of dissolved bisulfate and elemental sulfur from active crater lakes", *Journal of Volcanology and Geothermal Research,* vol. 97, no. 1-4, pp. 287-307.

Mambo, V.S., Yoshida, M. & Matsuo, S. 1991, "Partition of arsenic and phosphorus between volcanic gases and rock. Part I: analytical data and magmatic conditions of Mt. Usu, Japan", *Journal of Volcanology and Geothermal Research,* vol. 46, no. 1-2, pp. 37-47.

Mörth, C. M., Torssander, P., Kjonaas, J. O., Stuanas, A. O., Moldan, F., Giesler, R. 2005. "Mineralization of organic sulfur delays recovery from anthropogenic acidification", *Environmental Science and Technology*, vol. 39, pp. 5234-5240.

Nriagu, J.O. 1989, "A global assessment of natural sources of atmospheric trace metals", *Nature,* vol. 338, pp. 47-49.

Oddson, B. 2007, *The Grímsvötn Eruption in 2004: Dispersal and Total Mass of Tephra and Comparison with Plume Transport Models*, MSc edn, University of Iceland, Reykjavik, Iceland.

Oelkers, E.H. & Gislason, S.R. 2001, "The mechanism, rates and consequences of basaltic glass dissolution: I. An experimental study of the dissolution rates of basaltic glass as a function of aqueous Al, Si and oxalic acid concentration at 25 degrees C and pH=3 and 11.", *Geochimica et Cosmochimica Acta,* vol. 65, no. 21, pp. 3671-3681.

Parkhurst, D.L. & Appelo, C.A.J. 1999, *User's guide to PHREEQC (Version 2)- A computer program for speciation, batch-reaction, one-dimensional transport, and inverse geochemical calculations*, US Geological Survey.

Pokrovski, G., Gout, R., Schott, J., Zotov, A. & Harrichoury, J.C. 1996, "Thermodynamic properties and stochiometry of As(III) hydroxide complexes at hydrothermal conditions", *Geochimica et Cosmochimica Acta,* vol. 60, no. 5, pp. 737-749.

Pokrovski, G.S., Zakirov, I.V., Roux, J., Testemale, D., Hazemann, J., Bychkov, A.Y.u. & Golikova, G.V. 2002, "Experimental study of arsenic speciation in vapor phase to 500°C: implications for As transport and fractionation in low-density crustal fluids and volcanic gases", *Geochimica et Cosmochimica Acta,* vol. 66, no. 19, pp. 3453-3480.

Sahai, N. & Sverjensky, D.A. 1997, "Solvation and electrostatic model for specific electrolyte adsorption", *Geochimica et Cosmochimica Acta,* vol. 61, no. 14, pp. 2827-2848.

Sakai, H., Casadevall, T.J. & Moore, J.G. 1982, "Chemistry and isotope ratios of sulphur in basalts and volcanic gases at Kilauea volcano, Hawaii", *Geochimica et Cosmochimica Acta,* vol. 46, pp. 729-738.

Sigfusson, B., Meharg, A.A. & Gislason, S.R. 2008, "Regulation of Arsenic Mobility on Basaltic Class Surfaces by Speciation and pH", *Environmental science & technology,* vol. 42, no. 23, pp. 8816-8821.

Sigvaldason, G.E. & Oskarsson, N. 1976, "Chlorine in Basalts from Iceland", *Geochimica et Cosmochimica Acta,* vol. 40, no. 7, pp. 777-789.

Stefansdottir, M.B. & Gislason, S.R. 2005, "The erosion and suspended matter/seawater interaction during and after the 1996 outburst flood from the Vatnajökull Glacier, Iceland", *Earth and Planetary Science Letters,* vol. 237, no. 3-4, pp. 433-452.

Stefansson, A. 2008, *Numerical simulation of CO_2-water basalt interaction*, Science Institute, University of Iceland, Reykjavik.

Sverjensky, D.A. & Fukushi, K. 2006, "A predictive model (ETLM) for As(III) adsorption and surface speciation on oxides consistent with spectroscopic data", *Geochimica et Cosmochimica Acta,* vol. 70, no. 15, pp. 3778-3802.

Tester, J.W., Worley, W.G., Robinson, B.A., Grigsby, C.O. & Feerer, J.L. 1994, "Correlating quartz dissolution kinetics in pure water from 25 to 625°C", *Geochimica et Cosmochimica Acta,* vol. 58, no. 11, pp. 2407-2420.

Torssander, P. 1989, "Sulphur isotope ratios of Icelandic rocks", *Contributions to Mineralogy and Petrology,* vol. 102, pp. 18-23.

Vogfjörd, K., Jakobsdottir, S., Gudmundsson, G.B., Roberts, M.J., Agustsson, K., Arason, T., Geirsson, H., Karlsdottir, S., Hjaltadottir, S., Olafsdottir, U., Thorbjarnardottir, B., Skaftadottir, T., Sturkell, E., Jonasdottir, E.B., Hafsteinsson, G., Sveinbjörnsson, H., Stefansson, R. & Jonsson, T. 2005, "Forecasting and monitoring a subglacial eruption in Iceland", *EOS,* vol. 86, pp. 245-252.

6 Final Discussion

6.1 Introduction

Basaltic rocks are the primary product of magma processes at ocean ridges and they are further associated with mantle plumes (Jerram and Widdowson, 2005). Evidently, being formed by volcanic eruptions, basaltic rock occurrence is inherently associated with geothermal activity at some point in time. The activity may be non existent in old geothermal areas and far from volcanic regions whereas active areas are always associated with elevated temperatures near the Earth's surface compared to eg. Continental crustal areas. These elevated temperatures in combination with presence of abundant ground waters and rock permeability promote more rapid dissolution of the host rocks than at low temperature, therefore facilitating release of metals that may or may not precipitate into secondary minerals depending on the environmental conditions. One of these metals is arsenic (As) which varies from 0.18 to 113 mg kg^{-1} in basaltic rocks (Smedley and Kinniburgh, 2002).

The toxicity of arsenic is a well documented phenomenon (e.g. (Squibb, Fowler 1983, Lintschinger et al., 1998; Chakraborti et al., 2002; Mukhopadhyay et al., 2002; Hopenhayn, 2006; Cifuentes et al., 2009; Ventura-Lima et al., 2009). The oxidation of arsenite (As(III) to arsenate As(V) is commonly assumed to be carried out by microorganisms to derive energy from the oxidation of As(III) or it is presumed to be a detoxification mechanism (Salmassi et al., 2002). The toxicity of As(III) results from its affinity for sulfhydryl groups: various enzymes can be inactivated when As(III) binds to the cysteine residues of these proteins (Ferguson and Gavis, 1972; Summers and Silver, 1978). Arsenate, exerts a lower level of toxicity by substituting for phosphate in membrane transport systems and in ATP (Summers and Silver, 1978). Although the species may have different toxicity, there is evidence that the speciation once ingested is not the deciding attribute on the toxicity, but rather the transformations of arsenic species that may occur in the body after ingestion (Naranmandura et al., 2008). Regardless of transformations in the body, the speciation though always plays an important part on the mobility of As and determines the availability of the metal to the receptor.

The occurrence of As in ground-waters is of high concern throughout the world (Smedley and Kinniburgh, 2002) and while the source of As to these waters is not always understood numerous studies have been conducted on As removal from drinking waters with the aid of natural minerals, being either primary minerals in rocks (Singh et

al., 1996) or secondary minerals in soils (Lin and Puls, 2000; Herbel and Fendorf, 2006). Traditionally, the adsorption of arsenic (and other pollutants for that matter) was determined under set environmental conditions and an empirical relationship between the arsenic and the sorbent established, hence providing limited applicability of the data to other environments (Limousin et al., 2007). As analytical and computational power has advanced, the shift towards mechanistic models on adsorption has been observed in the literature (Sverjensky and Fukushi, 2006; Fukushi and Sverjensky, 2007). These models rely on stoichiometric reactions taking into account the chemical composition of the medium where they occur. Results generated on As sorption in the laboratory, which are validated by a mechanistic model taking into account competition of other ions and the ionic strength of the solution may be applied to other environments with confidence.

The widespread occurrence of basalts and the toxicity of As make research on their interaction important. While a considerable effort has been made on As research through the years the source and fate of arsenic in basaltic terrain is poorly understood (Arnorsson, 2003; Cabral and Beaudoin, 2007; Giroud, 2008). Therefore the aims of this thesis were:

- To provide an overview of the mobility of arsenite, As(III) and arsenate, As(V) oxyanions in contact with basaltic glass surfaces by carrying out laboratory experiments under controlled pH, Eh and ionic strength conditions.
- To use the coefficients generated to predict As transport where high temperature geothermal water is released into the natural environment.
- To quantify the percentage of thioarsenates in high temperature geothermal water and estimate the effect of thioarsenate complexation on the mobility.
- To combine experimental and field results to describe As cycling in a glacial outburst flood (jökulhlaup) following a sub glacial basaltic eruption.

In order to fulfil the aims of the thesis, the As/basalt interaction was studied in the range from small scale laboratory experiments in both Iceland and Scotland to field measurements in the vicinity of geothermal power plants and rivers draining from active volcanic eruptions. The data were then integrated by means of geochemical modeling in order to broaden our understanding on the release and transport of As in the basaltic crustal environment.

6.2 Key findings of this research

The work may be summarised into these key findings.

1. Arsenate (As(V)) mobility in basaltic porous media is highly dependent on the pH of the system. At low pH arsenate is nearly immobile and much less mobile than arsenite (As(III)). At high pH arsenate is highly mobile and much more mobile than arsenite. Arsenite was least mobile at near neutral conditions.
2. Arsenic is primarily bound to sulphur in high temperature geothermal waters in Iceland. These species are unstable at the surface and degrade rapidly once H_2S has been oxidised or degassed and as a consequence, the mobility in some non sulphidic environments may be predicted from experiments on arsenite and arsenate oxyanions.
3. Volcanic eruptions are a source of As Earth's surface. However basaltic eruptions may cause localised decrease in As concentrations in the ocean due to surface adsorption reactions.

6.2.1. Arsenite and arsenate mobility in basaltic porous media

In this thesis, basaltic glass has been considered as a mechanical mixture of amorphous silica-, iron- and aluminium oxides (Gislason and Oelkers, 2003). Consequently the surface of the glass has been assumed to derive it's properties in stochiometric proportions to the chemical composition of the glass. Of the three elements, Si is in highest abundance (16.8%) followed by Al (5.92% and finally Fe(3.28%) (Table 1, chapter 2). However when considering the equilibrium constants for surface reactions of arsenite on these surface sites it may be seen that the most important inner sphere surface reaction is the binding of As(III) to Fe sites (log K = 5.6) followed by adsorption to Al sites (log K = 4) and finally to Si sites (log K = 0.63). Similar tendency applies to As(V) adsorption and is due to different effective dielectric constants of the solids explaining the different magnitude of log K values (Fukushi and Sverjensky, 2007). This treatment of the basaltic glass allowed prediction of As transport in the laboratory, a necessary precursor for any reliable prediction under field conditions.

Arsenite is least mobile under near neutral conditions in basaltic aquifers. Near neutral conditions are though not very common in ground waters as the pH is raised

relatively fast to above 9 due to water/rock reactions by consumption of protons and there is not a resupply of bicarbonate from the atmosphere to neutralise the pH. Conversely, the pH of soils with basaltic parent material may be lower both due to a steady supply of bicarbonate and also due to formation of organic acids that may lower the pH (Sigfusson et al., 2006). Volcanic gases may lower the pH in ground waters (Delmelle et al., 2003) and could therefore increase As(III) mobility. Since the volcanic gases often include high proportion of H_2S the sulphur may effectively remove all As from the solution by formation of As-sulphides. The very high mobility of arsenic in basaltic terrain is presumably due to the fact that high pH is usually maintained and at high pH, both As(III) and in particularly As(V) are mobile and additionally formation of aqueous thioarsenic species is favoured over formation of As-sulphides (Planer-Friedrich et al., 2007).

Basaltic glass is one of many rock and soil constituents exhibiting variable charge on its surface. The variable charge is due to the surface's ability to accept and donate protons from its surrounding solution. This property leads to varying adsorption potential of ions with pH. Furthermore, the adsorption potential relies on the protonation of the anions in question.

Typically, peak sorption of oxyanions such as sulphate, carbonate, silicate and phosphate is observed at low pH and a complete sorption is essentially observed until a critical pH value is reached. For arsenic, this behaviour may be explained by the formation of two types of As(III) surface complexes (Sverjensky and Fukushi, 2006):

1) Formation of a strong inner sphere complex by ligand exchange. Here the surface complex is formed when two water molecules are replaced by the anion on the surface through two reactions, first the surface is protonated and H_3AsO_3 is adsorbed and deprotonated. In a second reaction water molecules are desorbed and an inner sphere surface complex is formed.

2) The formation of an outer sphere complex is essentially through hydrogen bonding. The surface is protonated to $–OH_2^+$ and the protonated surface site forms a H bond to the -OH group of the oxyanion. The formation occurs primarily around and below the first pK value of the oxyanion. Once the oxyanion has dissociated the H bond is not stable and as a consequence the oxyanion will not form an outer sphere complex.

The ratio of As inner sphere to outer sphere complexes depends on the surface. According to modeling carried out by Sverjensky and Fukushi (2006) on As(III) adsorption, inner sphere complex was prevalent on magnetite (Dixit and Hering, 2006) up to pH 4.2, on goethite (Dixit and Hering, 2003), ferrihydrite (Jain et al., 1999) and amorphous Fe (Goldberg and Johnston, 2001) over the whole pH range, on HFO (Dixit and Hering, 2003) up to pH 8.9, on amorphous Al (Goldberg and Johnston, 2001) up to pH 6.5 and gibbsite (Weerasooriya et al., 2003) over the whole pH range. The crossover points were though dependent on the As concentration, ionic strength of the solution and solution composition. In general it may though be said that As(III) inner sphere complexes predominate at low pH values and As(III) outer sphere complexes are increasingly important at high pH. However, on most oxides the As(III) inner sphere complex becomes more predominant over aqueous As(III) as pH is shifted from 3 upwards towards neutral pH.

Similarly, for As(V) three inner sphere surface complexes may be assumed from spectroscopic data (Fukushi and Sverjensky, 2007). The formation of these complexes occurs in similar manner as the inner sphere complex of As(III), that is the release of water molecules from the surface and adsorption of arsenate ion. Together, these surface complexes are primarily formed at low pH values whereas decreased sorption is observed as pH is increased and the arsenate dissociates. In all cases the highest tendency to form surface complex is on HFO, followed by ferrihydrite, goethite and then the aluminium bearing phases (Fukushi and Sverjensky, 2007).

6.2.2. The stability and mobility of thioarsenic species in geothermal powerplant wastewaters

Arsenic sulphur relationship was studied under three types of field conditions:

1) In high temperature geothermal water leaving a power plant with the arsenic primarily being on thioarsenic form

2) In surface stream with thioarsenic being both adsorbed to sulphides and degraded stepwise to arsenite and arsenate before being finally discharged into:

3) a shallow groundwater stream in a basaltic lava flow where the primary mechanisms for arsenic removal were presumably adsorption to basaltic glass and iron oxides in the absence of H_2S.

Field measurements confirmed published literature that As is primarily bound to sulphur in high temperature sulphidic waters at high pH (Planer-Friedrich et al., 2007;

Nordstrom and Archer, 2003). These thiorarsenic species were rapidly degraded in the absence of H_2S although the degradation was kinetically controlled and considerable discrepancies were observed between thermodynamic calculations and field measurements. The As levels in geothermal waters and ground waters were compared against the highly conservative chloride (Giroud, 2008) and the As was highly mobile in the in the presence of H_2S when it was mainly on the thiorarsenic form. However, surface discharge, associated with decrease of H_2S due to sulphide formation, degassing and oxidation promoted degradation of thioarsenic species and formation of arsenite and later arsenate presumably along with some incorporation of As into sulphides (Cleverley et al., 2003). The As oxyanions were then removed from ground waters relative to chloride due to a combination of surface adsorption reactions on basaltic glass and iron hydroxides since no sulphides were stable at these latter conditions in the postglacial lava.

During the field trials of the thesis the author sampled geothermal waters (pH 3-7.8) from boiling mud springs in Krísuvík and Hveradalir, Iceland. The mineralogy of these mud springs is characterised by iron sulphides and in a total of 14 samples acquired from 0-50 m from the source total arsenic concentrations were never above 0.2 $\mu g\ l^{-1}$ although the waters in Hveradalir are derived from the same source as geothermal waters in the Hellisheiði Power plant where the author repeatedly measured As concentrations around 150 – 200 $\mu g\ l^{-1}$.

It may therefore be inferred that although As can be highly mobile under reservoir conditions at high temperature and pressure it can be efficiently removed from the solution initially by incorporation into and onto sulphides and later onto oxides and basaltic glass provided that H_2S has been removed from the solution.

6.2.3 The fate of volcanically derived arsenic in a glacial outburst (Jökulhlaup) event

A modeling exercise was carried out to speculate on the fate of As from entering the Earth's surface until being discharged in the ocean few hours later. The 2004 Grímsvötn eruption was used for this purpose. The model could be verified to some extent by the means of sampling campaign on river water and suspended materials that was carried out during the volcanic eruption. The fresh unweathered tephra was also sampled allowing for prediction of mobility of various trace elements. According to geochemical calculations the dissolution of volcanic materials that travelled through the

flood-path was sufficient to explain the elevated flux of dissolved and adsorbed arsenic. No volatile arsenic was needed during the eruption as an external source. However, As from degassing magmas may reach the volcano's caldera (Pokrovski et al., 2002). This As is then presumably carried by steam being formed near the magma body and later dissolved in the Grímsvötn lake (Ballantyne and Moore, 1988). The 2004 Grímsvötn eruption was presumably too small to have any significant impact on the ocean due to dilution. Geochemical modeling of suspended material sea water interactions predicted adsorption of arsenate and phosphate from the ocean immediately upon mixing. The phosphate desorbed rapidly and was effectively not sorbed once floodwater had been diluted ten times with sea water. The arsenic was however adsorbed on the tephra surface until 1000 fold dilution had occurred. This means that a subglacial eruption or the much more common discharge of rivers with high suspended matter load may cause much more widespread localised decrease in aqueous arsenic than phosphate concentrations. These adsorption reactions may overcome the supply of anions leaching from the suspended particles as a result of chemical weathering thus making the suspended materials a short term sink followed by a long term source of nutrients to the ocean (Frogner et al., 2001; Jones and Gislason, 2008; Gabrielli et al., 2008; Stefansdottir and Gislason, 2006, Stefansdottir and Gislason, 2005).

6.3 Future work

The current research project merely touched on the subject of arsenic basalt interactions and it is evident that more research is needed in order to better understand the primary mechanisms responsible for arsenic mobility in basaltic terrain. The following projects are suggested to better understand arsenic – basalt interactions.

Conduct Synchrotron radiation spectroscopy to qualify arsenic surface interactions. Although a great variety of possible surface species coordination geometries may be proposed from these spectroscopy studies (Waychunas et al., 2005) and they cannot determine the protonation state of surface complexes (Fukushi and Sverjenski, 2007) they provide insight on the structure of surface complexes and may shed the light on weather simple surface complex modeling may be applied to such a complex matrix as basaltic glass. In other words, is it justifiable to assume basaltic glass is a mechanical mixture of three surface site types that don't interact or are other methods needed for modeling.

Carry out laboratory experiments in more complex solutions to quantify the effect of competing ions on As sorption. Numerous authors have studied the effect of competing ions in solution (Arai et al., 2004) and although silica, carbonate and chloride form weaker bonds than arsenic on eg. HFO (Dzombak and Morel, 1990) their concentrations exceed those of As by far in high temperature geothermal waters and as a consequence can have substantial impact on As mobility.

Instigate experiments with AEC-ICP-MS attached to the experiments outlet instead of HG-AAS or HG-AF. This allows for the determination of thioarsenic basaltic glass surface reactions. A concern has been put forward on the applicability of HG techniques to study arsenic speciation due to the instability of As aqueous species in the analytical system and formation of As-sulphides at low pH (Planer-Friedrich and Wallschlager, 2009). The usage of AEC-ICP-MS will eliminate that source of error and provide more robust data for interpretation.

Study arsenic dynamics on weathered rocks and also crystalline basalts. This would increase the applicability of the findings. The need for those experiments is though somehow determined by results generated from project 1 mentioned above. If basalt may in fact be considered to be a mechanical mixture of Si, Al and Fe –oxides, more weathered systems may be studied by altering the ratio between the abovementioned sites.

Carry out further modeling and measurements of the fate of trace elements adsorbed to river suspended materials once they enter the ocean. A considerable effort has been made to quantify the release of trace elements form suspended materials once entering the ocean, (Frogner et al., 2001; Jones and Gislason, 2008; Gabrielli et al., 2008; Stefansdottir and Gislason, 2006; Stefansdottir and Gislason, 2005) although less is known on the adsorption of some elements onto tephra grains. Initially a desk study might be carried out to revise data from experiments that does not take into account surface complexation reactions since they may be responsible for variable release rates of elements into solution rather than different leaching rates from the crystal lattice of bulk materials.

Deploy HPLC-ICP-MS at geothermal power plants to accurately quantify of As in geothermal waters and, hence, provide further insight on the transport of As in fluid dominated high temperature geothermal systems. This deployment prevents most uncertainties about sample preservation and analysis (Planer-Friedrich et al., 2007, Planer-Friedrich and Wallschlager, 2009, McCleskey et al., 2004) and would give a

deeper understanding of processes occurring within high temperature geothermal regions. Field application of AES-HG-AFS as in this thesis and AES to quantify sulphur species (Stefansson et al., 2009) have already demonstrated the limited usefulness of sample preservation with regards to redox sensitive species and all sulphur containing species in geothermal fluids.

References

Arai, Y., Sparks, D.L. & Davis, J.A. 2004, "Effects of dissolved carbonate on arsenate adsorption and surface speciation at the hematite-water interface", *Environmental science & technology,* vol. 38, no. 3, pp. 817-824.

Arnorsson, S. 2003, "Arsenic in surface- and up to 90 degrees C ground waters in a basalt area, N-Iceland: processes controlling its mobility", *Applied Geochemistry,* vol. 18, no. 9, pp. 1297-1312.

Ballantyne, J.M. & Moore, J.N. 1988, "Arsenic geochemistry in geothermal systems", *Geochimica et Cosmochimica Acta,* vol. 52, no. 2, pp. 475-483.

Cabral, A.R. & Beaudoin, G. 2007, "Volcanic red-bed copper mineralisation related to submarine basalt alteration, Mont Alexandre, Quebec Appalachians, Canada", *Mineralium Deposita,* vol. 42, no. 8, pp. 901-912.

Chakraborti, D., Rahman, M.M., Paul, K., Chowdhury, U.K., Sengupta, M.K., Lodh, D., Chanda, C.R., Saha, K.C. & Mukherjee, S.C. 2002, "Arsenic calamity in the Indian subcontinent: What lessons have been learned?", *Talanta,* vol. 58, no. 1, pp. 3-22.

Cifuentes, F., Bravo, J., Norambuena, M., Stegen, S., Ayavire, A. & Palacios, J. 2009, "Chronic Exposure to Arsenic in Tap Water Reduces Acetylcholine-induced Relaxation in the Aorta and Increases Oxidative Stress in Female Rats", *International journal of toxicology,* vol. 28, no. 6, pp. 534-541.

Cleverley, J.S., Benning, L.G. & Mountain, B.W. 2003, "Reaction path modelling in the As–S system: a case study for geothermal As transport", *Applied Geochemistry,* vol. 18, no. 9, pp. 1325-1345.

Delmelle, P., Delfosse, T. & Delvaux, B. 2003, "Sulfate, chloride and fluoride retention in Andosols exposed to volcanic acid emissions", *ENVIRONMENTAL POLLUTION,* vol. 126, no. 3, pp. 445-457.

Dixit, S. & Hering, J.G. 2006, "Sorption of Fe(II) and As(III) on goethite in single- and dual-sorbate systems", *Chemical Geology,* vol. 228, no. 1-3, pp. 6-15.

Dzombak, D.A. & Morel, F.M.M. 1990, *Surface Complexation Modeling: Hydrous Ferric Oxide,* Wiley-Interscience.

Ferguson, J.F. & Gavis, J. 1972, "A review of the arsenic cycle in natural waters", *Water Research,* vol. 6, no. 11, pp. 1259-1274.

Frogner, P., Gislason, S.R. & Oskarsson, N. 2001, "Fertilizing potential of volcanic ash in ocean surface water", *Geology,* vol. 29, no. 6, pp. 487-490.

Fukushi, K. & Sverjensky, D.A. 2007, "A predictive model (ETLM) for arsenate adsorption and surface speciation on oxides consistent with spectroscopic and theoretical molecular evidence", *Geochimica et Cosmochimica Acta,* vol. 71, no. 15, pp. 3717-3745.

Gabrielli, P., Barbante, C., Plane, J.M.C., Boutron, C.F., Jaffrezo, J.L., Mather, T.A., Stenni, B., Gaspari, V., Cozzi, G., Ferrari, C. & Cescon, P. 2008, "Siderophile metal fallout to Greenland from the 1991 winter eruption of Hekla (Iceland) and during the global atmospheric perturbation of Pinatubo", *Chemical Geology,* vol. 255, no. 1-2, pp. 78-86.

Giroud, N. 2008, *A chemical study of arsenic, boron and gases in high-temperature geothermal fluids in Iceland*, University of Iceland, Faculty of Science.

Gislason, S.R. & Oelkers, E.H. 2003, "Mechanism, rates, and consequences of basaltic glass dissolution: II. An experimental study of the dissolution rates of basaltic glass as a function of pH and temperature", *Geochimica et Cosmochimica Acta,* vol. 67, no. 20, pp. 3817-3832.

Goldberg, S. & Johnston, C.T. 2001, "Mechanisms of arsenic adsorption on amorphous oxides evaluated using macroscopic measurements, vibrational spectroscopy, and surface complexation modeling", *Journal of colloid and interface science,* vol. 234, no. 1, pp. 204-216.

Herbel, M. & Fendorf, S. 2006, "Biogeochemical processes controlling the speciation and transport of arsenic within iron coated sands", *Chemical Geology,* vol. 228, no. 1-3, pp. 16-32.

Hopenhayn, C. 2006, "Arsenic in drinking water: Impact on human health", *Elements,* vol. 2, no. 2, pp. 103-107.

Jain, A., Raven, K.P. & Loeppert, R.H. 1999, "Arsenite and arsenate adsorption on ferrihydrite: Surface charge reduction and net OH- release stoichiometry", *Environmental science & technology,* vol. 33, no. 8, pp. 1179-1184.

Jerram, D.A. & Widdowson, M. 2005, "The anatomy of Continental Flood Basalt Provinces: geological constraints on the processes and products of flood volcanism", *Lithos,* vol. 79, no. 3-4, pp. 385-405.

Jones, M.T. & Gislason, S.R. 2008, "Rapid releases of metal salts and nutrients following the deposition of volcanic ash into aqueous environments", *Geochimica et Cosmochimica Acta,* vol. 72, no. 15, pp. 3661-3680.

Limousin, G., Gaudet, J.P., Charlet, L., Szenknect, S., Barthes, V. & Krimissa, M. 2007, "Sorption isotherms: A review on physical bases, modeling and measurement", *Applied Geochemistry,* vol. 22, no. 2, pp. 249-275.

Lin, Z. & Puls, R.W. 2000, "Adsorption, desorption and oxidation of arsenic affected by clay minerals and aging process", *Environmental Geology,* vol. 39, no. 7, pp. 753-759.

Lintschinger, J., Schramel, P., Hatalak-Rauscher, A., Wendler, I. & Michalke, B. 1998, "A new method for the analysis of arsenic species in urine by using HPLC-ICP-MS", *Fresenius Journal of Analytical Chemistry,* vol. 362, no. 3, pp. 313-318.

McCleskey, R.B., Nordstrom, D.K. & Maest, A.S. 2004, "Preservation of water samples for arsenic(III/V) determinations: an evaluation of the literature and new analytical results", *Applied Geochemistry,* vol. 19, no. 7, pp. 995-1009.

Mukhopadhyay, R., Rosen, B.P., Pung, L.T. & Silver, S. 2002, "Microbial arsenic: from geocycles to genes and enzymes", *FEMS microbiology reviews,* vol. 26, no. 3, pp. 311-325.

Naranmandura, H., Suzuki, N. & Suzuki, K.T. 2008, "Reaction mechanism underlying the in vitro transformation of thioarsenicals", *Toxicology and applied pharmacology,* vol. 231, no. 3, pp. 328-335.

Nordstrom, D. & Archer, D. 2003, *Arsenic thermodynamic data and environmental geochemistry*.

Planer-Friedrich, B., London, J., McCleskey, R.B., Nordstrom, D.K. & Wallschlager, D. 2007, "Thioarsenates in geothermal waters of yellowstone national park: Determination, preservation, and geochemical importance", *Environmental science & technology,* vol. 41, no. 15, pp. 5245-5251.

Planer-Friedrich, B. & Wallschlager, D. 2009, "A critical investigation of hydride generation-based arsenic speciation in sulfidic waters", *Environmental Science and Technology,* vol. in press.

Pokrovski, G.S., Zakirov, I.V., Roux, J., Testemale, D., Hazemann, J., Bychkov, A.Y.u. & Golikova, G.V. 2002, "Experimental study of arsenic speciation in vapor phase to 500°C: implications for As transport and fractionation in low-density crustal fluids and volcanic gases", *Geochimica et Cosmochimica Acta,* vol. 66, no. 19, pp. 3453-3480.

Salmassi, T.M., Venkateswaren, K., Satomi, M., Nealson, K.H., Newman, D.K. & Hering, J.G. 2002, "Oxidation of arsenite by Agrobacterium albertimagni, AOL15, sp nov., isolated from Hot Creek, California", *Geomicrobiology Journal,* vol. 19, no. 1, pp. 53-66.

Sigfusson, B., Paton, G.I. & Gislason, S.R. 2006, "The impact of sampling techniques on soil pore water carbon measurements of an Icelandic Histic Andosol", *Science of the Total Environment,* vol. 369, no. 1-3, pp. 203-219.

Singh, D.B., Prasad, G. & Rupainwar, D.C. 1996, "Adsorption technique for the treatment of As(V)-rich effluents", *Colloids and Surfaces A-Physicochemical and Engineering Aspects,* vol. 111, no. 1-2, pp. 49-56.

Smedley, P.L. & Kinniburgh, D.G. 2002, "A review of the source, behaviour and distribution of arsenic in natural waters", *Applied Geochemistry,* vol. 17, no. 5, pp. 517-568.

Squibb, K.S. & Fowler, B.A. 1983, "The toxicity of arsenic and its compounds" in *Biological and environmental effects of arsenic*, ed. B.A. Fowler, Elsevier, Amsterdam, pp. 233-269.

Stefansdottir, M.B. & Gislason, S.R. 2006, "Suspended basaltic glass-seawater interactions", *Journal of Geochemical Exploration,* vol. 88, no. 1-3, pp. 332-335.

Stefansdottir, M.B. & Gislason, S.R. 2005, "The erosion and suspended matter/seawater interaction during and after the 1996 outburst flood from the Vatnajokull Glacier, Iceland", *Earth and Planetary Science Letters,* vol. 237, no. 3-4, pp. 433-452.

Stefansson, A., Arnorsson, S., Gunnarsson, I. & Kaasalainen, H. 2009, “Förgun brennisteins frá Hellisheiðarvirkjun – Jarðefnafræðileg athugun” in Icelandic. Science Institute report RH-14-2009, 84 pp,

Summers, A.O. & Silver, S. 1978, "Microbial Transformations of Metals", *Annual Review of Microbiology,* vol. 32, pp. 637-672.

Sverjensky, D.A. & Fukushi, K. 2006, "A predictive model (ETLM) for As(III) adsorption and surface speciation on oxides consistent with spectroscopic data", *Geochimica et Cosmochimica Acta,* vol. 70, no. 15, pp. 3778-3802.

Ventura-Lima, J., Fattorini, D., Regoli, F. & Monserrat, J.M. 2009, "Effects of different inorganic arsenic species in Cyprinus carpio (Cyprinidae) tissues after short-time exposure: Bioaccumulation, biotransformation and biological responses", *Environmental Pollution,* vol. 157, no. 12, pp. 3479-3484.

Waychunas, G., Trainor, T., Eng, P., Catalano, J., Brown, G., Davis, J., Rogers, J. & Bargar, J. 2005, "Surface complexation studied via combined grazing-incidence EXAFS and surface diffraction: arsenate an hematite (0001) and (10-12)", *Analytical and Bioanalytical Chemistry,* vol. 383, no. 1, pp. 12-27.

Weerasooriya, R., Tobschall, H.J., Wijesekara, H.K.D.K., Arachchige, E.K.I.A.U.K. & Pathirathne, K.A.S. 2003, "On the mechanistic modeling of As(III) adsorption on gibbsite", *Chemosphere,* vol. 51, no. 9, pp. 1001-1013.